

PROCESSING AND CHARACTERIZATION
OF CUTTLBONE REINFORCED
POLYMER COMPOSITES FOR
BIOMEDICAL APPLICATIONS

Thesis

Submitted in partial fulfillment of the requirements for the degree of
DOCTOR OF PHILOSOPHY

by

KAMALBABU P.



DEPARTMENT OF MECHANICAL ENGINEERING
NATIONAL INSTITUTE OF TECHNOLOGY KARNATAKA,
SURATHKAL, MANGALORE -575025.

October, 2017

DECLARATION

by the Ph.D. Research Scholar

I hereby declare that the Research Thesis entitled “**Processing and Characterization of Cuttlebone Reinforced Polymer Composites for Biomedical Applications**” which is being submitted to the National Institute of Technology Karnataka, Surathkal in partial fulfillment of the requirements for the award of the Degree of Doctor of Philosophy in **Department of Mechanical Engineering** is a bonafide report of the research work carried out by me. The material contained in this Research Thesis has not been submitted to any University or Institution for the award of any degree.

KAMALBABU P.

Register Number: ME09F02

Department of Mechanical Engineering

National Institute of Technology Karnataka

Place : NITK-Surathkal

Date :

CERTIFICATE

This is to certify that the Research Thesis entitled “**Processing and Characterization of Cuttlebone Reinforced Polymer Composites for Biomedical Applications**” submitted by **Kamalbabu P. (Register Number: ME09F02)** as the record of the research work carried out by him, is accepted as the Research Thesis submission in partial fulfillment of the requirements for the award of degree of Doctor of Philosophy.

Research Guide

Prof. G. C. Mohan Kumar

(Signature with Date and Seal)

Chairman – DRPC

(Signature with Date and Seal)

Dedicated to my beloved family members and well wishers.....

ACKNOWLEDGEMENTS

First and foremost, I would like to express my sincere gratitude to my supervisor, Dr. G.C. Mohan Kumar, Professor, Department of Mechanical Engineering for his guidance, encouragement, inspiration and constant support throughout my research work. He is an excellent adviser, who has always been there to answer my questions, and a great guide who has encouraged and helped me to learn many new skills.

I am grateful to Prof. Narendranath S., Head of the department, Prof. K. V. Gangadharan, and Prof. Prasad Krishna, Department of Mechanical Engineering, for providing facilities for my Ph.D. Research work in the Department of Mechanical Engineering, NITK, Surathkal. Also, I would like to give my special thanks to the National Institute of Technology Karnataka, Surathkal for a research fellowship.

I am also grateful to my Research Progress Assessment Committee members: Dr. M. C. Narasimhan, Professor, Department of Civil Engineering and Dr. Murigendrappa, Associate Professor, Department of Mechanical Engineering for their insightful suggestions, advices and patience.

This research work could not complete without having help from the colleagues and friends around me. My very special thanks go to Dr. T. Senthil, Haixi Institutes, Chinese Academy of Sciences, Fujian, P. R. China, for his constant supports and help during my research. He has always been there for discussions at most difficult times.

I am thankful to Director, SCTIMST, Thiruvananthapuram for permitting me to carry out cytotoxicity and hemocompatibility tests in his institute. Also, I thank Dr. A. Sabareeswaran, Scientist E, SCTIMST, Thiruvananthapuram for his support to my unforeseen technical needs.

I also own my grateful to Dr. Anandhan Srinivasan, Dr. K. Narayan Prabhu, Dr. I. Regupathi, Dr. N. K. Udayashankar, Dr. Nagaraja H.S., Dr. H. D. Saikala Dr. Saravanabavan D., Dr. Gibin George, Dr. Hemanth kumar and Mr. Sivananth, for their valuable assistance in different ways.

I am grateful to Prof. Lixin Wu, Haixi Institutes, Chinese Academy of Sciences, Fujian, P. R. China, Dr. Kishore Ginjupalle, Manipal Institute of Dental Science, Manipal, Dr. Keshav Prabhu, Konspec-Konkan Speciality polyproducts private limited, Mangalore, Dr. Nandini, Kasturba Medical College, Mangalore, Mr. Shenoy, Chemtrends private limited, Bangalore, Mr. Gokulakrishnan, Aqua Technologies, Coimbatore, for providing the necessary support in terms of facilities and equipments for executing this research work.

I must also extend warmest thanks to my friends: Dr. Melby Chacko, Dr. Akshata G. Patil, Dr. Kripa M. Suvarna, Mr. Gopinath kalaiarasan, Dr. Maheswari M., Mr. Vipin Allien, Mr. M. Mathusuthanan, Mr. K. Panneerselvam Mr. G. Arunkumar and Mr. A. Senthilnath for always being supportive, unfailing encouragement and loving.

I am also thankful to Dr. Sivamurthy, Dr. Manjunath Patel, Dr. Manjaiah, Mr. Kiran Pedanaboyina, Mr. Sreejesh M., Dr. Manoj Kumar N., Mr. Mahendra K., Mr. Pragadeesh K S, Dr. Viswanatha H. N. Mr. Abhinav K Nair, Dr. Mrunali Sona, Mr. Hargovind Soni, Dr. Rajesh M., Mr. Vimalanathan, Mr. Nagamadhu and other friends who constantly supported and helped me during the experimental work.

I would also like to thank rest of the faculty members, research scholars and technical staff in the Department of Mechanical Engineering.

An inspiration, role model and a hero to me; your dear son, I submit this thesis as a gratitude to my father Mr. T. S. Periasamy, who I wish was here with me to see as I excel in my research career. Thanks to my mother Smt. Kamalam, brother Dr. Kathiravan, sister-in-law Dr. Anbumalar and niece Joshita for giving their support, love, tolerance and understanding during the years of my doctoral study. Without them, I would not be where I am today... literally.

KAMALBABU P.

ABSTRACT

Utilization of sea coral in the development of biocomposites, especially for application as implants has been well documented. In this study, different cuttlebone derived bio-fillers were used as reinforcement in epoxy composites along with carbon fiber to improve mechanical and biocompatibility properties for low and high load bearing implant applications. Raw cuttlebone, heat treated cuttlebone particles (calcined at 400°C) and cuttlebone derived bio ceramics (calcium oxide, hydroxyapatite and tricalcium phosphate) obtained through either calcination at 800°C or mechanochemical method followed by calcination at higher temperature were derived. X-ray diffractometer and Fourier Transform-Infra Red spectroscopy was used to confirm the phase confirmation of different cuttlebone derived particles. Epoxy composites were prepared by hand layup method using different cuttlebone derived particles as reinforcement phase. Material properties like mechanical, physical, thermal, thermo-mechanical and biocompatibility of these composites were studied. Among the different composites studied, raw cuttlebone and hydroxyapatite reinforced epoxy composites showed a superior mechanical, physical, thermal and biocompatibility properties than the other composites even at a lower filler loading level (≤ 9 wt%). Material properties observed for these two composites establish them as a potential candidate for low load bearing orthopedic implant applications. Similarly, raw cuttlebone, heat treated cuttlebone, hydroxyapatite and tricalcium phosphate was used along with carbon fiber as reinforcement in epoxy composites. These hybrid composites were prepared by hand layup followed by hydraulic press method; their mechanical, physical, thermal and thermo-mechanical properties were found to be improvised than carbon fiber/epoxy composites. Among the hybrid composites examined, raw cuttlebone/carbon fiber reinforced epoxy composite demonstrates favorable biocompatible properties that substantiate them for high load bearing bone plate applications.

Keywords: *Biomaterials; Polymer composites; carbon fiber; Sea coral; Cuttlebone; Implants; Biocompatibility*

CONTENTS

Chapter No.	Description	Page No.
	LIST OF FIGURES	i
	LIST OF TABLES	vii
	NOMENCLATURE	ix
	ABBREVIATION	xi
Chapter 1	INTRODUCTION	1
1.1	Background	1
1.2	Hypothesis	4
1.3	Objective of this research work	4
1.4	Thesis Structure	5
Chapter 2	LITERATURE REVIEW	7
2.1	History of non-degradable implants	7
2.2	Biological Materials	8
2.2.1	Marine Calcium carbonate skeletons	8
2.2.1.1	Shells	9
2.2.1.2	Sea Urchins	9
2.2.1.3	Corals	10
2.2.1.4	Cuttlebone	10
2.2.1.5	Marine calcium carbonate biomaterials for biomedical applications	11
2.3	Calcium Phosphates	12
2.3.1	Chemically synthesized calcium phosphate through different methods	12
2.3.2	Calcium phosphate derived from natural sources	13
2.3.2.1	Corals	14
2.3.2.2	Cattle bone	14

2.3.2.3	Fish bones	15
2.3.2.4	Sea Shells	15
2.3.2.5	Cuttlebone derived calcium phosphates	16
2.4	Calcium carbonate as reinforcement in polymer composites	18
2.4.1	Synthetic calcium carbonate as reinforcement in thermoset polymer composites	19
2.4.2	Modified calcium carbonate as reinforcement in thermoset polymer composites	19
2.4.3	Calcium carbonate reinforced polymer composites for biomedical applications	20
2.4.4	Marine calcium carbonate as reinforcement in polymer composites	21
2.4.5	Cuttlebone as reinforcement in polymer composites	22
2.5	Calcium phosphate as reinforcement in polymer composites	22
2.5.1	Synthetic calcium phosphates/ thermoset polymer composites	23
2.5.2	Natural derived calcium phosphates and its composites for biomedical applications	23
2.5.3	Cuttlebone derived calcium phosphates/polymer composites	24
2.6	Fiber reinforced polymer composites	25
2.6.1	Fiber reinforced polymer composites for biomedical applications	25
2.6.2	Fiber/filler reinforced hybrid polymer composites	26
2.7	Mechanical properties of materials used in biomedical application	28
2.8	Summary of contribution	31

Chapter 3	MATERIALS AND METHODS	33
3.1	Materials	33
3.2	Preparation of cuttlebone (CB) and heat-treated cuttlebone particles	33
3.3	Preparation of calcium oxide(CO), hydroxyapatite (HA) and tricalcium phosphates from cuttlebone particles	34
3.4	Characterization of cuttlebone particles	35
3.5	Preparation of composites	37
3.5.1	Preparation of cuttlebone particles (CB, HB) / cuttlebone derived bio ceramics (CO, HA, CP) reinforced epoxy composites	37
3.5.2	Preparation of cuttlebone derived particles (CB, HB, HA, CP) and carbon fiber reinforced hybrid epoxy composites	38
3.6	Mechanical, Surface morphology, thermal and physical studies of composites	39
3.6.1	Mechanical properties of composites	39
3.6.2	Surface morphology of composites	41
3.6.3	Thermo-mechanical and thermal properties of composites	41
3.6.4	Physical properties of composites	42
3.7	Biocompatibility studies of composites	44
3.7.1	<i>“In vitro”</i> cytotoxicity study	44
3.7.2	<i>“In vitro”</i> hemocompatibility study	46
Chapter 4	Influence of cuttlebone bio-fillers as reinforcement in epoxy composites	49
4.1	Results and Discussions	49
4.1.1	Characterization of CB, HB and CC particles	49

	4.1.1.1	Thermo gravimetric analysis of CB, HB and CC particles	52
	4.1.1.2	Crystallographic structure and composition of CB, HB and CC particles	54
	4.1.2	Mechanical properties of EP, EP/CB, EP/HB and EP/CC composites	59
	4.1.3	Fracture morphology studies of EP, EP/CB, EP/HB and EP/CC composites	76
	4.1.4	Density and voids percentage of EP, EP/CB, EP/HB and EP/CC composites	77
	4.1.5	Physical properties of EP, EP/CB, EP/HB and EP/CC composites	78
	4.1.6	Thermo-mechanical and thermal properties of EP, EP/CB, EP/HB and EP/CC composites	81
	4.1.7	Biocompatibility properties of EP/CB and EP/HB composites	85
	4.1.8	Summary	89
Chapter 5		Influence of cuttlebone derived bio ceramics as reinforcement in epoxy composites	91
	5.1	Results and Discussions	91
	5.1.1	Characterization of CO, HA and CP particles	91
	5.1.1.1	Thermo gravimetric analysis of CO, HA and CP particles	96
	5.1.1.2	Crystallographic structure and composition of CO, HA and CP particles	98
	5.1.2	Mechanical properties of EP, EP/CO, EP/HA and EP/CP composites	103
	5.1.3	Fracture morphology studies of EP, EP/CO, EP/HA and EP/CP composites	119

	5.1.4	Density and voids percentage of EP, EP/CO, EP/HA and EP/CP composites	121
	5.1.5	Physical properties of EP, EP/CO, EP/HA and EP/CP composites	122
	5.1.6	Thermo-mechanical and thermal properties of EP, EP/CO, EP/HA and EP/CP composites	124
	5.1.7	Biocompatibility properties of EP/HA and EP/CP composites	129
	5.1.8	Summary	133
Chapter 6		Comparison of material properties of cuttlebone derived bio-fillers and bio-ceramics reinforced epoxy composites	135
	6.1	Results and Discussions	135
	6.1.1	Material Characterization of CB, HB, HA and CP particles.	135
	6.1.2	Mechanical properties of EP, EP/CB, EP/HB, EP/HA and EP/CP composites	136
	6.1.3	Fracture morphology studies of EP, EP/CB, EP/HB, EP/HA and EP/CP composites	142
	6.1.4	Voids percentage of EP, EP/CB, EP/HB, EP/HA and EP/CP composites	143
	6.1.5	Physical properties of EP, EP/CB, EP/HB, EP/HA and EP/CP composites	143
	6.1.6	Thermo-mechanical and thermal properties of EP, EP/CB, EP/HB, EP/HA and EP/CP composites	145
	6.1.7	Biocompatibility properties of EP/CB, EP/HB, EP/HA and EP/CP composites	148
	6.1.8	Assessment on material properties for potential requirement of low load bearing implants applications	151

	6.1.9	Summary	152
Chapter 7		Influence of cuttlebone derived bio-fillers and bio-ceramics/carbon fiber as reinforcement in hybrid epoxy composites	155
	7.1	Results and Discussions	155
	7.1.1	Mechanical properties of hybrid composites	155
	7.1.2	Fracture morphology studies of hybrid composites	167
	7.1.3	Density and voids percentage of hybrid composites	168
	7.1.4	Physical properties of hybrid composites	170
	7.1.5	Thermo-mechanical and thermal properties of hybrid composites	172
	7.1.6	Biocompatibility properties of hybrid composites	177
	7.1.7	Assessment on material properties for potential requirement of low load bearing implants applications	182
	7.1.8	Summary	183
Chapter 8		CONCLUSIONS	185
		FUTURE WORK	187
		REFERENCES	189
		LIST OF PUBLICATIONS	217
		BIO-DATA	219

LIST OF FIGURES

Figure No.	Captions	Page No.
1.1	Classification of polymer composites for biomedical applications	2
3.1	Process flowchart for conversion of cuttlebone to (a) hydroxyapatite and (b) tricalcium phosphates	34
3.2	Process flowchart for preparation of particle reinforced composites	37
3.3	Process flowchart for preparation of particle/fiber reinforced hybrid composites	38
3.4	(a) Schematic representation of area S1, S2 and S3 from TGA curve. (b) Plots of $\ln[\ln(1-\alpha)-1]$ Vs. θ for composites	42
3.5	Process flowchart for the cytotoxicity test using indirect test method	45
3.6	Process flowchart for the hemocompatibility test	46
4.1	Particle size distribution of (a) cuttlebone particles and (b) commercial CaCO_3	50
4.2	SEM micrograph of (a) cuttlebone particles (b) commercial CaCO_3 particles and EDX spectra of cuttlebone particles	51
4.3	(a) TG and DTG curve of cuttlebone particles and (b) its corresponding DTA curve with base line subtraction	53
4.4	(a) TG and (b) DTG curve of heat treated cuttlebone (HB) particles and commercial CaCO_3 (CC) particles.	54
4.5	X-ray diffractograms of raw cuttlebone and JCPDS 01-0628 for aragonite CaCO_3 .	54
4.6	X-ray diffractograms of heat treated cuttlebone particles (HB), commercial CaCO_3 particles (CC) and JCPDS 01-0837 for calcite CaCO_3 .	55
4.7	FT-IR spectra of (a) raw cuttlebone, (b) heat treated cuttlebone particles and (c) Commercial CaCO_3 particles.	56

4.8	XPS Spectra for raw cuttlebone and heat-treated cuttlebone particles.	57
4.9	(a) Ultimate tensile strength, (b) Tensile modulus, (c) Elongation percentage at break and (d) Load Vs. displacement curve of EP, EP/CB, EP/HB and EP/CC composites.	61
4.10	(a) Flexural strength, (b) Flexural modulus and (c) Load Vs. displacement curve of EP, EP/CB, EP/HB and EP/CC composites.	65
4.11	(a) Compression strength, (b) Compression modulus and (c) Load Vs. displacement curve of EP, EP/CB, EP/HB and EP/CC composites.	68
4.12	(a) Impact strength, and (b) Fracture toughness of EP, EP/CB, EP/HB and EP/CC composites.	72
4.13	Hardness of EP, EP/CB, EP/HB and EP/CC composites.	74
4.14	SEM micrograph of (a) EP, (b) EP/CB, (c) EP/HB and (d) EP/CC composites at 9 wt. % filler loading.	76
4.15	Water absorption and Wettability results of (a) EP, (b) EP/CB, (c) EP/HB and (d) EP/CC composites.	79
4.16	(a) TG and (b) DTG of EP, EP/CB, EP/HB and EP/CC composites	81
4.17	(a) Storage modulus and (b) $\tan \delta$ of EP, EP/CB, EP/HB and EP/CC composites.	83
4.18	“ <i>In vitro</i> ” cytotoxicity of EP/CB and EP/HB composites	86
4.19	Microscopic images of viable cells for (a) EP/CB composite prepared at 100% leach concentrations, (b-e) EP/HB composite prepared at 100, 50, 25 and 12.5% leach concentrations.	88
5.1	Particle size distribution of cuttlebone derived (a) Calcium oxide, (b) Hydroxyapatite and (c) tricalcium phosphate particles	92
5.2	SEM micrograph of cuttlebone derived (a-c) Calcium oxide (CO), (d-f) Hydroxyapatite (HA) and (g-i) tricalcium phosphate (CP) particles.	93
5.3	TEM micrograph of cuttlebone derived (a-c) Hydroxyapatite (HA) (d-f) tricalcium phosphate (CP) particles.	94
5.4	TG of cuttlebone derived calcium oxide (CO), hydroxyapatite (HA)	96

	and tricalcium phosphate (CP) particles	
5.5	X-ray diffractograms of cuttlebone derived CO and JCPDS 01-1160 for CaO	98
5.6	X-ray diffractograms of cuttlebone derived HA and JCPDS 009-0432 for Hydroxyapatite.	99
5.7	X-ray diffractograms of tricalciumphosphate CP and JCPDS 009-0346 for tricalcium phosphate	100
5.8	FT-IR spectra of cuttlebone derived (a) CO, (b) HA and (c) CP particles	102
5.9	(a) Ultimate tensile strength, (b) Tensile modulus, (c) Elongation percentage at break and (d) Load Vs. displacement curve of EP, EP/CO, EP/HA and EP/CP composites.	104
5.10	(a) Flexural strength, (b) Flexural modulus and (c) Load Vs. displacement curve of EP, EP/CO, EP/HA and EP/CP composites.	108
5.11	(a) Compression strength, (b) Compression modulus and (c) Load Vs. displacement curve of EP, EP/CO, EP/HA and EP/CP composites	112
5.12	(a) Impact strength, and (b) Fracture toughness of EP, EP/CO, EP/HA and EP/CP composites	115
5.13	Hardness of EP, EP/CO, EP/HA and EP/CP composites	118
5.14	SEM micrograph of (a) EP, (b) EP/CO, (c) EP/HA and (d) EP/CP composites at 6 wt% filler loading	120
5.15	Water absorption and Wettability results of (a) EP, (b) EP/CO, (c) EP/HA and (d) EP/CP composites	123
5.16	(a) TG and (b) DTG of EP, EP/CO, EP/HA and EP/CP composites	125
5.17	(a) Storage modulus and (b) $\tan \delta$ of EP, EP/CO, EP/HA and EP/CP composites.	126
5.18	“ <i>In vitro</i> ” cytotoxicity of EP/HA and EP/CP composites.	130
5.19	Microscopic images of viable cells for (a-d) EP/HA composite prepared at 100% leach concentrations, (e-h) EP/CP composite	131

prepared at 100, 50, 25 and 12.5% leach concentrations.

6.1	(a) Ultimate tensile strength, (b) Tensile modulus and (c) Elongation percentage at break of EP, EP/CB, EP/HB, EP/HA and EP/CP composites.	137
6.2	(a) Flexural strength and (b) Flexural modulus of EP, EP/CB, EP/HB, EP/HA and EP/CP composites.	138
6.3	(a) Compression strength and (b) Compression modulus of EP, EP/CB, EP/HB, EP/HA and EP/CP composites.	139
6.4	(a) Impact strength, and (b) Fracture toughness of EP, EP/CB, EP/HB, EP/HA and EP/CP composites.	140
6.5	Shore D Hardness of EP, EP/CB, EP/HB, EP/HA and EP/CP composites.	142
6.6	SEM micrograph of (a) EP, (b) EP/CB, (c) EP/HB (d) EP/HA and (e) EP/CP composites.	142
6.7	Voids percentage of EP, EP/CB, EP/HB, EP/HA and EP/CP composites.	143
6.8	Water absorption percentage of EP, EP/CB, EP/HB, EP/HA and EP/CP composites.	144
6.9	Wettability results for EP, EP/CB, EP/HB, EP/HA and EP/CP composites.	144
6.10	(a) TG and (b) DTG of EP, EP/CB, EP/HB, EP/HA and EP/CP composites.	145
6.11	(a) Storage modulus and (b) $\tan \delta$ of EP, EP/CB, EP/HB, EP/HA and EP/CP composites.	146
6.12	“ <i>In vitro</i> ” cytotoxicity of EP/CB, EP/HB, EP/HA and EP/CP composites.	149
7.1	(a) Ultimate tensile strength, (b) Tensile modulus, (c) Elongation percentage at break and (d) Load Vs. displacement curve of EP/CF, EP/CF/CB, EP/CF/HB, EP/CF/HA and EP/CF/CP composites.	157

7.2	(a) Flexural strength, (b) Flexural modulus and (c) Load Vs. displacement curve of EP/CF, EP/CF/CB, EP/CF/HB, EP/CF/HA and EP/CF/CP composites.	160
7.3	(a) Impact strength, and (b) Fracture toughness of EP, EP/CF/CB, EP/CF/HB, EP/CF/HA and EP/CF/CP composites.	162
7.4	(a) Hardness and (b) Interlaminar shear strength of EP/CF, EP/CF/CB, EP/CF/HB, EP/CF/HA and EP/CF/CP composites.	165
7.5	SEM micrograph of (a) EP/CF, (b) EP/CF/CB, (c) EP/CF/HB composites (d) EP/CF/HA composites and (e) EP/CF/CP composites.	167
7.6	Water absorption percentage of EP/CF, EP/CF/CB, EP/CF/HB, EP/CF/HA and EP/CF/CP composites.	170
7.7	Wettability results of EP/CF, EP/CF/CB, EP/CF/HB, EP/CF/HA and EP/CF/CP composites.	171
7.8	(a) TG and (b) DTG curve of EP/CF, EP/CF/CB, EP/CF/HB, EP/CF/HA and EP/CF/CP composites.	172
7.9	(a) Storage modulus and (b) $\tan \delta$ of EP/CF, EP/CF/CB, EP/CF/HB, EP/CF/HA and EP/CF/CP composites.	174
7.10	“ <i>In vitro</i> ” cytotoxicity of EP/CF/CB, EP/CF/HB, EP/CF/HA and EP/CF/CP composites.	178
7.11	Microscopic images of viable cells for (a-d) EP/CF/CB composite prepared at 100, 50, 25 & 12.5% leach concentration, (e-h) EP/CF/HB composite prepared at 100, 50, 25 & 12.5% leach concentration, (i-l) EP/CF/HA composite prepared at 100, 50, 25 & 12.5% leach concentration and (m-p) EP/CF/CP composite prepared at 100, 50, 25 and 12.5% leach concentration.	180

LIST OF TABLES

Table No.	Captions	Page No.
2.1	Cuttlebone derived calcium phosphates	17
2.2	Mechanical properties of composite materials for biomedical applications.	29
4.1	Volume percentage of particles at different size range and mean particle size of cuttlebone and commercial CaCO ₃ particles	50
4.2	Density, surface area and pore volume of cuttlebone and commercial CaCO ₃ particles	52
4.3	Percentage composition of elements in cuttlebone particles found by EDX and ICP-OES analysis	52
4.4	XPS parameters for Ca, C, O and N core levels from raw cuttlebone and heat treated cuttlebone particles and its surface composition	58
4.5	Theoretical density, actual density and void percentage of EP, EP/CB, EP/HB and EP/CC composites	78
4.6	Thermal properties of EP, EP/CB, EP/HB and EP/CC composites	82
4.7	Storage modulus, gain in storage modulus and glass transition temperature of EP, EP/CB, EP/HB and EP/CC composites	84
4.8	Swelling ratio, crosslink density and molecular weight between crosslinks of EP, EP/CB, EP/HB and EP/CC composites	85
4.9	Hemolysis percentage of EP/CB and EP/HB composites	88
5.1	Volume percentage of particles at different size range and mean particle size of cuttlebone derived CO, HA and CP particles	92
5.2	Density, surface area and pore volume of cuttlebone derived CO, HA and CP particles	93
5.3	Ca/P molar ratio of cuttlebone derived HA and CP by EDX and ICP-OES analysis	95
5.4	FWHM, d-spacing and crystallite size of the cuttlebone derived CO,	101

	HA and CP particles	
5.5	Theoretical density, actual density and void percentage of EP/CO, EP/HA and EP/CP composites	121
5.6	Thermal properties of EP, EP/CO, EP/HA and EP/CP composites	125
5.7	Storage modulus, gain in storage modulus and glass transition temperature of EP, EP/CO, EP/HA and EP/CP composites	127
5.8	Swelling ratio, crosslink density and molecular weight between crosslinks of EP, EP/CO, EP/HA and EP/CP composites	128
5.9	Hemolysis percentage of EP/HA and EP/CP composites	132
6.1	Thermal properties of EP, EP/CB, EP/HB, EP/HA and EP/CP composites	146
6.2	Storage modulus, gain in storage modulus and glass transition temperature of EP, EP/CB, EP/HB, EP/HA and EP/CP composites	147
6.3	Swelling ratio, crosslink density and molecular weight between crosslinks of EP, EP/CB, EP/HB, EP/HA and EP/CP composites	147
6.4	Hemolysis percentage of EP/CB, EP/HB, EP/HA and EP/CP composites.	150
7.1	Theoretical density, actual density and void percentage of EP/CF, EP/CF/CB, EP/CF/HB, EP/CF/HA and EP/CF/CP composites.	168
7.2	Thermal properties of EP/CF, EP/CF/CB, EP/CF/HB, EP/CF/HA and EP/CF/CP composites.	173
7.3	Storage modulus, gain in storage modulus and glass transition temperature of EP, EP/CF/CB, EP/CF/HB and EP/CF/HA and EP/CF/CP composites	175
7.4	Swelling ratio, crosslink density and molecular weight between crosslinks EP, EP/CF/CB, EP/CF/HB and EP/CF/HA and EP/CF/CP composites	176
7.5	Hemolysis percentage of EP/CF/CB, EP/CF/HB, EP/CF/HA and EP/CF/CP composites.	181

NOMENCLATURE

3D	Three dimensional
1D	One dimensional
t_l	Crystalline size (nm)
K_{IC}	Critical stress intensity factor (MPa.m ^{1/2})
P	Peak load (N)
S	Span length (mm)
y	Geometrical correction factor
θ	Swelling coefficient
χ	Crosslink density (mol/cm ³)
M_c	Molecular weight between crosslinks (Kg/mol)
T_g	Glass transition temperature (°C)
E_t	Activation energy (KJ/mol)
T_{max}	Temperature at the maximum rate of degradation (°C)
A^*	Area ratio of the total TGA experiment curve
K^*	Area Coefficient
T_i	Initial Temperature (°C)
T_f	Final Temperature (°C)
α	Decomposition fraction
R	Gas constant (8.316 J/ mol.K)
S_1, S_2 and S_3	Area of the three regions from TGA curve (m ²)
V_r	Volume fraction of polymers (%)
d_r	Density of the dry polymer (g/cm ³)
V_o	Molar volume of the solvent (cm ³)
γ	Huggins polymer-solvent interaction
SR	Swelling ratio
W_1	Weight of the composite before swelling (g)
W_2	Weight of the composite after swelling (g)
WA	Water absorption (%)

W_I	Initial weight of sample before immersed in water (g)
W_F	Final weight of sample after immersed in water (g)
V_V	Volume fraction of voids (%)
ρ_{ca}	Actual density of composites (g/cm^3)
ρ_{ct}	Theoretical density of composites (g/cm^3)
ρ_p	Density of the particle (g/cm^3)
ρ_M	Density of the matrix (g/cm^3)
W_P	Weight fraction of the particle (%)
W_M	Weight fraction of the matrix (%)
H_b	Hemoglobin

ABBREVIATION

CB	Raw cuttlebone particles
HB	Heat treated cuttlebone particles
CC	Commercial Calcium carbonate
CO	Cuttlebone derived calcium oxide particles
HA	Cuttlebone derived hydroxyapatite particles
CP	Cuttlebone derived tricalciumphosphate particles
EP	Neat epoxy
EP/CB	Raw cuttlebone reinforced epoxy composites
EP/HB	Heat treated cuttlebone reinforced epoxy composites
EP/CC	Commercial CaCO ₃ reinforced epoxy composites
EP/CO	Cuttlebone derived calcium oxide reinforced epoxy composites
EP/HA	Cuttlebone derived hydroxyapatite reinforced epoxy composites
EP/CP	Cuttlebone derived tricalciumphosphate reinforced epoxy composites
EP/CF	Carbon fiber reinforced epoxy composites
EP/CF/CB	Raw cuttlebone/carbon fiber reinforced epoxy composites
EP/CF/HB	Heat treated cuttlebone/carbon fiber reinforced epoxy composites
EP/CF/HA	Cuttlebone derived hydroxyapatite/carbon fiber reinforced epoxy composites
EP/CF/CP	Cuttlebone derived tricalciumphosphate/carbon fiber reinforced epoxy composites
wt%	Weight percentage
Vol%	Volume percentage
XRD	X-ray diffractometer
FTIR	Fourier transform infra-red spectroscopy

CaCO ₃	Calcium carbonate
CaO	Calcium oxide
BOC	Bone marrow derived osteoblast cells
BMP	Bone morphogenic protein
Ca/P	Calcium/Phosphorous
B-CP	Beta tricalciumphosphate
GBR	Guided Bone Regeneration
PEEK	Polyether ether ketone
DGEBA	Diglycidyl Ether of Bisphenol-A epoxy resin
H ₃ PO ₄	Phosphoric acid
DMF	<i>N,N</i> -dimethyl formamide
DMA	Dimethylacetamide
THF	Tetrahydrofuran
SEM	Scanning electron microscope
EDX	Energy dispersive X-ray
HR TEM	High Resolution Transmission electron microscope
TGA	Thermo gravimetric analysis
DTA	Differential thermal analysis
DTG	Differential thermo gravimetric
XPS	X-ray photoelectron spectroscopy
ICP-OES	Inductively coupled plasma-optical emission spectrometer
FWHM	Full width half maximum
UTM	universal testing machine
ASTM	American society for testing methods
ILSS	Inter laminar Shear strength
DMA	Dynamic mechanical analysis
IPDT	Integral procedure decomposition temperature
FBS	Foetal bovine serum
ISO	International standard organization

JCPDS	Joint committee for powder diffraction standard
UTS	Ultimate tensile strength
EPB	Elongation percentage at break

CHAPTER 1

CHAPTER 1

INTRODUCTION

1.1 Background

The use of natural or synthetic materials to assist tissue healing and/or to correct abnormalities in the event of traumatic or pathologic damage to human organs has a long history. Applications of biomaterials dates back to several centuries into human civilization with the findings of artificial eyes, ears and teeth in Egyptian mummies (Williams and Cunningham, 1979), use of prostheses since 1500 B.C. in India, 300 B.C. in China, and in European civilizations (Benoist, 1978). Over time, with the advancements in material development and medical technologies, such biomaterials are widely used in the form of implants and medical devices to correct, replace and/or restore the functions of traumatized and/or defective organs. Based on the purpose, implants/devices have been classified into three types (Khan et al., 2014). They are a) orthopedic implants for structural and mechanical support (reconstructive joint replacement, spinal and trauma), b) cardiovascular implants for functional support (pacing devices, cardiac stents and structural cardiac implants) and c) other medical implants for localized drug delivery (drug implants, ophthalmic implants and gastroenterological implants). Biomaterials, mostly biocomposites are now commonly used in orthopedic patients for both external and internal fixations and examples include bone plates, screws, wires, intramedullary nails, rods, pins, etc. Composites are man-made materials that are normally produced by coupling together two or more constituents or phases, typically a weak and compliant matrix phase and a stiff and strong reinforcement phase. The function of matrix is to transmit externally applied load to reinforcement via interface through shear stress, thus preventing mechanical damage/material failure. Biocomposites are composite materials in which one or more of these phase(s) are derived from a biological origin. Matrices are either naturally derived (e.g. starch) or synthetic (e.g. epoxy, polyester resin, polyethylene, polyether ether ketone, etc.) materials while reinforcements may be either fillers (e.g. alumina, zirconia

and calcium phosphates, naturally derived sea corals, etc.) or fibers (e.g. carbon, kevlar and glass fibers, etc.).

For orthopedic application, materials like metals, ceramics and polymers has few disadvantage like stress shielding, poor tissue response and low mechanical stability. Due to these disadvantages, composite materials become more attractive because of tailor made material properties (Navarro et al. 2008). Especially in the last two decades, most of the composite materials developed for bone replacement and fixations are made by polymer as matrix phase and fillers or fiber as reinforcement phase. Based on the tissue response to these composites, they are categorized as bioinert, bioactive and biodegradable.

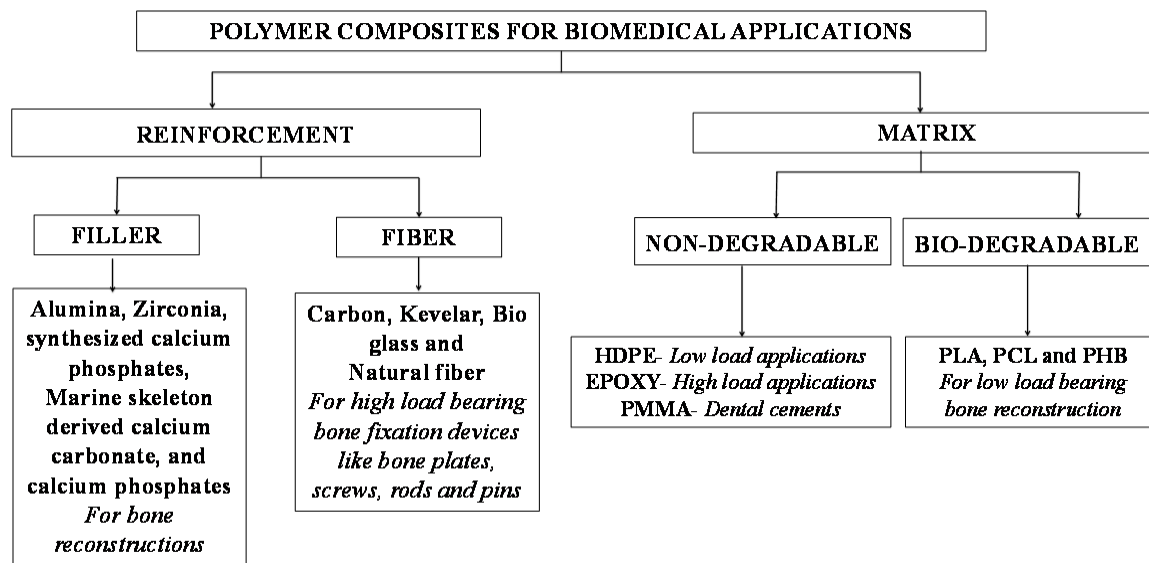


Figure 1.1 Classification of polymer composites for biomedical applications

Classification of polymer composites is based on the matrix and reinforcement phase (Figure 1.1). Based on the degradability of matrix phase, composites are classified as biodegradable and non-degradable. Polymers like polylactide, polyglycolide, poly-ε-caprolactone, and polyhydroxybutyrate are biodegradable and mainly used in bone graft applications. But these materials are not suitable for hard tissue implants because of low mechanical properties and long term durability. Epoxy, polyethylene, polypropylene, polymethylmetacrylate, polytetrafluoroethylene are non-degradable polymers. These polymers along with reinforcement are mainly used in hard tissue implant applications.

Based on the reinforcement material, composites are further classified as particle and fiber reinforced composites. High strength and stiffness fibers like carbon, kevlar and glass fibers are mostly reinforced in non-degradable polymers for hard tissue implants. Some of the examples are bone plates, screws, wires, intramedullary nails, rods and pins. Ceramic particles like alumina, zirconia and calcium phosphates are used as reinforcement for the improvement of mechanical properties in biodegradable polymer composites. Recently, marine corals are used in the development of composites (Ben-Nissan 2003). These materials offer the advantage of being used to derive biopolymers (e.g. polysaccharides, chitin, and chitosan), minerals (e.g. calcium carbonate) and ceramics (e.g. hydroxyapatite, calcium oxide and calcium phosphates) for composite applications either as a matrix or reinforcements for the improvement of mechanical strength and biocompatibility. Examples of some of the commonly used marine corals for composite development are crab shells, nacre, cuttlebone, glass sponge and cancer pagurus.

Several studies are currently focused on the development of biodegradable polymer composites for orthopedic applications. Although these materials fit well for the most low load bearing applications, non-degradable composites are still the choice of materials for high load bearing applications. Even for certain low load bearing applications (e.g. ear implants), non-degradable composite materials are essentially required to provide long term stability. However, there are many important issues that need to be addressed with respect to the mechanical and biological properties of non-degradable materials. Some of them are listed below:

1. In case of low load bearing applications (e.g. ear implants), fixation devices are desired to be not only non-degradable but bioactive. Hence, chemically synthesized hydroxyapatite reinforced non-degradable composites are used. In these composites, higher volume percentage (20 to 40 vol%) of fillers is used to improve the bioactivity. However, higher filler content leads to improper bonding between the matrix and reinforcement phase and reduce the long term mechanical stability.

2. For high load bearing applications (e.g. femur fractures, acetabular cups), metallic implants are still used. Due to the high stiffness property of metallic implants, fractured bone frequently encounters stress shielding.
3. Carbon fiber reinforced non degradable composites have been increasingly used to reduce the stress shielding due to metallic implants. However, both metallic implants and carbon fiber reinforced composites are biologically inert leading to poor adhesion with host tissues.

1.2 Hypothesis

To address the above mentioned issues, the present study is based on the following hypothesis:

1. Coral derived bio-fillers reinforced composites will improve the mechanical stability at lower filler percentage while retaining the bioactivity of non-degradable composites for low load bearing applications.
2. Coral derived bio-fillers/carbon fiber reinforced hybrid composites will improve the bioactivity of non-degradable materials (i.e. bioinert to bioactive), while retaining the required mechanical strength for high load bearing orthopedic applications.

1.3 Objectives of this research work

The objectives of the present research work are:

1. To prepare and characterize cuttlebone particles and heat treated cuttlebone particles derived from cuttlefish bone.
2. To develop and characterize the material properties of cuttlebone particle (cuttlebone and heat treated cuttlebone) reinforced epoxy composites.
3. To synthesize and characterize cuttlebone derived ceramic bio-fillers (calcium oxide, hydroxyapatite and tricalcium phosphate).
4. To develop and characterize the material properties of cuttlebone derived ceramics (calcium oxide, hydroxyapatite and tricalcium phosphate) reinforced epoxy composites.
5. To develop and characterize the material properties of cuttlebone derived bio-fillers/bio-ceramics and carbon fiber reinforced hybrid composites.

1.4 Thesis structure

On the basis of above findings, the dissertation is organized in eight chapters which are as follows.

- **Chapter 1** discusses about the introduction of biomaterials for implants, background of different existing materials for orthopedic applications, scope and objectives of the present research work.
- **Chapter 2** reviews the literatures related to marine CaCO_3 skeleton, utilization of commercial CaCO_3 , sea coral as reinforcement in polymer composites for various implants applications, conversion of sea corals into hydroxyapatite (HA) and tri-calcium phosphate (CP) with different techniques, utilization of converted HA, CP and its composites for various implants applications, bio-filler/fiber reinforced composites for load bearing application are described.
- **Chapter 3** presents the materials and methods for preparation of different cuttlebone derived bio-fillers (raw cuttlebone (CB), heat treated cuttlebone (HB), cuttlebone derived calcium oxide (CO), cuttlebone derived hydroxyapatite (HA) and cuttlebone derived calcium phosphate (CP)), processing of bio-fillers and bio-fillers/carbon fiber reinforced epoxy composites. Different testing procedures to evaluate the material properties like mechanical, thermal, physical and biocompatibility have also been presented.
- **Chapter 4** describes the characterization of cuttlebone derived bio-filler particles, CB, HB and commercial CaCO_3 (CC). Besides, different material properties (mechanical, physical, thermal, thermo-mechanical and biocompatibility) for the neat epoxy (EP), EP/CB, EP/HB and EP/CC composites are discussed.
- **Chapter 5** describes the characterization of cuttlebone derived ceramic bio-filler particles, CO, HA and CP. Different material properties (mechanical, physical, thermal, thermo-mechanical and biocompatibility) for EP, EP/CO, EP/HA and EP/CP composites are discussed.

- **Chapter 6** discusses the comparison of material properties like mechanical, physical, thermal, thermo-mechanical and biocompatibility for EP/CB, EP/HB, EP/CC, EP/CO, EP/HA and EP/CP composites.
- **Chapter 7** discusses the material properties like mechanical, physical, thermal, thermo-mechanical and biocompatibility for the cuttlebone derived bio-filler/carbon fiber reinforced hybrid epoxy composites (EP/CF/CB, EP/CF/HB, EP/CF/HA and EP/CF/CP).
- Finally, **Chapter 8** presents the summarized results and conclusions of present research work.
- A complete list of references and publications related to present research work is place at the end of the dissertation.

CHAPTER 2

CHAPTER 2

LITERATURE REVIEW

This chapter gives a survey of literature related to contemporary natural materials used for biomedical application, along with the discussion on the development of coral and fiber based polymer composites for implant applications.

2.1 History of non-degradable implants

Implants especially for high load bearing orthopedic applications like bone plate has been upgraded in three different time periods. During the initial periods (from 1940-1980) metallic implants were widely used for fracture fixation applications. These materials induced problems like stress shielding and encapsulation of implants by fibrous tissue during implant period. To overcome these issues, fiber reinforced polymer composites and stiffness graded metallic plates has been used during the period from 1980-2000. However these materials also come under the category of bio inert which does not have better interaction with host tissue (Navarro et al. 2008). These problems have been sorted out by making the implant material as bio active ones (2000 – at present). Synthetic bio-active ceramic filler coated metallic or polymer composites implants have been currently used for bone fixation applications.

Similarly, carbon-carbon prostheses have been widely used for long term low load bearing implants during the initial periods (until 1980). But these materials have disadvantages like release of carbon debris, cell detachment and lysis which lead to inflammation. Subsequently, Polyester and polytetrafluoroethylene has been used as alternate material for this application during the period of 1980-2000. Even though, these polymeric materials do not have enough biocompatible property. To overcome this issue, synthetic bioactive ceramic filler reinforced non degradable polymer composites has been used in the past 16 years (Navarro et al. 2008).

Incorporation of synthetic bioactive filler in polymer composites has comparable biocompatible properties than metallic implants in the aforementioned cases. Instead of

synthetic bio-active filler, addition of naturally derived bioactive fillers may give better biocompatibility along with improved mechanical properties. Developing a biomaterial with natural derived sources has become a research interest among the material scientists in the past 10 years. In this chapter detail literature survey for topics like different marine coral materials, marine coral derived ceramic materials, utilization of marine corals and marine coral derived ceramics as reinforcement in polymer and its fiber composites has been included.

2.2 Biological materials

In the present scenario, biological structures (marine skeletons) have inspired material scientists in the design of novel biomaterials. Due to its mechanical properties and hierarchical structure similar to human bone, biological materials can be used for various biomedical applications like bone grafts, cartilage replacements and nano sized biomimetic materials. Besides the structural and mechanical properties, exceptional biocompatible properties of these biological materials had distinct advantages over synthetic materials. Some of the examples for biological materials are a) arthropod exoskeleton (like crabs, lobsters and shrimps), b) antlers, c) tusks and teeth, d) Toucan and hornbill beak, e) sea urchin, f) sponge spicules, g) shells, h) corals and i) cuttlebone. These materials are mainly composed of minerals (various minerals with primary elements like Ca, Mg, Si, Fe, Mn, P, S and C) and organic components (proteins (like collagen, keratin and Elastin) and polysaccharides (like chitin and cellulose)). These components provide strength and ductility to the material which tends to withstand more energy before failure (Meyers et al. 2008).

2.2.1 Marine Calcium carbonate skeletons

Among the various biological materials available in nature, there are few marine skeletons which possess high content of calcium carbonate. The primary mineral phase (calcium carbonate) present in these marine skeletons are found to be either aragonite or calcite crystal structure. Similarly organic matters like protein and chitin are present as secondary phase. Besides this, element like strontium, magnesium and fluoride ions are

presents as traces. Examples for marine CaCO₃ skeleton are a) shells (Nacre, conch and giant clam), b) sea urchin, c) corals and d) cuttlebone. These marine CaCO₃ skeletons are found to have lamellar (shells) and interconnected porous structure (corals, cuttlebone and sea urchins with different pore size of 20-100 μm) with high compressive strength, biocompatibility, osteoconductivity and degradability at various rates depending on the skeleton porosity and the implant location (Chen et al. 2008). They have been successfully used for more than 10 years in orthopedic, trauma, craniofacial, dental, and neurosurgery (Ige et al. 2012). Moreover these marine CaCO₃ can be used along with polymeric material in the development of biocomposites for hard tissue fracture fixation applications.

2.2.1.1 Shells

Generally, shells provide protection to inner soft bodies of the animals by withstanding the external impact and compression loads. Combination of mineral and organic component phases presents in the shells, resulted in the development of intricate micro or macro structure with owing mechanical properties like toughness and strength (Meyers et al. 2008).

The microstructure of the conch, giant clam and nacre are found to be most organized, under organized and optimized hierarchically, respectively (Meyers et al. 2008). All the three materials exhibit greater compression strength during dynamic loading than quasi-static loading. Apart from that, hierarchically organized nacre has better compression strength than other two shell materials in both types of loading. Besides, conch shell has higher compressive strength than giant clam shell. In contrast, fracture strength of the conch shell is higher than nacre. Based on the analysis of these three shell materials, it can be concluded that properties of these materials are mainly dependent on its microstructure.

2.2.1.2 Sea urchins

Sea urchins are mainly composed of large single crystal magnesium rich calcium carbonate in calcite polymorph form. Sea urchins are smooth, continuous and have prominent internal structure (interconnected 3D porous structure) with pore size of 20-

50 μm (Tsafnat et al. 2012). Compared to monolithic CaCO_3 , sea urchins have been reported to be fairly flexible, possibly due to minimal amount of protein embedded with mineral phase (Zhang and Vecchio, 2013). This enhances the material properties like fracture resistance and elastic modulus and make Sea urchin as a potential biomaterial for biomedical applications.

2.2.1.3 Corals

Corals are marine invertebrate's derived from marine madreporic and have interconnected porous microstructure with the pore size greater than 100 μm . It's mainly composed of calcium carbonate mineral in aragonite or calcite polymorph form along with organic compounds. It has two major regions, hard outer layer and spongy inner core. The microstructure and pore size of the coral is very similar to human cancellous bone, which makes the material compatible to host tissue *in vivo*. Utilizing coral as bone graft material has been implemented by the researchers in the early of 1970's in animal and 1979 in humans. Later on, it was evaluated for various bone defects. Besides the use of coral for bone reconstruction, it can also be used as bone substitution. Even though coral has high degradability and less durability, it was modified as hydroxyapatite to improve the material properties so that it can be used for bone graft purposes (Zhang and Vecchio, 2013).

2.2.1.4 Cuttlebone

Cuttlebone (*Sepia officinalis*), a marine invertebrate endoskeleton comes under the class of cephalopods. These cephalopods have a wide range of bioactive substances with exceptional mechanical and physical properties. The unique multifunctional properties of cuttlebone like high flexural stiffness, high compressive strength and porosity are attributed to highly ordered and cross-linked chambered structure (Cadman et al. 2010). Understanding the structural and material properties of cuttlebone will lead to its better utilization in the development of novel composite materials.

Cuttlebone is structural rigid skeletal with two major portions called dorsal shield and lamellar matrix. Dorsal shield is thick and tough material which is used to protect the inner soft lamellar matrix. Furthermore, this dorsal shield is non-porous layer structure

with high amount (30-40 wt%) of organic matters. This organic matters lead to increase the toughness of dorsal shield by undergoing plastic deformation while loading. The lamellar matrix is in porous layered structured which is separated by numerous pillars. This lamellar matrix has mainly consists of calcium carbonate which is surrounded by minimal amount of organic matters on their surface (Birchall and Thomas 1983). Furthermore same researchers examined the mechanical strength of lamellar matrix by applying the load perpendicular to lamella plane. They found that crushing and bending strength of the lamella matrix was 1.1MPa and 1.8MPa, respectively. Besides, Denton and Gilpin-brown 1961 identified lamella matrix of the cuttlebone is in individual chamber format and act as a rigid buoyancy tank which helps the fish to float in certain level. Florek et al. 2009 examined and identified that cuttlebone consists of different elements like sodium, potassium, bromine, magnesium and strontium in traces form. Cusack and chung 2014 identified through electron backscatter diffraction that dorsal shield of cuttlebone is composed of aragonite needles which stacked one on each other. The properties and composition of cuttlebone has right potential to the development of biocomposites for implants applications.

2.2.1.5 Marine Calcium carbonate biomaterial for biomedical applications

Pai et al. 2011 developed aragonite based carbonate material which mimics the nacre material properties and structure at nano scale level. Furthermore they suggested this material to use as filler in composites for excellent bioactivity. Similarly, Ajikumar et al. 2005 developed a nano sized CaCO_3 thin film over a functionalized demineralized eggshell membrane for tissue engineering applications. Oteyakä et al. 2013 identified that fish heads of the species *Argyrosomus regius* had the composition of CaCO_3 in aragonite and calcite form and they suggested this material for bone graft application after hydroxyapatite transformation. Figueiredo et al. 2010 investigated the physical-chemical characteristic of Caroline CaCO_3 and they concluded that “*in vivo*” behaviors of these coral were mainly influenced by their morphological characteristics. Kato 2008 developed a nacre mimicked biomaterial using CaCO_3 and biomolecules derived organic polymer with improved material properties. Development of CaCO_3 nano crystals with

uniform rod shape from cockle shell powder using high pressure homogenizer via a micro emulsion system was achieved by Kamba et al. 2013. Corals along with bone marrow derived osteoblast cells (BOC) and bone morphogenic protein (BMP) have been used for the reconstruction of large bone defects by improving the stability, longevity and the biodegradation properties (Roux et al. 1988). Arnaud et al. 1994 and Yukna 1994 clinical examined the coral for spinal fusion and filler for periodontal defects. Petite et al. 2000 evaluated the coral implants for trans-cortical bony defects. Vacanti et al. 2001 prepared the coral scaffolds and examined in clinical settings for osseous regeneration of the distal phalanx of a thumb in an avulsion injury. Chen et al. 2002 examined coral with BOC for the restoration of human mandibular condyle. Demer's et al. 2002 evaluated the coral powders as a delivery system for cell growth by modifying the absorption condition and particle size.

2.3 Calcium phosphates

Calcium phosphate is classified under the category of ceramic material with chemical composition similar to that of biologically calcified tissues (human bone) and possessing good biocompatibility, bioresorbability and bioactivity properties. Therefore it has been used as an alternate biomaterial for bone reconstruction in maxillofacial, dental and orthopedic applications (Ignjatović and Uskoković 2008). Calcium phosphate can also be classified into 13 different types based on the molar ratio, stability and solubility parameters (Barinov 2010). Among the different calcium phosphates, hydroxyapatite and tricalcium phosphate are widely used in biomedical applications. In this literature review, synthesized and naturally derived calcium phosphates [hydroxyapatite (HA) and tricalcium phosphate (CP)] related to the research objective are discussed in detail as follows.

2.3.1 Chemically synthesized calcium phosphates through different methods

Synthetic hydroxyapatite and tricalcium phosphate provide high interfacial strength when used in bone implants and possess a stoichiometric Ca/P molar ratio of 1.67 and 1.5 respectively. Generally hydroxyapatite has low degradability, high strength

and more stability under physiological conditions. On the contrary, tricalcium phosphate has high degradability, low strength and less stability compared to hydroxyapatite (Dorozhkin 2012). Both the calcium phosphates have the potential to be used in various applications like bone grafts, coatings on metallic plates and fillers in polymer composites. They are normally synthesized either in dense or porous forms and the former possess better mechanical strength that are suitable for moderate load bearing scaffolds applications. Hydroxyapatite and tricalcium phosphate can be synthesized following different procedures and some of the most commonly applied methods are:

- Solvent casting method
- Freeze-drying method
- Wet chemical precipitation method
- Mechano-chemical method
- Hydrothermal method
- Electro deposition method

Numerous researchers have synthesized and developed calcium phosphates scaffolds in dense or porous structure with chemically synthesized different methods. Besides, few researchers developed composite scaffold using synthetic calcium phosphate and different bio active particles.

2.3.2 Calcium phosphates derived from natural sources

Generally, micro porous structure of marine skeleton withstands the mechanical load when used in implant materials. Marine skeleton converted calcium phosphates also have better biocompatibility and osteoconductivity than chemically synthesized calcium phosphates. These advantageous properties led researchers to turn their interest in the past two decades towards developing marine skeleton derived calcium phosphates. Numerous researchers investigated and developed naturally derived calcium phosphates with different morphology, crystalline size, improved degree of crystallinity and biocompatibility properties following various process methodologies and parameters. Some of the examples for natural sources of calcium phosphates are corals, bovine bone, fishbone, sea shells and cuttlebone.

2.3.2.1 Corals

During 1970's, researchers successfully developed calcium phosphates derived from different coral sources using various techniques. Sivakumar et al. 1996 and Hu et al. 2001 were able to convert *Goniopora* coral into HA following hydrothermal method. They obtained pure HA phase with retention of porous and inter connective structures after hydrothermal conversion. Zhaolin et al. 2009 examined the effect of strontium substitution during the conversion of *Goniopora* coral into HA. They found significant improvement in osteo conductive property with strontium substitution. Likewise Mehta et al. 2014 succeeded in converting *Goniopora* coral into calcium phosphate through wet chemical precipitation method. They obtained biphasic calcium phosphate (HA and β -CP) along with traces of calcium oxide and calcium carbonate.

Similarly, Jinawath et al. 2002 and Zhaolin et al. 2009 converted porites coral into HA. They identified converted coralline HA having nano rod shapes with rod length less than 5 μ m. Chou et al. 2007 developed sand coral derived calcium phosphates following hydrothermal method. They confirmed the conversion of sand coral into β -CP with preserved inter connective and porous structures. However, they observed the presence of calcium carbonate traces in the converted samples.

2.3.2.2 Cattlebone

Few researchers successfully derived calcium phosphates from cattlebone through the process of calcination (Thermal method). Ooi et al. 2007 studied the effect of calcination temperature on cattle bone and identified the formation of pure HA at 1000°C while biphasic calcium phosphate (HA and β -CP) was formed at 1200°C. Similarly, magnesium and sodium traces were observed along with HA when cattle bone was converted to calcium phosphate at 850°C (Younesi et al. 2011). Pramanik et al. 2013 prepared pure HA from bovine bone after calcination at 900 °C. Effects of three different methods of conversion of bovine bone into HA were evaluated by Barakat et al. 2008. They found that subcritical water and alkaline hydrolysis methods produced nano rod shaped carbonated HA. They also identified that pure HA in nano flake form was achieved following thermal method (Barakat et al. 2009). Figueiredo et al. 2010

examined the effects of calcination temperature on conversion of three different bones (human, bovine and porcine) into HA. They concluded that crystalline size and degree of crystallinity were higher in human bone than porcine and bovine bone. Moreover in all the three bones, degree of crystallinity, crystalline size and purity of HA phase increased with increasing calcination temperature. In contrast, porosity of the three bones decreased with increasing calcination temperature. Similarly, Mondal et al. 2012 compared HA derived from bovine and fish scale and reported sub microns size HA from both sources and absence of toxic effect under *in vitro* conditions.

2.3.2.3 Fish bones

In the recent years, researchers derived calcium phosphates from different fish bones. Rodríguez-Lugo et al. 2005 developed hydrothermal converted HA fibers from starfish bones. They identified that fiber diameter and length were decreased by increasing the reaction time. Prabakaran and Rajeswari 2006 prepared pure HA by calcined the Sier fish bone at 950°C. Coelho et al. 2006 derived HA from three different bones (Pintado, jaú and cachara fish bone) through mechano-chemical method. They confirmed that converted nano HA powders were in spherical form. Similarly in another research work (Coelho et al. 2007), they studied the effect of milling time in the material properties of converted HA. They found that thermal conductivity was increased and crystalline size was decreased by increasing the milling time. Pallela et al. 2011 obtained high purity HA from *Thunnus obesus* bone through polymer assisted thermal method. Similarly, Venkatesan et al. 2011 developed HA from *Thunnus obesus* bone through two different method. They identified that particle size and degree of crystallinity of the prepared HA was higher in thermal method than alkaline hydrolysis method. Bi phasic calcium phosphate was derived from Sword and tuna fish bones through thermal method (Boutinguiza et al. 2012). They concluded that pure HA phase was achieved while calcined at 650°C. But bi phasic calcium phosphate (HA and β -CP) was attained while calcined at 950 °C.

2.3.2.4 Sea shells

Extensive research work was carried out to derive calcium phosphates from different sea shells. Vecchio et al. 2007 prepared magnesium substituted HA from sea urchins shell through hydrothermal method. Also they found that 3D-porous structure was maintained after conversion taken place. Few researchers utilized recycled eggshell to derive calcium phosphate through different methods. Lee et al. 2003 attained HA and β -CP particles from recycled eggshell through mechano-chemical method by varying the stoichiometric ratio. Gergely et al. 2010 studied the effect of two different milling processes in deriving HA from Eggshell. They found that attrition milling process derived nano size homogenous particles than ball milling process. Bi phasic calcium phosphate (HA and β -CP) was derived from eggshell through thermal method while calcined at 950°C (Hui et al. 2010). Jones et al. 2011 utilized waste mussel shell for deriving HA through hydrothermal followed by thermal method. They found that degree of crystallinity was increased by increasing the calcination temperature. Oyster shell derived bi phasic calcium phosphate through mechano-chemical method was achieved by Wu et al. 2011. Similarly, Macha et al. 2015 derived whitlockite from ostrich shell through mechano chemical method. Few researchers converted Sea snail shells in to HA and β -CP through mechano-chemical method by varying the stoichiometric molar ratio (Ozyegin et al. 2012, Oktar et al. 2013 and Gunduz et al. 2014). They identified that converted powders were in brick like structure. Moreover this method is simple and economic than hydrothermal method. Similarly, Singh 2012 derived HA from sea snail shells. They concluded that chemical precipitation followed thermal method produced HA particles in high purity form and high surface area in the range of 15m²/g.

2.3.2.5 Cuttlebone derived calcium phosphates.

To best of our knowledge, first cuttlebone converted calcium phosphate scaffolds was prepared in the year 2005. In the past 12 years, few researchers prepared cuttlebone derived calcium phosphates through different methods and examined the prepared scaffolds for bone restoration applications. The detailed studies of cuttlebone derived

calcium phosphates by various researchers were given in table 2.3 according to chronological order.

Table 2.1: Cuttlebone derived calcium phosphate

Origin Material	Method	Material developed	Results	Authors and year
Cuttlebone	Hydrothermal method	Scaffolds HA	Pure HA was obtained at 200°C. Interconnected porous structure was retained after conversion.	Rocha et al. 2005
Cuttlebone	Hydrothermal method	Scaffolds (HA and β -CP)	Pure HA was obtained at 200°C. HA was stable upto 1350 °C during sintering. At 1400°C biphasic (HA+ β -CP) was formed	Rocha et al. 2005
Cuttlebone	Hydrothermal method	Powder (HA and β -CP)	HA nano rod was obtained at 140°C. Small amount of β -CP was evidenced on rod surface.	Zhang and Vecchino 2007
Fluorine substituted Cuttlebone	Hydrothermal method	Powder HA	Nano-sized crystallites were obtained. Carbonated apatite was formed	Kannan et al. 2007
Cuttlebone	Wet ball mill method	Powder (HA and β -CP)	HA and β -CP formed at cuttlebone and phosphoric acid powder ratio 1:1.2 and 1:1.4, respectively. Followed by calcined at 900 °C for 1h.	Lee et al. 2007
Cuttlebone	Hydrothermal method	Scaffolds HA rod	Porous HA was obtained at 200°C. During “ <i>in vivo</i> ” bone density increases around the HA rod implant area.	Kim et al. 2008
Cuttlebone	Hydrothermal method	Scaffolds HA	Specific surface area & total pore volume increased after conversion.	Ivankovic et al. 2009
Cuttlebone	Hydrothermal method	Scaffolds HA	Dandelion like HA spheres were formed. Interconnected porous structure was retained after conversion.	Ivankovic et al. 2010
Cuttlebone	Hydrothermal method	Scaffolds HA	Diffusion controlled 1D growth of HA was observed. Mean pore volume decreased after conversion.	Ivankovic et al. 2010

Cuttlebone	Vacuum assisted infiltration and calcination method	Scaffolds β -CP	Porous structure was retained after calcination. Scaffolds had compressive strength of 2.38MPa	Sarin et al. 2011
Cuttlebone	Hydrothermal method	Scaffolds HA	“ <i>In vitro</i> ” showed good biocompatibility and proliferation of human marrow mesenchymal stem cells. “ <i>In vivo</i> ” showed good bioresorption, degradation and biological active.	Li et al. 2013
Cuttlebone	Hydrothermal method	Scaffolds HA	Increase in crystalline size, degree of crystallinity and compressive strength after sintered at 900 °C	Aminatun et al. 2013
Fluorine substituted Cuttlebone	Hydrothermal method	Scaffolds HA	Carbonated-flour HA scaffolds was obtained and stabled upto 1300 °C	Tkalčec et al. 2014
Cuttlebone	Hydrothermal method	Scaffolds HA	“ <i>In vitro</i> ” showed enhanced of alkaline phosphate activity and osteocalcin level. “ <i>In vivo</i> ” showed bone formation near implant location.	Hongmin et al. 2014

2.4 Calcium carbonate as reinforcement in polymer composites

Amongst the various mineral fillers, calcium carbonate (CaCO_3) is one of the abundant bio minerals and extensively used fillers in polymer composites. Generally, it is used in polymer composites for rheology control, dimensional stability, sustainable improvement in mechanical strength and cost effectiveness. It is familiar that CaCO_3 has encountered three polymorphic forms in nature, i.e., calcite, aragonite and vaterite. Among these, rhombohedral calcite form is the most stable one thermo dynamically/thermo kinetically followed by orthorhombic aragonite and hexagonal vaterite forms.

2.4.1 Synthetic calcium carbonate as reinforcement in thermoset polymer composites

As like thermoplastic composites, thermoset composite materials were developed by reinforcing CaCO_3 filler. Nano CaCO_3 reinforced triglycidyl paraaminophenol epoxy resin composites showed good improvement in fracture toughness, impact and flexural strength with increasing filler content (Jin and Park 2008). Further, addition of nano CaCO_3 fillers also improved cross link density and thermal stability of the composites (Jin and Park 2009). Klu et al. 2012 examined CaCO_3 /vinyl ester composites that were post cured at two different temperatures, ambient and 60°C . They found that storage modulus, glass transition temperature and crosslink density was higher in composites post cured at 60°C than those post cured at ambient temperature. Verma et al. 2014 investigated the material properties of CaCO_3 / bagasse fiber/epoxy composites and reported improvement in flexural and compression strength with the addition of fillers. Mishra et al. 2005 studied the influence of nano CaCO_3 as reinforcement in epoxy composites and observed significant improvement in mechanical and flame retarding properties. Similarly, Shimpi and Mishra 2012 showed improvement in thermal and mechanical properties of nano CaCO_3 reinforced epoxy composites under ultrasonic cavitation technique.

2.4.2 Modified calcium carbonate as reinforcement in thermoset polymer composites

Li et al. 2005 treated nano CaCO_3 with silane coupling agent and observed significant improvement in flexural modulus and impact strength when used as reinforcement in epoxy composites. Similarly, He et al. 2011 reported improvement of thermal stability and mechanical properties like compression, flexural and impact strength when silane treated CaCO_3 was used as fillers in epoxy composites. He and Gao 2015 studied the material properties of CaCO_3 reinforced epoxy composites and observed improvement of compression strength and compression modulus after modification of filler with silane coupling agent. Cure behavior, adhesion and hardness of

polyester/epoxy blended composites were increased by the infusion of stearic acid coated nano CaCO_3 (Kalee et al. 2011).

2.4.3 Calcium carbonate reinforced polymer composites for biomedical applications

Jamali et al. 2002 prepared biomaterial by combining CaCO_3 and hydroxyapatite. The *in vivo* study of the prepared biomaterial in the rabbit model for bone regeneration applications revealed that it has slower resorption rate than plaster of paris. Lucas-girot et al. 2002 developed non-sintered porous biomaterial from synthetic aragonite CaCO_3 by compaction method. Besides, they optimized the porosity of material for bone regeneration application by varying the pore former concentration and different methods of pressure application. Oudadesse et al. 2004 fabricated synthetic aragonite CaCO_3 biomaterial with porosity. They evaluated mineral composition *in vivo* and found sustained absorption of CaCO_3 by bony matrix. Fujihara et al. 2005 fabricated guided bone regeneration (GBR) membrane using polycaprolactone/ CaCO_3 nano fiber composites and observed an increase in absorbance intensity. Olah et al. 2006 fabricated CaCO_3 /poly ϵ - caprolactone composites for bone tissue engineering with two different polymorphic forms of filler, aragonite and calcite. They concluded that composites prepared with aragonite fillers had higher compression strength than those using calcite fillers. Wang et al. 2006 developed polyelectrolyte multilayer film with porous CaCO_3 micro particles for sustained and controlled drug delivery. Medeiros 2007 investigated the addition of CaCO_3 in poly lactide carbonate composites and reported improvement in failure strength of implant material and the strength at bone-tendon interface. Lee et al. 2007 observed improvement in stability and malleability of the amorphous CaCO_3 /polyethylenimine composites and reported their potential for fabrication in various shapes required for different clinical applications. Jayasuriya and Bhat 2010 fabricated novel hybrid chitosan/ CaCO_3 micro particles for bone regeneration application. They observed osteoconductivity and structural integrity of the micro particles may be used as voids filler in orthopaedic and craniofacial applications. Bai et al. 2009 developed inorganic fillers (CaCO_3 , β -tricalcium phosphate and calcium sulphate

dihydrate) reinforced poly para-dioxanone composites. They found that improved thermal and mechanical properties and crystalline structure of composites had potential applications like bone fixation and tissue engineering. Olàh and Tuba 2010 investigated the effects of aragonite and calcite CaCO_3 as reinforcement in poly ϵ -caprolactone composite scaffolds. They found that calcite filled composites were stiffer and stronger than aragonite filled composites with comparable biocompatibility. Composites prepared from polyvinyl acetate/coralline calcium carbonate and calcium hydroxyapatite had compression strength similar to human trabecular bone and porosity was increased while in contact with simulated body fluid (Aragón et al. 2011). Aragón et al. 2012 reported potential usage of these composites as bone substitutes for cancellous bones.

2.4.4 Marine calcium carbonate as reinforcement in polymer composites

Few researchers have examined the effect of adding marine skeletons as reinforcement in polymer composites. Improvement in thermal stability of epoxy composites with conch shell CaCO_3 as reinforcing fillers has been reported by Mustata et al. 2012. Utilization of waste shellfish shell as reinforcing filler in polypropylene composites resulted in significant improvement of the mechanical properties of the composites (Li et al. 2012). Hamester et al. 2012 successfully enhanced the tensile and impact strength of polypropylene composite by using oyster mussel shell as reinforcing fillers. Similarly, addition of scallop shell as reinforcing filler resulted in improvement of impact strength and the degree of crystallization (Lin et al. 2013) of polypropylene composites. Modified clam shell reinforced polypropylene composites were found to possess improved thermal properties, but without compromising the balance of fracture toughness and stiffness (Yao et al. 2014). Improvement in thermo mechanical and thermal properties like storage modulus, glass transition temperature and thermal stability was achieved by reinforcing crab shell particles in polybenzoxazine composites (Ramdani et al. 2014).

Kauly et al. 2008 investigated the effects of surfactant treated (fatty acids like stearic, palmitic, lauric and valeric acid) natural CaCO_3 fillers as reinforcements in poly di methyl siloxane composites. They observed better mechanical and thermo mechanical

properties of untreated CaCO_3 filled composites, while fatty acid treated fillers degraded the material properties of the composites. Intharapat et al. 2013 utilized heat-treated and untreated eggshell as fillers in epoxidized natural rubber and observed that untreated eggshell filled rubber had better cure rate index, scorch time, tensile strength, storage modulus and glass transition temperature as compared to treated eggshell filled rubber.

2.4.5 Cuttlebone as reinforcement in polymer composites

The first report on application of cuttlebone as naturally derived CaCO_3 fillers in polymer composites published in 2008. Poompradub et al. 2008, reported significant improvement in the mechanical properties of natural rubber reinforced with cuttlebone particles. In 2009, Jasso-Gastinel et al. 2009 observed the tendency of poly (methyl methacrylate-co-styrene) bone cements reinforced with cuttlebone particles to reduce the peak temperature and maintain the mechanical properties suggesting the potential of these materials for cement arthroplasty applications. They also examined the response of bone cements as *in vivo* implants and reported better interaction of material with host tissue (García-Enriquez et al. 2010). Improvement in tensile properties and lower biodegradation rate was achieved by reinforcing cuttlebone bio-filler in thermoplastic starch composites (Bootklad and Kaewtatip 2014). Similarly, Klungsuwan and Poompradub 2011 extracted organic compounds from cuttlebone particles and studied the thermal stability of natural rubber reinforced with cuttlebone particles. Shang et al. 2014 developed cuttlebone/waterborne polyurethane composites with significant improvement in properties such as strength, stiffness and thermal stability.

2.5 Calcium phosphates as reinforcement in polymer composites

Utilization of calcium phosphates for various biomedical applications started in the early 1920's. Amongst the different types of calcium phosphates, hydroxyapatite (HA), tricalcium phosphates (CP) and biphasic calcium phosphates (HA+CP) are widely used in bone regeneration and implant applications. These calcium phosphates are mainly used in the form of dense and porous structured scaffolds (sintered ceramic biomaterial), as well as a reinforcing phase in polymer composites (biocomposites scaffolds) and

coatings in metallic bone plates. Presently, biocomposites are majorly used as scaffolds rather than sintered ceramic scaffolds. The main reason is the addition of calcium phosphate as reinforcement in polymer matrix enhances the mechanical properties (especially compressive strength) along with the osteoconductive properties of the prepared composite material. Furthermore, the structure and properties of these composites are similar to the natural bone tissues.

2.5.1 Synthetic calcium phosphates/ thermoset polymer composites

Few researchers developed thermoset based polymer composites with synthetic calcium phosphate as reinforcement for tissue engineering applications. Peter et al. 1997 investigated that composites made with β -CP/Poly (Propylene Fumarate) had adequate mechanical properties even after undergone three month of degradation. Epoxy/ sodium bio-glass ceramic composites exhibited better modulus of rupture and bioactivity during simulated body fluid degradation study (Pattanayak and Srivastava 2005). Roesse and Amico 2009 fabricated HA reinforced epoxy composites and they found that composite strength was increasing by increasing the filler content. Jayabalan et al. 2010 identified that addition of HA in poly (propylene fumarate) increased the composite strength, interfacial bonding and crosslink density. Moreover, through “*in vivo*” animal study they found that prepared composites were biocompatible and osteo compatible. Similarly, Murali et al. 2013 identified that HA/ poly (propylene fumarate) composites were non hemolytic, non-cytotoxic, blood biocompatible along with higher mechanical properties and it has the potential for bone plate application.

2.5.2 Natural derived calcium phosphates and its composites for biomedical applications

In the past two decades, various researchers developed novel biocomposites material by utilizing natural derived calcium phosphates. Cho et al. 1998 examined a material prepared with coral derived hydroxyapatite/avitene/autologous blood and they found it has potential for bone substitution applications. Similarly, Suter et al. 2002 identified through long term clinical study that cattle bone derived HA implants has low rate of long term complications. Composites prepared using zirconia and Indian coral

derived HA was in biphasic form (HA and β -CP) (Sivakumar and Manjubala 2000). In the another research work, Sivakumar and Rao 2002 developed coral derived HA/gelatin/gentamicin composites and found it was suitable for controlled drug delivery applications. Ben-Nissan et al. 2004 converted Australian coral into pure HA scaffolds. Later on they coated the scaffolds with sol-gel derived HA to enhance the biaxial strength, durability and longevity. Crab shell derived HA/chitosan composites through biomorphic mineralization synthesis have high tensile modulus and it was pertinent for bone tissue engineering applications (Ge et al. 2010). Likewise, Pramanik et al. 2014 identified that different portion of cattle bone derived hydroxyapatite through sintering has the potential for soft and hard tissue engineering applications. Silver loader coralline HA scaffolds shown better cytotoxicity and antibacterial properties (Zhang et al. 2010). Nandi et al. 2015 investigated coralline converted HA/insulin material through animal study and concluded that scaffolds increases the rate of new bone regeneration.

2.5.3 Cuttlebone derived calcium phosphates/ polymer composites

To the best of our knowledge, so far two research group developed cuttlebone derived hydroxyapatite scaffold coated with polymer material. Kim et al. 2013 developed cuttlebone derived HA through hydrothermal method by maintained the microstructure as well. Besides they examined the effects of poly caprolactone coating on cuttlebone derived HA composite scaffold and found the improvement in compression strength and bioactivity. In another research work (Kim et al. 2014), they fabricated porous poly caprolactone scaffold infiltrated by cuttlebone derived HA. They observed that prepared composite scaffold has higher bone formation during rabbit animal study. Another research group (Milovac et al. 2014a) developed cuttlebone derived HA coated with poly caprolactone through vacuum impregnation technique. They identified the improvement in mechanical properties together with apatite formation during “*in vitro*” degradation study. In another study (Milovac et al. 2014b) they found that prepared composites have better cell proliferation, cell attachment and DNA content than neat poly caprolactone scaffold.

2.6 Fiber reinforced polymer composites

During 1950-1980's, metallic materials like stainless steel, chromium-cobalt, and titanium based alloys were used as internal fixations for bone fractures. It provides mechanical supports while bone healing in the form of plates, screws, rods, pins and wires. To overcome the limitations of metallic fixations like high modulus of elasticity and low fatigue life, carbon fiber reinforced polymer composites has gained the attention in the period of 1980-2000. These fiber reinforced polymer composites has less stiffness compared to metallic implants and its strength and stiffness were stable during “*in vivo*” conditions because of its non-resorbable property. However, both metallic and fiber reinforced polymer composites has disadvantages of bio inert property which induces the formation of fibrous tissue around the implants. For these cases, polymer composites with integrated bio-active surfaces need to be developed. To achieve this property, bio-active ceramic filler was added with polymer matrix and a hybrid fiber reinforced polymer composites were developed in the last decade. The detail literature of carbon fiber reinforced polymer composites and hybrid fiber reinforced composites for orthopedic application are discussed below.

2.6.1 Fiber reinforced polymer composites for biomedical applications

Bidirectional carbon fiber/epoxy composite bone plate was fabricated by Bradley et al. 1980. They found these plates has better flexural and fatigue strength than metallic implants. Tayton et al. 1982 examined through animal study for the period of 17 months that carbon fiber did not induced any malignant change near the implant location. Howard et al. 1985 investigated through clinical study and concluded that carbon fiber/epoxy composites did not shown any significant histological difference with stainless steel plates. Ali et al. 1990 examined through “*in vitro*” and “*in vivo*” animal study and identified that carbon fiber reinforced epoxy bone plates has better biocompatibility than steel and titanium implants. Bader et al. 2003 reviewed and identified that carbon fiber reinforced polymer composites have been used in the different implants application like joint replacement, tumor surgery and spinal operations. Carbon fiber reinforced polyetheretherketone composites were developed by Scotchford et al.

2003. They found that osteoblast attachment and cell proliferation results conducted through “*in vitro*” has not been significantly different than titanium alloy. Similarly, Fujihara et al. 2004 developed knitted carbon fabric reinforced polyetheretherketone composites. They identified these composites has good bending stiffness and found suitable for forearm implants, where higher deformation required. Peterson 2011 fabricated carbon fiber/ epoxy composites and found that these composite shown comparable osteoconductivity during animal study along with the improvement in bone percentage near the midtibial area. Later on in 2014, he (Peterson 2014) reviewed and suggested that improvement in osteoconductive properties of fiber reinforced polymer composites will be achieved by the addition of bio-active fillers in matrix material or by coating on implant surfaces. Similarly, Hak et al. 2014 reviewed and concluded that carbon fiber/PEEK composites has higher fatigue strength than metal implants, comparable elastic modulus of human bone and good radiolucent property.

Few researchers examined the carbon fiber reinforced polymer composites for other bio implants applications. Fredriksson et al. 1998 identified through clinical examination of 236 patients over a period of 2 to 3 years, that carbon fiber/epoxy post for teeth restoration application was superior to conventional cast post and cores. Similar kind of observation was conducted by Ferrari et al. 2000 for 200 patients over a period of 4 years. They also suggested that carbon fiber/epoxy post system has better success rate than conventional cast post and cores system. Saringer et al. 2002 prepared carbon fiber/epoxy composite for cranioplasty implants application. They found through clinical study that these material shown better performance in complicated cranial defects. Kotela et al. 2009 fabricated carbon fiber/Epoxy composite clamps and found it has similar mechanical strength, stability and less stiffness than metallic clamps.

2.6.2 Fiber/Filler reinforced hybrid polymer composites

Few researchers examined the interaction between carbon fiber, bio-active ceramic fillers and polymer matrix. Ha et al. 1997 identified that vacuum plasma spray method was the suitable one for HA coating on carbon fiber/PEEK implant material. Park and Vasilos 1997 examined and identified that carbon fiber/calcium phosphate

composites has significant improvement in ductility and slight degrade in flexural strength. Ślósarczyk et al. 2000 developed calcium phosphate coated carbon fiber/HA composites and found the improvement in flexural strength and modulus due to the better adhesion between coated fiber and HA matrix material. Carbon fiber surface coated with β -tricalcium phosphate/hydroxyapatite composites has better mechanical properties than uncoated ones (Su-ping et al. 2008). Addition of carbon nano fiber as reinforcement in HA composites shown improvement in fracture toughness and bone like apatite formation after simulated body fluid immersion study (Kobayashi and Kawai 2007). While coating of HA on carbon fibers through bio mineralization techniques, Para amino benzoic acid treated carbon fiber had better homogeneous coating than nitric acid treated carbon fibers (Su-ping et al. 2004). Cieřlik et al. 2009 developed poly lactide-glycolide co-polymer with reinforcement phase of carbon fiber or HA. They identified through “*in vivo*” study that both composite were biocompatible and induced the new bone formation. Similarly, Poly (propylene fumarate-co-caprolactone diol) reinforced with HA or Kevlar fiber composites were developed by jayabalan 2009. He identified that HA reinforced composites had better compression properties than fiber reinforced composites. Canal and Ginebra 2011 has reviewed and concluded that mechanical properties of calcium phosphate cements was improved by the addition of various polymer and ceramic fibers like polyamide, aramid, carbon and glass.

Some researchers investigated the improvement on bioactivity of prepared polymer composites either by the addition of bioactive filler with matrix or coating on prepared composites. Carbon fiber/surface modified HA/ epoxy composites were fabricated by Zhao et al. 2004 and they found the improvement in impact toughness and flexural properties of the composites. Similarly, prepared carbon fiber/HA/ epoxy composites were prepared by Fu and Zhao 2004. They summarized that the mechanical properties of the composites was comparable with human cortical bone and the addition of HA in composites reduced the toxicity of epoxy resin. Auclair-Daigle et al. 2005 investigated and concluded that mechanical stability of carbon fiber/polyamide composites coated with HA was consistent during simulated body fluid conditioning.

Novel carbon fiber/HA/polyamide 12 composites for hip replacement were developed by Dimitrievska et al. 2009. They found through “*in vivo*” study that these composite has better osteoconductive properties than titanium alloys. Shen et al. 2009 fabricated carbon fiber/HA/ poly lactic acid composites and they identified that mechanical properties of composites was slightly reduced after the “*in vitro*” degradation study. Jianfeng et al. 2010 developed carbon fiber/HA/ poly methyl methacrylate hybrid composites and found the improvement in young’s modulus, flexural modulus and strength. Brockett et al., 2012 developed carbon fiber/PEEK composites for hip replacements. They identified that the wear rate was reduced by the cobalt ceramic coating on the prepared composites.

Recently, Bagheri et al. 2013 developed carbon fiber/ flax fiber/ epoxy composites for bone plate applications. They identified that tensile and flexural properties were similar to human cortical bone. In their continuation work (Bagheri et al. 2014a) they examined the fatigue strength through thermographic analysis and conventional fatigue test. They summarized that prepared composites had higher fatigue strength and suggested as potential material for bone plate application. In another research work (Bagheri et al. 2014b), they examined the plate axial stiffness and surface stress shield of the prepared composites. They concluded that these properties of the prepared composites were comparable with clinical metallic plates. Finally, they examined (Bagheri et al. 2015) the cytotoxicity and osteogenesis of prepared composites. They found that gene expression level for bone formation and cell viability results were better than clinical metal plates.

2.7 Mechanical properties of materials used in biomedical application

In furtherance of various biomedical applications, implants material should have adequate mechanical properties. Based on these mechanical properties like stiffness, strength, toughness and hardness ,behavior of implants materials has been determined. Besides it should have good wear, corrosion resistance and machining ability. The material properties attained by various reachears for low (middle ear) and high load (bone

plates) bearing implants applications are summarized and listed below along with human cortical and trabecular bone.

Table 2.2: Mechanical properties of composite materials for biomedical applications.

Material developed	Method	Results	Authors and year
Human cortical bone	----	<ul style="list-style-type: none"> Elastic modulus is 16-23GPa on longitudinal axes Elastic modulus is 6-13GPa on Transverse axes Tensile strength is 80-150MPa on longitudinal axes Tensile strength is 50-60MPa on Transverse axes Fracture toughness of 4-6MPa.m^{1/2} on longitudinal axes Fracture toughness of 2-4MPa.m^{1/2} on Transverse axes 	Roeder et al. 2008
Human trabecular bone	----	<ul style="list-style-type: none"> Elastic modulus is 0.05-0.5GPa Tensile strength is 1-6MPa 	Roeder et al. 2008
Hydroxyapatite polyethelene Composites	Extrusion and compression moulding	<ul style="list-style-type: none"> Young's modulus is 4.6 GPa at 40 vol. % after 3 month of incubation in SBF Ultimate tensile strength is 20 MPa at 40 vol. % after 3 month of incubation in SBF Elongation % at 40 vol. % shows brittle nature (3.25%) after 3 month of incubation in SBF Composities showed better cell proliferation rate 	Huang et al 1997
Hydroxyapatite polyethelene Composites	Compounding and compression moulding	<ul style="list-style-type: none"> Young's modulus is 7.7 GPa at 50 vol. % Ultimate tensile strength is 24 MPa at50 vol. % Elongation % at 50 vol. % shows brittle nature (7%) Fracture toughness shows 3MPa.m^{1/2} at 50 vol. % 	Bonfield 1998

Hydroxyapatite polyethelene Composites	Compounding and compression moulding	<ul style="list-style-type: none"> • Young's modulus is 4.29 GPa at 40 vol. % • Ultimate tensile strength is 20.67 MPa at 40 vol. % • Elongation % at 40 vol. % shows brittle nature (2.6%) 	Wang et al. 1998
Hydroxyapatite polyethelene Composites	Extrusion and compression moulding	<ul style="list-style-type: none"> • Composities with 20 wt. % of HA showed better cell proliferation rate than 40 wt. % 	Di Silvio et al. 1998
Hydroxyapatite high density polyethelene Composites	Compounding and Extrusion	<ul style="list-style-type: none"> • Young's modulus is 1.8 GPa at 50 vol. % • Ultimate tensile strength is 27 MPa at 50 vol. % • Elongation % at 50 vol. % shows ductile nature (15%) • Impact strength is 9 KJ/m² at 50 vol. % 	Husin et al. 2011
Hydroxyapatite/carbon fiber/epoxy Composites	Resin transfer molding	<ul style="list-style-type: none"> • Impact toughness of 280KJ/m² at 25 wt% of carbon fiber and 16.7 wt% of HA • FlexuralStrength of 520 MPa at 25 wt% of carbon fiber and 16.7 wt% of HA • Flexural modulus of 50 GPa at 25 wt% of carbon fiber and 16.7 wt% of HA 	Zhao et al. 2004
Hydroxyapatite/carbon fiber/epoxy Composites	Resin transfer molding	<ul style="list-style-type: none"> • Flexural modulus of 25 GPa at 35 wt% of carbon fiber and 20 wt% of HA • Flexural strength of 400 MPa at 35 wt% of carbon fiber and 20 wt% of HA 	Fu et al 2004
Carbon fiber/Flax fiber/epoxy Composites	Compression molding	<ul style="list-style-type: none"> • Flexural modulus of 57 • Flexural strength of 510 MPa • Young's modulus of 41.7 GPa • Flexural strength of 399 MPa • Rockwell E Hardness 72.43 	Bagheri et al. 2013
Carbon fiber/Flax fiber/epoxy Composites	Compression molding	<ul style="list-style-type: none"> • Stiffness is 645N/mm • Dynamic modulus is 47GPa 	Bagheri et al. 2014 _{a & b}

Carbon fiber/Flax fiber/epoxy Composites	Compression molding	• Composites showed good cell viability	Bagheri et al. 2015
--	------------------------	--	---------------------------

2.8 Summary of contribution

The far-reaching literature survey shows an overview of different marine CaCO_3 skeletons and its polymer composites for biomedical applications which are related to this thesis. Numerous research works has been carried out by using marine CaCO_3 for bone graft applications either in as such manner or by converting it as calcium phosphates. Likewise, most of the researchers followed hydro thermal method for converting marine CaCO_3 especially cuttlebone into calcium phosphates. But, use of mechano-chemical method was found to be fast and easy approach for the preparation of marine CaCO_3 derived calcium phosphate in particle form without compromising the crystallinity percentage. Even though few researcher works showed the improvement in material properties like mechanical, physical and thermal properties by reinforcing marine CaCO_3 as filler in polymer composites. As far the low load bearing application concern, there is no work has been carried out by utilizing the marine CaCO_3 skeleton and marine skeleton derived calcium phosphates as reinforcement in non-degradable polymer composites.

Similarly, in the past decade fiber reinforced polymer composites has been widely used as alternate material for metallic bone plates. Despite of its bio inert property, these composites showed better mechanical properties than metallic plates. Few researchers experimented for improving the bioactivity of fiber reinforced polymer composites either by addition of synthetic bio-active filler or coating on the surfaces. But so far to the best of our knowledge, no work has been carried out by adding marine CaCO_3 or marine skeleton derived calcium phosphates particles into fiber reinforced polymer composites for the improvement of bioactive property. We expect that, addition of natural derived filler may have better interaction with polymer matrix and good biocompatible properties than synthetic added ones which lead to the more success rate during clinical application.

CHAPTER 3

CHAPTER 3

MATERIALS AND METHODS

3.1 Materials

Cuttlebone samples were obtained from sea food industry of M/S Blue Water Foods and Exports Private Limited, Mangalore, India. Commercial CaCO_3 (CC) filler without any surface treatment supplied by M/S Fisher Scientific Pvt. Ltd, Mumbai, India, was used. A commercial grade of Diglycidyl Ether of Bisphenol-A (DGEBA) liquid epoxy resin (EP) with an epoxide equivalent of 182–200 g/eq and modified polyamine adducts-curing agent (low toxic) from M/S Roto Polymers and Chemicals Private Limited, Chennai, India, was used. Fiber material used in this work was a twill type 3K yarn woven carbon fiber fabric with the thickness of 0.28mm and weight of 200g/m². Analytical grade phosphoric acid (H_3PO_4), dimethylformamide (DMF), dimethylacetamide (DMA), tetrahydrofuran (THF), and toluene of purity >99% were obtained from SRL private Ltd., Mumbai, India, and were used without further purification.

3.2 Preparation of cuttlebone (CB) and heat treated cuttlebone (HB) particles

Cuttlebone samples were washed with plain water and a wire brush was used to remove residual flesh and other wastes. Subsequently, it was rinsed in distilled water and dried at room temperature for one week. Dried cuttlebones were crushed and grounded by a pulverizer and sieved with a 37- μm mesh sieve. Before using the cuttlebone particles (CB) as reinforcing filler, it was pre-dried in a furnace at 100°C for 1 h. Heat treated cuttlebone particle (HB) was prepared by heating at 400°C for 3 h, cooled to ambient temperature and stored in a desiccator to avoid moisture absorption.

3.3 Preparation of calcium oxide (CO), hydroxyapatite (HA) and tricalcium Phosphate (CP) from cuttlebone particles

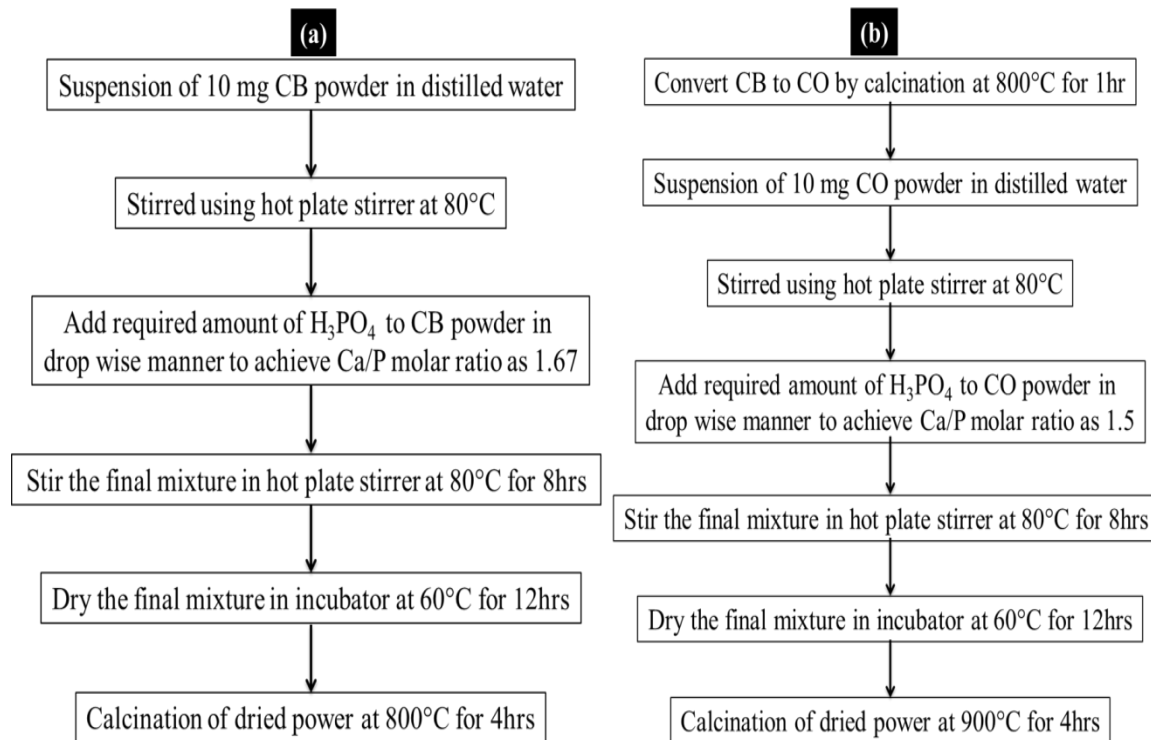


Figure 3.1. Process flowchart for conversion of cuttlebone to (a) hydroxyapatite and (b) tricalcium phosphate

Calcium oxide was obtained from cuttlebone particles, by calcining the samples upto 800°C for 1 h at the heating rate of 5°C/min. Bioactive ceramic particles viz. hydroxyapatite and tricalcium phosphate were derived from cuttlebone by mechanochemical method. This method is simple, fast and efficient for the production of coralline derived calcium phosphates. The detailed process flowchart for the conversion of cuttlebone into hydroxyapatite and tricalcium phosphate is shown in Figure 3.1. Initially, the exact percentage content of calcium carbonate (CaCO₃) in raw cuttlebone particles was determined by thermogravimetry (TGA/DTA) analysis. 10mg of cuttlebone particles was suspended in distilled water and the solution was transferred to a conical flask and kept in a hot plate stirrer at 80°C. To attain the stoichiometric molar ratio of 1.67 (Ca/P), ortho phosphoric acid (H₃PO₄) was added to the suspended cuttlebone

particle solution in drop wise manner at the rate of 12drops/min. Afterwards the final mixture was stirred continuously for 8 h at 80°C and the mixture in slurry form was dried in an incubator at 60°C overnight. The final dried powder was calcined at 800°C for 4h.

For converting coralline CaCO₃ into CP, 10mg of calcined cuttlebone powder (which is in pure CaO phase) was suspended in distilled water and the solution was transferred to a conical flask and kept in a hot plate stirrer at 80°C. Ortho phosphoric acid was added to the suspended cuttlebone particle solution in drop wise manner at the rate of 12drops/min to attain the final stoichiometric molar ratio of 1.5 (Ca/P). Later, the mixture was stirred continuously for 8 h at 80°C and the mixture in slurry form was dried in an incubator at 60°C overnight. The final dried powder was calcined at 900°C for 4h.

3.4 Characterization of cuttlebone particles

The density of CB, CC, CO, HA and CP particles were determined based on the true volume of particles using Pycnometer. The test was repeated five times and the mean density value is reported. Surface area and pore volume of CB, CC, CO, HA and CP particles were measured using surface area analyzer (M/S Smart Instrument Co. Pvt. Ltd Model no: Smart Sorb 92/93). The particle size distribution of CB, CC, CO, HA and CP particles were analyzed using laser particle size analyzer (Ankersmid CIS-50S, USA). To measure the particle size, particles were dispersed in distilled water in a cuvette and scanned with a focused He-Ne laser beam, rotating at a constant frequency by a wedge prism. Morphology of the CB, CC, CO, HA and CP particles were analyzed using scanning electron microscopy (SEM) (JEOL JSM-6380LA, Japan) with energy dispersive X-ray (EDX) (Link ISIS-300 Micro-analytical System, Oxford Instruments, UK) spectroscopy. The particles were dispersed in acetone using bath sonicator for 30 minutes and poured on a glass microscope slide. Gold-sputtering was done on the samples using JFC 1600 auto fine coater (JEOL, Japan), to avert charge accumulation with an accelerating voltage of 20 kV. Inductively coupled plasma-optical emission spectrometer (ICP-OES) (Perkin Elmer- Optima 7000DV) was used to enumerate the elements present in the cuttlebone particles; 50 mg of dried cuttlebone powder was dissolved in diluted

nitric acid and analyses were performed. Further, ICP-OES and SEM-EDX were used to determine Ca/P molar ratio of HA and CP particles.

The thermal degradation of CB, HB and CC particles was analyzed using thermogravimetric analyzer (TGA) (EXSTAR 6000 TG/DTA 6300-Japan), in a nitrogen atmosphere. Twenty milligrams of cuttlebone powder was placed in a platinum pan and heated up to 1000°C at the rate of 10°C/min and nitrogen flow was maintained at 50 mL/min. The polymorphic crystal form of CB, HB, CC, CO, HA and CP particles was identified by a JEOL X-Ray Diffractometer (XRD) (DX-GE-2P, Japan), using CuK α radiation. The filament was operated at 30 kV and the diffraction angle (2θ) was in the range of 20° to 80° at a scanning rate of 2°/min. The approximate crystalline or grain size (t) of the particles were calculated from the XRD pattern using Scherrer's equation (Patterson 1939)

$$t = \frac{k\lambda}{\beta \cos \theta} \quad (1)$$

where, λ is the wavelength of X-rays (CuK α = 1.542 nm); k denotes the Scherrer constant, which is in the range of 0.87–1.0; θ is Bragg angle and β represents full width of the peak at half maximum intensity (FWHM). The sharp and influential diffraction planes from the XRD pattern of the individual particles were used to calculate the corresponding crystalline size of particles (t). A Thermo, Nicolet Avatar 330 FT-IR spectroscopy was used to characterize the presence of organic and mineral phases in CB, HB, CC, CO, HA and CP particles, in the spectral range of 4000–400 cm⁻¹ by KBr pellet-pressing method. XPS analysis of CB and HB was done by AXIS- Ultra instruments using Al K α . The excitation energy was 15kV and 15mA. C1s hydrocarbon peak at 284.80eV was used to calibrate the binding energies because of charge compensations. High-resolution transmission electron microscopic (HRTEM) images of HA and CP particles were obtained by a transmission electron microscope (JEOL, JEM 2100, Tokyo, Japan) operating at an accelerating voltage of 200 kV.

3.5 Preparation of Composites

3.5.1 Preparation of cuttlebone particle (CB, HB) / cuttlebone derived ceramics (CO, HA, CP) reinforced epoxy composites

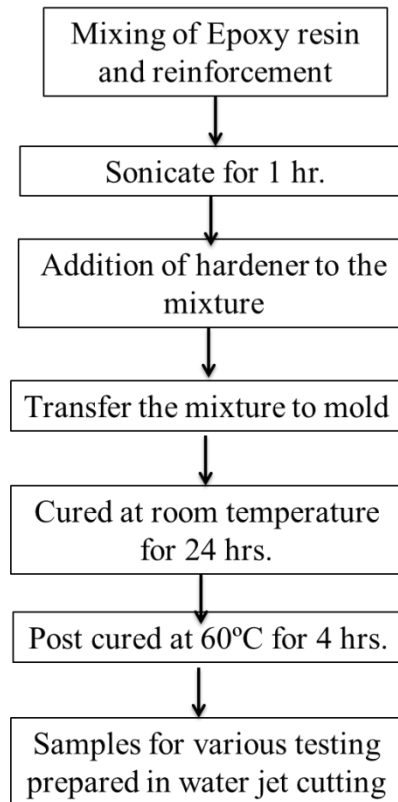


Figure 3.2. Process flowchart for preparation of particle reinforced composites

composite (EP/CB) was prepared at different weight fractions (3, 6, 9, 12 and 15%). At room temperature, epoxy resin was mixed well with required amount of reinforcing filler under mechanical stirring for 30 min. To avoid agglomeration and achieve uniform dispersion of filler in epoxy resin, mixture was transferred to capped bottle and immersed in bath sonicator for 1 h. Then required amount of hardener was added by manual stirring and the final mixture was degassed in vacuum at 60°C for 20 min. A mild steel mold of size 200 X 200 X 3.2 mm was used to cast the composites in sheet form. For compression test samples, a mild steel mold in the size of 70 X 70 X 25.4 mm was used. Before cast, mold releasing agent was applied on the surface for easy removal of composites after curing. The final mixture was poured into the mold and

allowed to cure at room temperature for 24 h. After curing, the casted composite was removed from the mold and post cured in hot air oven at 80°C for 4 h. Similarly, heat treated cuttlebone reinforced epoxy composites (EP/HB), commercial CaCO₃ reinforced epoxy composites (EP/CC), cuttlebone converted calcium oxide reinforced epoxy composites (EP/CO), cuttlebone derived hydroxyapatite reinforced epoxy composites (EP/HA) and cuttlebone derived tri-calcium phosphate reinforced epoxy composites (EP/CP) were prepared at different weight fractions. Neat epoxy sheet (EP) was also prepared based on the above procedure for comparison purpose.

3.5.2 Preparation of cuttlebone derived particles (CB, HB, HA, CP) and carbon fiber reinforced hybrid epoxy composites.

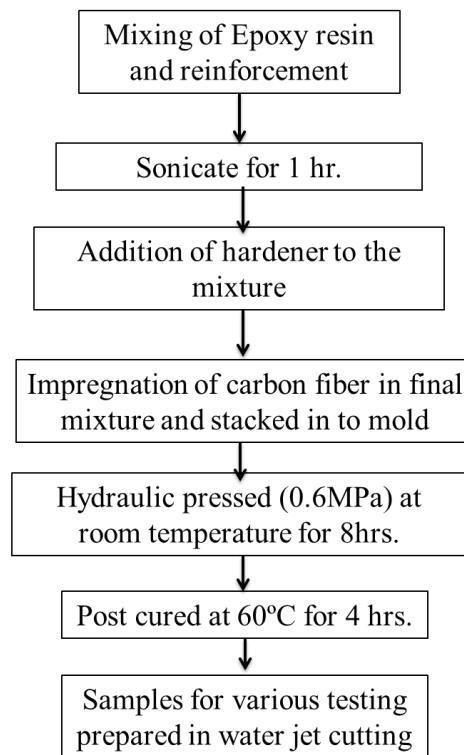


Figure 3.3. Process flowchart for preparation of particle/fiber reinforced hybrid composites

Cuttlebone derived bio-fillers (particles (CB/HB) and ceramics (HA/CP)) and carbon fiber reinforced hybrid epoxy composites were prepared by hand layup followed by compaction in hydraulic press. Initially, four filler material with known weight

fraction (CB at 9 wt%, HB at 9 wt%, HA at 6 wt% and CP at 6 wt%) were added with epoxy resin individually to obtain different composition. Proper mixing was attained by mechanical stirring followed by bath sonication for 1h. Subsequently, required amount of hardener was added to the resin filler mixture manually. To avoid air bubble formation, final mixture was degassed under vacuum at 60°C for 20 min. Five plies of carbon fiber with the size of 200 X 200 mm were fully impregnated in to the final mixture by hand lay-up method. Thereafter, these plies were stacked up in to the teflon mold and a pressure of 0.6 MPa was applied by hydraulic press at room temperature for 8h, followed by post curing in hot air oven at 80°C for 4 h. Volume fraction of carbon fiber in the prepared composites was 35%. The hybrid composites were labeled respectively as EP/CF/CB (cuttlebone and carbon fiber reinforced hybrid epoxy composite), EP/CF/HB (heat treated cuttlebone and carbon fiber reinforced hybrid epoxy composite), EP/CF/HA (cuttlebone derived hydroxyapatite and carbon fiber reinforced hybrid epoxy composite) and EP/CF/CP (cuttlebone derived tricalcium phosphate and carbon fiber reinforced hybrid epoxy composite). Neat epoxy/carbon fiber composite (EP/CF) was also prepared for comparison purpose. Specimens for mechanical, thermal, physical and biocompatibility studies were cut down from these composite sheets using water jet cutting. Before testing, the specimens were conditioned at ambient temperature $23 \pm 2^\circ\text{C}$ and $50 \pm 5\%$ relative humidity for 48 h.

3.6 Mechanical, surface morphology, thermal and physical studies of composites

3.6.1 Mechanical properties of composites

Mechanical tests like tensile, flexural, compression, fracture toughness and inter laminar shear strength were conducted in universal testing machine (UTM) Tinius Olsen (Model H75K-S) equipped with a load cell capacity of 50 kN. Tensile test was performed as per ASTM standard D638 type-I specimen at a crosshead speed of 5 mm/min. The tensile properties (tensile modulus, ultimate tensile strength and elongation percentage at break) were calculated from the load and displacement data. Three-point flexural test was conducted according to ASTM standard D790 at a crosshead speed of 1.32 mm/min.

Flexural strength and modulus was obtained from the load vs. displacement curve. Compressive properties of the prepared composites were determined as per ASTM standard D695 at a crosshead speed of 1.3 mm/min. Cylindrical specimen was used to conduct the compression test and properties like compression strength and modulus were obtained from load vs. displacement curve. Fracture toughness of the composites was determined in terms of critical stress intensity factor (K_{IC}) using single-edge notched 3 point bending test. Test was conducted according to ASTM standard D5045 at a cross head speed of 0.5 mm/min. Before the test, a pre crack was introduced in the specimen to obtain the results in plane strain condition. Based on the peak load obtained from the load vs. displacement curve, fracture toughness was calculated using the following equation:

$$K_{IC} = \frac{3PSy\sqrt{a}}{2tw^2} \quad (2)$$

$$y = 1.93 - 3.07\left(\frac{a}{w}\right) + 14.53\left(\frac{a}{w}\right)^2 - 25.11\left(\frac{a}{w}\right)^3 + 25.8\left(\frac{a}{w}\right)^4 \quad (3)$$

Where **P** is the peak load (N), **S** is the span length (mm), **y** is the geometrical correction factor **a** is the notch length (mm), **t** is thickness of the specimen (mm) and **w** is width of the specimen (mm).

Short beam shear test was conducted as per ASTM standard D2344 to measure the inter-laminar shear strength (ILSS) of the prepared hybrid epoxy composites. Test was conducted in 3-point bending test mode at a displacement rate of 0.5 mm/min. Specimen breaking load was measured from the load vs. displacement curve and the load value was used in the following equation to calculate the ILSS of the composites.

$$ILSS = \frac{3P}{4wt} \quad (4)$$

Where **P** is the breaking load (N), **w** is width of the specimen (mm) and **t** is thickness of the specimen (mm).

Impact test was carried out according to the ASTM standard D256 using Zwick Roell impact tester (Model no: HIT50P). Notch was created in composite specimens and tests were done with an impact velocity of 3.458 m/s to find the impact strength. Hardness of the composites was measured as per ASTM standard D2270 with a shore D

durometer (Mextech Shore D Hardness tester-Model no: HT6510-D). Hardness was determined by the penetration depth of the indenter in to the sample under a constant applied force for 60 seconds.

All mechanical tests were performed at room temperature. Five samples for each composition of the tests were conducted and mean value is reported. Based on the mechanical properties of various composite materials (with different reinforcement materials (CB/HB/CC/CO/HA/CP) at different weight ratios) 12 composite material with best mechanical properties were identified for further physical, thermal properties and surface morphology studies.

3.6.2 Surface morphology of composites

Cross section of the fractured tensile and impact specimens was used to observe the surface morphologies of composites by scanning electron microscopy (SEM).

3.6.3. Thermo-mechanical and thermal properties of composites

Dynamic mechanical analyzer (DMA8000, PerkinElmer, USA) was used to measure the dynamic mechanical properties of composites in single cantilever mode at a frequency of 1 Hz. Test was performed at varying temperatures that ranged from room temperature to 150°C at a heating rate of 5°C/min under nitrogen atmosphere. Properties like storage modulus, loss modulus, $\tan \delta$ was obtained and glass transition temperature (T_g) was measured from the peak value of $\tan \delta$. The thermal stability of composites was analyzed by TGA at a heating rate of 10°C/min from 30 to 650°C. Besides the weight loss calculation, thermal stability factors like activation energy (E_i), integral procedure decomposition temperature (IPDT), temperature at the maximum rate of degradation (T_{max}) and char yield at 650°C were evaluated. Following equations were used to calculate the IPDT from the TGA curve.

$$IPDT = A^* K^* (T_f - T_i) + T_i \quad (5)$$

$$A^* = (S_1 + S_2) / (S_1 + S_2 + S_3) \quad (6)$$

$$K^* = (S_1 + S_2) / S_1 \quad (7)$$

Where A^* is the area ratio of the total experimental curve to the total TGA thermogram. K^* , T_i and T_f are the coefficient, initial temperature (30°C) and final temperature (650°C), respectively. S_1 , S_2 and S_3 are the areas of three regions from TGA curve which is indicated in Figure 3.2 (a).

The decomposition activation energy (E_t) was calculated from the following equation adapted by Horowitz and Metzger using integral method (Jin and Park 2009).

$$\ln[\ln(1-\alpha)^{-1}] = \frac{E_t \theta}{RT_{\max}^2} \quad (8)$$

Where, α is the decomposition fraction, $\theta = T - T_{\max}$ and R is gas constant [8.3146 J / (mol K)]. Plots for $\ln[\ln(1-\alpha)^{-1}]$ Vs θ is shown in Figure 3.2(b). Equation 8 was used to calculate E_t of the composites from the slope of the straight line (in Figure 3.2(b)).

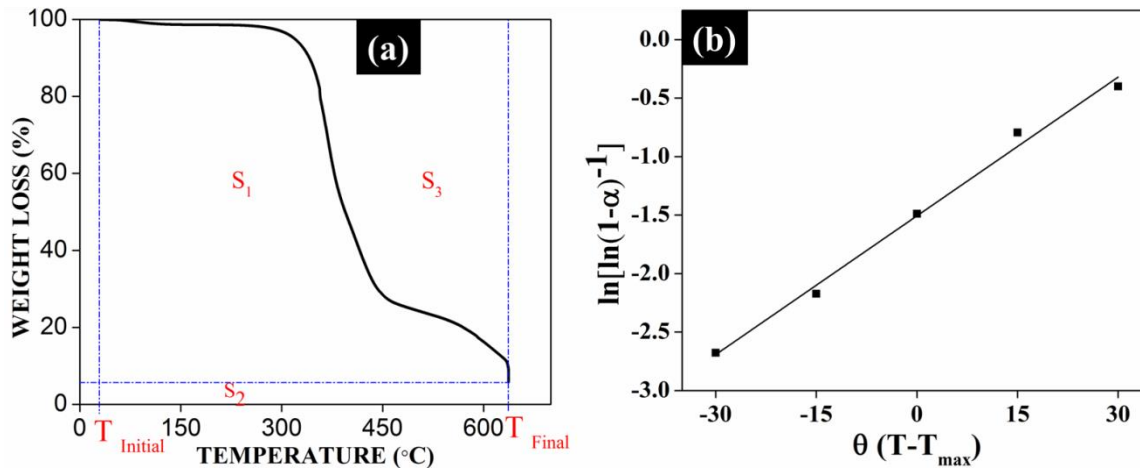


Figure. 3.4. (a) Schematic representation of area S_1 , S_2 and S_3 from TGA curve. (b) Plots of $\ln[\ln(1-\alpha)^{-1}]$ vs. θ for composites

3.6.4. Physical properties of the composites

The effective crosslink density of composites and average number of molecular weight between successive cross links were determined through swelling co-efficient (θ). The optimal solvent for measuring the swelling coefficient of composites under study was identified by immersing the samples in different solvents like dimethylformamide (DMF), dimethylacetamide (DMA), tetrahydrofuran (THF), toluene and water.

Maximum swelling was observed in dimethylformamide and was used to measure the swelling co-efficient. Samples weighing about 0.2 to 0.25 g were cut from respective composite sheets and allowed to swell and weighed after 48 hours. Swelling coefficient was calculated using the following equation:

$$\text{Swelling coefficient}(\theta) = \frac{\text{weight of the solvent in swollen composite}}{\text{weight of the swollen composite}} \times \frac{\text{density of the composite}}{\text{density of the solvent}} \quad (9)$$

Crosslink density (χ) and molecular weight between crosslinks (M_c) of the composites were determined using Flory-Rehner equation

$$\chi = \frac{-[V_r + \gamma V_o V_r^2 + \ln(1 - V_r)]}{d_r V_o (V_r^{1/3} - \frac{V_r}{2})} = \frac{1}{M_c} \quad (10)$$

Where $V_r = 1/(1+\theta)$ is the volume fraction of the polymer, d_r is the density of dry polymer, V_o is the molar volume of the solvent (82.628 cm³) and γ is the Huggins polymer-solvent interaction parameter (0.34 in this study). Swelling ratio (SR) of the composites was measured at diffusion equilibrium state by the following equation.

$$SR = \frac{W_2 - W_1}{W_1} \quad (11)$$

Where, W_1 and W_2 are weight of the composite before and after swelling, respectively. Water absorption test for prepared composites was conducted as per ASTM standard D570. Initially, samples were pre-dried in a vacuum oven at 70°C to achieve constant weight. The samples were then immersed in distilled water for a period of 30 days. Weight gain of the composites was measured at frequent time interval, by removing the sample from container and wiping off the excess water with dry cloth. Percentage of water absorption (WA.) was calculated by the following formula.

$$WA = \frac{W_F - W_I}{W_I} * 100 \quad (12)$$

Where, W_I and W_F are the respective weights of composites before and after water absorption. Wettability of the composites was measured by water contact angle

using a dynamic contact angle analyzer (FTA 200, First Ten Angstroms, Virginia, USA) by sessile drop technique. In detail, 10 μ L of double distilled water was dispensed on the surface of the specimen by syringe, and the digital images of the drops were taken by a charged couple device camera at specific time interval. Images were analyzed by FTA image analysis software to measure the contact angle.

The volume fraction of voids (V_V) in composite material was determined according to ASTM standard D2734 using the following equation

$$V_V = \frac{\rho_{ct} - \rho_{ca}}{\rho_{ct}} \quad (13)$$

Where, ρ_{ca} and ρ_{ct} are the actual and theoretical density of the composites. The actual density of the composite material (ρ_{ca}) was calculated by displacement method using electronic balance with ± 0.1 mg precision. The theoretical density of the composite material (ρ_{ct}) in terms of weight fraction was calculated from the following equation.

$$\rho_{ct} = \frac{1}{\left(\frac{W_P}{\rho_P}\right) + \left(\frac{W_M}{\rho_M}\right)} \quad (14)$$

Where, W and ρ denotes the weight fraction and density respectively. The subscripts P and M represent the particle and matrix respectively.

3.7 Biocompatibility studies of composites

3.7.1 *In vitro* cytotoxicity study

In vitro cytotoxicity of the composites was evaluated using mammalian mouse fibroblast cell line L-929 by indirect MTT assay. The MTT assay was performed to measure the metabolic activity of cells and assessed through “color-change” phenomenon from yellow colored tetrazolium salt, MTT {3-(4,5-diamethyl thiazol- 2-yl)-2,5-diphenyltetrazolium bromide} to purple colored formazan. Initially, specimens were sterilized by steam sterilization at 120°C for 20 min followed by conditioning in culture medium for 15 min. Extract was prepared by incubating the sample with total surface area of 1.82cm² in 1.45ml culture medium containing foetal bovine serum (FBS) at 37 \pm 1°C for 24 \pm 2 h. After 24 h, the extract was diluted further using same culture medium

to obtain 50%, 25% and 12.5%. Cells cultured in normal medium were considered as cell control. Negative and positive controls were prepared by incubating 1.25cm² ultra high molecular weight polyethylene and 1.3 mg/ml phenol with culture medium containing FBS at 37±1°C for 24±2h, respectively. Equal volume (100µL) of various dilutions (100%, 50%, 25% and 12.5%) of test specimens, extract of negative, positive and cell control were placed on sub-confluent monolayer of L-929 cells and incubated at 37±1°C for 24±2h.

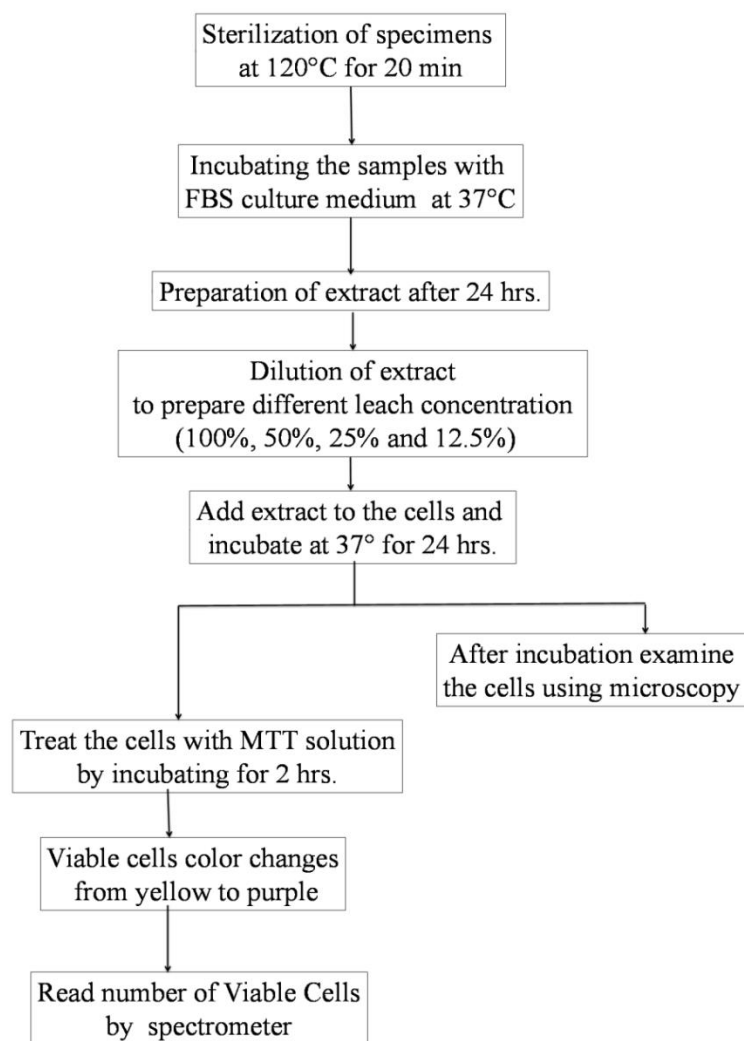


Figure 3.5. Process flowchart for the cytotoxicity test using indirect test method

After incubation, cell monolayer was examined microscopically for understanding the cell response to specimen. Later, extract and control medium in cultured cell was

replaced with 50 μ L of MTT (1mg/ml medium without supplements), wrapped with aluminum foil and were incubated at 37 \pm 2 $^{\circ}$ C for 2 h. After discarding the MTT solution, 100ml of isopropanol was added to all wells and swayed the plates. The color developed was quantified by measuring absorbance at 570nm using a spectrophotometer. The detailed process flowchart for the cytotoxicity test using indirect test method was shown in figure 3.3. Test was performed for six replicates and specimen results were compared with cell control.

3.7.2 *In vitro* hemocompatibility study

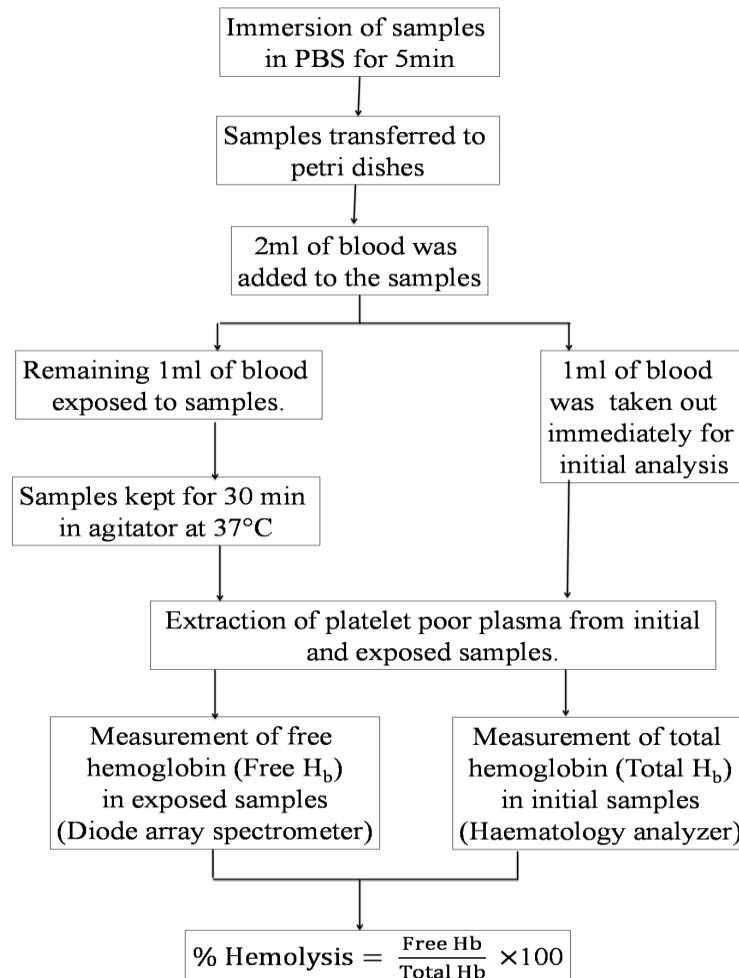


Figure 3.6. Process flowchart for the hemocompatibility test

In vitro hemocompatibility study was conducted as per ISO 10993 Part-4 to understand the interaction between composites and blood. Figure 3.4 shows the process

flowchart for hemocompatibility test. Composite samples with the size of 1.2 x 1.2 cm² were used for this study. Blood from human volunteers was collected into the anticoagulant, CPD-A. Initially, samples were transferred to polystyrene petri dishes and immersed in phosphate buffer saline for 5 min before they were exposed to blood. 2ml of blood was added to each petri dish that contains sample and 1ml of blood was taken out immediately for initial analysis.

The remaining 1ml blood was exposed to sample for 30min under agitation at 70±5 rpm using an Environ shaker thermo at 35±2°C (as per WPTRU012). Test was done in triplicate and as a reference four empty polystyrene petri dishes were exposed with blood. The platelets poor plasma was aspirated from initial samples and blood samples exposed to specimens by centrifuging at 4000 rpm for 15 min as per WPTRU006. The total hemoglobin (Total Hb) in the initial samples was measured using automatic haematology analyzer (Sesmex-K 4500) as per WPTRU015. Similarly, free hemoglobin (Free Hb) liberated into the plasma after exposure was measured by Diode array Spectrophotometer as per WPTRU022. Hemolysis percentage was calculated using the following formula.

$$\% \text{ Hemolysis} = \frac{\text{Free Hb}}{\text{Total Hb}} \times 100 \quad (15)$$

Results were compared with average % hemolysis of four reference samples after 30 min exposure.

CHAPTER 4

CHAPTER 4

INFLUENCE OF CUTTLBONE BIO-FILLERS AS REINFORCEMENT IN EPOXY COMPOSITES

This chapter describes the utilization of cuttlebone particles as reinforcement in epoxy composites. Different polymorph of cuttlebone particles was attained by heat-treatment method. Presence of polymorph form, elemental composition and thermal stability were confirmed with different characterization techniques. Composites were prepared with different polymorph form cuttlebone particles and also commercially available CaCO_3 as reinforcement in epoxy matrix. Material properties like mechanical, physical, thermal, thermo-mechanical and biocompatibility of the composites developed were analyzed. Cuttlebone reinforced epoxy composites showed favorable material properties for biomedical applications.

4.1 Results and Discussions

4.1.1 Characterization of CB, HB and CC particles

Figure 4.1 shows the particle size distribution of cuttlebone particles and commercial CaCO_3 . The percentage of derivative volume of particle (dV/dD) against particle size is shown in these plots. The average particle size for cuttlebone particles and commercial CaCO_3 are 10.32 and 10.10 μm , respectively. The cumulative volume percentage of these two particles at different size range, mean particle size and standard deviation value are shown in Table 4.1. In all, 90% of commercial CaCO_3 particles were in the size of less than 10 μm . But for cuttlebone particles the size distribution was broader because of irregular flake form of structure. Almost 20% of cuttlebone particles were in the size of less than 5 μm and remaining 70% of particles were in the range of 5 to 10 μm .

Density, surface area and pore volume of cuttlebone particles and commercial CaCO_3 are presented in Table 4.2. The density of commercial CaCO_3 was slightly higher

than cuttlebone particles. However, the surface area of cuttlebone particles was higher than commercial CaCO_3 because of the particle shape and aspect ratio.

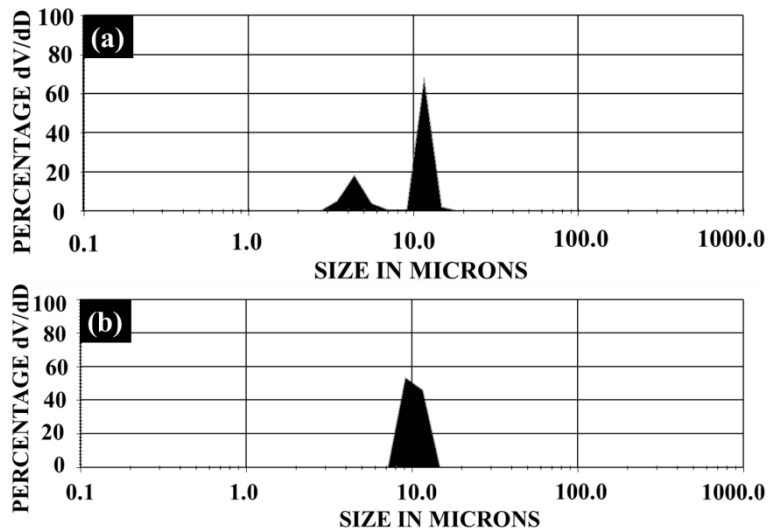


Figure 4.1. Particle size distribution of (a) cuttlebone particles and (b) commercial CaCO_3 .

Table 4.1. Volume percentage of particles at different size range and mean particle size of cuttlebone and commercial CaCO_3 particles.

Material	Cumulative volume %				Mean particle size with standard deviation (μm)
	< 25 μm	< 15 μm	< 10 μm	< 5 μm	
Cuttlebone particles	100.0	100.0	70.0	20.0	10.32 \pm 3.72
Commercial CaCO_3	100.0	100.0	91.48	9.94	10.10 \pm 0.44

Figure 4.2a to c shows the morphology of cuttlebone, commercial CaCO_3 particles and EDX spectra of cuttlebone particles, respectively. The particle size of cuttlebone particles was heterogeneous in nature and varied from fine to large-size flaky form of particles. But commercial CaCO_3 particles consisted of fine particles in spherical shape. Elements present in the cuttlebone particles and its percentage composition was determined by both EDX spectra and ICP-OES method and their percentage composition are presented in Table 4.3. Both results ensured that cuttlebone particles were composed of calcium carbonate and organic matters.

Particle size analysis revealed broad size distribution in cuttlebone particles than commercial CaCO_3 particles. The size distribution for commercial CaCO_3 was narrow because of even spherical structure. Cuttlebone has a dorsal shield and a lamellar structure inside separated by thin pillars. Thickness of these lamellae is less than $5\ \mu\text{m}$. The dorsal shield of cuttlebone is normally stiffer than the lamellae resulting in longer pulverizing time and broader particle size distribution. The diameter to thickness ratio of flake particles is generally high and signifies the fact that the aspect ratio of flake-type cuttlebone particles is higher than the spherical-type commercial CaCO_3 particles (Cao et al. 2014).

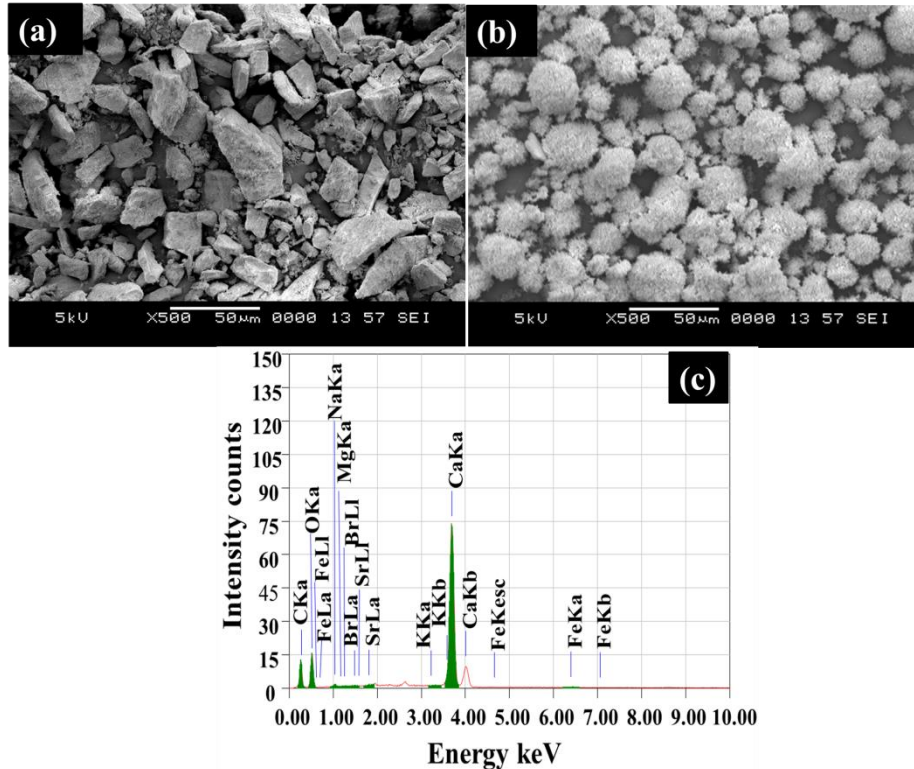


Figure 4.2. SEM micrograph of (a) cuttlebone particles (b) commercial CaCO_3 particles and (c) EDX spectra of cuttlebone particles.

The cuttlebone particles may therefore have higher surface area than commercial CaCO_3 particles. Calcite structure CaCO_3 has lower density than aragonite structure CaCO_3 (Tuba et al. 2010). However, cuttlebone particle in aragonite form had lower

density than commercial CaCO₃ in calcite form. It is noteworthy that density of the coral skeletons was preponderate by the environmental condition of seawater.

Table 4.2. Density, surface area and pore volume of cuttlebone and commercial CaCO₃ particles.

Material	Density (g/cm ³)	Surface area (m ² /g)	Pore volume (cm ³ /g)
Cuttlebone particles	2.4	5.08	0.0059
Commercial CaCO ₃	2.5	3.74	0.00128

Table 4.3. Percentage composition of elements in cuttlebone found by EDX and ICP-OES analysis

	Elements								
	Na	K	Mg	Fe	Sr	Ca	C	O	Br
ICP-OES in wt%	1.341	0.079	0.060	0.012	0.281	35.06	--	--	--
EDX in wt%	1.041	0.23	1.253	0.05	0.29	38.07	15.10	45.31	0.20

EDX and ICP-OES analysis also revealed that cuttlebone was mainly composed of CaCO₃ followed by organic components. Apart from that sodium (Na), bromine (Br), iron (Fe), magnesium (Mg), potassium (K) and strontium (Sr) were found in minor quantities. Ca and Sr elements determined in cuttlebone particles ensured their aragonite forms. C is the common element for the organic and inorganic components. Presence of small trace elements Br, Na and Mg confirmed the presence of organic matters in cuttlebone particles (Florek et al. 2009).

4.1.1.1 Thermo gravimetric analysis of CB, HB and CC particles

Figure 4.3 shows the TGA, differential thermo gravimetric (DTG) and differential thermal analysis (DTA) curves for cuttlebone particles. TGA curve exhibits three stages of degradation as shown in Figure 4.3a. First step of degradation occurred at 30 to 75°C because of removal of moisture. The second step of major degradation started at 280°C and ended at 340°C. A moderate intensity broad peak at 320°C in DTG curve (Figure

4.3a) showed the decomposition of organic compounds like protein and chitin. The weight loss of cuttlebone particles up to 350°C was around 7.5%. Third step of degradation started at 640°C and increased up to 780°C. The DTG curve showed a maximum degradation rate at 757°C. This sharp peak revealed that the CaCO_3 decomposed completely and converted into calcium oxide (CaO) and carbon dioxide (CO_2) (Florek et al. 2009). The weight loss at 800°C was around 51%. The DTA curve with baseline subtraction in Figure 4.3b clearly showed an endothermic peak at the region of 51°C due to removal of moisture content from the sample. At 330°C an exothermic peak was observed. At this temperature, phase transformation from aragonite to calcite occurred in cuttlebone particles. Again a broad endothermic peak appeared in the temperature region of 700 to 800°C because of the decomposition of CaCO_3 into CaO and CO_2 .

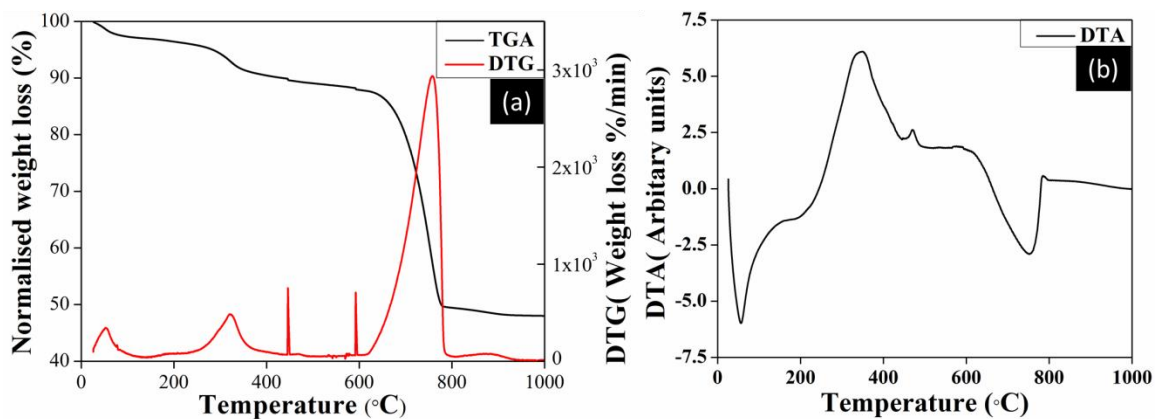


Figure 4.3. (a) TG and DTG curve of cuttlebone particles and (b) its corresponding DTA curve with baseline subtraction.

TGA curve for HB (Figure 4.4a) revealed smaller amount of degradation at the temperature range of 350-410°C. But CC was stable up to 600°C. Similarly as like cuttlebone, major degradation of HB and CC materials occurred in the temperature range of 600-800°C with the decomposition of CaCO_3 into CaO and CO_2 . Figure 4.4b showed that CC had higher rate of decomposition than other materials. The possible reason could be smaller particle size of CC as compared to CB and HB, leading to efficient heat

transfer and decomposition. Furthermore, maximum decomposition rate for CB, HB and CC materials occurred at a temperature of 757.46, 723.44 and 733.03°C, respectively.

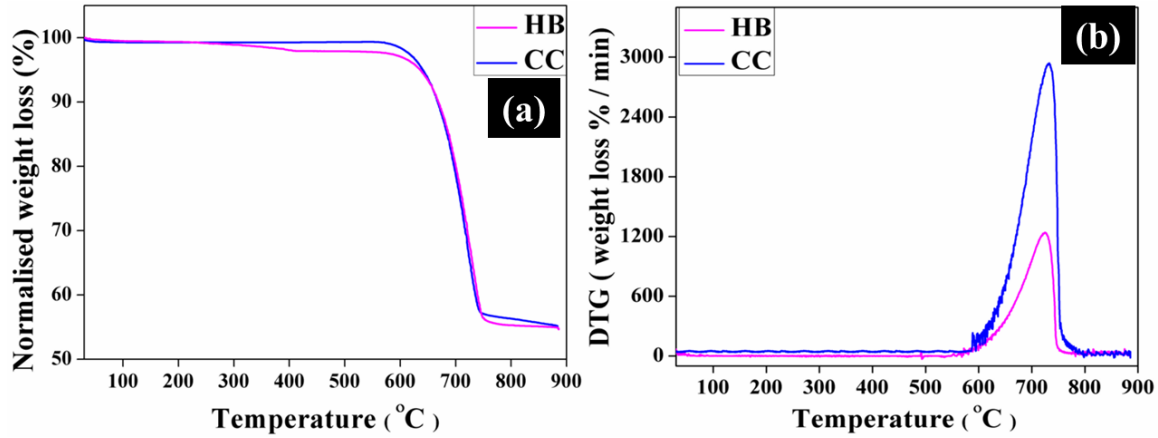


Figure 4.4. (a) TG and (b) DTG curve of heat treated cuttlebone (HB) particles and commercial CaCO_3 (CC) particles.

4.1.1.2 Crystallographic structure and composition of CB, HB and CC particles

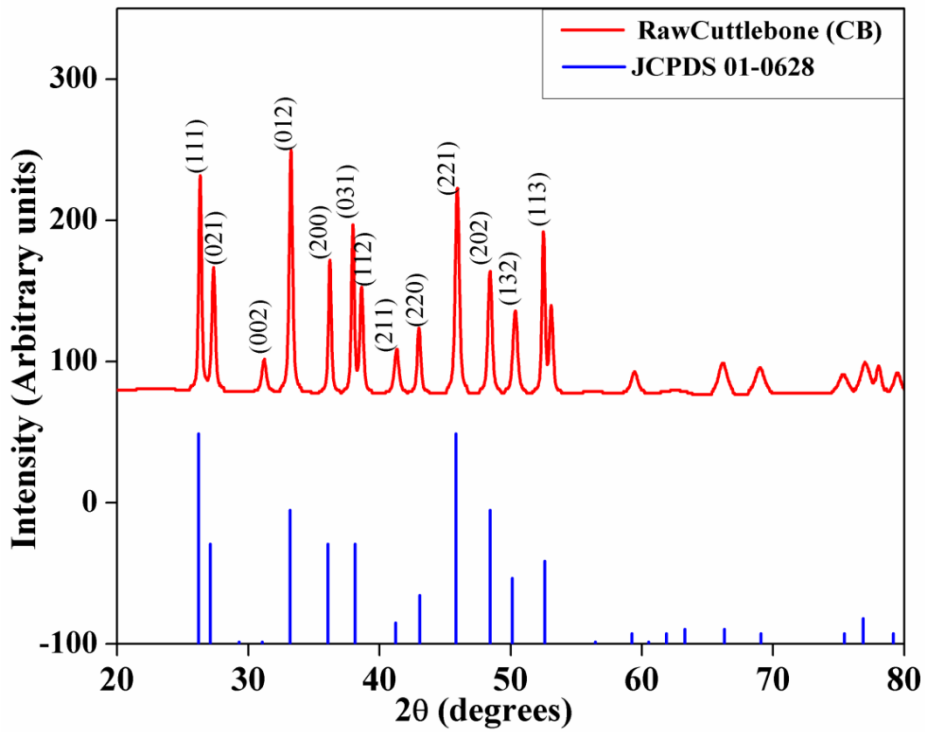


Figure 4.5. X-ray diffractograms of raw cuttlebone and JCPDS 01-0628 for aragonite CaCO_3 .

The crystallographic study of cuttlebone particle was done using XRD. Figure 4.5 shows the XRD pattern of raw cuttlebone particles along with the standard reference pattern. XRD pattern of cuttlebone particles coincided with the Joint Committee on Powder Diffraction Standards (JCPDS) card no: 01-0628 for aragonite. Especially, three major intensities of diffraction peak planes (111), (012) and (221) and their corresponding reflexes location (2θ) 26° , 33° and 46° agreed well with the standard. It clearly showed that the cuttlebone was fully composed of aragonite polymorph form of CaCO_3 in orthorhombic shape. XRD pattern of commercial CaCO_3 (CC) and cuttlebone particles heated at 400°C (HB) were matched with JCPDS card no: 01-0837 for standard calcite form as shown in Figure 4.6. Cuttlebone particles heated at 400°C showed influential diffraction peak plane (104) typical of calcite polymorphs, although certain peaks corresponding to aragonite polymorphs were also present (Figure 4.6).

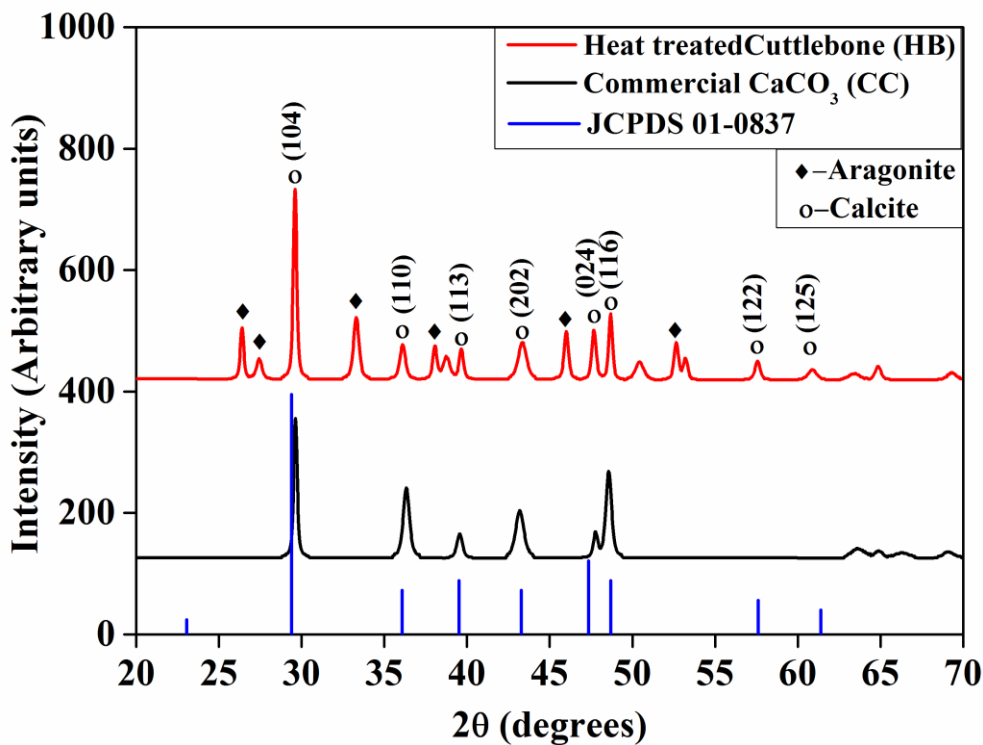


Figure 4.6. X-ray diffractograms of Heat treated cuttlebone particles (HB), commercial CaCO_3 particles (CC) and JCPDS 01-0837 for calcite CaCO_3 .

The FT-IR spectra of raw cuttlebone, heat treated cuttlebone and commercial CaCO_3 particles are illustrated in Figure 4.7. Figure 4.7a shows the presence of aragonite and chitin from their characteristic bands in raw cuttlebone particles. The strong aragonite structure carbonate group peaks were confirmed at 1081.63 (ν_1), 704.63 and 698.82cm^{-1} (ν_4 doublet -C-O in plane bend) and 853.34cm^{-1} (ν_2 -out-of plane bend). Beyond that, band at 1444.9cm^{-1} (ν_3 -asymmetric stretch) was observed because of the internal vibration mode of CO_3^{2-} ions. The bands at 2524.6 and 1786cm^{-1} were also influenced as a result of (C = O bond) vibration of the carbonate ions. A small amount of organic compounds like chitin and protein were confirmed by the band characteristics in the region of $1030\text{-}1110\text{ cm}^{-1}$ (stretching C-O), 1649cm^{-1} (amide II) and 1470cm^{-1} (amide band for protein). Bands in the region of $3100\text{-}3400\text{cm}^{-1}$ were found for α - chitin. Raw cuttlebone had weak OH and NH group absorption peaks in the range of $3450\text{-}3800\text{cm}^{-1}$ because of the stretching vibration of water molecules. The FT-IR spectra of heat treated cuttlebone and commercial CaCO_3 particles is shown in Figure 4.7b –c respectively. It was clearly identified that the particles were in calcite polymorph form.

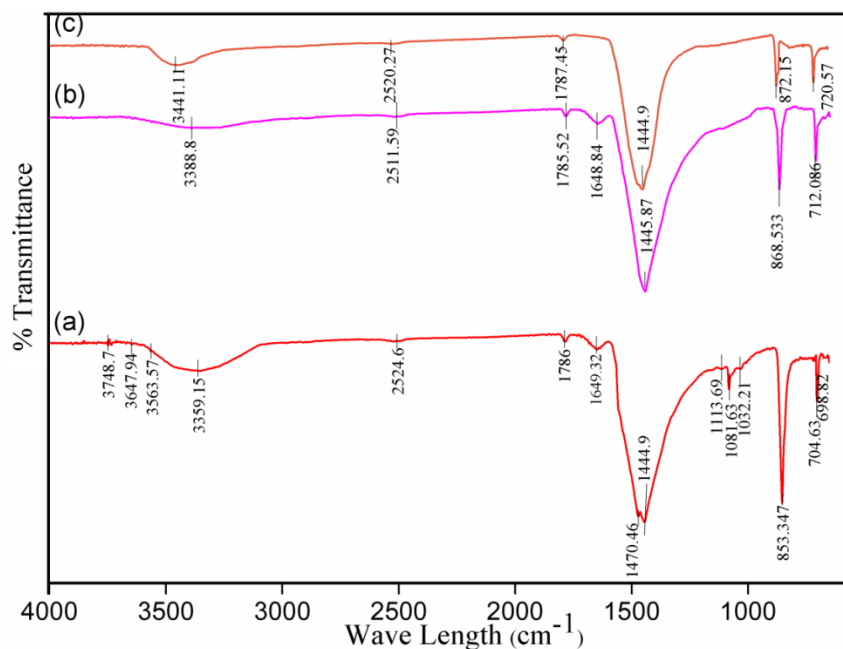


Figure. 4.7. FT-IR spectra of (a) raw cuttlebone, (b) heat treated cuttlebone and (c) Commercial CaCO_3 particles.

X-ray photoelectron spectroscopy (XPS) spectra of CB and HB particles (Figure 4.8) indicated the core level of each element like calcium (Ca2p), carbon (C1s), oxygen (O1s) and nitrogen (N1s) detected from CaCO₃ and organic components. Binding energy peak values along with the surface composition in terms of atomic percentage are shown in Table 4.4. Electron density of these elements in CB and HB were similar, as the orientation of carbonate ions (CO₃²⁻) in lattice were parallel to *ab* plane (Gopinath et al. 2002).

Element peak (N1s) in cuttlebone denoted the presence of organic matter like chitin which is covalently linked to protein (Poompradub et al. 2008). Binding energy peak position of Ca2p element (347.1) for both materials attributed that calcium was surrounded by hydroxyl groups making them most stable. Compared to HB, CB had poor amount of calcium composition on their surfaces because of aragonite crystalline nature.

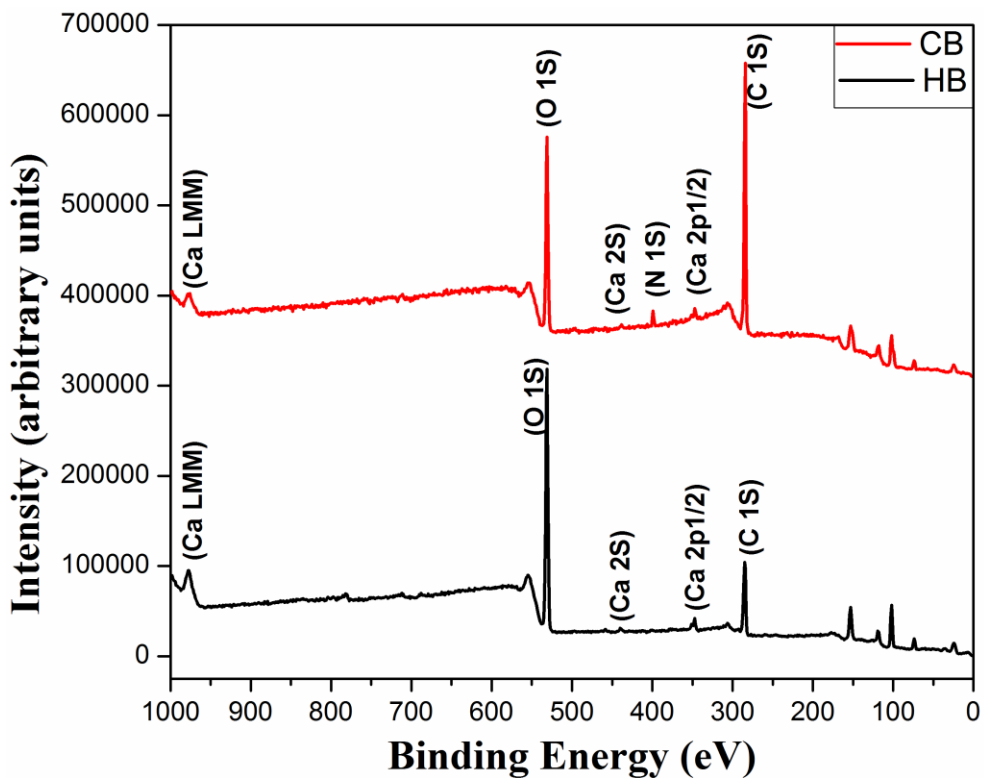


Figure 4.8. XPS Spectra for raw cuttlebone and heat-treated cuttlebone particles.

Table 4.4: XPS parameters for Ca, C, O and N core levels from raw cuttlebone and heat treated cuttlebone particles and its surface composition

Material	Binding energy (eV)				Atomic Percentage			
	Ca2p	C1s	O1s	N1s	Ca	C	O	N
Cuttlebone (CB)	347.13	284.32	531.22	399.06	0.6	70.97	26.34	2.09
Heat treated Cuttlebone (HB)	347.13	284.5	531.4	399.31	1.26	38.45	60.15	0.14

Based on the above TGA, XRD, FT-IR and XPS analysis, the thermal stability, polymorph structure and effects in polymorph structure by heat treatment of cuttlebone particles were analyzed. TGA curve of cuttlebone particles showed their stability up to 300°C. In the XRD analysis, pattern of raw cuttlebone and commercial CaCO₃ comprised of orthorhombic form aragonite and rhombohedral form calcite crystal structure, respectively. FT-IR analysis showed that the strong stretching band (ν_3) at 1444.9cm⁻¹ for aragonite was overlapped by the presence of organic matters in the raw cuttlebone, but it became sharper in heat treated cuttlebone particles [Figure 4.7(b)]. It clearly showed that organic matter started degrading, although with the deduction of water absorption bands at 3450-3800cm⁻¹.

Organic matters started decomposing at 320°C and aragonite crystal structure got converted in to calcite form at 300 to 400°C [shown in Figure 4.3(a)]. But heat treated cuttlebone particles showed higher order of calcite polymorph with low amount of aragonite forms. It clearly indicates that heat treated cuttlebone particles did not ensure complete aragonite-calcite transition. Even after 400°C, some parts of organic compounds did not decompose because of strong interaction with minerals. It was confirmed by XPS, TGA and FT-IR techniques. XPS analysis of HB particles [Figure 4.8] revealed that detected nitrogen peaks confirmed the presents of organic matters. Likewise TGA analysis of HB particles [Figure 4.4(a)] denoted the decomposition of organic matrix in the temperature range of 350-410°C. Besides, it was also evidenced in FT-IR spectra. After heat treatment, the strong aragonite peaks at 1083, 701.3, 698.82 and 851cm⁻¹ disappeared, while new peaks appeared at 712 and 875cm⁻¹ which strongly

indicated the phase transformation from aragonite to calcite [Figure 4.7(b)]. However, even after heat treatment at 400°C, some organic content peaks at 1648 and 3388 cm^{-1} were still observed. Generally, organic matters in cuttlebone are present in between the boundary of dorsal shield and lamellar matrix as well as on the surface of each lamella. During heat treatment, dorsal shield got converted into calcite form completely as compared to lamellar region (Ivankovic et al. 2009). Further organic matters present on the surface of lamella decomposed at 600°C which was clearly identified in the DTG curve [shown in Figure 4.3(a)]. The stepwise peaks at 446°C and 592°C of DTG curve attribute to the complete removal of organic matters and thermally induced crystal conversion of cuttlebone particle from metastable aragonite state to calcite state. Major degradation of cuttlebone particles occurred at the temperature range of 640°C to 780°C. The high amount of weight loss at this temperature range clearly indicates that volatile minerals in the cuttlebone decomposed as CaO and CO₂. Thermal decomposition reaction in sea corals headed from outer surface of the particles to inner solid. This reaction termed as shrinking core model finally turned out with converted solid material (Kamba et al. 2013). Beyond 800°C the sample weight was same. Temperature of maximum rate of degradation showed that CB was more stable thermally than HB and CC because of the presence of organic matters. Due to the great thermal stability, cuttlebone particles could be used as bio filler in polymer composites.

4.1.2 Mechanical properties of EP, EP/CB, EP/HB and EP/CC composites

In this topic three different groups of composites (EP/CB, EP/HB and EP/CC) were analyzed. Each test group consists of six different sets (0, 3, 6, 9, 12 and 15 wt%). Results are expressed in the form of mean \pm Standard deviation of 5 experiments. For all mechanical properties, statistical analyses were performed by one-way ANOVA. Tukey's honestly significant difference method was used for all post hoc analysis to identify the significant difference between each set of individual test group. Furthermore, significant difference between highest values of three test group was also determined by tukey's test. In all the tests, statistical significance was set at $p < 0.05$. Letters in lower case (a, b, c, d, and e), letters in upper case (A, B, C, D and E) and numbers (1, 2, 3, 4 and 5) was used to

denote the statistical results in EP/CB, EP/HB and EP/CC test group, respectively. Likewise, symbols (♠, ♦ and ●) were used to denote the statistical results among the highest value of three test groups.

Figure 4.9 shows the tensile strength, tensile modulus, elongation percentage at break and load vs. deformation curve of EP/CB, EP/HB and EP/CC composites. Ultimate tensile strength (UTS) in all the three composites increased with filler content in the matrix material as shown in Figure 4.9a. UTS increased until certain weight fraction of filler content and then it decreased. The UTS of neat epoxy matrix was 24MPa while UTS of EP/CB, EP/HB and EP/CC composites (at 9 wt%) were 38.84, 41.30 and 34.16MPa, respectively. Further, increased weight fraction (beyond 9 wt%) of filler content in composites led to reduction in UTS because of poor dispersion of filler in matrix material.

In figure 4.9a, insets indicate that EP/CB composites prepared at 9 and 12 wt% have significantly higher tensile strength value than neat epoxy samples. However, there was no significant difference found between these two samples. Besides, significant difference was found between EP/CB composites at 3 and 9 wt%. For EP/HB composites, 6, 9 and 12 wt% samples have significantly higher value compared to neat epoxy, but there was no significant difference was found within these three samples. In addition to, EP/CC composites at 9 wt% has significantly higher than neat epoxy. On the other hand, there was no significant difference was found between the highest tensile strength of three composites (EP/CB, EP/HB and EP/CC at 9 wt%).

Figure 4.9b shows the tensile modulus plotted versus different weight ratio of filler content for EP/CB, EP/HB and EP/CC composites. The tensile modulus for neat epoxy was 659MPa. It increased until certain weight fraction of the filler content in both EP/CC and EP/CB composites and then decreased. The maximum modulus value of EP/CC composite was 701MPa (at 6wt%) and EP/CB composite was 776MPa (at 12 wt%). For EP/HB composites, tensile modulus increased by increasing the filler content and the maximum modulus value was 889MPa (at 15 wt%). Among the cuttlebone filled composites, EP/HB composites had better tensile modulus than EP/CB composite.

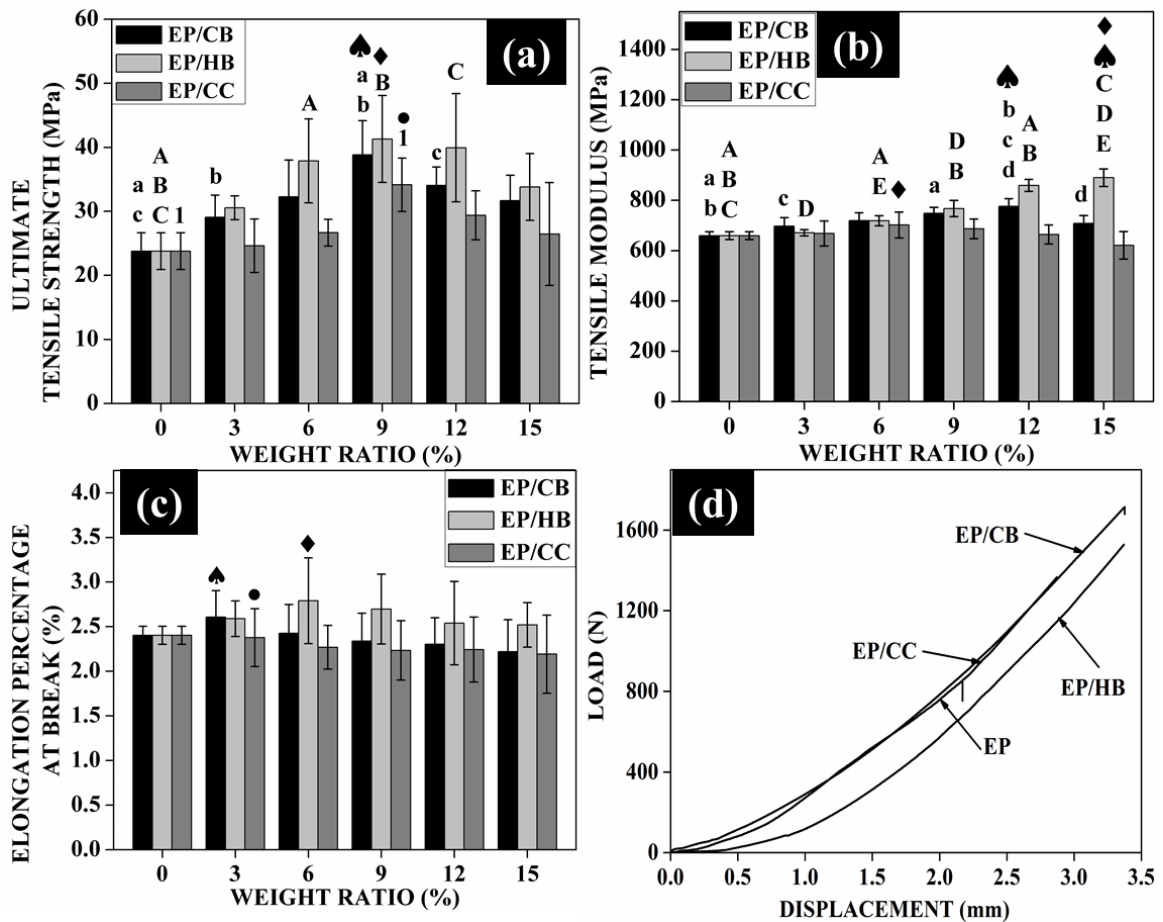


Figure 4.9. (a) Ultimate tensile strength, (b) Tensile modulus, (c) Elongation percentage at break and (d) Load Vs. displacement curve of EP, EP/CB, EP/HB and EP/CC composites. Symbols, numbers, letters in lower case and upper case (inset in figure) indicate pairwise comparison, that they were significantly different ($p < 0.05$).

In figure 4.9b, insets indicate that EP/CB composites prepared at 9 and 12 wt% have significantly higher tensile modulus value than neat epoxy samples. However, there was no significant difference found between these two samples. Furthermore, within EP/CB composites, 3 & 12 wt% and 12 and 15 wt% samples have significant difference in modulus values. For EP/HB composites, 6, 9, 12 and 15 wt% samples have significantly higher value compared to neat epoxy. Moreover within EP/HB composites, samples between 6 & 12 wt%, 9 & 12 wt%, 3 & 15 wt% and 6 & 15 wt% have significantly different values. Besides in EP/CC composites, none of the samples do not

have significant differences. Amongst the highest tensile modulus of three composites (EP/CB, EP/HB and EP/CC at 12, 15 and 6 wt%, respectively), significant difference was found between EP/CB & EP/HB and EP/CC & EP/HB composites. However, there was no significant difference was found between EP/CB (at 12 wt%) and EP/CC (at 6 wt%) composites.

Elongation percentage at break (EPB) for EP/CB, EP/HB and EP/CC composites at different weight ratio are shown in Figure 4.9c. The elongation percentage for EP/CC composites reduced in a continuous manner from 2.4% (neat epoxy) to 2.19% (at 15 wt %). Reduction in elongation percentage was due to poor adhesion between rigid filler material and matrix. For EP/CB and EP/HB composites, EPB increased up to certain weight fraction and then gradually decreased. The maximum elongation percentage for EP/CB and EP/HB composites were 2.6% (at 3 wt%) and 2.79% (at 6 wt%), respectively. Addition of filler at higher weight fraction (15 wt%) resulted in improper bonding between matrix and filler material and decreased the EPB value of composites than neat epoxy (Abdul Khalil et al. 2013). In figure 4.9c, insets indicates that EPB value of all three composites at different weight ratios have no significant difference with neat epoxy sample. Amongst the highest EPB value of three composites (EP/CB, EP/HB and EP/CC at 3, 6 and 3 wt%, respectively), none of the combinations does not have significant difference in values.

Figure 4.9d, demonstrates the typical tensile load-deformation curve for neat epoxy, EP/CB, EP/HB and EP/CC composites at 9 wt%. The graph presents that both neat epoxy and three composites do not shown any yield and necking region. All four materials exhibit typical brittle behavior like large elastic deformation followed by sudden rupture. As expected, the addition of CB, HB and CC particles in epoxy matrix exhibit higher tensile modulus and tensile strength than neat epoxy. There was non-significant reduction in elongation percentage at break found in EP/CB and EP/CC composites than neat epoxy. But in contrast, there was slight improvement in EPB value of EP/HB composites than neat epoxy.

Analysis of tensile properties revealed increase in tensile strength of all three composites until certain level of filler loading and gradual decline subsequently. Tensile strength in particle-reinforced composites generally decreases with increasing filler loading because of the debonding between matrix and filler. This debonding occurs because of uneven particle shape and poor adhesion of fillers with matrix which leads to the crack initiation and reduction in the tensile properties of composites. But in some cases due to proper adhesion between filler and matrix, tensile strength increased with increasing filler loading. Stress transfer from matrix to filler is also beneficial and allows composites to withstand more amount of load with better tensile modulus. EP/HB and EP/CB composites had superior tensile strength than the EP/CC composites (at 9 wt%), because of good interaction between cuttlebone filler and polymer matrix. Some amount of remnant organic matter present in cuttlebone gave good compatibility between the filler and matrix material (Li et al. 2012).

According to percolation theory, distance between the nearest neighbor particles is reduced by increased filler loading resulting in increase in the tensile modulus and decrease in the flexibility of polymer composites (Rout and Satapathy 2012). Experimental results of EP/HB composites showed constant improvement in tensile modulus with increasing filler content, thus indicating adequate adhesion between filler and matrix. Cuttlebone and commercial CaCO_3 particles having the tendency to agglomerate at high filler loading reduce the interfacial adhesion between matrix and filler. However, in EP/CB and EP/CC composites at high filler content tensile modulus decreased due to agglomeration and non-uniform distribution of particles in matrix. Proper bonding at lower weight fraction was also evidenced by the EPB results. In EP/CB and EP/HB composites, EPB increased until certain filler loading and decreased gradually. Thus initial increment in EPB value was based on percolation theory and toughening effect of rigid particles initiated further plastic deformation (Kim and Michler 1998).

Calcite particles have better adhesion than aragonite particles which induces plastic flow at high filler content. As heat treated cuttlebone particles were in calcite

crystal state, it is imperative that calcite filled polymer composites had better tensile strength and modulus than aragonite-filled composites. Even though commercial CaCO_3 particles were in calcite form, the mechanical properties of its composites were lesser than cuttlebone filled composites due to agglomeration phenomenon. Similar observations were made by researchers (Oláh and Tuba 2010) on aragonite/calcite CaCO_3 filled poly-caprolactone composites.

Figure 4.10 shows the flexural strength, flexural modulus and load vs. deformation curve of EP/CB, EP/HB and EP/CC composites. As shown in Figure 4.10a, flexural strength in all the three composites increased until certain weight fraction of filler content and then it decreased. As compared to the neat epoxy resin (54.79MPa), flexural strength of EP/CB, EP/HB and EP/CC composites was increased and reached its maximum value of 69.58MPa (6 wt%), 68.1MPa (6 wt%) and 59.99MPa (3 wt%), respectively. With the further increment of filler content in all the three composites, leads to a substantial reduction in flexural strength. The reason for deterioration of tensile strength at higher filler content could be the same for flexural strength viz. weak interfacial bonding between filler and matrix material due to poor dispersion.

In figure 4.10a, insets indicate that EP/CB composites prepared at 3, 6 and 9 wt% have significantly higher than neat epoxy samples. It denotes that, addition of CB at 3, 6 and 9 wt% in epoxy matrix improved the flexural strength at significant level than neat epoxy. Though, there was no significant difference found between 3 & 6 wt%, 3 & 9 wt% samples. Moreover, the flexural strength of EP/CB composites prepared at 12 and 15 wt% does not have any significant difference with neat samples. It states that strength value of EP/CB composites at 12 and 15 wt% has significantly reduced compared to 3, 6 and 9 wt% samples. For EP/HB composites, samples at 3, 9, 12 wt% do not have significant difference with neat epoxy samples. However, there was a significant difference found between neat and 6 wt% samples. It clearly shown that addition of 6 wt% of HB in epoxy matrix has a good influence on the improvement of flexural strength of composites at significant level compare to neat epoxy. On the other hand, composite at

15 wt% significantly different with all other combinations which denote that strength reduction is in substantial level.

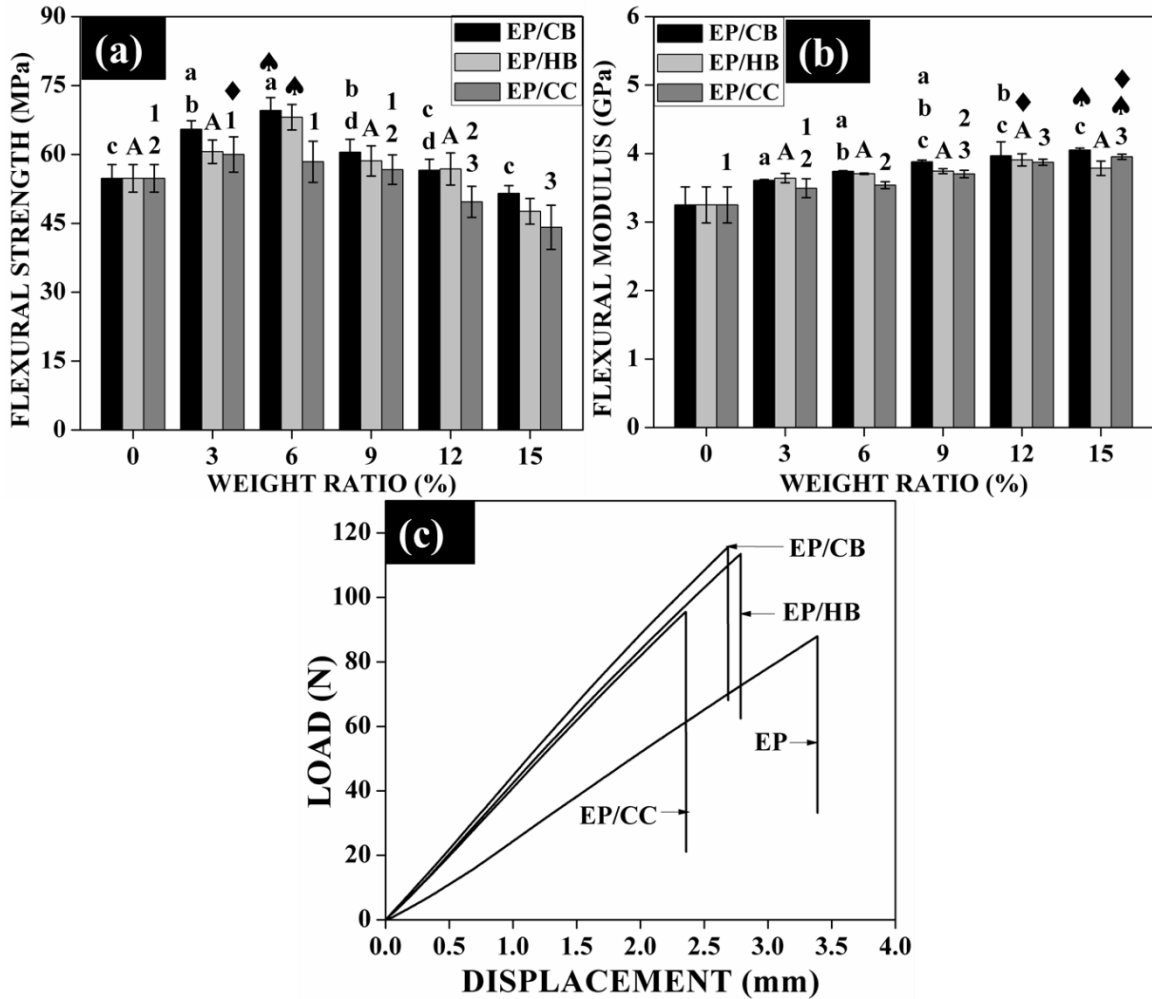


Figure 4.10. (a) Flexural strength, (b) Flexural modulus and (c) Load Vs. displacement curve of EP, EP/CB, EP/HB and EP/CC composites. Symbols, numbers, letters in lower case and upper case (inset in figure) indicate pairwise comparison, that they were significantly not different ($p \geq 0.05$).

In the case of EP/CC composites, the improvement in flexural strength value at 3, 6 and 9 wt% has not significant with neat epoxy. Similarly, values of EP/CC composites at 15 wt% has significantly different with neat, 3, 6, 9 wt% samples which clearly indicates that the reduction in flexural strength at higher filler content is in extensive level. Amongst the maximum flexural strength of three composites, there was no

significant difference was found between EP/CB and EP/HB composites. However, the maximum flexural strength of EP/CC composites value was significantly lesser than other two composites. It concludes that addition of CB and HB particles as reinforcement in epoxy matrix has a significant level of improvement in flexural strength than CC added epoxy composites.

Flexural modulus of EP/CB, EP/HB and EP/CC composites at different weight ratio are shown in figure 4.10b. The neat epoxy has a flexural modulus value of 3.25GPa. In EP/CB and EP/CC composites, flexural modulus was increased continuously by increasing the filler content. The maximum flexural modulus value for EP/CB and EP/CC composites were 4.05GPa (15 wt%) and 3.95GPa (15 wt%), respectively. Besides in EP/HB composites, the maximum modulus value of 3.90GPa was attained at 12 wt%. Beyond that, the modulus value was slightly reduced (3.78GPa at 15 wt%). This result shows that addition of CB, HB and CC particles in epoxy matrix enhances the stiffness property of composites.

Insets in figure 4.10b denote that in EP/CB composites there was significant difference found between neat epoxy and five different filler content samples. In EP/HB composites, there was no significant difference was found between the samples prepared at different weight ratios. But these samples were significantly different with neat sample. It clearly denotes that addition of CB and HB particles in epoxy matrix as a minimal level has significant improvement in modulus values. But there was not a much significant improvement in modulus value of EP/CB and EP/HB composites by increasing the filler content. In EP/CC composites, 6, 9, 12 and 15 wt% samples were statistically different with neat samples. But there was no significant difference was found between neat epoxy and 3 wt% samples. From the above post hoc analysis it's concluded that addition of filler particles into matrix leads to almost a linear improvement in flexural modulus but not in the significant level. Amongst the highest value of three composites, EP/CB has significantly higher value than EP/HB composites. Besides, all other combinations like EP/CB & EP/CC and EP/HB & EP/CC were significantly not different. Its states that EP/CB composite has better stiffness than other composites.

Figure 4.10c displays the flexural load vs. deflection curve of neat epoxy and EP/CB, EP/HB and EP/CC composites prepared at 6 wt%. All four materials exhibit linear trend until failure which confirms the brittle deformation. In comparison with neat epoxy, the initial slope of the EP/CB, EP/HB and EP/CC composites was higher which denotes the increase in stiffness of composites (Rahman et al. 2012). It could be attributed to the reduction of deflection value at break. Moreover, the load taking capability of the epoxy matrix was increased by incorporating the CB, HB and CC particles.

In general, the addition of rigid filler particles in polymer matrix makes the composite become stiffer. The better intermolecular interface between the components of epoxy resin and different filler materials restricts the chain mobility which leads to the increment in flexural modulus. EP/CB and EP/HB composites had better flexural modulus than EP/CC composite is the direct consequence of the organic components present in the filler material. These organic components augment the dispersion of filler in polymer matrix. Despite, slight increment in flexural modulus of composites from 6 to 15 wt%, significant improvement was achieved in lower filler percentage (3 wt%) compare to neat polymer. It shows that better homogeneous dispersion was attained only at lower filler percentage than higher ones. It corroborates with the results of flexural strength. The reduction in flexural modulus of EP/HB composites at 15wt% has due to agglomerations which cause the flow characteristics of rigid fillers and made the composites in porous manner (Fombuena et al. 2014). This could be the reason for the deterioration of material properties of composites.

Usually, addition of smaller particle size filler in epoxy matrix leads to the improvement in flexural strength due to the higher amount of interface regions. Similarly, proper bonding also increases the effective stress transfer between the composite constituent and tends to the improvement in flexural strength. In this case, all the three composites showed a declined trend in flexural strength at the filler content from 9 to 15 wt%.

Poor interface bonding and existence of voids due to particle agglomeration at high filler loading may cause the drop in flexural strength. EP/CB and EP/HB composites had significantly better flexural strength than EP/CC composites. Organic components present in the cuttlebone particles and the high specific surface area has improved the flexural strength of EP/CB and EP/HB composites than EP/CC composites (Khalil et al. 2013, Yao et al. 2013).

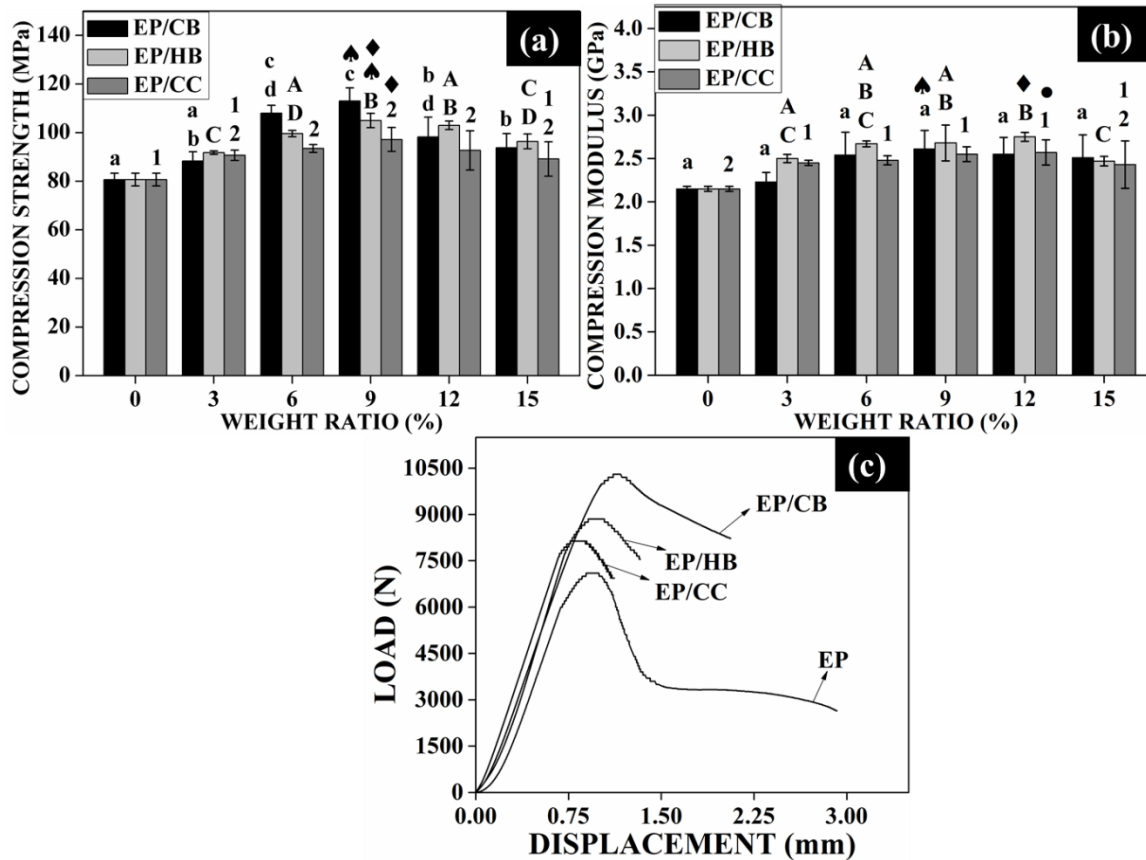


Figure 4.11. (a) Compression strength, (b) Compression modulus and (c) Load Vs. displacement curve of EP, EP/CB, EP/HB and EP/CC composites. Symbols, numbers, letters in lower case and upper case (inset in figure) indicate pairwise comparison, that they were significantly not different ($p \geq 0.05$).

The compression properties and compression load vs. deflection curve of EP, EP/CB, EP/HB and EP/CC composites was presented in figure 4.11. Figure 4.11a indicate that addition of CB, HB and CC particles in epoxy matrix was found to increase

in the strength of the composites until certain weight ratio, and then decrease continuously. The neat epoxy has compression strength of 80.7MPa. The maximum compressive strength of EP/CB, EP/HB and EP/CC composites was attained at 9 wt% filler ratio and it has the value of 113MPa, 105MPa and 97.2MPa, respectively. Beyond this optimum weight ratio of the filler content, compression strength was decreased in all three types of composites. However, formation of more amounts of aggregates at high filler loading acts as a barrier in the improvement of composite strength (Mahshuri and Malina 2014).

In figure 4.11a, insets indicate that EP/CB composites prepared at 6, 9, 12 and 15 wt% have significantly higher than neat epoxy samples. In that, 6 and 9 wt% have higher significant value than other combinations. It denotes that addition of filler content at 6 and 9 wt% has greater influence on the improvement of compression strength of EP/CB composites. However, there was no significant difference found between neat epoxy & 3 wt%, 3 & 12 wt% and 3 & 15 wt% samples. Composites at higher filler percentage (12 & 15 wt%) tend to significant reduction in strength and its almost equal to 3 wt% samples. Similarly, EP/HB composites prepared at five different filler loading have significant improvement than neat epoxy. But there was not much significant difference found within the samples. In EP/CC composites, there was no significant difference found between neat epoxy, 3 and 15 wt% samples. Likewise, no significant difference was found between the samples prepared at five different filler loading. Amongst the highest compression strength of three different composites, EP/CB has significantly higher than EP/CC composites. On the other hand, there was no significant difference found between EP/CB & EP/HB and EP/HB & EP/CC. This results shown that addition of CB particles as reinforcement in epoxy matrix has better enhancement in compression strength than other HB & CC particles.

Compression modulus of EP/CB, EP/HB and EP/CC composites at different weight ratio are shown in figure 4.11b. As like compression strength, compression modulus was also increased continuously upto certain weight percentage and then it decreased. As compared to the neat epoxy resin (2.15GPa), compression modulus of

EP/CB, EP/HB and EP/CC composites was increased and reached its maximum value of 2.61GPa(9 wt%), 2.75GPa and 2.57GPa (12 wt %), respectively. However, beyond these filler content, compression modulus decreased for all three composites. In most of the composites at higher filler percentage, strength was reduced due to premature failure which led by more amounts of stress concentration regions (He and Gao 2015).

In EP/CB composites, samples prepared at different filler loading has no significant difference in compression modulus with neat epoxy sample. Besides, within the different filler loading samples also does not have significant difference (shown in figure 4.11b). It concludes that there was not much improvement in compression modulus of EP/CB composites by the addition of CB particles. Similarly in EP/CC composites, samples prepared at 3, 6, 9 and 12 wt% have significant difference with neat epoxy samples. In addition to, samples at 15 wt% does not have any significant difference with all other samples. The results delivers that addition of CC particles in epoxy matrix from 3 to 12 wt% has significant improvement in compression modulus of the composites. On the other hand, EP/HB composites prepared at different filler loading has significantly different with neat epoxy but there was not much significant difference found within the samples. Amongst the highest modulus value of composites, all three combinations have significantly different with each other. In conveys that, addition of CB and HB particles has given better modulus value of composites than CC particles added ones.

Figure 4.11c represents the compressive load vs. deflection curve of neat epoxy, EP/CB, EP/HB and EP/CC composites. In both tension and flexural, neat epoxy behave in linear manner and rupture suddenly. Nevertheless, in compression it unveiled plastic deformation behavior before failure. Neat epoxy has the tendency of large strain softening region after yielding along with more amount of displacement during failure. Addition of rigid filler particles in epoxy matrix declines the strain softening region (Chen et al. 2013). Moreover it withstands more loads and become more brittle. In EP/CB composites, the strain softening zone is comparatively lower than neat epoxy but it withstand more load without sacrificing the strain at failure. In EP/HB and EP/CC composites, the material failed after yielding point followed by small amount of strain

softening which denotes the brittle failure. However, these composites also withstand more load than neat epoxy but have a significant reduction in strain at failure.

In general, polar groups (hydroxyl group) presents in epoxy resin have better interaction with polar fillers like CaCO_3 which consists of carbonyl or hydroxyl group. Besides, the presence of polar amide groups in CB particles (organic components like protein and chitin) have the tendency to react with epoxide ring groups and induce better bonding between CB fillers and epoxy matrix (He et al. 2011). Due to this capability of organic components present in CB particles, makes the composites as toughened ones. It correlated from the above compression results of EP/CB composites, whereas compression strength increased significantly by increasing the filler content and the modulus was not improved significantly.

In general, addition of rigid filler in epoxy matrix leads to the increase in strength and stiffness but gave adverse effect in strain to failure (He et al. 2013). Nevertheless, the better bonding between filler and matrix makes the effective stress transfer in composite constituent (from matrix to fillers) which leads more plastic deformation. Additionally, these rigid particle filled composites induces the deformation process of composites rather than matrix ones. The reduction in strain softening region was correlated by the better dispersion of filler particles in polymer matrix. This better dispersion induces the localized shear band by high stress concentration region developed around the equilateral plane of filler particles. These localized shear bands join together and bring about dispersed deformation zone by dissipating the energy from matrix to particles in the composite system (Jasso-Gastinel et al. 2009).

Figure 4.12 shows the impact strength and fracture toughness properties of EP/CB, EP/HB and EP/CC composites prepared at different weight ratios. As shown in Figure 4.12a the neat epoxy has impact strength of 2.60KJ/m^2 , and it has increased continuously by increasing the filler content in EP/CB and EP/CC composites. However in EP/HB composites, the impact strength increased until certain weight percentage and then slightly decreased. The maximum impact strength of EP/CB, EP/HB and EP/CC composites was attained of 4.35KJ/m^2 (15 wt%), 3.91KJ/m^2 (12 wt%) and 4.0KJ/m^2 (15

wt%), respectively. Addition of rigid filler particles in epoxy matrix tends to absorb more deformation energy and it's improved the impact strength of the composites (He et al. 2011).

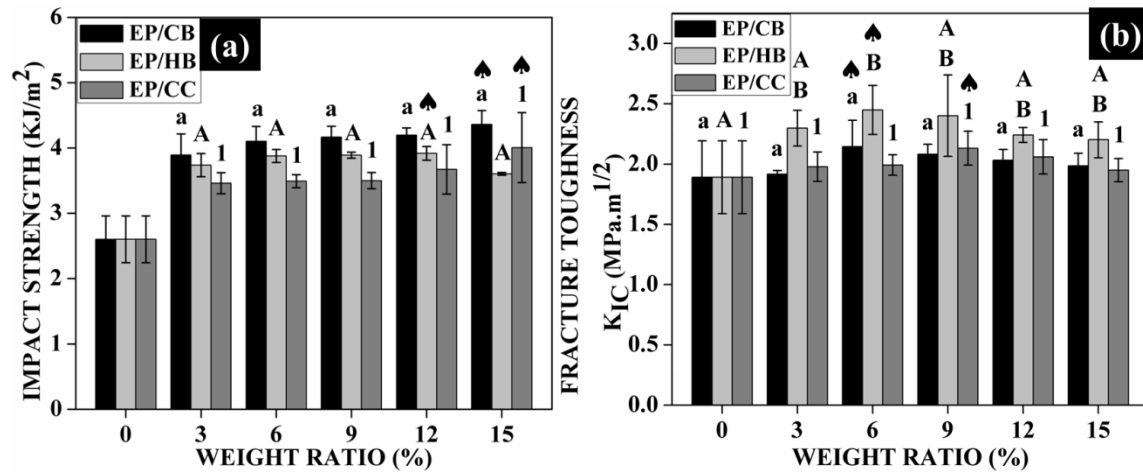


Figure 4.12. (a) Impact strength, and (b) Fracture toughness of EP, EP/CB, EP/HB and EP/CC composites. Symbols, numbers, letters in lower case and upper case (inset in figure) indicate pairwise comparison, that they were significantly not different ($p \geq 0.05$).

In EP/CB composites, samples prepared at 3, 6, 9, 12 and 15 wt% have significantly higher impact strength than neat epoxy. Besides, there was no significant difference was found between the samples prepared at different weight ratios. Similar kind of trend was observed in EP/HB and EP/CC composites. It clearly indicates that addition of filler at smaller weight ratio (3 wt%) led to the significant improvement in impact strength of all three composites than neat epoxy. Furthermore, there was no significant improvement was attained in impact strength of all three composites by increasing the filler content beyond 3 wt%. Similarly, there was no significant difference was found among the highest value of three composites. Even though the impact strength of EP/CB and EP/HB composites was higher than EP/CC composite, but it was not in the significant level. The results concluded that addition of CB and HB particles in epoxy matrix has similar behavior during impact loading.

Over the three composites, EP/CB and EP/HB has slightly higher impact strength than EP/CC composites. The possible reason could be the higher surface area of CB and

HB particles than CC which results in good interfacial combination of filler and matrix by van der Waals and hydrogen bonding (Yao et al. 2013). In addition, organic compounds present in cuttlebone particles lead to better interaction in EP/CB and EP/HB composites and gave better strength by restrict the matrix deformation and crack pinning mechanism. These mechanisms may prolong the crack path length and absorb more energy before failure. At higher filler loading in EP/HB composites, particle-particle interaction makes weak interface region between matrix and filler which may leads the feeble stress transfer mechanism (Sunny et al. 2016). Therefore, the ability to resist the impact load was reduced in composite systems.

Fracture toughness of EP/CB, EP/HB and EP/CC composites prepared at different weight ratio is shown in figure 4.12b. The neat epoxy has the fracture toughness value of $1.89 \text{ MPa}\cdot\text{m}^{1/2}$. Addition of filler particles tends to improve the fracture toughness property of composites until certain weight and then decreased continuously in all three composites. The maximum fracture toughness value of EP/CB, EP/HB and EP/CC composites was reached to $2.14 \text{ MPa}\cdot\text{m}^{1/2}$ (6 wt%), $2.45 \text{ MPa}\cdot\text{m}^{1/2}$ (6 wt%) and $2.13 \text{ MPa}\cdot\text{m}^{1/2}$ (9 wt%), respectively. The results followed the similar trend of impact strength. Owing to proper interaction at lower filler loading, the rigid filler particles restrict the crack propagation and tends to absorbed more amount of energy followed by the improvement in fracture toughness (Zhu et al. 2012).

Insets in figure 4.12b denote that in EP/CB composites, none of the combinations does not have any significant difference in fracture toughness values. Correspondingly, EP/CC composites also following the same trend. It resulted that addition of CB and CC particles in epoxy matrix has slight improvement in fracture toughness property but it was not upto the significant level. Besides, there was no significant difference found by increasing the filler content in composites. On the other hand, in EP/HB composites there was a significant difference was found between neat epoxy and 6 wt% samples. Besides, there was no significant difference was found between neat epoxy, 3, 9, 12 and 15 wt% samples. Similarly, there was no significant difference was found among the highest value of three composites. It concludes that CB and HB particles do not have much

influence in the improvement of fracture toughness property of composites compared to CC particle reinforced composites.

In general, addition of rigid filler particles induces the localized shear band in polymer matrix and development of void growth due to internal cavitation by particles (Teh et al. 2008, Srikanth et al. 2012). The better bonding between rigid filler and matrix leads to the crack deflection along with plastic deformation around the particles resulted in the enhancement of toughness property (Jin and Park 2008, Chen et al. 2013). Besides in few cases, voids present in composites act as barrier for crack propagation. This could be the reason for the initial increment in fracture toughness of all three composites. However, poor dispersion and cluster formation at higher filler loading diminish the resistance of crack propagation followed by deteriorate the fracture toughness of composites.

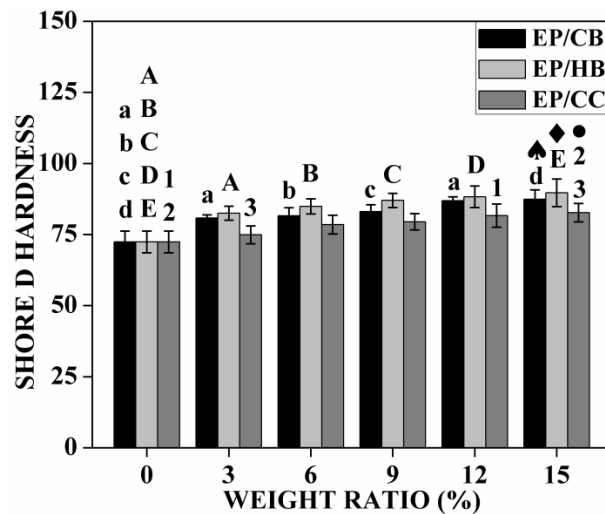


Figure 4.13. Hardness of EP, EP/CB, EP/HB and EP/CC composites. Symbols, numbers, letters in lower case and upper case (inset in figure) indicate pairwise comparison, that they were significantly different ($p < 0.05$).

Shore D hardness of EP/CB, EP/HB and EP/CC composites at different weight ratio are shown in figure 4.13. The neat epoxy has a hardness value of 72.4. In all the three composites, hardness value increased by increasing the filler content. The

maximum hardness value of EP/CB, EP/HB and EP/CC composites were 87.4, 89.7 and 82.7, respectively.

In general, addition of rigid filler particles in epoxy matrix enhanced the hardness of composites. Insets in figure 4.13 indicates that in EP/CB composites there was significant difference found between neat epoxy and 3, 6, 9 & 15 wt% samples. Nevertheless, there was no significant difference found within the samples prepared at 3, 6, 9 and 15 wt%. In addition, neat epoxy, 3 and 12 wt% samples has significant difference between them. In EP/HB composites, samples prepared at different filler content has significantly higher value than neat epoxy. However, there was no significant difference found within the samples. The result clearly states that addition of small amount of CB and HB filler content in epoxy matrix tends to significantly improve the hardness value of composites. On the other hand, there was no significant improvement attained by the increase of filler content in epoxy matrix. In EP/CC composites, combination like neat epoxy & 12 wt%, neat epoxy & 15 wt% and 3 & 15 wt% has been significantly different. It confirms that addition of CC particles at higher filler percentage (12 & 15 wt%) tends to give significant improvement in hardness values. Amongst the highest hardness value of three composites, each one is significantly different with other composites.

In general, addition of hard and brittle phase of particles in soft matrix tends to the improvement in hardness of composites (Fombuena et al. 2014). The results of EP/CB and EP/HB composites corroborated with the above justification by the addition of smaller filler content itself. Besides, EP/CC composites have significant improvement in hardness only at higher filler percentage (12 and 15 wt%) due to its soft nature compared to CB and HB particles. This could be the reason for the lower hardness value of EP/CC composites than EP/CB and EP/HB composites. Similarly, the absence of organic content and volatile matters in HB particle reinforced composites (EP/HB) leads to the superior hardness value than EP/CB composites (Ahmed et al. 2012).

4.1.3 Fracture morphology studies of EP, EP/CB, EP/HB and EP/CC composites

The micrograph of neat epoxy, EP/CB, EP/HB and EP/CC composites (at 9 wt%) are shown in Figure 4.14. A coarse and brittle type fracture surface was observed (indicated by the arrow) in the morphology of neat epoxy as shown in Figure 4.14a. Compared to neat epoxy, EP/CB and EP/HB composites Figure 4.14b–c had smooth fracture surface morphology, thus confirming even distribution of filler particles in matrix material and better interaction between the filler and matrix material. Such morphology appears to initiate the plastic flow and increase the strength and strain of composites. But in EP/CC composite (Figure 4.14d), fracture surface showed “stress whitening” due to debonding between the filler and matrix material. Because of uneven dispersal of filler material in matrix and agglomeration of filler particles (indicated in black circle), the strength and elongation percentage of EP/CC composites got reduced.

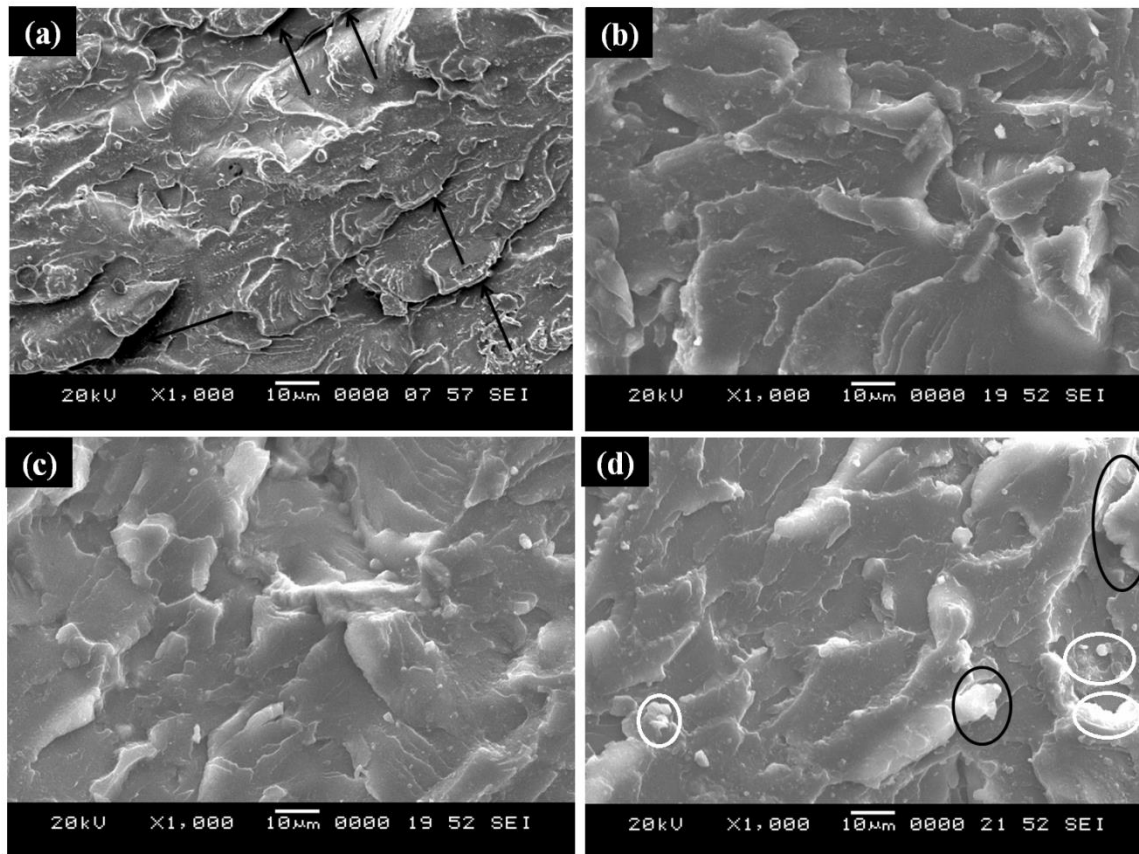


Figure 4.14. SEM micrograph of (a) EP, (b) EP/CB, (c) EP/HB and (d) EP/CC composites at 9 wt% filler loading.

In particle-filled polymer composites debonding of the filler and matrix determines the deformation mechanism. While using rigid fillers, failure occurs by debonding of filler due to stress concentration and it starts shear yielding than crazing. Due to shear yielding mechanism the material withstands more amount of energy before fracture (Zuiderduin et al. 2003).

SEM images of neat epoxy showed brittle type of fracture while EP/CB and EP/HB composites showed smooth fracture surfaces. Previous studies (Intharapat et al. 2013, Li et al. 2012, Hamester et al. 2012 and Poompradub et al. 2008) have reported the use of organic compounds to improve the interaction between CaCO_3 and matrix. Cuttlebone particles having organic compounds on the surface by nature induced good interaction between filler and composites. This was observed to be true even in HB particles that showed remnants of organic compounds even after heat treatment at 400 °C, the findings confirmed by TGA and FT-IR. Hence EP/CB and EP/HB composites had smooth fracture surface than EP/CC composites as a result of higher fracture resistance ensured by shear yielding mechanism. In EP/CC composites, failure occurred due to particle agglomeration and improper bonding of filler with matrix. Hence inorganic fillers are generally subjected to surface modification to improve the adhesion with matrix (Kango et al. 2013). Figure 4.14d shows certain level of agglomeration (indicated by white circle) because of no surface treatment done on the filler surface in EP/CC composites. These agglomerations create voids and debonding that resulted in pre-failure of material.

4.1.4 Density and voids percentage of EP, EP/CB, EP/HB and EP/CC composites

Preparing composites through hand-layup technique leads to the presence of voids and it is ineluctable. The voids percentage of neat epoxy matrix was 2.561% and augmentation of voids percentage was observed by increasing the filler content (from 3 wt% to 15 wt%) in composites. Voids percentage existed in the range of 2.198 to 3.519%, 2.117 to 3.366% and 2.436 to 4.978% for EP/CB, EP/HB and EP/CC composites, respectively. Addition of filler content at 3 wt% in composites showed lesser

voids percentage compared to neat epoxy matrix inferring that up to 3 wt% of filler content in composites reduces the voids percentage. Beyond 3 wt% of filler content, voids percentage in composites was higher than the epoxy matrix because of agglomerations during mixing and debonding of filler and matrix material (Abdul Khalil et al. 2013).

Table 4.5: Theoretical density, actual density and void percentage of EP/CB, HB/EP and CC/EP composites

F.W.R.	EP/CB Composites			EP/HB Composites			EP/CC Composites		
	T.D.	A.D.	V.C.	TD.	A.D.	V.C.	T.D.	A.D.	V.C.
0	1.21	1.179	2.561	1.21	1.179	2.561	1.21	1.179	2.561
3	1.228	1.201	2.198	1.228	1.202	2.117	1.229	1.199	2.436
6	1.247	1.211	2.886	1.247	1.215	2.566	1.248	1.204	3.505
9	1.266	1.225	3.238	1.266	1.231	2.764	1.268	1.216	4.101
12	1.286	1.243	3.343	1.286	1.248	2.954	1.289	1.234	4.267
15	1.307	1.261	3.519	1.307	1.263	3.366	1.312	1.246	4.978

F.W.R.: Filler weight ratio (%); T.D.: Theoretical density (g/cm^3);

A.D.: Actual density (g/cm^3); V.C.: Voids content (%)

At lower weight fraction, filler particles tend to fill the voids created during crosslinking of neat epoxy polymers (Abdul Khalil et al. 2013). However, increase in the void content beyond 3 wt% of filler loading clearly indicates imbalance in the dispersal of filler in the matrix. Compared to EP/CC composite, EP/CB and EP/HB composites had lesser percentage of voids because cuttlebone particles interacted with matrix material in a better way than commercial CaCO_3 .

4.1.5 Physical properties of EP, EP/CB, EP/HB and EP/CC composites

Based on the mechanical, morphological and voids content results of EP/CB, EP/HB and EP/CC composites prepared at different weight fractions, it can be concluded that composites prepared at 9 wt% filler fraction had relatively more advantageous

properties as compared to other filler fraction. Hence these weight fraction composites along with neat epoxy were further subjected to water absorption, wettability, thermal and thermo-mechanical studies.

Figure 4.15a shows the water absorption behavior of EP/CB, EP/HB and EP/CC composites. After 30 days, the maximum amount of water uptake for EP, EP/CB, EP/HB and EP/CC composites was around 0.46%, 0.51%, 0.53% and 0.47%, respectively. However, the best fit curve equation for EP and EP/HB composites was in third order polynomial form with R^2 value of 0.99 and 0.99, respectively. Similarly, the best fit curve equation for EP/CB and EP/CC composites was in second order polynomial ($R^2=0.99$) and logarithmic ($R^2=0.95$) form, respectively.

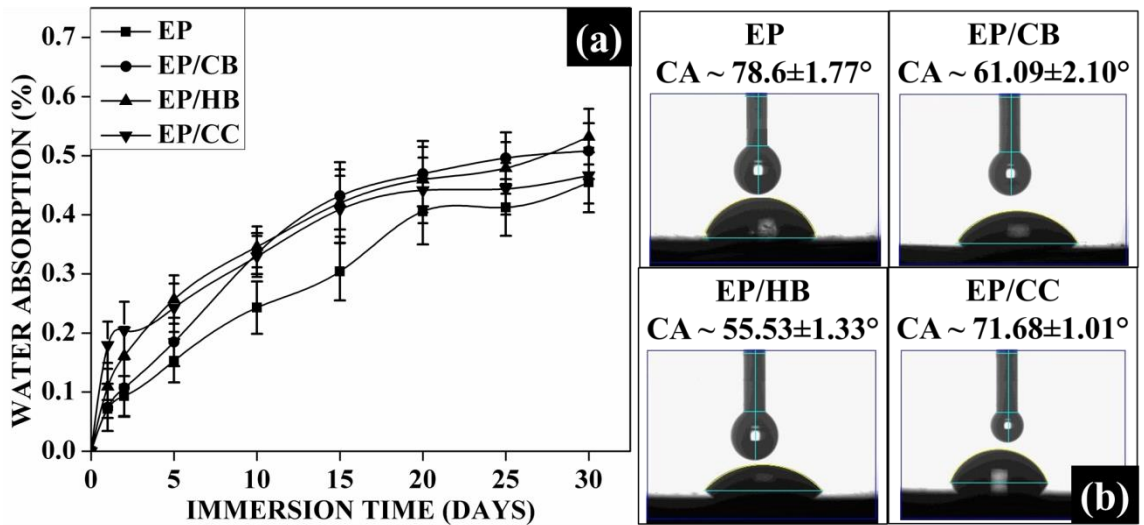


Figure 4.15: Water absorption and Wettability results of (a) EP, (b) EP/CB, (c) EP/HB and (d) EP/CC composites.

The corresponding best fit curve equation for EP, EP/CB, EP/HB and EP/CC composites was mentioned in equation 4.1 to 4.4, respectively.

$$Y = 6 \times 10^{-6} X^3 - 0.0006 X^2 + 0.0281 X + 0.0257 \quad \dots\dots\dots (4.1)$$

$$Y = -0.0007 X^2 + 0.0374 X + 0.0231 \quad \dots\dots\dots (4.2)$$

$$Y = 4 \times 10^{-5} X^3 - 0.0025 X^2 + 0.054 X + 0.0372 \quad \dots\dots\dots (4.3)$$

$$Y = 0.0916 \ln(X) + 0.1456 \quad \dots\dots\dots (4.4)$$

The results indicates that addition of CB, HB and CC particles as reinforcement in epoxy composites leads to the slight improvement in water absorption properties for a period of 30days. Researchers stated that hydrophilic nature of reinforcement particles and free volume of the polymer could be the reason for improvement in water absorption properties of neat matrix and composites (Raju and Kumarappa 2011). In general, CaCO_3 contains hydroxyl group which appeal to water molecules through hydrogen bonding (Abdul Khalil et al. 2013). However, none of the composites reached the saturation level of water absorption even after 30 days. The impenetrable reinforcement particles in composites make the water molecules to diffuse in tortuous pathway which induce the unsaturation level of water absorption at the end of experiment (Kornmann et al. 2005). In our case, CB and HB particle reinforced composite has higher percentage of water absorption compared to CC particle reinforced composites. Even though, EP/CC composites has higher voids percentage and lower cross link density (which discussed in upcoming topic), the water absorption percentage is lesser than other two composites. Owing to the hydrogen bonding between filler and matrix, presents of amide based organic components in CB particles and hygroscopic nature of HB particles leads to the more water absorption property than EP/CC composites (Zhao and Zhang 2008 and Bagheri et al. 2015).

Moreover, these results are well agreed with contact angle studies. The water contact angle for EP, EP/CB, EP/HB and EP/CC composites was $78.6 \pm 1.77^\circ$, $61.09 \pm 2.10^\circ$, $55.53 \pm 1.33^\circ$ and $71.68 \pm 1.01^\circ$, respectively. However, all four materials showed a hydrophilic behavior because of its contact angle was less than 90° . The addition of reinforcement filler in epoxy matrix tends to increase the wettability of composites. In that, EP/HB and EP/CB composites have higher wettability/lower contact angle than EP and EP/CC ones.

4.1.6 Thermo-mechanical and thermal properties of EP, EP/CB, EP/HB and EP/CC composites

Figure.4.16a shows the thermal Stability of EP, EP/CB, EP/HB and EP/CC composites. The composites exhibit two stages of degradation. The initial stage of degradation occurred in the temperature range of 25°C to 280°C. The possible reason could be the breaching of uncured epoxy resin and/or the traces of impurities from the cured parts (Zhu et al. 2012). The second major weight loss occurred in the temperature range of 300°C to 400°C, which was due to the thermal degradation of composites and epoxy network. Temperature at the maximum rate of degradation (T_{max}) was calculated from the DTG curve of composites (Figure 4.16b). Besides, thermal stability factors like activation energy (E_a), integral procedure decomposition temperature (IPDT) and char yield at 650°C (CY) were presented in table 4.6.

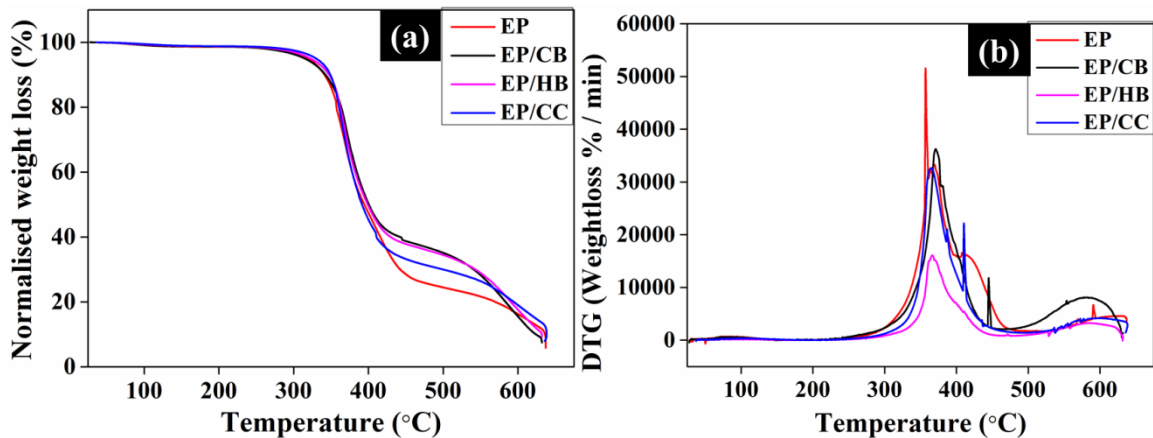


Figure 4.16 (a) TG and (b) DTG of EP, EP/CB, EP/HB and EP/CC composites

TGA results showed that addition of CB, HB and CC fillers improved the thermal properties of the composites than neat epoxy. EP/CB and EP/HB composites had higher T_{max} than EP/CC and EP composites. Moreover, IPDT clearly showed EP/CB had good thermal stability followed by EP/HB, EP/CC and EP composites. Amide group present in the organic matters of CB and HB particles made a proper interaction between epoxy resin and fillers which significantly slow down the degradation process. This, in turn, increases the T_{max} and IPDT value of the EP/CB and EP/HB composites. Similarly, activation energy increased with the addition of the CB, HB and CC reinforcement filler

in EP because of the high surface contact area between reinforcing filler and matrix (Shimpi and Mishra 2012).

Table 4.6: Thermal properties of EP, EP/CB, EP/HB and EP/CC composites

Composite	T _{max} (°C)	IPDT (°C)	E _t (KJ/mol)	Char Yield (%)
EP	356.8	453.3	117.1	5.82
EP/CB	371.8	480.8	130.4	7.46
EP/HB	366.3	490.0	133.8	9.28
EP/CC	364.7	474.1	150.3	7.95

But activation energy of EP/CC composites was higher than neat epoxy and other composites. During decomposition of EP/CC composites, pure calcite form CC particles led to reduce the heat diffusion which resulted in more activation energy. Besides, the char yield at 650°C was found to be increased in EP/CB, EP/HB and EP/CC composites compared to neat epoxy. Overall, TGA results revealed EP/CB and EP/HB composites showing better thermal stability than EP and EP/CC. Similar observations had been reported with epoxy/ mineral nanoparticles composites (Jin and Park 2012, Shimpi and Mishra 2012 and Ramdani et al. 2014).

Figure 4.17 shows the (a) storage modulus and (b) mechanical loss factor ($\tan\delta$) with respect to temperature for EP, EP/CB, EP/HB and EP/CC composites. Furthermore, the storage modulus, gain in percentage of storage modulus and glass transition temperature of all four materials are summarized in table 4.7. The storage modulus for neat epoxy was 2.57GPa. By the addition of different reinforcement particle in epoxy matrix tends to increase the storage modulus of composites. The storage modulus of EP/CB, EP/HB and EP/CC composites increased and reaches the value of 4.48GPa, 5.04GPa and 3.93GPa, respectively. As presented in table 4.7, the increase in percentage of storage modulus for EP/CB, EP/HB and EP/CC composites with respect to neat epoxy was 74.31%, 96.1% and 52.91%, respectively. The increase in storage modulus of composites was probably due to the addition of stiffened CaCO₃ particles in epoxy matrix which restricts the matrix deformation (Ramdani et al. 2014).

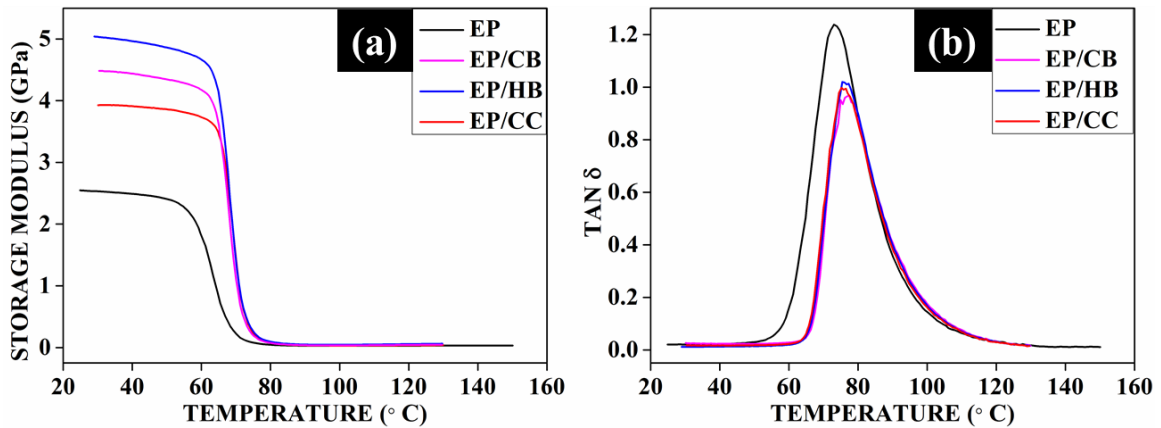


Figure 4.17 (a) Storage modulus and (b) $\tan\delta$ of EP, EP/CB, EP/HB and EP/CC composites.

As shown in figure 4.17a, storage modulus of all four composites has a gradual drop upto glass transition region. At the region of glass transition there was sudden drop in storage modulus identified in all four composites. These changes denote that material has transferred from glassy to rubbery region. In this case, the storage modulus of EP/CB and EP/HB composites was enhanced tremendously due to the increase in interfacial bonding between filler and matrix through covalent bond. Besides, the storage modulus of EP/CC composites was comparatively lower than other two composites. The possible reason could be the poor dispersion of particles in matrix which leads to poor interactions (Ramdani et al. 2014).

The glass transition temperature (T_g) of composites was determined from the peak point of $\tan\delta$ curve (shown in figure 4.17b). As compared to the neat epoxy, composites filled with CB, HB and CC particles as reinforcement has a slight enhancement in T_g values. The T_g value of EP, EP/CB, EP/HB and EP/CC composites was 73.03°C, 77.41°C, 75.48°C and 75.18°C, respectively. The possible reason could be the better matrix/particle interaction in composites and also the restriction in matrix mobility through the filler material (Rahman et al. 2013). Apart from the T_g , damping factor of the prepared composites was extracted from the $\tan\delta$ curve (shown in figure 4.17b). Addition of stiffened CaCO_3 particles in epoxy matrix tends to decline in the damping factor

through diminishes in peak intensity along with the peak broadening (Mohd Zulfli et al. 2013).

In general, composite material relaxation phenomenon was estimated through T_g values. The possible reason for the enhancement in T_g value is mainly due to the reduction in free volume of polymers, increase in number of successive cross links and decrease in chain mobility of polymers (Yasmin and Daniel 2004). The intensity of $\tan\delta$ will increase by faster the molecular motion along with transition. The reduction in molecular mobility leads to the broadening of peaks along with the decrease in $\tan\delta$ peak intensity, due to the heterogeneity of polymer network (Núñez et al. 2002). In this case, the T_g value of EP/CC and EP/HB composites were lower than EP/CB composites. The higher in T_g value of these two composites could be attributed through the amide group present in the organic components of CB and HB particles have an good interaction with hydroxyl group present in the epoxy matrix (Wang and Qin 2007).

Table 4.7: Storage modulus, gain in storage modulus and glass transition temperature of EP, EP/CB, EP/HB and EP/CC composites

Composite	Storage Modulus (GPa)	Gain in Storage Modulus (%)	Glass transition Temperature from $\tan\delta$ ($^{\circ}\text{C}$)
EP	2.57	--	73.03
EP/CB	4.48	74.31	77.41
EP/HB	5.04	96.10	75.48
EP/CC	3.93	52.91	75.18

The swelling ratio, crosslink density and molecular weight between crosslinks of EP, EP/CB, EP/HB and EP/CC composites were presented in table 4.8. The swelling ratio of neat epoxy was 0.6004. Similarly, the swelling ratio of EP/CB, EP/HB and EP/CC composites was 0.372, 0.4142 and 0.461, respectively. As compared to the neat epoxy, the swelling ratio of all three composites was decreased. It showed that addition of rigid filler particles in epoxy matrix tends to restrict the penetration of solvent in composites due to the better bonding between filler and matrix material (Ku et al. 2013 and Ahmed 2015).

Table 4.8: Swelling ratio, crosslink density and molecular weight between crosslinks of EP, EP/CB, EP/HB and EP/CC composites

Composite	Swelling ratio (S.R)	Crosslink density (ν) (mol/cm^3)	Molecular weight between crosslinks (M_c)
EP	0.6004	0.0047	212.43
EP/CB	0.372	0.0073	136.71
EP/HB	0.4142	0.0063	159.23
EP/CC	0.461	0.0059	168.85

Amongst the three composites, the swelling ratio was higher in EP/CC followed by EP/HB and EP/CB. Organic components present in CB particles leads to give better bonding with polymer matrix. Similarly, slight amount of organic components present in HB particles tends to give comparatively higher swelling ratio than EP/CB composites. But in the case of EP/CC composite, the particle-matrix interaction is poor which leads to more voids formation. This may attribute to absorb more solvent and gave maximum swelling ratio.

Addition of CB, HB and CC particles in epoxy matrix tends to increase the cross link density of composites. As compared to neat epoxy ($0.0047\text{mol}/\text{cm}^3$), EP/CB composites has higher cross link density ($0.0073\text{mol}/\text{cm}^3$) followed by EP/HB ($0.0063\text{mol}/\text{cm}^3$) and EP/CC ($0.0059\text{mol}/\text{cm}^3$). This cross link density behavior of all four composites is well agreed with their corresponding glass transition temperature. The addition of thermally stable rigid filler in epoxy matrix attributes the interlocking formation of matrix which induces more cross link density (Ahmed et al. 2012 & Rahman et al. 2013). Furthermore, the average molecular weight between crosslinks was inversely proportional to cross link density. In that EP/CB composite has lower value compare to other two composites.

4.1.7 Biocompatible properties of EP/CB and EP/HB composites

Based on the thermal, thermo-mechanical, and physical properties results of EP, EP/CB, EP/HB and EP/CC composites it can be concluded that EP/CB and EP/HB

composites had relatively more advantageous properties as compared to other two materials. Hence these two composites were further subjected to biocompatibility studies.

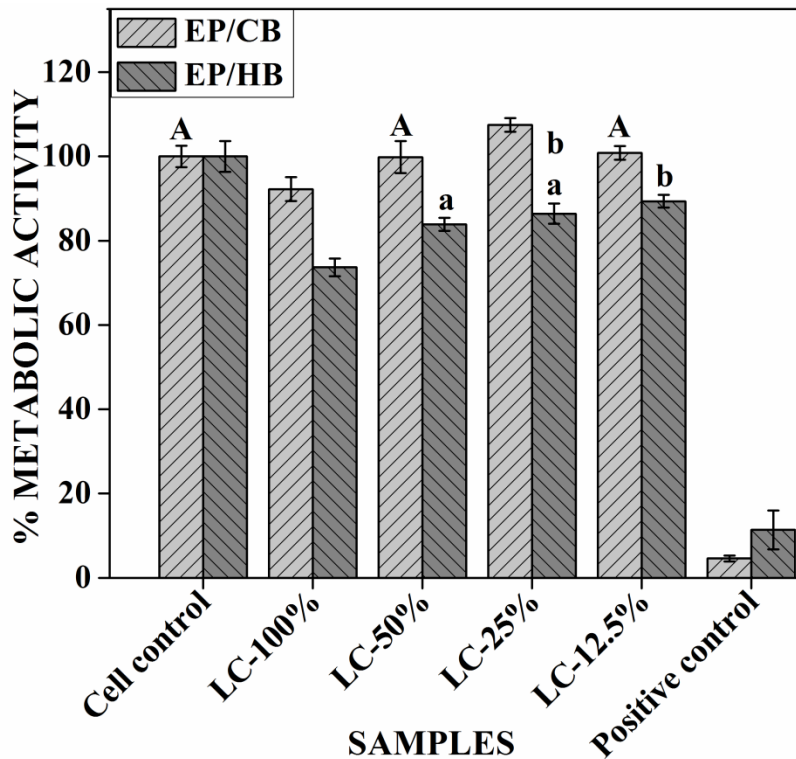


Figure 4.18 “*In vitro*” cytotoxicity of EP/CB and EP/HB composites. Data are expressed as percentage of control mean \pm S.D. of six independent experiments. Letters indicate pairwise comparison, that they were significantly not different ($p \geq 0.05$).

In this topic two different groups of composites (EP/CB and EP/HB) were analyzed. Each test group consists of five different sets (cell control, 100%, 50%, 25% and 12.5% leach concentration). Results are expressed in the form of mean \pm Standard deviation of 6 experiments. Statistical analyses were performed by one-way ANOVA and Tukey’s honestly significant difference method was used for all post hoc analysis to identify the significant difference between each set of individual test group. In all the tests, statistical significance was set at $p < 0.05$. Letters in upper case (A and B) and lower case (a, and b) was used to denote the statistical results in EP/CB and EP/HB test group, respectively.

Figure 4.18 shows the cell viability percentage of EP/CB and EP/HB composites at various leach concentration (LC). For EP/CB composites, the cell viability percentage at 100%, 50%, 25% and 12.5% leach concentrations were 92.23%, 99.83%, 107.51% and 100.81%, respectively. Similarly for EP/HB composites, the cell viability percentage at 100%, 50%, 25% and 12.5% LC were 73.69%, 83.9%, 86.42% and 89.36%, respectively. The results clearly indicate that EP/CB composites do not show any toxic effect at all LC.

As compared to control sample, there was a significant decrease was found in the cell viability percentage of EP/CB composites prepared at 100% leach concentration. Besides, reduction in LC percentage (upto 25%) tends to increase the cell viability percentage of EP/CB composites. EP/CB composite samples prepared at 50 and 12.5% LC does not shown any significant difference with control sample. Proliferation of cells was identified in EP/CB composite sample prepared at 25% leach concentration. In addition, the increment in cell viability percentage was significantly different with control samples.

In the case of EP/HB composites, samples at 100% LC shown slight toxic (73.69%). Besides, there was a continuous improvement in cell viability % by further reducing the LC. The cell viability percentage of samples prepared at four different concentrations has significantly different with control samples. But there was no significant difference was found between the combinations of 50 & 25% and 25 & 12.5%.

Moreover, the viability of cell at different LC for EP/CB and EP/HB composites is shown in figure 4.19. In EP/CB composites, more number of viable cells was identified (figure 4.19a). In EP/HB composites at 100% LC showed the depletion of more number of viable cells (figure 4.19b). However, by reducing the LC the number of viable cells was increased (figure 4.19c-e).

The results suggest that addition of CB as reinforcement has diminished the toxic level of epoxy matrix. Apart from that, presence of organic components in CB particles tends to prolife the cells at lower level leach concentrations (25 & 12.5%). On the other hand, EP/HB composite (removal of organic compound from cuttlebone by heat treatment) at 100% LC does not diminish the toxic level of epoxy resin (Fu and Zhao

2004). Nevertheless, by reducing the LC % (from 50 to 12.5%) in EP/HB composites tends to give the better cell viability. From the above results it's concluded that organic matters play a vital role in improving the biocompatibility property of epoxy composites.

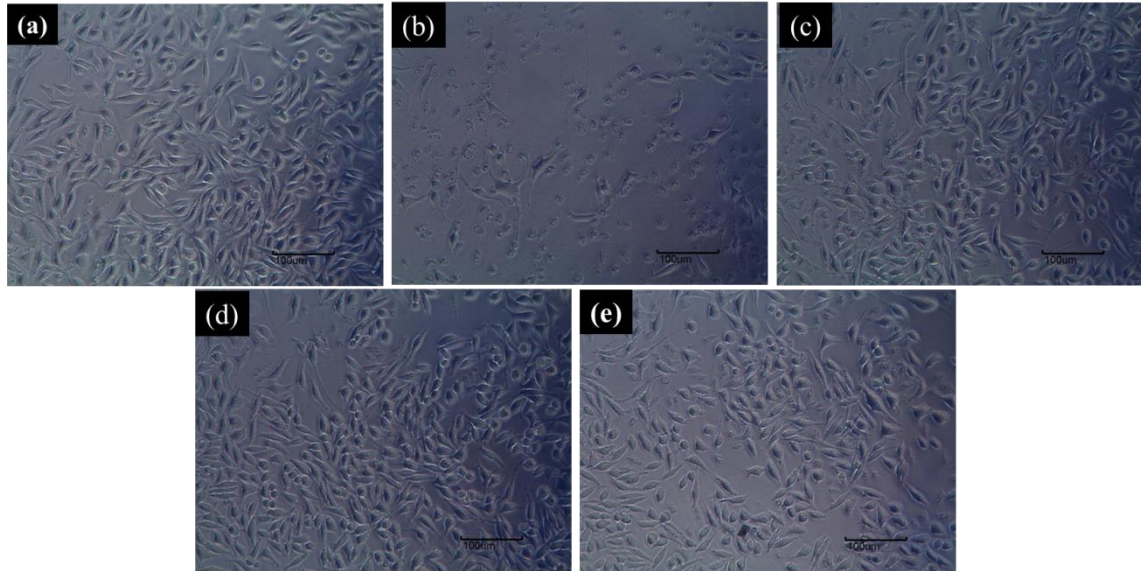


Figure 4.19 Microscopic images of viable cells for (a) EP/CB composite prepared at 100% leach concentrations, (b-e) EP/HB composite prepared at 100, 50, 25 and 12.5% Leach concentrations.(scale bar:100µm)

Table 4.9 shows the hemolytic activity of the prepared composite samples. The average percentage of hemolysis was 0.07%. Hemolysis % of EP/CB and EP/HB samples were found to be 0.033 and 0.033, respectively. From the above results it is concluded that both the sample are in non-hemolytic nature.

Table 4.9: Hemolysis percentage of EP/CB and EP/HB composites.

Samples	% Hemolysis	Average Hemolysis %	Normal Hemolysis
EP/CB	0.033	0.07	< 0.1%
EP/HB	0.033	0.07	

There was no significant difference was found between two samples. There are many reasons that could improve the blood compatibility of the composites. The possible reason could be a) hydrophilic nature, b) surface roughness of particles and c)

biocompatibility CaCO_3 fillers (Selvakumar et al. 2014 and Janaki et al. 2008). The observed results may confirm that addition of CB and HB particles in epoxy matrix tends to improve the blood compatibility of composites.

4.1.8 Summary

To summarize the results from this chapter, the influence of cuttlebone bio-filler & commercial CaCO_3 reinforced epoxy composites (EP, EP/CB, EP/HB and EP/CC) was discussed. CB particles are in flake form with higher surface area than CC particles. CB consists of CaCO_3 in aragonite polymorph form with small amount of organic matters. HB & CC consists of CaCO_3 in calcite polymorph form. EP/HB composites have better tensile modulus, tensile strength, elongation % at break, hardness and fracture toughness. EP/CB have better strength (flexural, compression and impact) and modulus (flexural and compression). EP/CB and EP/HB shown smooth fracture surface. EP/CB composites shown more voids in higher filler percentage than other composites. EP/CC composites required high activation energy to decompose than EP/CB and EP/HB composites. EP/CB composite showed higher T_g than EP/HB and EP/CC composites. EP/CB composite shown higher crosslink density than EP/HB and EP/CC composites. EP/HB and EP/CB composites absorbed more water than other composites. All four materials shown hydrophilic surface. EP/CB composite shown better metabolic activity at all leach concentration. But EP/HB shown slight toxic at 100% leach concentration. Both EP/CB and EP/HB are non-hemolytic.

CHAPTER 5

CHAPTER 5

INFLUENCE OF CUTTLBONE DERIVED BIO CERAMICS AS REINFORCEMENT IN EPOXY COMPOSITES

This chapter describes the utilization of cuttlebone derived bio ceramics as reinforcement in epoxy composites. Different cuttlebone derived bioceramics (calcium oxide, hydroxyapatite and tricalcium phosphate) used in composites was attained by mechano-chemical method and/or followed by heat-treatment. Ceramic phase confirmation, elemental composition, particle morphology and thermal stability were confirmed with different characterization techniques. Composites were prepared with different cuttlebone derived bioceramics as reinforcement in epoxy matrix. Material properties like mechanical, physical, thermal, thermo-mechanical and biocompatibility of the composites developed were analyzed. Cuttlebone derived hydroxyapatite reinforced epoxy composites showed favorable material properties for biomedical applications.

5.1 Results and Discussions

5.1.1 Characterization of CO, HA and CP particles

Figure 5.1 shows the particle size distribution of cuttlebone derived calcium oxide (CO), hydroxyapatite (HA) and tricalcium phosphate (CP). The percentage of derivative volume of particle (dV/dD) against particle size is shown in these plots. The average particle size for CO, HA and CP particles are 6.24, 0.74 and 1.01 μm , respectively. The cumulative volume percentage of these three particles at different size range, mean particle size with standard deviation value is shown in Table 5.1. Similarly as like cuttlebone particles, there was broad distribution in particle size was found for CO particles even after calcinated at 800°C. As a whole, 40% of CO particles were in the size of less than 5 μm and the remaining 60% of particles were in the size range of 5-10 μm . But for HA and CP particles the size distribution was narrow because of higher

processing time period in hot plate stirrer. As a result of, cuttlebone derived HA and CP particles were in the size range of 0.5-1 μm and 0.5-1.5 μm , respectively.

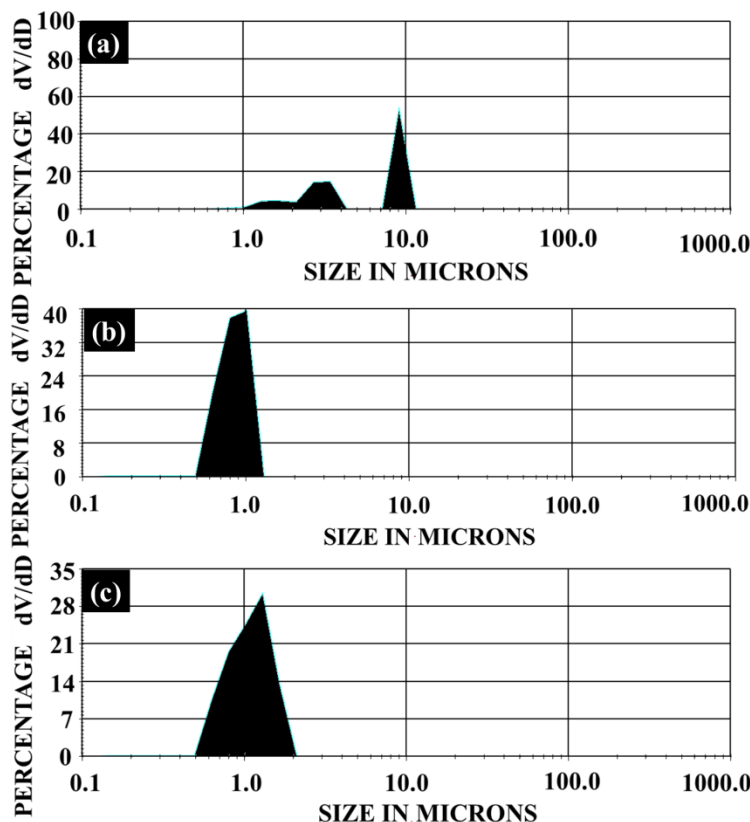


Figure 5.1. Particle size distribution of cuttlebone derived (a) Calcium oxide, (b) Hydroxyapatite and (c) tri calcium phosphate particles.

Table 5.1. Volume percentage of particles at different size range and mean particle size of cuttlebone derived CO, HA and CP particles.

Material	Cumulative volume %						Mean particle size with standard deviation (μm)
	<18 μm	<15 μm	<10 μm	<5 μm	<1.5 μm	<1 μm	
CO	100	100	100	40	10	-	6.24 \pm 3.32
HA	100	100	100	100	100	100	0.74 \pm 0.05
CP	100	100	100	100	100	45	1.01 \pm 0.26

Density, surface area and pore volume of CO, HA and CP particles are presented in Table 5.2. The density of CO was slightly higher than HA and CP particles. However,

the surface area of HA and CP particles were higher than CO because of the particle size and aspect ratio.

Table 5.2. Density, surface area and pore volume of cuttlebone derived CO, HA and CP particles.

Material	Density (g/cm ³)	Surface area (m ² /g)	Pore volume (cm ³ /g)
Calcium Oxide (CO)	2.29	4.47	0.0046
Hydroxyapatite (HA)	2.14	9.12	0.0247
TriCalcium Phosphate (CP)	1.83	8.38	0.0198

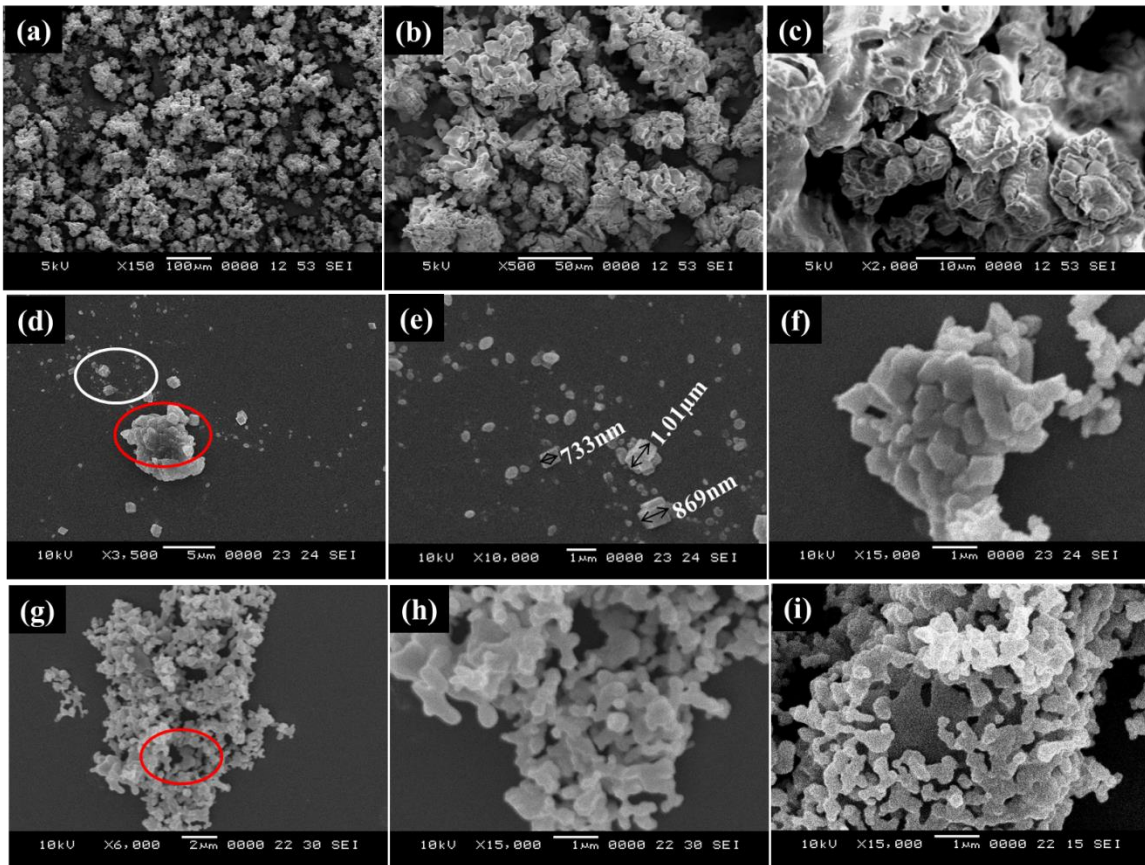


Figure 5.2. SEM micrograph of (a-c) CO (d-f) HA and (g-i) CP particles.

Figure 5.2a to i shows the morphology of CO, HA and CP particles. The CO particles (figure 5.2a to c) were diverse in size which varied from fine to large spherical shape of particles. However, both HA and CP particles were in sub microns level and

shows higher degree of agglomeration. The SEM results shows that the size of HA and CP particles were in the range of 1-3 μm due to the agglomeration phenomenon, but the dominant size were in the range of 0.5-1 μm . However all three particles were in white colored and smooth surface in nature. The agglomeration and particle shape for HA and CP particles was further corroborated with TEM results (Figure 5.3). Particle shape of HA particles were in the mixed form of cubical and spherical form (figure 5.3a to c). But figure 5.3d to f shows that CP particles were in rod structure. Besides, aggregates were also evidenced in both the samples at lower magnification (Figure 5.3 a & d).

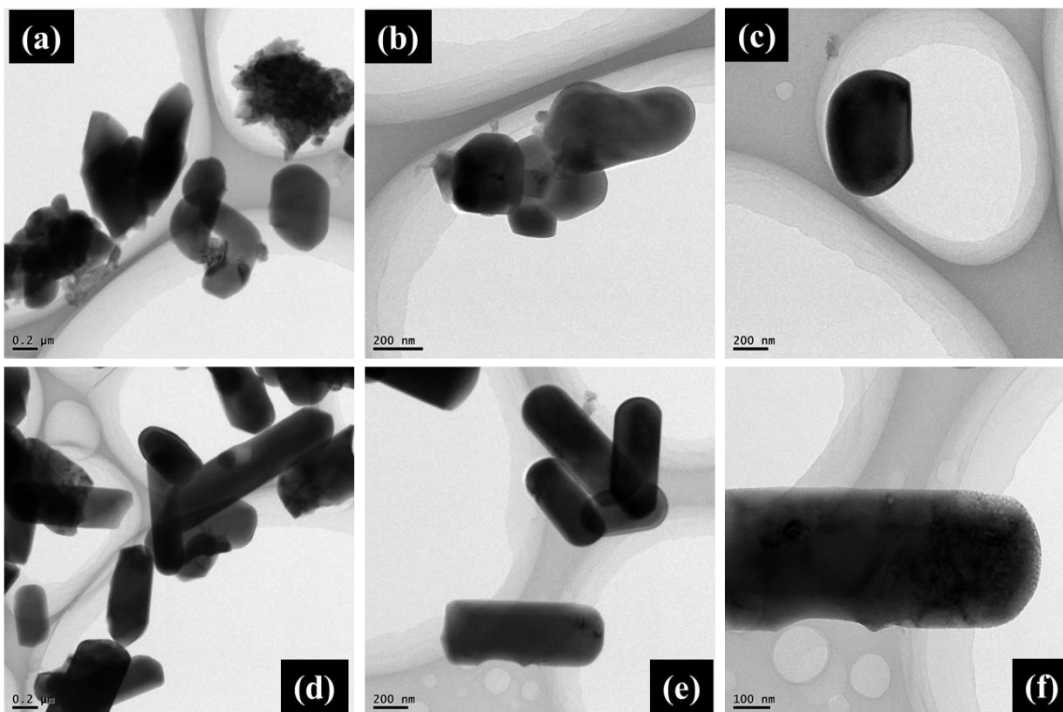


Figure 5.3. TEM micrograph of (a-c) HA (d-f) CP particles.

The Ca/P molar ratio for HA and CP particles was confirmed through ICP-OES and the values are 1.72 and 1.53, respectively. Similarly, SEM-EDX was also used to measure the Ca/P molar ratio for these two particles and it was marginally higher (HA: 1.95 and CP: 1.62) than ICP-OES results.

Based on the characterization results it's concluded that density of HA and CP particles were lesser as compared to CO particles due to the addition of phosphoric acid

during synthesis. Besides, higher phosphate content in synthesized particles tends to show the lower density. The density trend for the three different materials are in the order of CO > HA > CP.

Table 5.3. Ca/P molar ratio of cuttlebone derived HA and CP samples by EDX and ICP-OES analysis

	Ca/P molar ratio	
	HA	CP
ICP-OES in wt%	1.72	1.53
EDX in wt%	1.90	1.62

The particle size of CO particles was slightly lower than cuttlebone particles. The reduction in size occurred because of sintering effects and attrition in particles due to higher calcination temperature (Zhu et al. 2011). However, size distribution was broad and as similar as cuttlebone particles. Similarly the HA and CP particles prepared through mechanochemical followed by calcination method has remarkable reduction in particle size. Both the particles were in sub-micron size after synthesis process. This could be obtained by the continuous grinding during hot plate stirring and the subsequent high temperature calcination process. Owing to higher calcination temperature during conversion process, the particle size distribution of these two particles was even. It was reported by Li et al. 2013 that calcination temperature has higher influence on the crystalline phase, particle size and its distribution during the preparation of calcium phosphates. The reduction in particle size was further corroborated with surface area results. The specific surface area for HA and CP particles were in 8-9m²/g which denotes that the particles were in sub-micron level. Though Wang and shaw 2009 reported that the surface area for submicron particles was slightly higher than these range. It clearly indicates that the prepared HA and CP particles were in agglomerated form. Similarly in CO particles, the reduction in surface area was due to the particle sintering. The aggregates of particles were further validated through SEM and TEM analysis.

The SEM results of CO particles shown slight aggregation at lower magnifications (Figure 5.2a & b). Similarly HA and CP particles also shown higher amount of agglomeration. The result for both particles shows wide range of size distribution from sub-micron to few microns. During synthesis process, mechanical stirring for higher time period having the tendency to reduction of particle size from microns range to sub-micron level. Further calcination leads to the aggregates of primary particles and forms secondary particles in agglomerated form at micron size range (Sanosh et al. 2009). These primary particles presents in sub-micron range was further validated by TEM analysis. The SEM results clearly indicate that HA and CP particles have tendency to get agglomerate due to high surface area. To short out these agglomerations, ultrasonication treatment has been conducted to break the agglomeration. The Ca/P molar ratio identified through ICP-OES varies with experimental values. The variation for HA samples was marginally high compared to CP samples. This could be happened during stirring and calcination time period. These variations may leads to the presence of carbonate groups and formation of biphasic crystalline form which is further evaluated through XRD and FT-IR techniques.

5.1.1.1 Thermo gravimetric analysis of CO, HA and CP particles

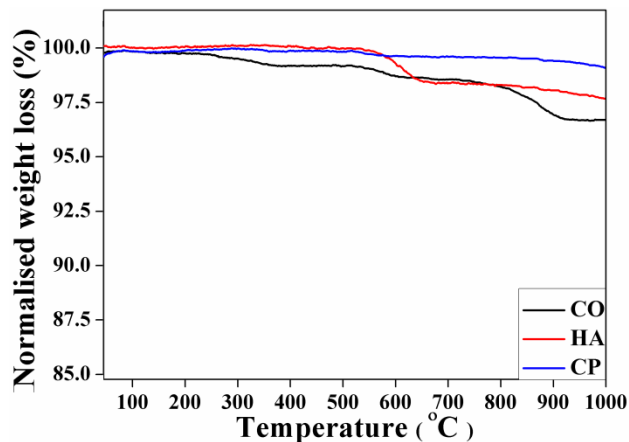


Figure 5.4. TG of cuttlebone derived calcium oxide (CO), Hydroxyapatite (HA) and tricalcium phosphate (CP) particles.

Figure 5.4 shows the TGA curves for CO, HA and CP particles. The TGA curve for CO particles exhibits three stages of degradation as shown in Figure 5.4. The initial

stage of degradation occurred at 250 to 350°C. The weight loss at 350 °C was around 0.5%. The second minor stage degradation starts at 500°C and ends at 600°C. The total weight loss at 600°C was around 1%. The reason could be the decomposition of hydroxide. The third stage of degradation occurred in the temperature range of 750-900 °C and the weight loss in this stage was around 2%. The calcium carbonate present as traces in CO samples was decarbonized at this temperature range. The total weight loss for CO samples at 900°C was around 3%. The HA samples were thermally stable up to 550°C. This samples exhibits slight degradation at the temperature range of 550-650 °C and the weight loss was around 1.25%. The degradation of hydroxide compounds could be the possible reason for the weight loss. Besides, there was no weight loss observed up to 1000°C. Similar kind of observation was identified for CP samples. The sample was thermally stable up to 1000°C and the total weight loss was less than 1%. Based from the TG analysis it has been concluded that HA and CP samples were thermally more stable than CO samples. Besides, small amount of CaCO₃ in traces form and slight phase conversion from calcium oxide to calcium hydroxide was also identified in CO samples.

These CO particles was prepared through decarbonation process by calcined the cuttlebone particle at 800°C. These decarbonation process induce CO₂ dissociation which proceeds from particle outer surface to inner one. During the dissociation has taken place inside the particles, a thin CO₂ layer has formed concurrently on the outer surface which tends to the recarbonation of particles to CaCO₃. This could be possible reason for the presence of CaCO₃ as traces in CO particles. As mentioned in previous chapter (TG curve of cuttlebone particles (figure 4.3a & b)) cuttlebone consists of CaCO₃ has decomposed into CaO at the temperature of 757.46°C. However even after calcinated at 800°C, cuttlebone was not fully converted into CaO. Consequently, predicted decomposition temperature of cuttlebone derived CaCO₃ into CaO through TG analysis was inadequate. While calcinating in muffle furnace these temperature should be higher than 800°C for thorough decomposition. The CO₂ concentration in furnace atmosphere, particle size and partial pressure greatly influence the decarbonation process (Ngamcharussrivichai et al. 2010). Besides, direct exposure of CO particles to air leads to

the phase conversion from CaO to Ca(OH)₂ by hydration reaction. However, there was 3% weight loss in CO samples but it was not in the substantial level and thermally stable. Additionally, slight degradation in HA samples also denotes the expulsion of water molecules from CaO mineral in Ca(OH)₂ form which was presented as secondary phase.

5.1.1.2 Crystallographic structure and composition of CO, HA and CP particles particles

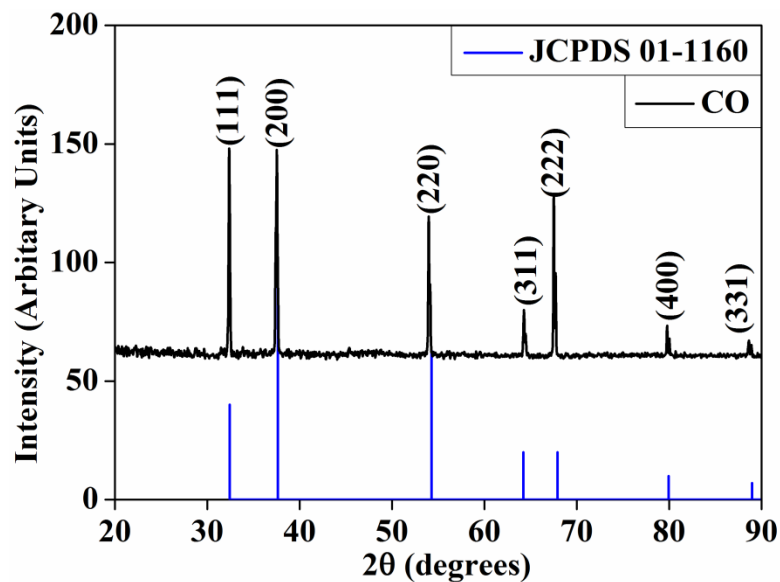


Figure 5.5. X-ray diffractograms of cuttlebone derived CO and JCPDS 01-1160 for CaO.

The crystalline phase of cuttlebone derived bio ceramics was confirmed through XRD. Figure 5.5 shows the XRD pattern of cuttlebone derived CO particles along with the standard reference pattern. The major reflection locations at 32.44°, 64.18°, 67.86° and 79.87° and its corresponding planes (111), (200), (220), (311), (222) and (400) are coincide with the JCPDS card no: 01-1160 for CaO. It clearly denotes that converted CO particles were in calcium oxide phase with cubic crystal form. At this temperature, cuttlebone was fully decomposed and converted into high purity calcium oxide phase.

XRD pattern of cuttlebone derived HA particles shown in Figure 5.6. It's revealed that the particles were in biphasic crystalline form. The major crystalline phase present in the particles was hydroxyapatite. Besides, CaO was also presented as the second major ones. Especially, major intensities of diffraction peak planes (002), (211),(112) and (221)

and their corresponding reflexes location (2θ) 25.89° , 31.77° , 32.18° and 32.90° agreed well with the standard JCPDS card no: 009-0432 for hydroxyapatite. So it is well known that the obtained hydroxyapatite particles were in hexagonal crystal structure and it can be expressed as $\text{Ca}(\text{PO}_4)_3(\text{OH})$. Besides, two peaks in the reflection location of 37.64° , and 54.28° denotes the presence of calcium oxide as second major phase in the prepared particles.

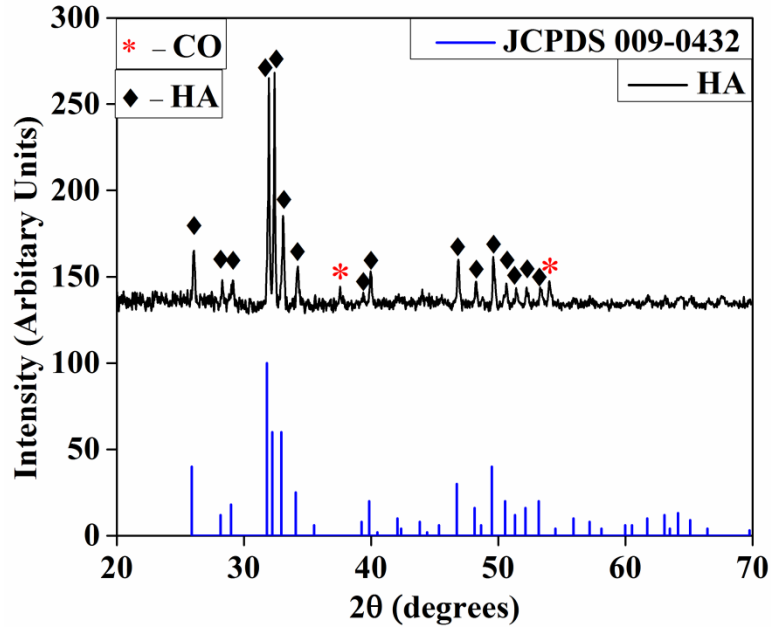


Figure 5.6. X-ray diffractograms of cuttlebone derived HA and JCPDS 009-0432 for Hydroxyapatite.

The volume fraction of CaO phase was evaluated from the following equation (Balakrishnan et al. 2007).

$$V_{CaO} = \frac{I_{CaO_1} + I_{CaO_2}}{I_{CaO_1} + I_{CaO_2} + I_{HA}} \quad (5.1)$$

Whereas I_{CaO_1} , I_{CaO_2} are the two intensities of the CaO phase and I_{HA} is the strongest intensity peaks of the HA Phase. Based from the above equation the estimated volume fraction of CaO phases in HA samples were 12.72%.

Similarly, figure 5.7 shows the XRD pattern of cuttlebone derived CP particles along with the standard reference pattern. The major reflection locations at 27.68° , 28.87° , 32.55° , and 34.55° and its corresponding planes (202), (203), (008), and (205) are coincide with the JCPDS card no: 01-1160 for tricalcium phosphates. It clearly denotes that converted CP particles were in tricalcium phosphate phase with tetragonal crystal form and it can be expressed as $3\text{CaO}\cdot\text{P}_2\text{O}_5$. Moreover, it didn't show any other crystalline peak which indicates that tricalcium phosphate in pure form has been prepared through this mechanochemical method.

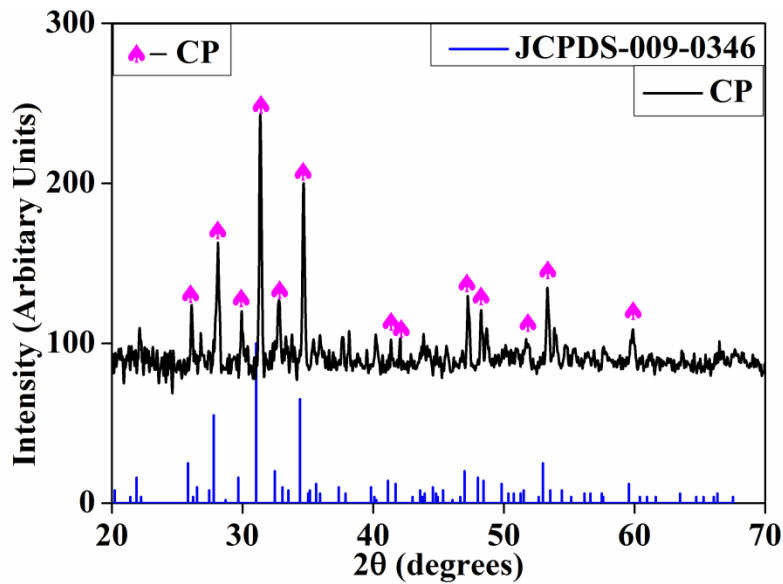


Figure 5.7. X-ray diffractograms of cuttlebone derived CP and JCPDS 009-0346 for tricalcium phosphate.

The crystalline parameters of cuttlebone derived CO, HA and CP are presented in Table 5.4. The sharp and influential diffraction planes from the XRD pattern of CO particles (200), HA particles (211) and CP particles (008) were used to calculate the corresponding crystalline size of particles (t). During bio ceramic conversion, the average crystalline size of prepared particles was found to be decreased. The grain size of the prepared CO, HA and CP particles are 22.62nm, 7.54nm and 8.48nm. The grain size value for CO particles is consistent with the Rodriguez-Navarro et al. 2009 for calcite decomposed into calcium oxide in air atmosphere.

Table 5.4. FWHM, d-spacing and crystallite size of the cuttlebone derived CO, HA and CP particles.

Material	FWHM (2 θ $^{\circ}$)	d-spacing (A°)	t (nm)
CO	0.0720 for (2 0 0) plane	2.39618	22.62
HA	0.2160 for (2 1 1) plane	2.79990	7.54
CP	0.1920 For(0 0 8) plane	2.85417	8.48

Moreover, larger amount of thermodynamically stable calcium oxide phase was developed while calcined the natural corals at 800 $^{\circ}$ C (Ngamcharussrivichai et al. 2010). Similarly, cuttlebone converted HA particles were in good crystallinity which enhances the chemical adhesion with hard tissue and also reduces the bioresorption activity. The presence of biphasic form was due to the variation in stoichiometric ratio. Few researchers (Lee et al. 2007) confirmed the formation of CaO phase, while Ca/P molar ratio is nearer to 1.75. In this case, it has been already confirmed through ICP-OES that the experimental value (1.72) has largely varied from the calculated value (1.67). Nevertheless, CP particles were in high purity form which is further corroborated through ICP-OES results that there is only marginal variation between the experimental and predicted values. However, CP particles are resorbable and osteoconductive which helps for faster bone formation. Based from the results, it is evidenced that nearer stoichiometric ratio and higher calcination temperature (>800 $^{\circ}$ C) gave better crystallinity and high purity HA and CP particles.

The FT-IR spectra of CO, HA and CP particles are illustrated in Figure 5.8. In general, CaO has major absorption in the range of 300 cm^{-1} which is in out of FT-IT range. In figure 5.8a peak at 864 cm^{-1} denotes the presence of weak absorbance band which confirms the carbonate species. Similarly, small amount of carbonate group was identified from the symmetric stretching vibration band at 1419.89 cm^{-1} 1473.54 cm^{-1} . Besides, Sharp OH peak at 3638.05 cm^{-1} associated with the vibration band of Ca(OH)₂

phase and small peak at 864.91 cm^{-1} denotes the CaO phase. On the whole, there should be the substantial reduction of carbonate and OH group in CaO samples (Tas 2007). Owing to high reactive surface of CaO to air leads to the formation of CO_2 and H_2O which forms OH group and carbonate species on the surface of CaO particles.

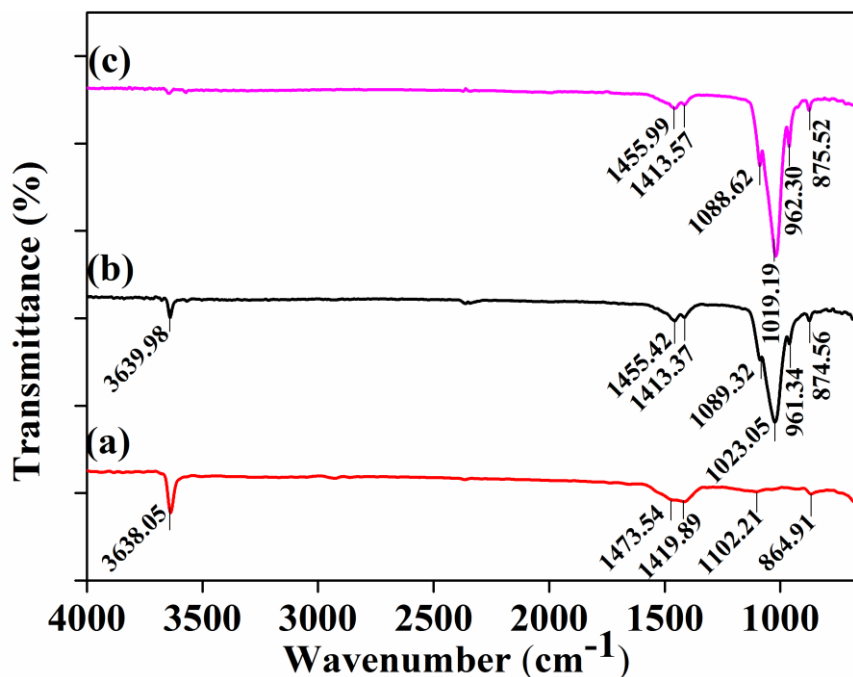


Figure. 5.8. FT-IR spectra of cuttlebone derived (a) CO, (b) HA and (c) CP particles.

In figure 5.8b & c, peak at 874 cm^{-1} denotes the presence of carbonate group which is formed as carbonated apatite with b-type substitution (Mehta and Singh 2014). Besides, a residue amount of carbonate group was identified from the peaks at 1413 cm^{-1} and 1455 cm^{-1} . Stretching mode (ν_1) of PO_4^{3-} group was identified through the Peaks at 961 cm^{-1} . Furthermore stretching mode (ν_3) of PO_4^{3-} group was identified through the band between $1018\text{-}1090\text{ cm}^{-1}$ in both HA and CP samples. Peak at 3639 cm^{-1} denotes the presence of surface OH band probably connected to the CaO surface.

From the FT-IR results, it clearly shown that CO samples has consist of CaO with minimal amount of carbonate group and $\text{Ca}(\text{OH})_2$ phase. It is also evidenced from the TGA results. Similarly, HA and CP samples show the presence of carbonate group as traces. But contradictorily, XRD does not show any carbonate and calcium hydroxide

peaks. The volume of these two phases is negligible and it could not be identified through XRD analysis.

5.1.2 Mechanical properties of EP, EP/CO, EP/HA and EP/CP composites

In this topic three different groups of composites (EP/CO, EP/HA and EP/CP) were analyzed. Each test group consists of five different sets (0, 3, 6, 9 and 12 wt%). Results are expressed in the form of mean \pm Standard deviation of 5 experiments. For all mechanical properties, statistical analyses were performed by one-way ANOVA. Tukey's honestly significant difference method was used for all post hoc analysis to identify the significant difference between each set of individual test group. Furthermore, significant difference between highest values of three test group was also determined by tukey's test. In all the tests, statistical significance was set at $p < 0.05$. Letters in lower case (a, b, c, d, and e), letters in upper case (A, B, C, D and E) and numbers (1, 2, 3, 4 and 5) was used to denote the statistical results in EP/CO, EP/HA and EP/CP test group, respectively. Likewise, symbols (\spadesuit , \diamond and \bullet) were used to denote the statistical results among the highest value of three test groups.

Figure 5.9 shows the tensile strength, tensile modulus, elongation percentage at break and load vs. deformation curve of EP/CO, EP/HA and EP/CP composites. Ultimate tensile strength (UTS) in EP/HA composites increased with filler content in the matrix material as shown in Figure 5.9a. In EP/CO and EP/CP composites, UTS increased until certain weight fraction of filler content and then it decreased. The UTS of neat epoxy matrix was 24MPa while maximum UTS of EP/CO, EP/HA and EP/CP composites were 36.3MPa (at 9 wt%), 45.7MPa (at 12 wt%) and 48.05MPa (at 6 wt%), respectively. Further, increased weight fraction of filler content in EP/CO (beyond 9 wt%) and EP/CP (beyond 6 wt%) composites led to reduction in UTS because of poor dispersion of filler in matrix material.

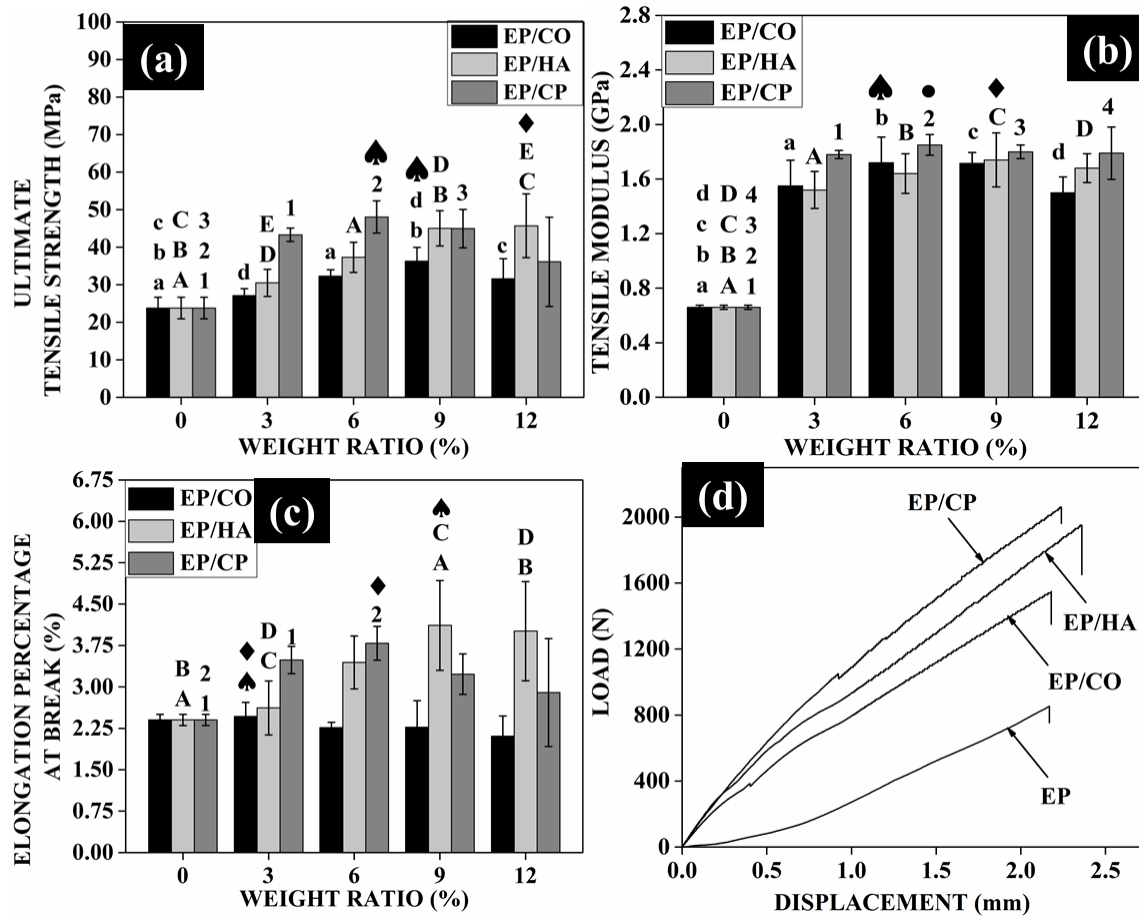


Figure 5.9. (a) Ultimate tensile strength, (b) Tensile modulus, (c) Elongation percentage at break and (d) Load Vs. displacement curve of EP, EP/CO, EP/HA and EP/CP composites. Symbols, numbers, letters in lower case and upper case (inset in figure) indicate pairwise comparison, that they were significantly different ($p < 0.05$).

In figure 5.9a, insets indicate that EP/CO composites prepared at 6, 9 and 12 wt% have significantly higher tensile strength value than neat epoxy samples. However, there was no significant difference found between these three samples. Besides, significant difference found between EP/CP composites at 3 & 9 and 3 & 12 wt%. Similar trend was observed for EP/HA composites. For EP/HA composites, 6, 9 and 12 wt% samples have significantly higher value compared to neat epoxy, but there was no significant difference was found within these three samples. In addition to, EP/CP composites at 3, 6 and 9 wt% has significantly higher than neat epoxy and there was no significant difference

found between these three composites. Amongst the highest tensile strength of three composites, significant difference found only between the EP/CO and EP/CP composites. Besides, other two combinations (EP/CO & EP/HA and EP/CP & EP/HA) didn't show any significant difference.

Figure 5.9b shows the tensile modulus plotted versus different weight ratio of filler content for EP/CO, EP/HA and EP/CP composites. The tensile modulus for neat epoxy was 0.659GPa. It increased until certain weight fraction of the filler content in all three composites and then decreased. The maximum modulus value of EP/CO, EP/HA and EP/CP composites were 1.72GPa (at 6 wt%), 1.74GPa (at 9 wt%) and 1.85GPa (at 6 wt%), respectively. Among the three composites, EP/HA and EP/CP composites had better tensile modulus than EP/CO composite. In that, EP/CP composites had better modulus than EP/HA composites. In figure 5.9b, insets indicate that all three composites prepared at 3, 6, 9 and 12 wt% have significantly higher tensile modulus value than neat epoxy samples. However, in all three composites there was no significant difference found between the four weight percentages. There was no significant difference found among the highest tensile modulus of three composites (EP/CO, EP/HA and EP/CP at 6, 9 and 6 wt%, respectively). The results indicates that the addition of smaller amount of (3 wt%) filler content in matrix material shown significant improvement in tensile modulus as compared to neat epoxy, in all three composites. However, there was no significant improvement in tensile modulus found while increasing the filler content beyond 3 wt% in all these composites.

Elongation percentage at break (EPB) for EP/CO, EP/HA and EP/CP composites at different weight ratio are shown in Figure 5.9c. The elongation percentage for EP/CO, EP/CB and EP/HB composites increased up to certain weight fraction and then gradually decreased. The maximum elongation percentage for EP/CO, EP/HA and EP/CP composites were 2.47% (at 3 wt%), 4.11% (at 9 wt%) and 3.79% (at 6 wt%), respectively. Addition of filler at higher weight fraction in EP/CO composites (6 to 12 wt%) resulted in improper bonding between matrix and filler material and decreased the EPB value of composites than neat epoxy (Abdul Khalil et al. 2013). In figure 5.9c, insets

indicates that EPB value of EP/CO composites at different weight ratios have no significant difference with neat epoxy sample. In EP/HA composites, 9 & 12 wt% samples have significantly higher EPB value than neat epoxy and 3 wt% samples. However there was no significant difference found within the samples (9 & 12 wt% and neat epoxy and 3 wt%). Similarly in EP/CP composites, there was significant improvement in EPB value was found in 3 & 6 wt% as compared to neat epoxy sample. Amongst the highest EPB value of three composites (EP/CB, EP/HB and EP/CC at 3, 9 and 6 wt%, respectively), EP/CO & EP/HA and EP/CO & EP/CP combinations have significant difference in values. It concludes that only EP/HA and EP/CP composites shown significant improvement in EPB value by the addition of filler content in matrix material.

Figure 5.9d, demonstrates the typical tensile load-deformation curve for neat epoxy, EP/CO, EP/HA and EP/CP composites at 9, 12 and 6 wt%, respectively. The graph presents that neat epoxy and three composites curve shown merely linear improvement without any yield and necking region. All four materials exhibit typical brittle behavior like large elastic deformation followed by sudden failure. As expected, the addition of CO, HA and CP particles in epoxy matrix exhibit higher tensile modulus and tensile strength than neat epoxy. There was non-significant reduction in elongation percentage at break found in EP/CO composites than neat epoxy. But in contrast, there was significant improvement in EPB value found on EP/HA and EP/CP composites than neat epoxy.

Mechanical properties of composites have be influenced by matrix material, geometry of reinforcement, weight fraction of reinforcement and interaction between filler and matrix material (Mirsalehi et al. 2015). In general, addition of ceramic particles as reinforcement in matrix led to the improvement in tensile strength of the composites. It is clear that the improvement in tensile strength of HA and CP particle filler composites has been significantly higher than CO particle reinforced composites. The possible reason could be the nanoparticles having better homogeneous dispersion and higher contact surface leads to the proper stress transfer between filler and matrix. However deteriorated

in tensile strength of EP/CP composites at higher filler loading level has been significantly higher than other two composites. Nanoparticles have higher amount of free surface energy which induced filler-filler interaction and further leads to more stress concentration region followed by failure of the material (Sezavar et al. 2015).

Similarly, addition of rigid ceramic filler in epoxy matrix tends to improve the stiffness and modulus properties of the composites. It is seen that there is significant effect on the modulus of composites prepared with micro and nano filler. As mentioned by Njoku et al. 2011 that the modulus of composites has been improvement by varying the filler particle size from micron to nano scale. Similar kind of observation has been evidenced in the present study that addition of nano sized HA and CP particles lead to efficient interaction with matrix which increases the stiffness and modulus of composites. Even at higher filler loading, modulus of EP/HA and EP/CP composites has been improved due to the even dispersion of nano filler in matrix. Consequently, EPB value of composites has been improved due to the proper bonding between nano filler and matrix material. Since the chemical nature of the HA and CP filler are different, their contribution in tensile properties improvement is in equal level due to the nano size particles.

Figure 5.10 shows the flexural strength, flexural modulus and load vs. deformation curve of EP/CO, EP/HA and EP/CP composites. The neat epoxy has the flexural strength of 54.79MPa. As shown in Figure 4.10a, flexural strength of EP/CO composites increased by increasing the filler content and reached its maximum strength value of 71.3MPa at 12 wt%. However flexural strength of EP/HA and EP/CP composites increased until certain weight fraction of filler content and then it decreased. The maximum flexural strength of EP/HA and EP/CP composites were 104.6MPa (6 wt%) and 94.85MPa (6 wt%), respectively. With the further increment of filler content in these two composites, led to a substantial reduction in flexural strength. The reason for deterioration of flexural strength of EP/HA and EP/CP composites at higher filler content could be the weak interfacial bonding between filler and matrix material due to poor dispersion.

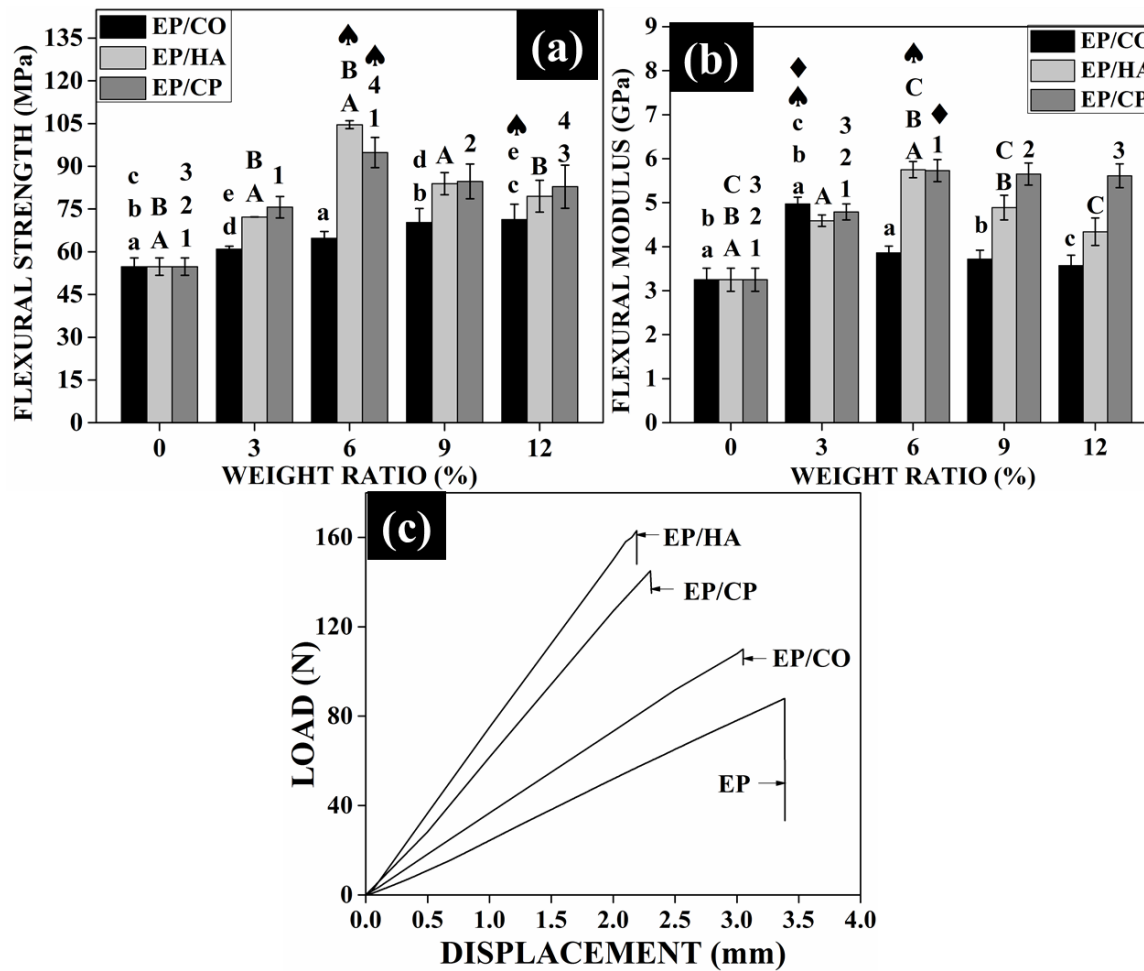


Figure 5.10. (a) Flexural strength, (b) Flexural modulus and (c) Load Vs. displacement curve of EP, EP/CO, EP/HA and EP/CP composites. Symbols, numbers, letters in lower case and upper case (inset in figure) indicate pairwise comparison, that they were significantly different ($p < 0.05$).

In figure 5.10a, insets indicate that EP/CO composites prepared at 6, 9 and 12 wt% have significantly higher than neat epoxy samples. Similarly, 3 wt% sample have significant lower value than 9 & 12 wt% samples. It denotes that, addition of CO at 6, 9 and 12 wt% in epoxy matrix improved the flexural strength at significant level than neat epoxy and 3 wt% samples. Though, there was no significant difference found between 6, 9 & 12 wt% samples. For EP/HA and EP/CP composites, all samples prepared at different wt% have significant different with neat epoxy samples. Furthermore, there was

a significant difference found within the samples (3, 6 & 9 wt% for EP/HA and 3 & 6 wt% for EP/CP). It clearly shown that addition of 6 wt% of HA and CP particles in epoxy matrix has a good influence on the improvement of flexural strength of composites compare to neat epoxy. Amongst the maximum flexural strength of three composites, there was significant difference was found between all three samples. However the maximum flexural strength of EP/HA composites value was significantly higher than other two composites. It concludes that addition of HA particles as reinforcement in epoxy matrix has highest significant level of improvement in flexural strength than CP and CO added epoxy composites.

Flexural modulus of EP/CO, EP/HA and EP/CP composites at different weight ratio are shown in figure 5.10b. The neat epoxy has a flexural modulus value of 3.25GPa. In all three composites, flexural modulus was increased until certain weight fraction and then decreased. The maximum flexural modulus value for EP/CO, EP/HA and EP/CP composites were 4.97GPa (3 wt%), 5.75GPa and 5.73GPa (6 wt%), respectively. With the further increment of filler content in all three composites, led to a substantial reduction in flexural modulus. This result shows that addition of CO, HA and CP particles in epoxy matrix enhance the stiffness property of composites.

Insets in figure 5.10b denotes that in EP/CO composites there was significant difference found between neat epoxy and 3, 6 & 9 wt% samples. However there was no significant difference found between neat epoxy and 12 wt% samples. It clearly indicates that addition of CO particles at higher filler weight fraction led to the significant reduction in modulus value and it's almost nearer to neat epoxy value. In both EP/HA and EP/CP composites, significant difference was found between neat epoxy and all different weight fraction samples. The results indicate that addition of HA and CP particles up to 6 wt% in epoxy matrix have significant improvement in modulus values. Beside the weight fraction, significant reduction in flexural modulus was observed in EP/HA composites. Nevertheless in EP/CP composites, the reduction in modulus value beyond 6 wt% was in non-significant manner. Amongst the highest value of three composites, EP/HA and EP/CP has significantly higher value than EP/CO composites. Besides, there was no

significant difference found between the highest modulus value of EP/HA and EP/CP composites. It states that EP/HA and EP/CP composite has better stiffness than EP/CO composites.

Figure 5.10c displays the flexural load vs. deflection curve of neat epoxy and EP/CO, EP/HA and EP/CP composites prepared at 12, 6 and 6 wt%, respectively. All four materials exhibits linear trend until failure which confirms the brittle deformation. In comparison with neat epoxy, the initial slope of the EP/CO, EP/HA and EP/CP composites was higher which denotes the increase in stiffness of composites (Rahman et al. 2013). It could be attributed by the reduction of deflection value at break. Moreover, the load taking capability of the epoxy matrix was increased by incorporating the CO, HA and CP particles.

Flexural strength of EP/CO composites increased monotonically while adding the filler content, whereas in EP/HA and EP/CP composites strength was increased until 6 wt% and decreased beyond that filler content. Hence, the continuous improvement in flexural strength of EP/CO composites denotes the effective stress transfer from matrix to filler via interface. Even though there was a continuous improvement, maximum flexural strength value of EP/CO composites has significantly lesser than other two composites. The reason for this phenomenon could be that nano particle reinforced composites having high interface region which makes better static adhesion strength and interfacial stiffness than micro particle reinforced ones. Furthermore, reduction in flexural strength of EP/HA and EP/CP composites at higher filler fraction was in significant level compared to the 6 wt% one. This was probably due to the poor dispersion of filler particles which act as stress concentrator and leads to the pre failure of material under loading.

In the case of flexural modulus, it has been improved in all three composites until certain weight fraction and then decreased. In general, addition of rigid particles in matrix tends to the improvement in stiffness property of composites. These rigid particles having good stiffness than matrix which leads to the improvement of composite modulus. Similarly as like flexural strength, maximum flexural modulus of EP/CO composites was significantly lower than EP/HA and EP/CP composites. As compared to the micro

particles, nano particle reinforced composites having high interfacial region. Additionally, these rigid nano fillers withstand more stress under loading condition and do not allow the molecular deformation in matrix system. This will contribute to the overall enhancement in composite modulus. The drop in flexural modulus of EP/CO and EP/HA composites was significantly different compared to their corresponding highest modulus values. But in the case of EP/CP composites, drop in the modulus was not up to significant level. As compared the results of flexural strength and modulus, HA and CP particles having better dispersion in epoxy matrix rather than CO filled ones.

The compression properties and compression load vs. deflection curve of EP, EP/CO, EP/HA and EP/CP composites was presented in figure 5.11. Figure 5.11a indicate that addition of CO and CP particles in epoxy matrix was found to increase in the strength of the composites until certain weight ratio, and then decrease continuously. The neat epoxy has compression strength of 80.7MPa. The maximum compressive strength of EP/CO and EP/CP composites has the value of 87.3MPa (at 6 wt%) and 97.5MPa (at 9 wt%), respectively. Beyond this optimum weight ratio of the filler content, compression strength was decreased in these two composites. However, formation of more amounts of aggregates at high filler loading acts as a barrier in the improvement of composite strength (Ang et al. 2015). Besides, compression strength of EP/HA composites was increased with increasing the filler content and attained its maximum compression strength of 97.4MPa at 12 wt% filler content.

In figure 5.11a, insets indicate that EP/CO composites prepared at different weight fraction does not have significant difference with neat epoxy samples. The results denote that addition of CO particles up to 9 wt% does not influence the improvement of compression strength of composites. Besides, addition of CO particles at higher filler fraction (12 wt%) have significantly reduce the compression strength than 6 wt% sample. However, in EP/HA composites significant improvement in strength was attained by the addition of filler particles at 9 and 12 wt%. Similarly, EP/CP composites prepared at 6 and 9 wt% have significant improvement in strength than neat epoxy.

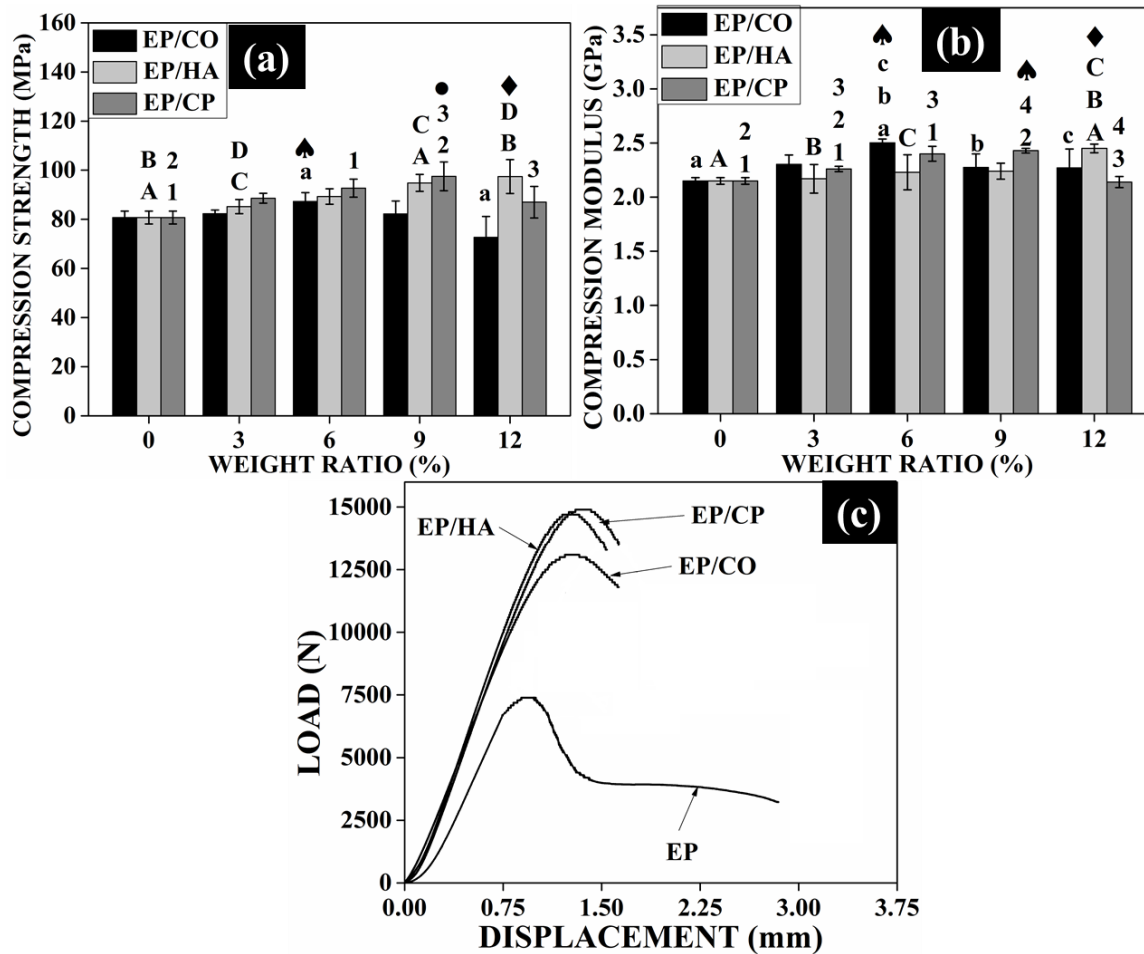


Figure 5.11. (a) Compression strength, (b) Compression modulus and (c) Load Vs. displacement curve of EP, EP/CO, EP/HA and EP/CP composites. Symbols, numbers, letters in lower case and upper case (inset in figure) indicate pairwise comparison, that they were significantly different ($p < 0.05$).

Besides, significant different was found between 9 and 12 wt% samples in EP/CP composites which denote that reduction in strength was in substantial level. Amongst the highest compression strength of three composites, none of the combination shows any significant difference. As compared to EP/CO composites, highest strength of EP/HA and EP/CP composites have significantly different with neat epoxy.

Compression modulus of EP/CO, EP/HA and EP/CP composites at different weight ratio are shown in figure 5.11b. As like compression strength, compression

modulus of EP/CO and EP/CP composites was also increased continuously upto certain weight percentage and then it decreased. However in EP/HA composites, compression modulus was increased continuously with the addition of filler content. As compared to the neat epoxy resin (2.15GPa), compression modulus of EP/CO, EP/HA and EP/CP composites was increased and reached its maximum value of 2.50GPa (6 wt%), 2.45GPa (12 wt%) and 2.43GPa (9 wt%), respectively. Though, compression modulus of EP/CO and EP/CP composites was decreased at high filler fraction. In most of the composites at higher filler percentage, modulus was reduced due to premature failure which led by more amounts of stress concentration regions (Li et al. 2004).

In EP/CO composites, samples prepared at 6 wt% has significant higher compression modulus than 9 wt%, 12 wt% and neat epoxy samples. Besides, EP/CO composites prepared at higher filler loading (9 and 12 wt%) has found significantly different with 6 wt% sample. It concludes that there was significant reduction in modulus of EP/CO composites was attained at higher filler fraction. In EP/HA composites, samples at 12 wt% filler fraction have significant different with neat epoxy, 3 and 6 wt% samples. It clearly indicates that addition of HA particles at 12 wt% have greater influence on the improvement of composite modulus. In EP/CP composites, addition of filler content up to 6 wt% has found significant improvement in modulus values. Additionally, EP/CP composites prepared at 6 and 12 wt% has significant difference in their modulus values. It shows that considerable amount of reduction in modulus was attained at higher filler fraction (12 wt%). Amongst the highest modulus value of composites, EP/CO & EP/CP have significantly different with each other. Besides, two combinations (EP/CO & EP/HA and EP/HA and EP/CP) does not have significant difference in their modulus values. It conveys that, addition of CO particles has given better modulus value of composites than HA and CP particles added ones.

Figure 5.11c represents the compressive load vs. deflection curve of neat epoxy, EP/CO, EP/HA and EP/CP composites. In both tension and flexural, neat epoxy behave in linear manner and rupture suddenly. Nevertheless, in compression it unveiled plastic deformation behavior before failure. Neat epoxy has the tendency of large strain

softening region after yielding along with more amount of displacement during failure. Addition of rigid ceramic fillers in epoxy matrix declines the strain softening region (Xu et al. 2013). Moreover it withstands more loads and become more brittle. In EP/CO, EP/HA and EP/CP composites, the strain softening zone is comparatively lower than neat epoxy and the material failed after yielding point followed by small amount of strain softening which denotes the brittle failure. However, these composites also withstand more load than neat epoxy but have a significant reduction in strain at failure.

In general, ceramic particles have the tendency to withstand more load than matrix which leads to improve the strength and modulus of the composites. Based on the degree of adhesion between ceramic fillers and matrix material, composite strength behavior has been analyzed. Addition of these rigid ceramic particles at right proportion makes the homogeneous dispersion of fillers in matrix and tends to improve the compression properties of composites. At higher filler loading level, free radicals have been released during polymerization which makes weak interaction between filler and matrix. This improper adhesion and non-homogeneity dispersion of filler particles in matrix lead to the decline in composite strength.

In EP/HA composites, the enhancement in compression strength is continuous by increasing the filler content. It denotes that the inclusion of HA nano filler dispersed in even manner which makes better bonding between filler and matrix. Furthermore in EP/CP composites, strength was increased until 9 wt% filler content and decreased significantly at 12 wt%. However, maximum strength of these two composites is almost equal. Similar trend was observed for compression modulus of both composites. Addition of nano particles in epoxy matrix tends to occupy the space between the polymer chains which increases the resistance against matrix deformation and crack growth (Li et al. 2004). Furthermore these HA and CP fillers prevent the crack initiation by occupying the voids space presents in the matrix.

Similarly in EP/CO composites, the compressive properties increased up to 6 wt% and then start declined. Though the strength of the EP/CO composites is lower than other two composites but it was not significantly different. However, modulus of EP/CO

composites is comparatively higher than EP/HA and EP/CP composites. Reasons for the reduction in compression properties of EP/CO and EP/CP composites at higher filler loading could be due to the particle agglomeration and lack of matrix material. While curing, thermal stresses have been developed around the particle agglomeration regions due to the disparity of thermal coefficient expansion in composite phases. This may initiate the crack propagation and makes the premature failure of composites during loading.

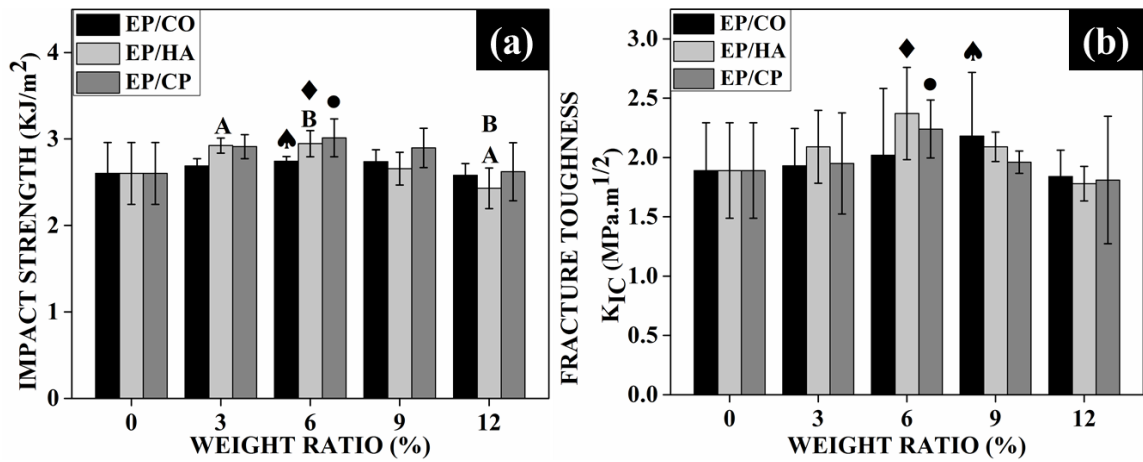


Figure 5.12. (a) Impact strength, and (b) Fracture toughness of EP, EP/CO, EP/HA and EP/CP composites. Symbols, numbers, letters in lower case and upper case (inset in figure) indicate pairwise comparison, that they were significantly different ($p < 0.05$).

Figure 5.12 shows the impact strength and fracture toughness properties of EP/CO, EP/HA and EP/CP composites prepared at different weight ratios. As shown in Figure 5.12a the neat epoxy has impact strength of 2.60KJ/m², and it has increased continuously by increasing the filler content up to 6 wt% in all three composites. The maximum impact strength of EP/CO, EP/HA and EP/CP composites was attained of 2.74KJ/m², 2.95KJ/m² and 3.01KJ/m² (6 wt%), respectively. Addition of rigid ceramic fillers in epoxy matrix tends to absorb more deformation energy and it's improved the impact strength of the composites (He et al. 2011).

In EP/CO and EP/CP composites, none of the combinations (neat epoxy and five different weight fractions) have significant difference. Similarly in EP/HA composites

samples prepared at different weight fraction do not have significant with neat epoxy. However 3 & 12 wt% and 6 & 12 wt% combinations have significant in their impact strength values. It clearly indicates that EP/HA composites prepared at higher filler fractions (12 wt%) have significant reduction in their composite impact strength. Similarly, there was no significant difference was found among the highest value of three composites. Even though the impact strength of EP/HA and EP/CP composites was higher than EP/CO composite, but it was not in the significant level. The results concluded that addition of CO, HA and CP particles in epoxy matrix have similar behavior during impact loading.

Impact behavior of composites has been influenced by various factors like molecular weight of matrix, filler material, sample geometry, processing and testing parameters (Zhang and Tanner 2008). Over the three composites, none of them has shown significant improvement in impact strength. The possible reason could be the addition of rigid filler particles in rigid matrix. Therefore the particle matrix interface was very poor which may lead to voids formation. This may assist crack initiation and propagation which reduced the impact strength of composites. However, there was a small increment in impact strength has been evidenced because of the mechanical interlocking at particle/matrix interfaces (Kavitha et al. 2012). Besides, EP/HA and EP/CP has slightly higher impact strength than EP/CO composites. In general, nano particle filled composites shown better impact properties than micro particle filled ones. At same filler loading, it has more contact area which leads to the prolongation in crack path and withstand more energy. Though, the difference in maximum impact strength of EP/HA, EP/CP and EP/CO was not up to the significant level. Moreover at higher filler loading, EP/HA composites shown significant reduction in impact strength due to the particle agglomeration which restricts the energy dissipation from filler to matrix (He et al. 2011).

Fracture toughness of EP/CO, EP/HA and EP/CP composites prepared at different weight ratio is shown in figure 5.12b. The neat epoxy has the fracture toughness value of $1.89 \text{ MPa.m}^{1/2}$. Addition of filler particles tends to improve the fracture toughness

property of composites until certain weight and then decreased continuously in all three composites. The maximum fracture toughness value of EP/CO, EP/HA and EP/CP composites was reached to $2.18 \text{ MPa}\cdot\text{m}^{1/2}$ (9 wt%), $2.37 \text{ MPa}\cdot\text{m}^{1/2}$ (6 wt%) and $2.24 \text{ MPa}\cdot\text{m}^{1/2}$ (6 wt%), respectively. Owing to proper interaction at lower filler loading, the rigid filler particles restrict the crack propagation and tends to absorbed more amount of energy followed by the improvement in fracture toughness (Zhu et al. 2011).

Insets in figure 5.12b denote that in all three composites, none of the combination does not have any significant difference in fracture toughness values. The results denote that addition of CO, HA and CP particles in epoxy matrix have slight improvement in fracture toughness property but it was not upto the significant level. Besides, there was no significant difference found by increasing the filler content in composites. Similarly, there was no significant difference was found among the highest value of three composites. Even though the fracture toughness of EP/HA and EP/CP composites was higher than EP/CO composite, it concludes that CO, HA and CP particles do not have much influence in the improvement of fracture toughness property of composites.

In general, fracture toughness property of polymer composites is mainly depends on the addition of reinforcing fillers. Factors like particle size, shape, chemical structure, surface properties and volume fraction has influenced more on the fracture toughness property (Khanal et al. 2016). In all three composites, fracture toughness has increased slightly until certain weight fraction and then decreased continuously. However, the improvement is not up to significant level. Addition of rigid ceramic particles in epoxy matrix leads to deflecting the path of crack propagation through particle/matrix interface and absorb more energy before failure (Kobayashi and Kawai 2007). This could be the possible reason for the slight improvement in fracture toughness property at lower filler fraction. Moreover, there was no significant difference found between the maximum fracture toughness values of three composites. Though nano fillers reinforced composites (EP/HA and EP/CP) have better fracture toughness value than micro filled ones (EP/CO) but it was not up to the significant level. It clearly indicates that all three ceramic filler having same kind of toughness behavior with matrix material.

Shore D hardness of EP/CO, EP/HA and EP/CP composites at different weight ratio are shown in figure 5.13. The neat epoxy has a hardness value of 72.4. In all the three composites, hardness value increased by increasing the filler content. The maximum hardness value of EP/CO, EP/HA and EP/CP composites were 82.5, 87.5 and 89.3 (at 12 wt%), respectively.

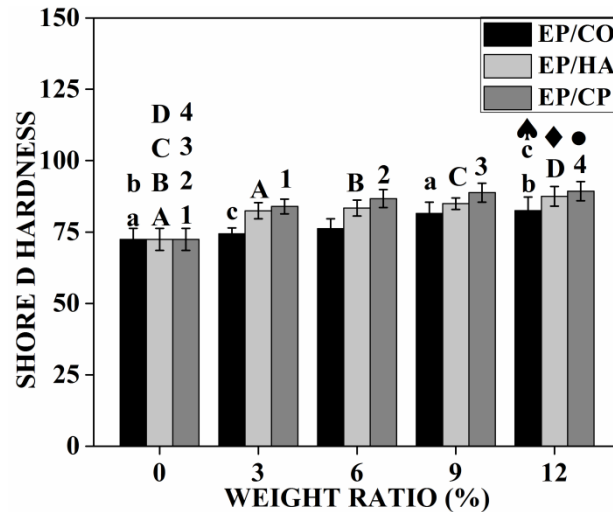


Figure 5.13. Hardness of EP, EP/CO, EP/HA and EP/CP composites. Symbols, numbers, letters in lower case and upper case (inset in figure) indicate pairwise comparison, that they were significantly different ($p < 0.05$).

In general, addition of rigid filler particles in epoxy matrix enhanced the hardness of composites. Insets in figure 5.13 indicates that in EP/CO composites there was significant difference found between neat epoxy & 9 and neat epoxy & 12 wt% samples. Similarly, there was significant difference found between the 3 & 12 wt% samples. The results denotes that addition of CO particles at higher filler fraction (9 & 12 wt%) has significant influence on the improvement in hardness values. In both EP/HA and EP/CP composites, samples prepared at different filler content has significantly different than neat epoxy. Likewise, there was significant difference found within the samples. The result clearly states that addition of small amount of HA and CP filler content in epoxy matrix tends to significantly improve the hardness value of composites. On the other hand, there was no significant improvement attained by the increase of filler content in

epoxy matrix. Amongst the highest hardness value of three composites, there was no significant difference found in any of the combinations.

In general, addition of hard phase of particles in matrix tends to the improvement in hardness of composites (Fombuena et al. 2014). The result indicates that addition of reinforcing particles at different loading level dominates the hardness property of composites. Enhancement in hardness was due to the presence of hard ceramic filler in epoxy matrix which tends to increase the brittleness property. In EP/CO composites, addition of filler at higher loading (9 and 12 wt%) showed the significant improvement in hardness values. But in EP/HA and EP/CO composites, addition of 3 wt% filler content itself showed significant improvement in hardness. It denotes that nano fillers (HA & CP) having good interfacial adhesion with matrix rather than micro (CO) ones.

5.1.3 Fracture morphology studies of EP, EP/CO, EP/HA and EP/CP composites

The fracture morphology of neat epoxy, EP/CO, EP/HA and EP/CP composites (at 6 wt%) conducted after tensile test are shown in Figure 5.14. SEM images of neat epoxy and three composites showed brittle type of fracture with rough fracture surface. Neat epoxy had relatively smoother fracture surface than other composites. In the ceramic reinforced epoxy composites, crack proliferation deflected more towards the filler-matrix interface region leading to increased crack propagation and rough fracture surface.

Furthermore, notable micro voids were observed on the fracture surface of EP/CO and EP/HA composites, that could have possibly played a role in increasing the crack propagation (Abdul Khalil et al. 2013). Apart from that, fractured surface of EP/HA and EP/CP composites showed particle agglomeration that acted as weak points for initial failure and subsequent crack propagation. In general, ceramic particle reinforced matrix tended to be shear yielding due to matrix plasticity, thus resulting in toughening of composites (Jumahat et al. 2010).

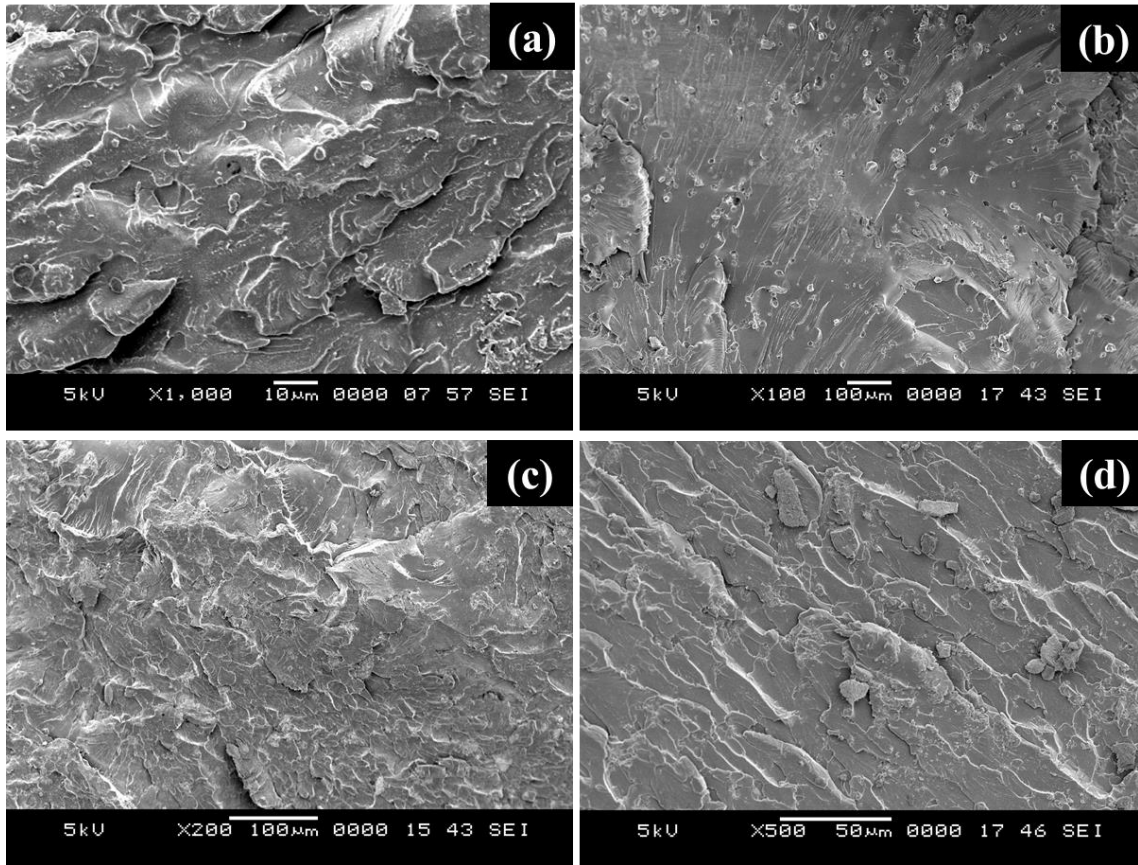


Figure 5.14. SEM micrograph of (a) EP, (b) EP/CO composites, (c) EP/HA composites and (d) EP/CP composites at 6 wt% filler loading.

From the figure 5.14a, the lines indicate the direction of crack propagation. The combination of lines denotes the rapid crack propagation which absorbed less energy before specimen failure. This induces the brittle type failure due to less resistance to crack propagation. Besides there was no micro voids presents in the sample. In particle reinforced epoxy composites, agglomerated particles play an important role in the formation of stress concentration. The amount of stress near particle agglomerated region is very high and induces rapid failure due to faster crack propagation. In EP/CO and EP/HA composites, fracture surface has consists of micro voids which induced by poor particle/matrix adhesion. During loading condition, poor adhesion leads to more amounts of particle debonding throughout the composite and tend to form more amount of voids.

As compared to the micro particles, nano particle reinforced composites has consists of more amount of voids because it consists more amount of surface contact area (Abdul Khalil et al. 2013). This statement was further corroborated with the voids percentage of composites (discussed in next topic). In that EP/HA and EP/CP composites has consists of more amount of voids as compared to EP/CO composites. Besides, nano particle reinforced composites shown rough fracture surface compared to micro particle filled ones. It happened due to the reduction in inter particle distance which deflects the crack propagation points and makes the rough surface.

5.1.4 Density and voids percentage of EP, EP/CO, EP/HA and EP/CP composites

Table 5.5: Theoretical density, actual density and void percentage of EP/CO, EP/HA and EP/CP composites

F.W.R.	EP/CO Composites			EP/HA Composites			EP/CP Composites		
	T.D.	A.D.	V.C.	TD.	A.D.	V.C.	T.D.	A.D.	V.C.
0	1.21	1.179	2.561	1.21	1.179	2.561	1.21	1.179	2.561
3	1.222	1.192	2.464	1.222	1.188	2.811	1.226	1.197	2.358
6	1.234	1.198	2.906	1.235	1.192	3.538	1.242	1.199	3.498
9	1.247	1.201	3.647	1.248	1.192	4.470	1.259	1.202	4.577
12	1.260	1.213	3.719	1.261	1.197	5.094	1.277	1.202	5.828

F.W.R.: Filler weight ratio (%); T.D.: Theoretical density (g/cm^3);

A.D.: Actual density (g/cm^3); V.C.: Voids content (%)

Theoretical and actual density along with voids percentage of EP/CO, EP/HA and EP/CP composites at different weight fractions are presented in Table 5.5. The actual density of composites was smaller than their corresponding theoretical density, thus confirming the presence of voids in composites. Theoretical and actual density of neat epoxy matrix was 1.21 and 1.179 g/cm^3 , respectively. Densities of the composites increased by the addition of filler particles into matrix due to higher density of fillers (2.29 g/cm^3 for CO, 2.14 g/cm^3 for HA and 1.83 g/cm^3 for CP) than matrix material. The

maximum density values of composites (1.260 g/cm³ of EP/CO, 1.261 g/cm³ of EP/HA and 1.277 g/cm³ of EP/CP) were observed at higher filler weight fraction of 12 wt%.

Preparing composites through hand-layup technique leads to the presence of voids and it is unavoidable. The voids percentage of neat epoxy matrix was 2.561% and augmentation of voids percentage was observed by increasing the filler content (from 3 wt% to 12 wt%) in composites. Voids percentage existed in the range of 2.464 to 3.719%, 2.811 to 5.094% and 2.358 to 5.828% for EP/CO, EP/HA and EP/CP composites, respectively. Addition of filler content at 3 wt% in EP/CO composites showed lesser voids percentage compared to neat epoxy matrix inferring that up to 3 wt% of filler content in composites reduces the voids percentage. Beyond 3wt% of filler content, voids percentage in composites was higher than the epoxy matrix because of agglomerations during mixing and debonding of filler and matrix material (Abdul Khalil et al. 2013).

At lower weight fraction, filler particles tend to fill the voids created during crosslinking of neat epoxy polymers (Abdul Khalil et al. 2013). However, increase in the void content beyond 3 wt% of filler loading clearly indicates imbalance in the dispersal of filler in the matrix. Compared to EP/CO composite, EP/CP and EP/HA composites had higher percentage of voids because these filler are in nano size range which develops cavity at higher weight fraction due to poor interaction with matrix material.

5.1.5 Physical properties of EP, EP/CO, EP/HA and EP/CP composites

Based on the mechanical, morphological and voids content results of EP/CO, EP/HA and EP/CP composites prepared at different weight fractions, it can be concluded that composites prepared at 6 wt% filler fraction had relatively more advantageous properties as compared to other filler fraction. Hence these weight fraction composites along with neat epoxy were further subjected to water absorption, wettability, thermal and thermo-mechanical studies.

Figure 5.15a shows the water absorption behavior of EP/CO, EP/HA and EP/CP composites. After 30 days, the maximum amount of water uptake for EP, EP/CO, EP/HA

and EP/CP composites was around 0.46%, 1.17%, 0.43% and 0.57%, respectively. However, the best fit curve equation for EP, EP/HA and EP/CP composites was in third order polynomial form with R^2 value of 0.99, 0.98 and 0.99, respectively. Similarly, the best fit curve equation for EP/CO composites was in second order polynomial ($R^2=0.99$) form. The corresponding best fit curve equation for EP, EP/CO, EP/HA and EP/CP composites was mentioned in equation 4.1 to 4.4, respectively.

$$Y = 6 \times 10^{-6} X^3 - 0.0006 X^2 + 0.0281 X + 0.0257 \quad \dots\dots\dots (4.1)$$

$$Y = -0.0007 X^2 + 0.0578 X + 0.0604 \quad \dots\dots\dots (4.2)$$

$$Y = 1 \times 10^{-5} X^3 - 0.001 X^2 + 0.0315 X + 0.0278 \quad \dots\dots\dots (4.3)$$

$$Y = 2 \times 10^{-5} X^3 - 0.0012 X^2 + 0.0391 X + 0.0302 \quad \dots\dots\dots (4.4)$$

The result indicates that addition of CO, HA and CP particles as reinforcement in epoxy composites leads to the slight improvement in water absorption properties for a period of 30 days.

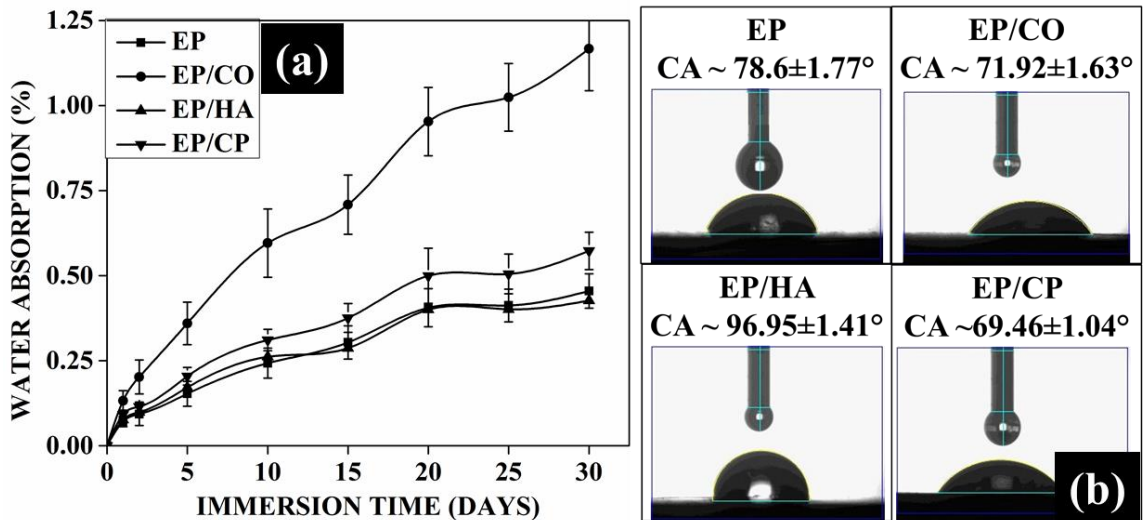


Figure 5.15: Water absorption and Wettability results of (a) EP, (b) EP/CO, (c) EP/HA and (d) EP/CP composites.

Researchers stated that hydrophilic nature of reinforcement particles and free volume of the polymer could be the reason for improvement in water absorption properties of neat matrix and composites (Raju and Kumarappa 2011). In general, CaO particles contains minimal amount of Ca(OH)_2 phase. Moreover, these CO particles were

in hygroscopic nature which appeals to water molecules through OH bonding (Zhao and Zhang 2008). However, none of the composites reached the saturation level of water absorption even after 30 days. The impenetrable reinforcement particles in composites make the water molecules to diffuse in tortuous pathway which induce the unsaturation level of water absorption at the end of experiment (Kornmann et al. 2005). In our case, CO and CP particle reinforced composite has higher percentage of water absorption compared to HA particle reinforced composites. Even though, EP/CO composites has lower voids percentage and cross link density (which discussed in upcoming topic), the water absorption percentage is higher than other two composites. Owing to the presents of hydroxyl components and hygroscopic nature of CO particles leads to more water absorption property than other three composites (Zhao and Zhang 2008 and Bagheri et al. 2015).

Moreover, these results are well agreed with contact angle studies. The water contact angle for EP, EP/CO, EP/HA and EP/CP composites was $78.6\pm 1.77^\circ$, $71.92\pm 1.63^\circ$, $996.95\pm 1.41^\circ$ and $69.46\pm 1.04^\circ$, respectively. Amongst the four materials, three composites (EP, EP/CO, and EP/CP) showed a hydrophilic behavior because of its contact angle was less than 90° . However, EP/HA composites showed a hydrophobic nature and the results were further corroborated with water uptake capability which denotes less percentage of absorption than neat epoxy. Addition of reinforcement filler in epoxy matrix tends to increase the wettability of composites. In that, EP, EP/CO and EP/CP composites have higher wettability/lower contact angle than EP/HA ones.

5.1.6 Thermo-mechanical and thermal properties of EP, EP/CO, EP/HA and EP/CP composites

Figure.5.16a shows the thermal Stability of EP, EP/CO, EP/HA and EP/CP composites. The composites exhibit two stages of degradation. The first stage of degradation occurred in the temperature range of 25°C to 280°C with a minimal weight loss. In this stage, disrupt of uncured epoxy resin and removal of moisture absorption and impurities has taken place (Zhu et al. 2011). The second major weight loss occurred in

the temperature range of 300°C to 400°C, which was due to the thermal degradation of composites and epoxy network. Temperature at the maximum rate of degradation (T_{max}) was calculated from the DTG curve of composites (Figure 5.16b). Besides, thermal stability factors like activation energy (E_t), integral procedure decomposition temperature (IPDT) and char yield at 700°C (CY) were presented in table 5.8.

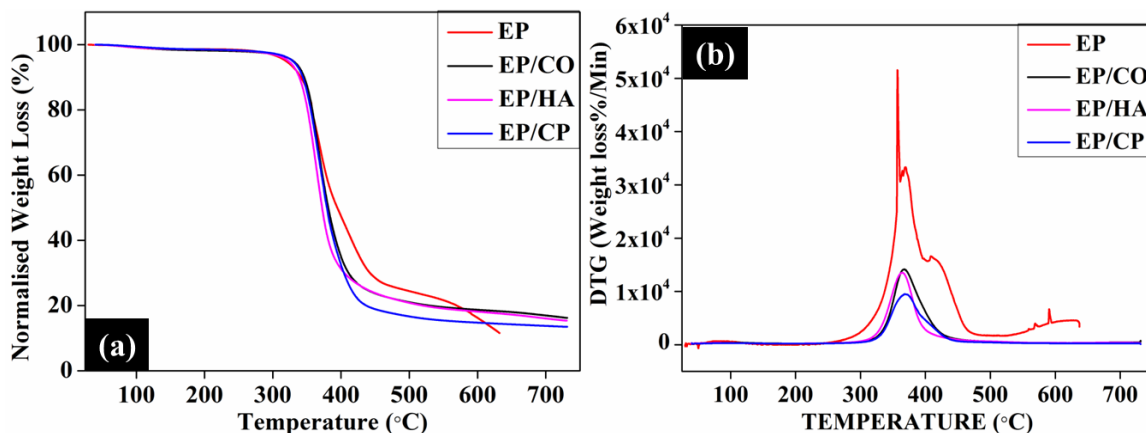


Figure 5.16 (a) TG and (b) DTG of EP, EP/CO, EP/HA and EP/CP composites

Table 5.6: Thermal properties of EP, EP/CO, EP/HA and EP/CP composites

Composite	T_{max} (°C)	IPDT (°C)	E_t (KJ/mol)	Char Yield (%)
EP	356.8	453.3	117.1	5.82
EP/CO	367.1	577.9	167.0	16.2
EP/HA	364.3	561.4	160.4	15.39
EP/CP	368.1	530.8	162.3	13.49

TGA results showed that addition of cuttlebone derived bio ceramic fillers (CO, HA and CP) improved the thermal properties of the composites than neat epoxy. As compared to neat epoxy, all three composites had higher T_{max} value due to the particle/matrix adhesion. Moreover, IPDT clearly showed addition of ceramic filler tends to improve the thermal stability of composites significantly compared to the neat epoxy. In that EP/CO had good thermal stability followed by EP/HA, EP/CP composites. Polar group presents in epoxy resin had a good interaction with hydroxyl group presents in CO HA and CP particles. This may lead the proper interaction between filler and matrix

which significantly slow down the degradation process and increases the IPDT value of the EP/CO, EP/HA and EP/CP composites. However there was not much significant difference found in IPDT value of three composites. Similarly, activation energy increased with the addition of the CO, HA and CP reinforcement filler in EP because of the high surface contact area between reinforcing filler and matrix (Shimpi and Mishra 2012). Interestingly, composites with small particle size fillers (HA and CP) required relatively high activation energy than composite with bigger particle size (CO). The possible explanation for the observed results (contrary to the expectation) could be lowered thermal stability of HA and CP particles due to their phosphate content. Besides, the char yield at 650°C was found to be increased in EP/CO, EP/HA and EP/CP composites compared to neat epoxy. Overall, TGA results revealed all three composites showing better thermal stability than EP. In that, EP/CO composites have slightly better thermal stability than EP/HA and EP/CP composites.

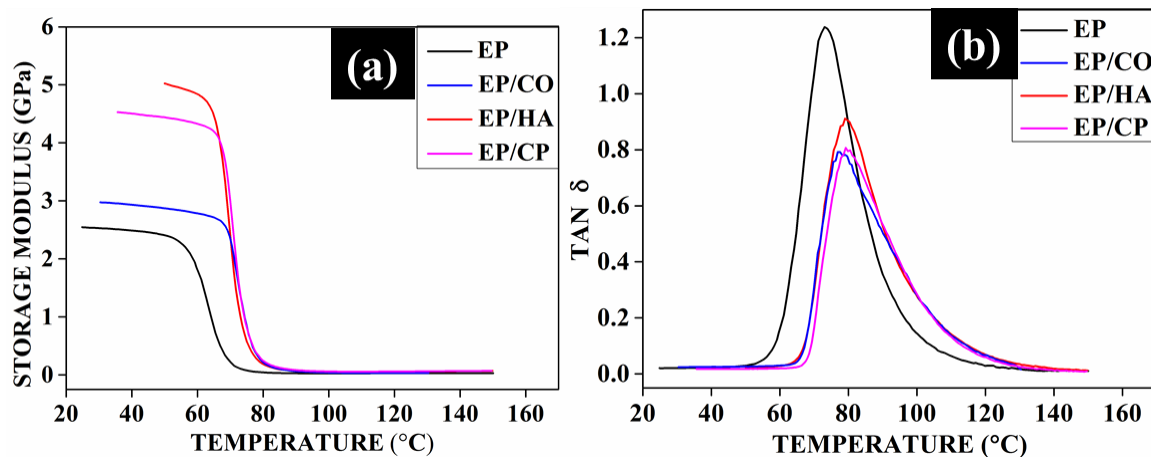


Figure 5.17 (a) Storage modulus and (b) $\tan\delta$ of EP, EP/CO, EP/HA and EP/CP composites.

Figure 5.17 shows the (a) storage modulus and (b) mechanical loss factor ($\tan\delta$) with respect to temperature for EP, EP/CO, EP/HA and EP/CP composites. Furthermore, the storage modulus, gain in percentage of storage modulus and glass transition temperature of all four materials are summarized in table 5.7. The storage modulus for neat epoxy was 2.57GPa. By the addition of different reinforcement particle in epoxy

matrix tends to increase the storage modulus of composites. The storage modulus of EP/CO, EP/HA and EP/CP composites increased and reaches the value of 2.98GPa, 5.02GPa and 4.53GPa, respectively. As presented in table 5.7, the increase in percentage of storage modulus for EP/CO, EP/HA and EP/CP composites with respect to neat epoxy was 15.95%, 95.33% and 76.27%, respectively. The increase in storage modulus of composites was probably due to the addition of rigid ceramic particles in epoxy matrix which restricts the molecular mobility (Ramdani et al. 2014). Consequently, the storage modulus of EP/HA and EP/CP composites was enhanced tremendously due to the increase in interfacial bonding between filler and matrix. Besides, the storage modulus of EP/CO composites was significantly lower than other two composites. The possible reason could be the nano particles (HA and CP) have better dispersion and interaction than micro particle reinforced composites (Ramdani et al. 2014). As shown in figure 5.17a, storage modulus of all four materials has a gradual drop upto glass transition region. At the region of glass transition there was sudden drop in storage modulus identified in all four composites. These changes denote that material has transferred from glassy to rubbery region.

Table 5.7: Storage modulus and glass transition temperature of EP, EP/CO, EP/HA and EP/CP composites

Composite	Storage Modulus (GPa)	Gain in Storage Modulus (%)	Glass transition Temperature from $\tan\delta$ ($^{\circ}\text{C}$)
EP	2.57	--	73.03
EP/CO	2.98	15.95	76.77
EP/HA	5.02	95.33	79.24
EP/CP	4.53	76.27	79.04

The glass transition temperature (T_g) of composites was determined from the peak point of $\tan\delta$ curve (shown in figure 5.17b). As compared to the neat epoxy, composites filled with CO, HA and CP particles as reinforcement has a slight enhancement in T_g values. The T_g value of EP, EP/CO, EP/HA and EP/CP composites was 73.03°C , 76.77°C , 79.24°C and 79.04°C , respectively. The possible reason could be the better

matrix-particle interaction in composites and also the restriction in matrix mobility through the filler material (Rahman et al. 2013). Apart from the T_g , damping factor of the prepared composites was extracted from the $\tan\delta$ curve (shown in figure 5.17b). Addition of stiffened cuttlebone derived ceramic particles in epoxy matrix tends to decline in the damping factor through diminish in peak intensity along with the peak broadening (Mohd Zulfli et al. 2013).

Composites relaxation phenomenon was evaluated through T_g value which estimated from dissipation factor ($\tan \delta$). The possible reason for the enhancement in T_g value is mainly due to the reduction in free volume of polymers, increase in number of successive cross links and decrease in chain mobility of polymers (Yasmin and Daniel 2004). It implies that addition of hard ceramic particles tends to restrict the motion of matrix phase. The reduction in molecular mobility leads to the broadening of peaks along with the decrease in $\tan\delta$ peak intensity, due to the heterogeneity of polymer network. In this case, the T_g value of EP/HA and EP/CP composites were higher than EP/CO composites. The higher in T_g value of these two composites could be attributed through the increase in degree of interaction between matrix and cuttlebone derived ceramic particle surface (Zabihi et al. 2011).

Table 5.8: Swelling ratio, crosslink density and molecular weight between crosslinks of EP, EP/CO, EP/HA and EP/CP composites

Composite	Swelling ratio (S.R)	Crosslink density (ν) (mol/cm^3)	Molecular weight between crosslinks (M_C)
EP	0.6004	0.0047	212.43
EP/CO	0.2886	0.0093	107.13
EP/HA	0.1044	0.0201	79.73
EP/CP	0.1929	0.0125	49.64

The swelling ratio, crosslink density and molecular weight between crosslinks of EP, EP/CO, EP/HA and EP/CP composites were presented in table 5.8. The swelling ratio of neat epoxy was 0.6004. Similarly, the swelling ratio of EP/CO, EP/HA and EP/CP composites was 0.2886, 0.1044 and 0.1929, respectively. As compared to the neat

epoxy, the swelling ratio of all three composites was decreased. It showed that addition of rigid ceramic particles in epoxy matrix tends to restrict the penetration of solvent in composites due to the better bonding between filler and matrix material (Ku et al. 2013 and Ahmed 2015). Amongst the three composites, the swelling ratio was higher in EP/CO followed by EP/CP and EP/HA. Addition of nano particles in polymer matrix tends to give better bonding than micro filled ones due to high surface contact area. Similarly, presence of hydroxyl group in HA samples have better interaction with epoxy matrix which tends to give lower swelling ratio. Besides, hygroscopic nature of CO particles tends to absorb more solvent and gave maximum swelling ratio.

Addition of CO, HA and CP particles in epoxy matrix tends to increase the cross link density of composites. As compared to neat epoxy (0.0047mol/cm^3), EP/HA composites has higher cross link density (0.0201mol/cm^3) followed by EP/CP (0.0125mol/cm^3) and EP/CO (0.0093mol/cm^3). This cross link density behavior of all four materials is well agreed with their corresponding glass transition temperature. The addition of thermally stable rigid filler in epoxy matrix attributes the interlocking formation of matrix which induces more cross link density (Ahmed et al. 2012 & Rahman et al. 2013). Furthermore, the average molecular weight between crosslinks was inversely proportional to cross link density. In that EP/CP composite has lower value compare to other two composites.

5.1.7 Biocompatible properties of EP/HA and EP/CP composites

Based on the thermal, thermo-mechanical, and physical properties results of EP, EP/CO, EP/HA and EP/CP composites it can be concluded that EP/HA and EP/CP composites had relatively more advantageous properties as compared to other two materials. Hence these two composites were further subjected to biocompatibility studies.

In this topic two different groups of composites (EP/HA and EP/CP) were analyzed. Each test group consists of five different sets (cell control, 100%, 50%, 25% and 12.5% leach concentration). Results are expressed in the form of mean \pm Standard deviation of 6 experiments. Statistical analyses were performed by one-way ANOVA and

Tukey's honestly significant difference method was used for all post hoc analysis to identify the significant difference between each set of individual test group. In all the tests, statistical significance was set at $p < 0.05$. Letters in upper case (A and B) and lower case (a, b and c) was used to denote the statistical results in EP/HA and EP/CP test group, respectively.

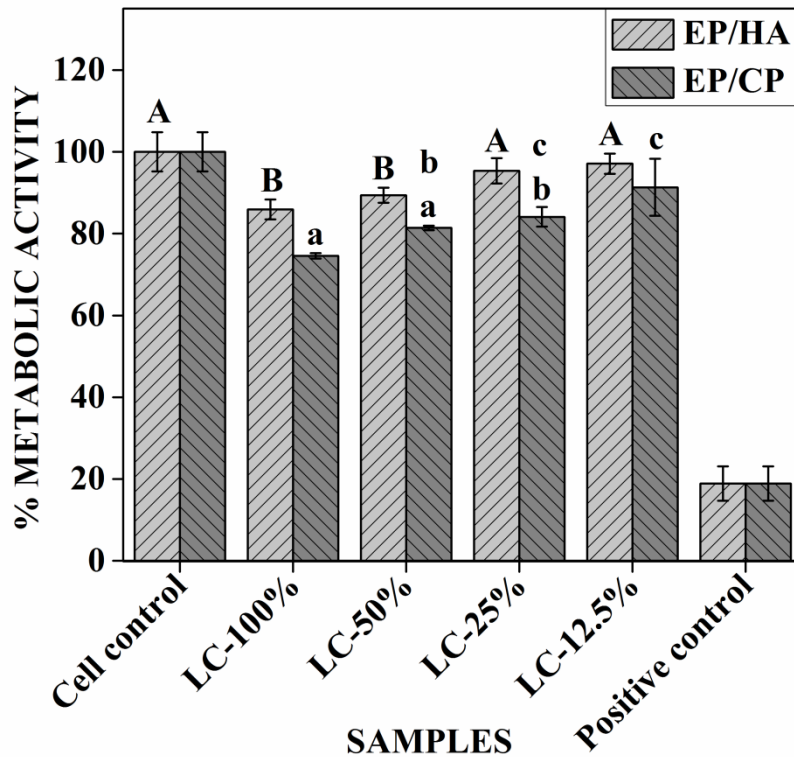


Figure 5.18 “*In vitro*” cytotoxicity of EP/HA and EP/CP composites. Data are expressed as percentage of control mean \pm S.D. of six independent experiments. Letters indicate pairwise comparison, that they were significantly not different ($p \geq 0.05$).

Figure 5.18 shows the cell viability percentage of EP/HA and EP/CP composites at various leach concentration (LC). For EP/HA composites, the cell viability percentage at 100%, 50%, 25% and 12.5% leach concentrations were 85.93%, 89.41%, 95.35% and 97.1%, respectively. Similarly for EP/CP composites, the cell viability percentage at 100%, 50%, 25% and 12.5% LC were 74.57%, 81.4%, 84.1% and 91.33%, respectively. The results clearly indicate that EP/HA composites do not show any toxic effect at all

LC. While reducing the leach concentration from 100 to 12.5%, the percentage of metabolic activity (cell viability) was increased continuously.

As compared to control sample, there was a significant reduction was found in the cell viability percentage of EP/HA composites prepared at 100 & 50% LC. However, there was no significant difference found between 100 and 50% LC samples. Similarly, EP/HA composites done at 25 & 12.5% LC does not have any significant difference with control sample. Besides, there was no significant difference found with the samples (EP/HA at 25 and 12.5% LC). Moreover, none of the EP/HA composite samples shown cell proliferation.

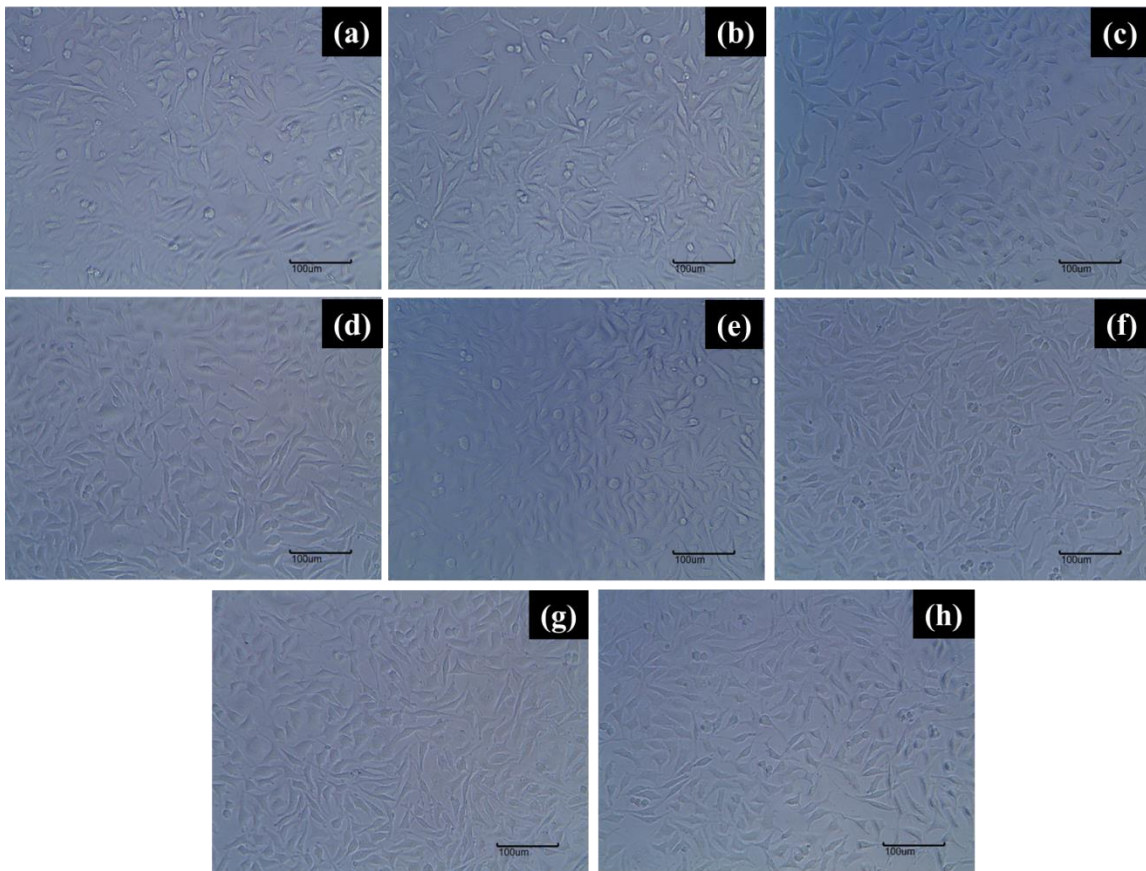


Figure 5.19 Microscopic images of viable cells for (a-d) EP/HA composite prepared at 100% leach concentrations, (e-h) EP/CP composite prepared at 100, 50, 25 and 12.5% Leach concentrations.(scale bar:100µm)

In the case of EP/CP composites, samples at 100% LC shown slight toxic (74.57%). Besides, there was a continuous improvement in cell viability % by further reducing the LC. The cell viability percentage of samples prepared at four different concentrations has significantly different with control samples. But there was no significant difference was found between the combinations of 100 & 50%, 50 & 25% and 25 & 12.5%. Similarly as like EP/HA composites, EP/CP composites also not shown cell proliferation at all concentration.

Moreover, the viability of cell at different LC for EP/HA and EP/CP composites is shown in figure 5.19. In EP/HA composites, more number of viable cells was identified at 25 and 12.5% LC (figure 5.19c&d). In EP/CP composites at 100% LC showed the depletion of more number of viable cells (figure 5.19e). However, by reducing the LC the number of viable cells was increased (figure 5.19f-h).

EP/CP composite at 100% LC does not diminish the toxic level of epoxy resin (Fu and Zhao 2004). Nevertheless, by reducing the LC % (from 50 to 12.5%) in EP/CP composites tends to give the better cell viability. The results suggest that addition of HA as reinforcement in epoxy matrix has shown better adhesion with cells rather CP filled ones.

Table 5.9: Hemolysis percentage of EP/HA and EP/CP composites.

Samples	% Hemolysis	Average Hemolysis %	Normal Hemolysis
EP/HA	0.053	0.04	
EP/CP	0.046	0.04	< 0.1%

Table 5.9 shows the hemolytic activity of the prepared composite samples. The average percentage of hemolysis was 0.04%. Hemolysis % of EP/HA and EP/CP samples were found to be 0.053 and 0.046, respectively. From the above results it is concluded that both the sample are in non-hemolytic nature. There was no significant difference was found between two samples. There are many reasons that could improve the blood compatibility of the composites. The possible reason could be a) hydrophilic nature, b) surface roughness of particles and 3) biocompatibility of cuttlebone derived HA and CP

fillers (Janaki et al. 2008). Hydrophobic nature of the HA particles tends to show slightly higher hemolysis % compared to average hemolysis %. The observed results may confirm that addition of HA and CP particles in epoxy matrix tend to improve the blood compatibility of composites.

5.1.8 Summary

To summarize the results from this chapter, the influence of cuttlebone derived calcium oxide, hydroxyapatite and tri calcium phosphate reinforced epoxy composites (EP, EP/CO, EP/HA and EP/CP) was discussed. HA and CP particles are in sub-micron size range with higher surface area than CO particles. Prepared CO & CP particles are in pure calcium oxide and tricalcium phosphate form. However HA particles are in biphasic crystalline form with the combination of hydroxyapatite and minimal amount of calcium oxide. EP/HA composites have better elongation % at break, flexural strength, flexural modulus and fracture toughness properties. EP/CP has better ultimate tensile strength, tensile modulus, compression strength, compression modulus, impact strength and hardness properties. All three composites show rough fracture surface and more voids in higher filler percentage. EP/CO composites required high activation energy to decompose than EP/HA and EP/CP composites. EP/HA composite showed higher T_g than EP/CP and EP/CO composites. Similar trend was observed in crosslink density results. EP/CO composites absorbed more water than other composites. EP/HA shows hydrophobic surface nature. EP/HA composite shows better metabolic activity at all leach concentrations. However, EP/CP shows slight toxicity at 100% leach concentration. Both EP/HA and EP/CP are non-hemolytic.

CHAPTER 6

CHAPTER 6

COMPARISON OF MATERIALS PROPERTIES OF CUTTLEBONE DERIVED BIO FILLERS AND BIO CERAMICS REINFORCED EPOXY COMPOSITES

Based on the results of last two chapters, epoxy composites prepared using cuttlebone derived bio fillers (EP/CB and EP/HB prepared at 9 wt% filler fraction) and cuttlebone derived bio ceramics (EP/HA and EP/CP prepared at 6 wt% filler fraction) as reinforcement has shown good material properties. Material properties like mechanical, physical, thermal, thermo-mechanical and biocompatibility properties of these four composites along with neat epoxy has been compared in this chapter. From the comparison results, suitable composite with required material properties (mechanical and biocompatibility) for low load bearing implant applications has been recommended.

6.1 Results and Discussions

6.1.1 Material characterization of CB, HB, HA and CP particles

The average particle size for CB, HB, HA and CP particles are 10.32, 10.32, 0.74 and 1.01 μm , respectively. The particle size distribution for CB and HB particles were broad in nature. But in the case of HA and CP, it was narrow and shows higher degree of agglomeration. The particle morphology for CB and HB was in flake structure. Likewise, HA and CP particles are in cubic and rod structure, respectively. The density of CB, HB, HA and CP particles are 2.4, 2.4, 2.14 and 1.83g/cm³, respectively. Furthermore, surface area for CB, HB, HA and CP particles are 5.08, 5.08, 9.12 and 8.38m²/g, respectively. The ICP-OES result for CB particles confirms the presence of elements like Na, K, Mg, Fe, Sr and Ca. Similarly, the Ca/P molar ratio for cuttlebone derived HA and CP particles were identified through ICP-OES and the values are 1.72 and 1.53, respectively. The TGA results indicates that cuttlebone derived bio fillers (CB & HB) and bio ceramics (HA &

CP) particles were thermally stable up to 600°C and 1000°C, respectively. The crystallographic structure and components presents in these four particles was confirmed through XRD and FT-IR. The CB and HB particles were composed of CaCO₃ in aragonite and calcite polymorph form, respectively. Moreover, HA particles were in biphasic form and composed of hydroxyapatite and calcium oxide phases. But, CP particles were in pure tri calcium phosphate phase. Besides, organic components like protein and chitin were detected as secondary major phase in CB.

6.1.2 Mechanical properties of EP, EP/CB, EP/HB, EP/HA and EP/CP composites

In this topic five different composites (EP, EP/CB, EP/HB, EP/HA and EP/CP) were analyzed. Results are expressed in the form of mean \pm Standard deviation of 5 experiments. For all mechanical properties, statistical analyses were performed by one-way ANOVA. Tukey's honestly significant difference method was used for all post hoc analysis to identify the significant difference between five different composites. In all the tests, statistical significance was set at $p < 0.05$. Symbols (\spadesuit , \clubsuit , \diamond and \heartsuit) were used to denote the statistical results between the composites.

Figure 6.1 shows the ultimate tensile strength, tensile modulus and elongation percentage at break of different composites. Ultimate tensile strength (UTS) of all four composite increased significantly by the addition of different filler content in matrix material as shown in Figure 6.1a. In that, EP/CP has highest UTS (48.05MPa) followed by EP/HB (41.30MPa), EP/CB (38.84MPa), EP/HA (37.3MPa) and neat epoxy of 23.78MPa. There was no significant difference found between EP/CB, EP/HB and EP/HA combinations. Similarly, combinations between EP/CB, EP/HB and EP/CP did not shown any significant difference among them. The result clearly indicates that addition of different filler in epoxy matrix leads to the significant improvement in UTS, but no significant difference found between the four composites.

The tensile modulus for neat epoxy was 0.659GPa (shown in figure 5.1b). Addition of different filler content in matrix material leads to the significant improvement in tensile modulus of composites. EP/CP (1.85GPa) and EP/HA (1.64GPa) composites

shown higher tensile modulus than EP/HB (0.767GPa) and EP/CB (0.748GPa). Among the five different materials, EP/CB and EP/HB composites did not shown any significant difference in tensile modulus of composites. Besides, all other combination has shown the significant difference. It concludes that EP/HA and EP/CP composites have greater influence on the improvement of tensile modulus than EP/CB and EP/HB composites. Similarly, EP/CP composite shows significantly higher tensile modulus than EP/HA composite.

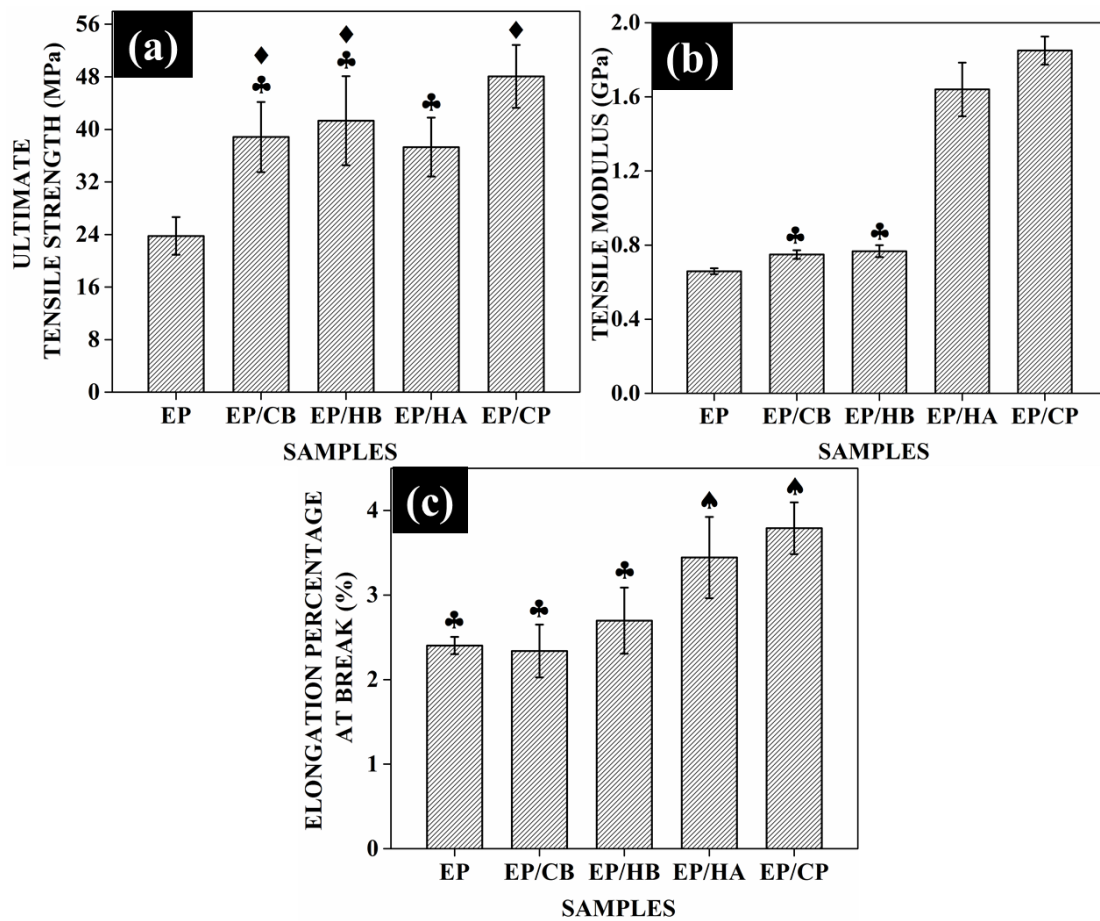


Figure 6.1 (a) Ultimate tensile strength, (b) Tensile modulus and (c) Elongation percentage at break of EP, EP/CB, EP/HB, EP/HA and EP/CP composites. Symbols (inset in figure) indicate pairwise comparison, that they were significantly not different ($p \geq 0.05$).

Elongation percentage at break (EPB) for neat epoxy and four different composites are shown in Figure 6.1c. As compared to neat epoxy (2.40 %), the EPB value for EP/CB composites reduced slightly but it was not up to the significant level. Besides, EP/HB, EP/HA and EP/CP composites has shown higher EPB value than neat epoxy. There was no significant difference found between the EPB value of neat epoxy, EP/CB and EP/HB composites. Nevertheless, EP/HA and EP/CP composites has shown significant improvement in EPB as compared to other composites. Furthermore, there was no significant difference found between these two (EP/HA and EP/CP) composites. Similarly as like tensile modulus, EP/HA and EP/CP composites has greater improvement in EPB value as compared to neat epoxy, EP/CB and EP/HB composites.

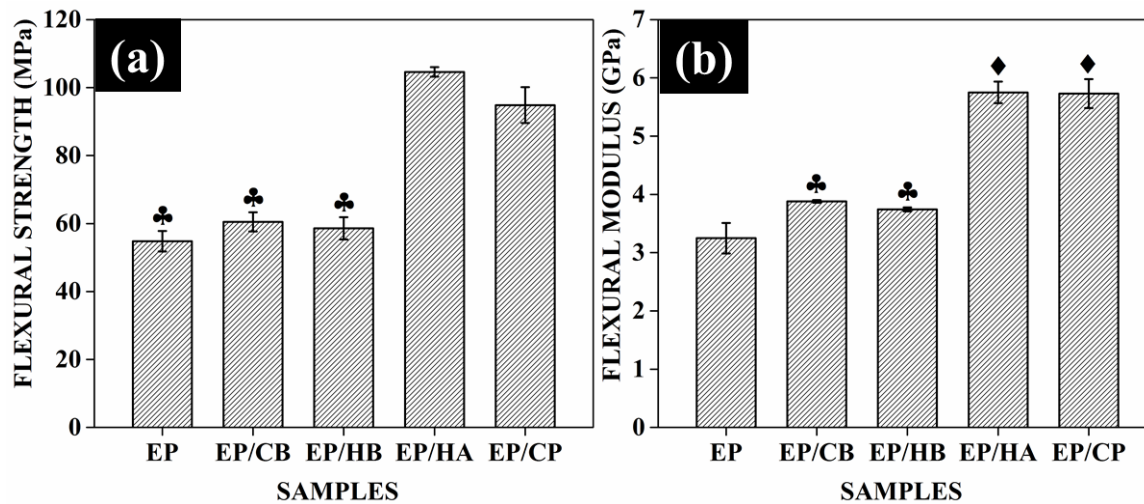


Figure 6.2. (a) Flexural strength and (b) Flexural modulus of EP, EP/CB, EP/HB, EP/HA and EP/CP composites. Symbols (inset in figure) indicate pairwise comparison, that they were significantly not different ($p \geq 0.05$).

Figure 6.2 shows the flexural strength and flexural modulus of different composites. The neat epoxy has the flexural strength of 54.79MPa. As shown in Figure 6.2a, by the addition of different filler in epoxy matrix tends to increase the flexural strength of all four composites. Flexural strength of EP/HA (104.6MPa) and EP/CP (94.85MPa) was higher than EP/CB (60.5MPa) and EP/HB (58.59MPa) composites. The one-way ANNOVA result indicates that combinations like neat epoxy, EP/CB and EP/HB does not shown any significant difference in the flexural strength. However,

EP/HA and EP/CP composites has significant improvement in flexural strength than other three material. On the other hand, there was a significant difference found between the flexural strength of EP/HA and EP/CP composites.

The flexural modulus for neat epoxy was 3.25GPa (shown in figure 6.2b). The flexural modulus value for EP/CB, EP/HB, EP/HA and EP/CP composites were 3.88GPa, 3.74GPa, 5.75GPa and 5.73GPa, respectively. As compared to neat epoxy, EP/CB and EP/HB composites show significant improvement in flexural modulus. Similarly, flexural modulus of EP/HA and EP/CP composites was significantly higher than other three materials. However, combinations like EP/CB & EP/HB and EP/HA & EP/CP does not any significant difference in flexural modulus. Besides, the results concluded that addition of HA and CP particles in epoxy matrix tend to shown substantial increment in flexural properties than CB and HB reinforced ones.

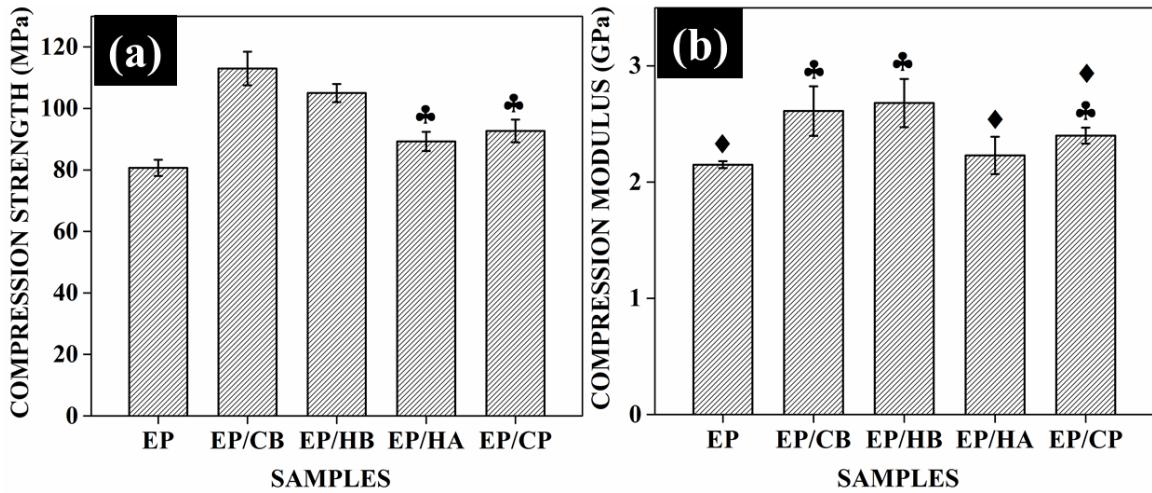


Figure 6.3. (a) Compression strength and (b) Compression modulus of EP, EP/CB, EP/HB, EP/HA and EP/CP composites. Symbols (inset in figure) indicate pairwise comparison, that they were significantly not different ($p \geq 0.05$).

The compression strength and modulus for neat epoxy and different composites was presented in figure 6.3. Figure 6.3a indicates that addition of CB & HB filler as reinforcement in epoxy matrix tends to increase the compression strength of composites rather than HA and CP filler ones. As compared to neat epoxy (80.7MPa), compression strength of EP/HA (89.29MPa) and EP/CP (92.7MPa) composites was increased

significantly. However, there was no significant difference found between EP/HA and EP/CP composites. On the other hand, EP/CB (113MPa) and EP/HB (105MPa) composites compression strength was higher than other materials. Besides, compression strength of EP/CB was significantly higher than EP/HB ones. Lastly, EP/CB composite has higher compression strength than other composites.

As like compression strength, compression modulus of different composites was higher than neat epoxy. The compression modulus for neat epoxy was 2.15GPa. The compression modulus for EP/CB, EP/HB, EP/HA and EP/CP composites were 2.61GPa, 2.68GPa, 2.23GPa and 2.4GPa, respectively. As compared to neat epoxy, compression modulus for EP/CB and EP/HB composites was significantly different. However, there was no significant found between these two composites. Similarly, improvement in compression modulus for EP/HA and EP/CP composites was not significantly different with neat epoxy. Likewise, there was no significant difference found between EP/HA and EP/CP composites. Based from the results, it was found that addition of CB and HB particles in epoxy matrix have greater influence on the improvement of compression modulus of composites.

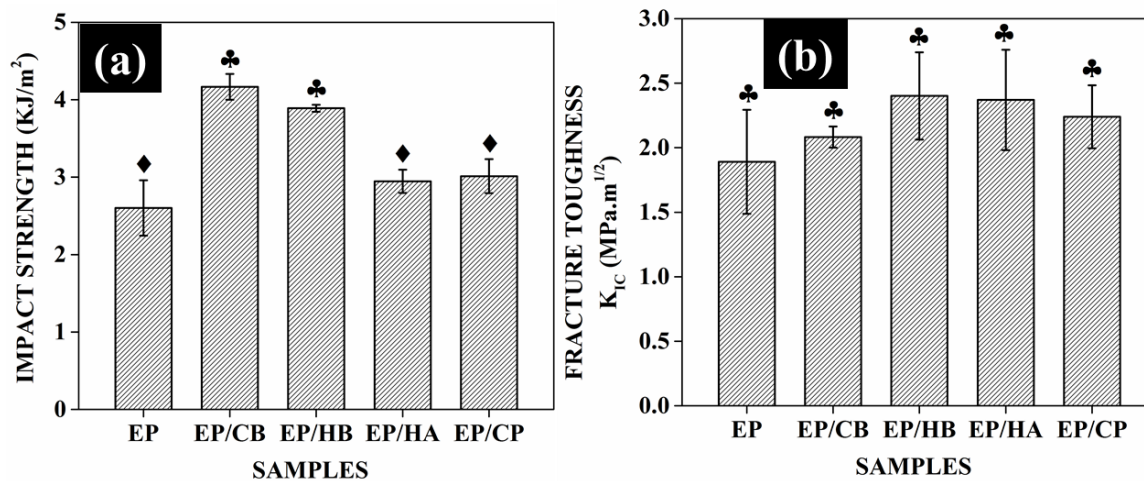


Figure 6.4. (a) Impact strength, and (b) Fracture toughness of EP, EP/CB, EP/HB, EP/HA and EP/CP composites. Symbols (inset in figure) indicate pairwise comparison, that they were significantly not different ($p \geq 0.05$).

Figure 6.4 shows the impact strength and fracture toughness properties of neat epoxy and four different composites. As shown in Figure 6.4a the neat epoxy has impact strength of 2.60KJ/m^2 , and it was higher in all four composites. The impact strength of EP/CB, EP/HB, EP/HA and EP/CP composites was attained of 4.16KJ/m^2 , 3.89KJ/m^2 , 2.95KJ/m^2 and 3.01KJ/m^2 , respectively. As compared to neat epoxy, the improvement in impact strength was not significantly higher in EP/HA and EP/CP composites. Furthermore in EP/CB and EP/HB composites, the improvement in impact strength was significantly higher compared to neat epoxy and other composites. However, there was no significant difference found between EP/CB and EP/HB composites. The results concluded that addition of CB and HB particles in epoxy matrix tends to improve the impact strength of composites at significant level.

Fracture toughness of neat epoxy and four different composites is shown in figure 6.4b. The neat epoxy has the fracture toughness value of $1.89\text{MPa.m}^{1/2}$. Addition of four different filler in epoxy matrix tends to improve the fracture toughness of composites. The fracture toughness value of $2.08\text{MPa.m}^{1/2}$, $2.40\text{MPa.m}^{1/2}$, $2.37\text{MPa.m}^{1/2}$ and $2.24\text{MPa.m}^{1/2}$ was obtained for EP/CB, EP/HB, EP/HA and EP/CP composites, respectively. The result of one-way ANNOVA indicates that none of the combinations shown significant difference in fracture toughness value. It concludes that improvement in fracture toughness of composites was not up to the significant level as compared to neat epoxy.

Shore D hardness of neat epoxy and four different composites are shown in figure 6.5. The neat epoxy has a hardness value of 72.4. The hardness value of four composites was significantly higher as compared to neat epoxy. In this, EP/HB composite has higher hardness value (87) followed by EP/CP (86.7), EP/HA (83.4) and EP/CB (83.1) composites. The results indicate that addition of four different fillers in epoxy matrix leads to the significant improvement in hardness property. However, there was no significant difference found between the hardness values of four composites.

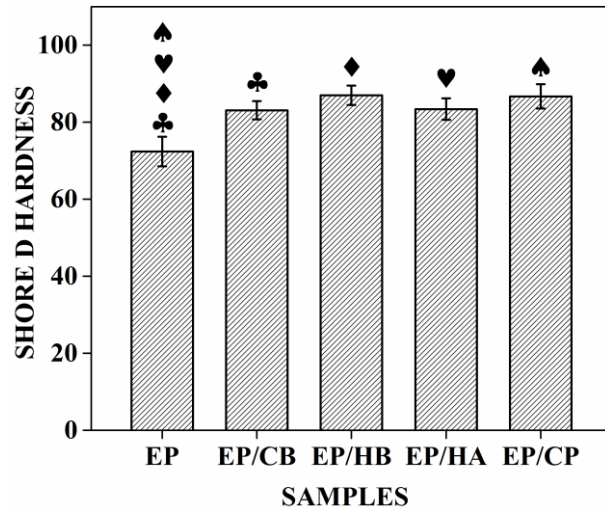


Figure 6.5. Shore D Hardness of EP, EP/CB, EP/HB, EP/HA and EP/CP composites. Symbols (inset in figure) indicate pairwise comparison, that they were significantly different ($p < 0.05$).

6.1.3 Fracture morphology studies of EP, EP/CB, EP/HB, EP/HA and EP/CP composites

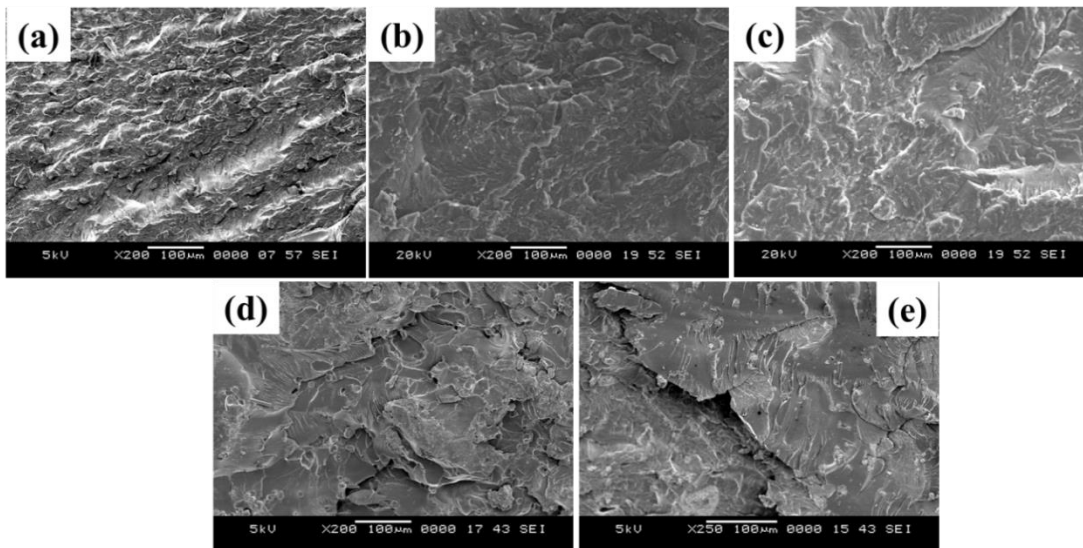


Figure 6.6. SEM micrograph of (a) EP, (b) EP/CB, (c) EP/HB (d) EP/HA and (e) EP/CP composites.

The micrograph of neat epoxy (EP), EP/CB, EP/HB, EP/HA and EP/CC composites are shown in Figure 6.6. A coarse and brittle type fracture surface was observed in the

morphology of neat epoxy as shown in Figure 6.6a. Compared to neat epoxy, EP/CB and EP/HB composites (shown in Figure 6.6b–c) had smooth fracture surface morphology. As compared to neat epoxy and other two composites, the fracture surface of EP/HA and EP/CP was quite rough. Furthermore, notable amount of voids were observed on the fracture surface of EP/HA and EP/CP composites.

6.1.4 Voids percentage of EP, EP/CB, EP/HB, EP/HA and EP/CP composites

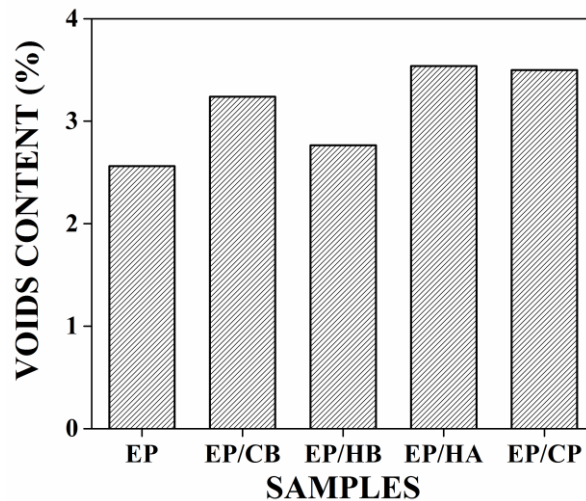


Figure 6.7. Voids percentage of EP, EP/CB, EP/HB, EP/HA and EP/CP composites.

Voids percentage of composites was calculated based on the actual and theoretical density of composites. The results are presented in figure. 6.7. The voids percentage of neat epoxy matrix was 2.561%. As compared to neat epoxy, the voids percentage of all four composites increased due to the addition of different filler content. The voids percentage of EP/CB, EP/HB, EP/HA and EP/CP composites was 3.24%, 2.76%, 3.54% and 3.50%, respectively. In that, EP/HA and EP/CP composites show higher voids percentage compare to EP/CB and EP/HB composites. Besides, voids percentage in EP/CB was higher than EP/HB composites.

6.1.5 Physical properties of EP, EP/CB, EP/HB, EP/HA and EP/CP composites

Figure 6.8 shows the water absorption behavior of EP, EP/CB, EP/HB EP/HA and EP/CC composites. After 30 days, the maximum amount of water uptake for EP, EP/CB,

EP/HB and EP/CC composites was around 0.46%, 0.51%, 0.53%, 0.43% and 0.47%, respectively. At the end of 30 days, water uptake percentage for EP/CB, EP/HB and EP/CP composites was higher than neat epoxy. In that, water uptake percentage for EP/HA and EP/CP composites was significantly lesser than EP/CB and EP/HB composites. Nevertheless, water uptake percentage of EP/HA composite was lower than neat epoxy.

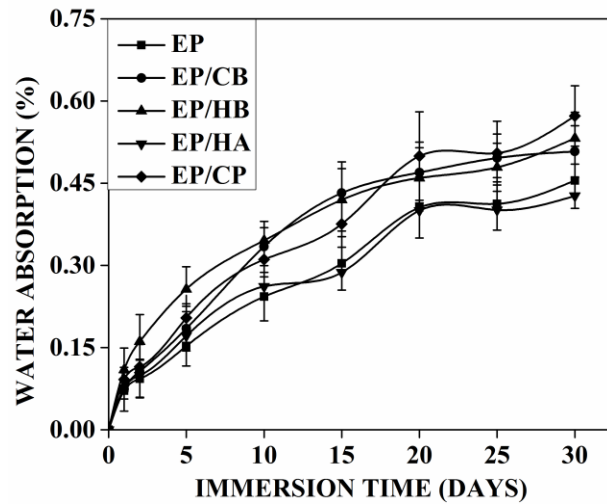


Figure 6.8. Water absorption percentage of EP, EP/CB, EP/HB, EP/HA and EP/CP composites.

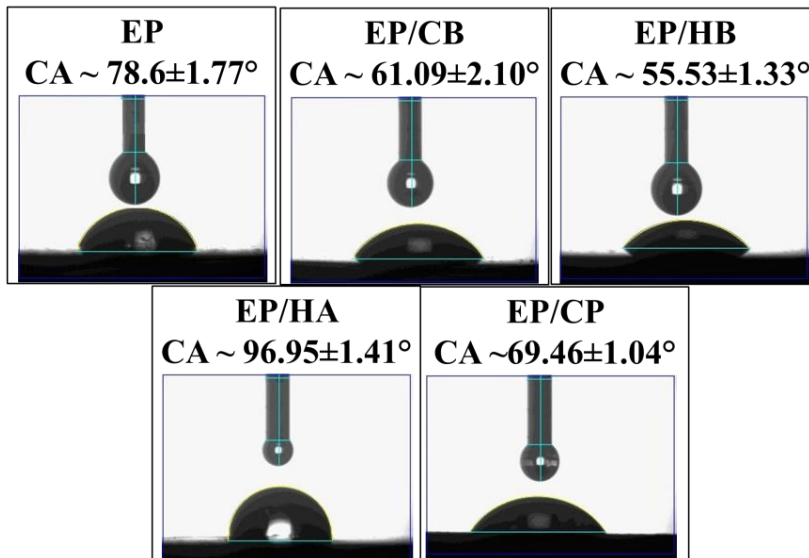


Figure 6.9. Wettability results for EP, EP/CB, EP/HB, EP/HA and EP/CP composites.

The water contact angle for EP, EP/CB, EP/HB and EP/CC composites was $78.6 \pm 1.77^\circ$, $61.09 \pm 2.10^\circ$, $55.53 \pm 1.33^\circ$, $96.95 \pm 1.41^\circ$ and $71.68 \pm 1.01^\circ$, respectively. Amongst the five materials, neat epoxy and three composites (EP, EP/CB, EP/HB and EP/CP) showed a hydrophilic behavior because of its contact angle was less than 90° . However, EP/HA composites showed a hydrophobic nature.

6.1.6 Thermo-mechanical and thermal properties of EP, EP/CB, EP/HB, EP/HA and EP/CP composites

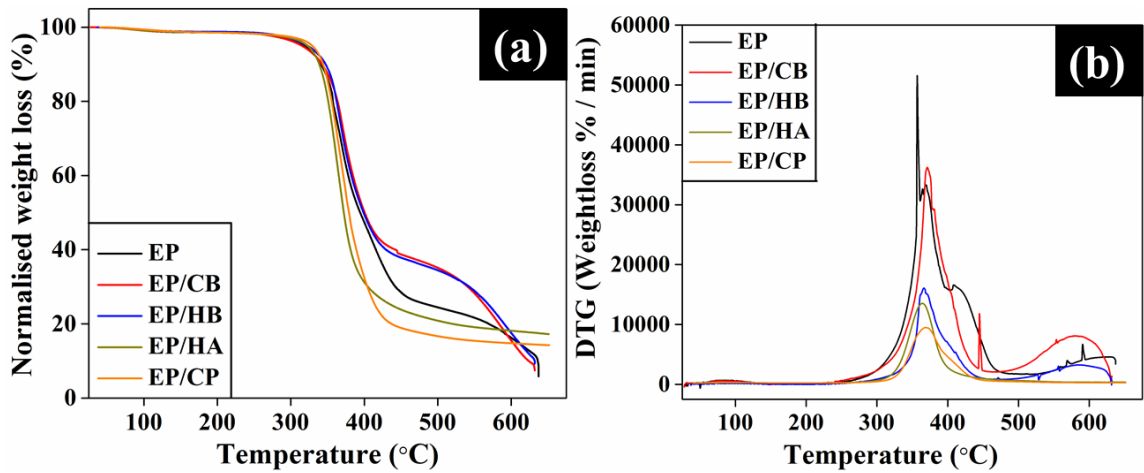


Figure 6.10 (a) TG and (b) DTG of EP, EP/CB, EP/HB, EP/HA and EP/CP composites

Figure. 6.10a shows the thermal Stability of neat epoxy and four different composites. The composites exhibit two stages of degradation. The first stage of degradation occurred in the temperature range of 25°C to 280°C with a minimal weight loss due to moisture absorption. The second major weight loss occurred in the temperature range of 300°C to 400°C , which was due to the thermal degradation of filler and epoxy network. Besides, thermal stability factors like Temperature at the maximum rate of degradation (T_{\max}), activation energy (E_t), integral procedure decomposition temperature (IPDT) and char yield at 650°C (CY) were presented in table 6.1.

TGA results showed that addition of cuttlebone derived bio fillers (CB, HB, HA and CP) improved the thermal properties of composites than neat epoxy. As compared to neat epoxy, all four composites had higher T_{\max} , IPDT, E_t and char yield value. It clearly shows that addition of filler in epoxy matrix tends to improve the thermal stability of

composites. In that EP/HA has better thermal stability followed by EP/CP, EP/HB and EP/CB composites. It clearly indicates that addition of bio ceramic particles (HA and CP) as reinforcement in epoxy matrix tends to improve the thermal stability of composites substantially rather than EP/CB and EP/HB composites.

Table 6.1: Thermal properties of EP, EP/CB, EP/HB, EP/HA and EP/CP composites

Composite	T_{max} (°C)	IPDT (°C)	E_t (KJ/mol)	Char Yield (%)
EP	356.8	453.3	117.1	5.82
EP/CB	371.8	480.8	130.4	7.46
EP/HB	366.3	490.0	133.8	9.28
EP/HA	364.3	561.4	160.4	15.39
EP/CP	368.1	530.8	162.3	13.49

Figure 6.11 shows the (a) storage modulus and (b) mechanical loss factor ($\tan\delta$) with respect to temperature for neat epoxy and four different composites. Furthermore, the storage modulus, gain in percentage of storage modulus and glass transition temperature of all five materials are summarized in table 6.2. The storage modulus for neat epoxy was 2.57GPa. By the addition of different reinforcement particle in epoxy matrix tends to increase the storage modulus of composites.

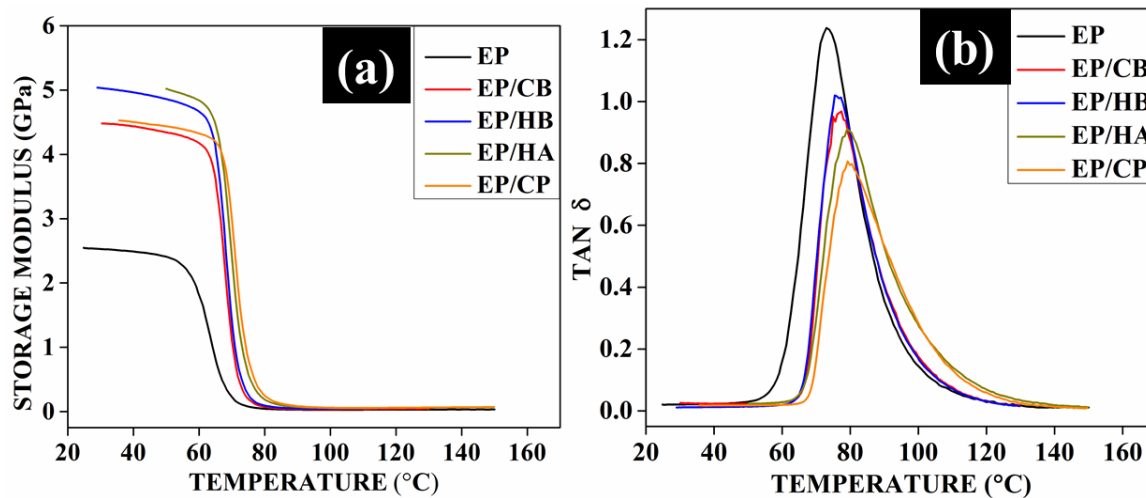


Figure 6.11 (a) Storage modulus and (b) $\tan\delta$ of EP, EP/CB, EP/HB, EP/HA and EP/CP composites.

The storage modulus of EP/CB, EP/HB, EP/HA and EP/CP composites was 4.48GPa, 5.04GPa, 5.02GPa and 4.53GPa, respectively. As presented in table 6.2, the increase in percentage of storage modulus for EP/CB, EP/HB, EP/HA and EP/CP composites with respect to neat epoxy was 74.31%, 96.10%, 95.33% and 76.27%, respectively. The results clearly indicate that EP/HB composite has highest storage modulus followed by EP/HA, EP/CP and EP/CB composites.

Table 6.2: Storage modulus and glass transition temperature of EP, EP/CB, EP/HB, EP/HA and EP/CP composites

Composite	Storage Modulus (GPa)	Gain in Storage Modulus (%)	Glass transition Temperature from $\tan\delta$ ($^{\circ}\text{C}$)
EP	2.57	--	73.03
EP/CB	4.48	74.31	77.41
EP/HB	5.04	96.10	75.48
EP/HA	5.02	95.33	79.24
EP/CP	4.53	76.27	79.04

Table 6.3: Swelling ratio, crosslink density and molecular weight between crosslinks of EP, EP/CB, EP/HB, EP/HA and EP/CP composites

Composite	Swelling ratio (S.R)	Crosslink density (ν) (mol/cm^3)	Molecular weight between crosslinks (M_c)
EP	0.6004	0.0047	212.43
EP/CB	0.372	0.0073	136.71
EP/HB	0.4142	0.0063	159.23
EP/HA	0.1044	0.0201	79.73
EP/CP	0.1929	0.0125	49.64

The glass transition temperature (T_g) of composites was determined from the peak point of $\tan\delta$ curve (shown in figure 6.11b). As compared to the neat epoxy, composites filled with CB, HB, HA and CP particles as reinforcement has a slight enhancement in T_g values. The T_g value of EP, EP/CB, EP/HB, EP/HA and EP/CP composites was 73.03°C , 77.41°C , 75.48°C , 79.24°C and 79.04°C , respectively. In that, EP/HA and EP/CP

composites has higher T_g temperature than EP/CB and EP/HB composites. It clearly indicates that bio ceramic (HA and CP) reinforcement have better interaction and bonding with epoxy matrix rather than bio fillers (CB and HB).

The swelling ratio, crosslink density and molecular weight between crosslinks of neat epoxy and four different composites were presented in table 6.3. The swelling ratio of neat epoxy was 0.6004. The swelling ratio of EP/CB, EP/HB, EP/HA and EP/CP composites was 0.372, 0.4142, 0.1044 and 0.1929, respectively. As compared to the neat epoxy, the swelling ratio of all four composites was decreased. In that EP/HA and EP/CP composites has lower swelling ratio than EP/HB and EP/CB composites. Similarly, EP/HA and EP/CP composites has higher crosslink density than EP/HB and EP/CB composites. It concludes that addition of bio ceramic particles (HA and CP) in epoxy matrix tends to show better bonding with matrix material rather than bio fillers (CB and HB). Amongst the four composites, EP/HA composites has higher cross link density (0.0201 mol/cm^3) followed by EP/CP (0.0125 mol/cm^3), EP/CB (0.0073 mol/cm^3) and EP/HB (0.0063 mol/cm^3) composites. Furthermore, the average molecular weight between crosslinks was inversely proportional to cross link density. In that EP/CP composite has lower value compared to other four composites.

6.1.7 Biocompatible properties of EP/CB, EP/HB, EP/HA and EP/CP composites

In this topic four different groups of composites (EP/CB, EP/HB, EP/HA and EP/CP) were analyzed. Each test group consists of five different sets (cell control, 100%, 50%, 25% and 12.5% leach concentration). Results are expressed in the form of mean \pm Standard deviation of 6 experiments. Statistical analyses were performed by one-way ANOVA and Tukey's honestly significant difference method was used for all post hoc analysis to identify the significant difference between each set of individual test group. In all the tests, statistical significance was set at $p < 0.05$. Letters in upper case (A), Letters in lower case (a and b), symbols (α and β) and symbols (\clubsuit , \heartsuit and \diamondsuit) was used to denote the statistical results in EP/CB, EP/HB, EP/HA and EP/CP test group, respectively.

Similarly, numbers (1), (2), (3) and (4, 5 and 6) was used to denote the statistical results in leech concentration 100%, 50%, 25% and 12.5%, respectively.

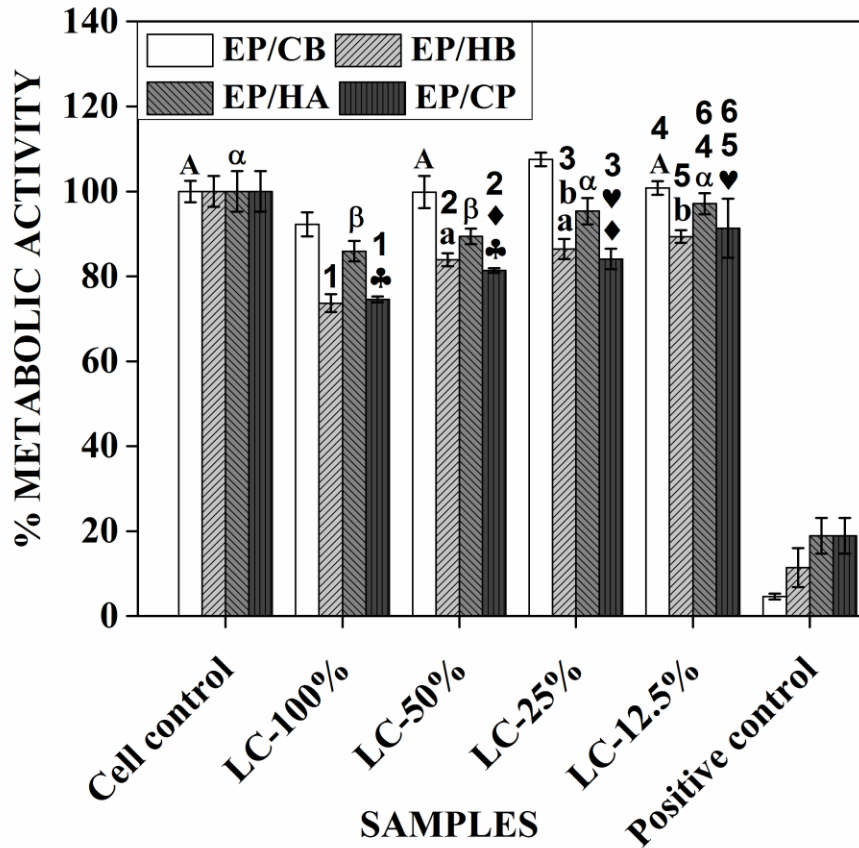


Figure 6.12 “*In vitro*” cytotoxicity of EP/CB, EP/HB, EP/HA and EP/CP composites. Data are expressed as percentage of control mean \pm S.D. of six independent experiments. Letters in upper case, lower case, symbols and numbers indicate pairwise comparison, that they were significantly not different ($p \geq 0.05$).

Figure 6.12 shows the cell viability percentage of EP/CB, EP/HB, EP/HA and EP/CP composites at various leach concentration (LC). The cell viability percentage for EP/CB composites at 100%, 50%, 25% and 12.5% leach concentrations were 92.23%, 99.83%, 107.51% and 100.81%, respectively. For EP/HB composites, the cell viability percentage at 100%, 50%, 25% and 12.5% leach concentrations were 73.69%, 83.9%, 86.4% and 89.6%, respectively. In the case of EP/HA composites, 85.93%, 89.41%,

95.35% and 97.1% cell viability was attained at the leach concentration of 100%, 50%, 25% and 12.5%, respectively.

Similarly for EP/CP composites, the cell viability percentage at 100%, 50%, 25% and 12.5% LC were 74.57%, 81.4%, 84.1% and 91.33%, respectively. The results clearly indicate that EP/CB and EP/HB composites do not show any toxic effect at all LC. Moreover, EP/HB and EP/CP composites showed slight toxic at 100% leach concentration. Among the four composites, EP/CB composite at 25 and 12.5% leach concentration shown slight amount of cell proliferation. As compared to control sample, EP/CB composites at 50 and 12.5% leach concentration did not shown any significant difference. In EP/HB composites, combinations like 50 & 25% and 25 & 12.5% did not shown significant difference. In the case of EP/HA composites at 25 and 12.5% did not shown significant difference with cell control samples. Besides, there was no significant difference found between EP/HA composite samples at 100 and 50% LC. For EP/CP composites, there was no significant difference found between the combinations like cell control & 100%, 100 & 50% and 50 & 25%.

Furthermore, significant difference was found between four different composites at particular leach concentration. The results clearly indicate that EP/HB and EP/CP composites do not have significant difference in cell viability percentage at 100, 50 and 25% leach concentration. At lower leach concentration level (12.5%), combinations like EP/CB & EP/HA, EP/HB & EP/CP and EP/HA and EP/CP did not shown significant difference in cell viability percentage. Based from the above cytotoxicity study, EP/CB and EP/HA composites have better biocompatibility property than other two composites.

Table 6.4: Hemolysis percentage of EP/CB, EP/HB, EP/HA and EP/CP composites.

Samples	% Hemolysis	Average Hemolysis %	Normal Hemolysis
EP/CB	0.033	0.07	
EP/HB	0.033	0.07	
EP/HA	0.053	0.04	< 0.1%
EP/CP	0.046	0.04	

Table 6.4 shows the hemolytic activity of four different composites. The average percentage of hemolysis was 0.07 for EP/CB & EP/HB composites. Similarly, for EP/HA and EP/CP composites, the average hemolysis % value was 0.04. Hemolysis % of EP/CB, EP/HB, EP/HA and EP/CP samples were found to be 0.033, 0.033, 0.053 and 0.046, respectively. There was no significant difference was found between four composites. From the above results it is concluded that both all four composites are in non-hemolytic nature.

6.1.8 Assessment on material properties for potential requirement of low load bearing implants application.

For few clinical applications, produced implants should be non-degradable and bioactive. Some of the examples are orbital floor prosthesis, middle ear implants and maxillofacial surgery (Mahyudin et al. 2016). So far, hydroxyapatite reinforced with non-degradable polymer (like polyethelene and polyetheretherketone) composites has been used for this application (Rakin and Sedmak 2006). Presence of hydroxyapatite in composite surface tends to make it as bioactive and it gets attached with host tissue in fast manner (Tanner 2010). For that, utilization of higher filler fraction (40 wt%) in composites gave better bioactivity property. However, it leads to poor processability followed by reduction in mechanical properties (Mahyudin et al. 2016).

In the present work, prepared composites has comes under the category of non-degradable (epoxy matrix) ones. However, utilization of cuttlebone derived bio fillers (CB, HB, HA and CP) at lower filler fraction (<9 wt%) as reinforcement in epoxy composites tends to improve the mechanical and bioactive property. The tensile properties of these four composites has comes in the range of 40-48MPa (UTS), 0.8-2.0GPa (tensile modulus) and 2.2-3.8% (EPB). Similarly, attained flexural properties are in the range of 60-105MPa (flexural strength) and 4-6GPa (flexural modulus). Likewise compression strength, compression modulus, impact strength and fracture toughness are comes in the range of 85-110MPa, 2.2-2.5GPa, 3-4.2KJ/m² and 2.2-2.5MPa.m^{1/2}. The substantial improvement in mechanical properties tends to show the better interaction

between filler and matrix. It indicates that obtained mechanical properties fulfill the required mechanical properties of implants. Moreover, the mechanical properties of contemporary composite materials used for this application become lesser than the obtained ones (Wang et al. 1998 & Huang et al. 1997). Besides, better thermal stability, crosslink density and wettability also obtained in the prepared composites. It denotes that addition of bio fillers in epoxy matrix tends to have better bonding due to particle size, shape and components presents in cuttlebone particles. Furthermore, the increase in cross link density reduced the uncured monomers presents in composite system which may help to improve the biocompatibility. Amongst the four composites, EP/CB and EP/HA composites shown better biocompatibility (% of metabolic activity and % hemolysis) properties. In that, EP/CB composite showed cell proliferation at lower leach concentration (25 and 12.5%) level. It concludes that prepared EP/CB and EP/HA composites has been found as alternate composite material for bio active low load bearing non degradable implants application. The major advantage of prepared composites is attained higher mechanical and bioactivity properties at lower filler fraction. This may give better mechanical stability during “in-vivo” condition for long term implant period.

6.1.9 Summary

To summarize the results from this chapter, material properties like mechanical, thermal, thermo-mechanical, physical and biocompatibility of epoxy composites reinforced with four different cuttlebone derived bio filler (EP/CB, EP/HB, EP/HA and EP/CP) was compared.

Based from the particle characterization, HA and CP particles are having less in size, density and high in surface area than CB and HB particles. Moreover, HA and CP particles are thermally stable than CB and HB particles. Among the four different composites, EP/HA and EP/CP composites have better tensile and flexural properties, respectively. Moreover, compression strength, compression modulus and impact strength was higher in EP/CB and EP/HB composites rather than other two composites. Besides,

none of the composites have significant improvement in fracture toughness property compared to neat epoxy. On the other hand, hardness of all four composites was significantly higher than neat epoxy. However there was no significant difference found between the four composites. The results indicate that all four composites have good mechanical properties to satisfy the requirement for low load bearing implant applications. Besides, EP/HA and EP/CP composites has better thermal stability, storage modulus, glass transition temperature, cross link density and lower water uptake percentage rather than EP/CB and EP/HB composites. It denotes that HA and CP particle reinforced epoxy composites have better interaction between filler/matrix. Additionally, EP/HA and EP/CP composites have better wettability properties than EP/CB and EP/HB composites. In contrast, EP/HA and EP/CP composites has higher amount of voids percentage than other two composites. Though EP/CB and EP/HB composites has lesser thermal and physical properties than EP/HA and EP/CP composites, but it fulfills the requirements for implants applications. Finally, EP/CB and EP/HA composites has good biocompatibility property (% metabolic activity) than EP/CP and EP/HB composites. Furthermore, blood compatibility was good in all four composites. It concludes that only EP/CB (prepared at 9 wt% filler fraction) and EP/HA (prepared at 6 wt% filler fraction) composites has fulfill the criteria (mechanical, physical and biocompatibility properties) for implant. These two composites found suitable for the bioactive non degradable category implants destined for low load bearing applications.

CHAPTER 7

CHAPTER 7

INFLUENCE OF CUTTLBONE DERIVED BIO FILLERS AND BIO CERAMICS/CARBON FIBER AS REINFORCEMENT IN HYBRID EPOXY COMPOSITES

This chapter describes the utilization of cuttlebone derived bio fillers and bio ceramics/carbon fiber as reinforcement in epoxy composites. Based from the previous chapter results, cuttlebone derived bio fillers [raw cuttlebone (CB) and heat treated cuttlebone (HB) at 9 wt%] and cuttlebone derived bio-ceramics [hydroxyapatite (HA) and tricalcium phosphate (CP) at 6 wt %] has been used as reinforcement along with bi-directional carbon fiber woven fabric (35 vol%) in epoxy matrix composites. Material properties like mechanical, physical, thermal, thermo-mechanical and biocompatibility of the developed hybrid composites were analyzed. Raw cuttlebone/carbon fiber reinforced epoxy composites showed favorable material properties for high load bearing implant applications.

7.1 Results and Discussions

7.1.1 Mechanical properties of hybrid composites

In this topic five different composites (EP, EP/CB, EP/HB, EP/HA and EP/CP) were analyzed. Results are expressed in the form of mean \pm Standard deviation of 5 experiments. For all mechanical properties, statistical analyses were performed by one-way ANOVA. Tukey's honestly significant difference method was used for all post hoc analysis to identify the significant difference between five different composites. In all the tests, statistical significance was set at $p < 0.05$. Symbols (\spadesuit , \clubsuit , \diamond and \heartsuit) were used to denote the statistical results between the composites.

Figure 7.1 shows the ultimate tensile strength, tensile modulus, elongation percentage at break and load vs. deformation curve of EP/CF, EP/CF/CB, EP/CF/HB,

EP/CF/HA and EP/CF/CP composites. As compared to unfilled carbon fiber/epoxy composites, cuttlebone derived filler added hybrid composites has shown better UTS (shown in figure 7.1a). The unfilled carbon fiber/epoxy composite has UTS of 193MPa. The UTS for EP/CF/CB, EP/CF/HB, EP/CF/HA and EP/CF/CP composites was 217MPa, 218MPa, 285MPa and 270MPa, respectively. However, EP/CF/HA and EP/CF/CP composites have higher UTS compared to EP/CF/CB and EP/CF/HB composites. The results stated that addition of nano filler in epoxy resin has better interaction between fiber and matrix rather than micro size filler added ones.

In figure 7.1a, insets indicate that filler reinforced hybrid composites has significant improvement in UTS than unfilled carbon fiber/epoxy composites. In that, EP/CF/CB and EP/CF/HB composites do not have significant difference between them. However, UTS of EP/CF/HA and EP/CF/CP composites has significantly higher than EP/CF/CB and EP/CF/HB composites. Similarly, there was significant difference found between EP/CF/HA and EP/CF/CP composites.

Figure 7.1b shows the tensile modulus plotted of different hybrid composites. The tensile modulus for neat epoxy was 3.65GPa. Similarly as like UTS, tensile modulus of hybrid composites has improved substantially compared to unfilled carbon fiber/epoxy composites. The tensile modulus value of EP/CF/CB, EP/CF/HB, EP/CF/HA and EP/CF/CO composites was 5.43GPa, 6.06GPa, 6.51GPa and 5.62GPa, respectively. EP/CF/HA composites have higher tensile modulus compared to other three hybrid composites. It denotes that addition of fillers in fiber reinforced composites tends to improve the stiffness property in significant level.

In figure 7.1b, insets indicate that all four hybrid composites have significantly higher tensile modulus value than unfilled carbon fiber/epoxy composites. However, there was no significant difference found among EP/CF/CB, EP/CF/HB and EP/CF/CP composites. Moreover, EP/CF/HA composite had higher modulus than other three hybrid composites. Furthermore, there was no significant difference between EP/CF/HA and EP/CF/HB composites.

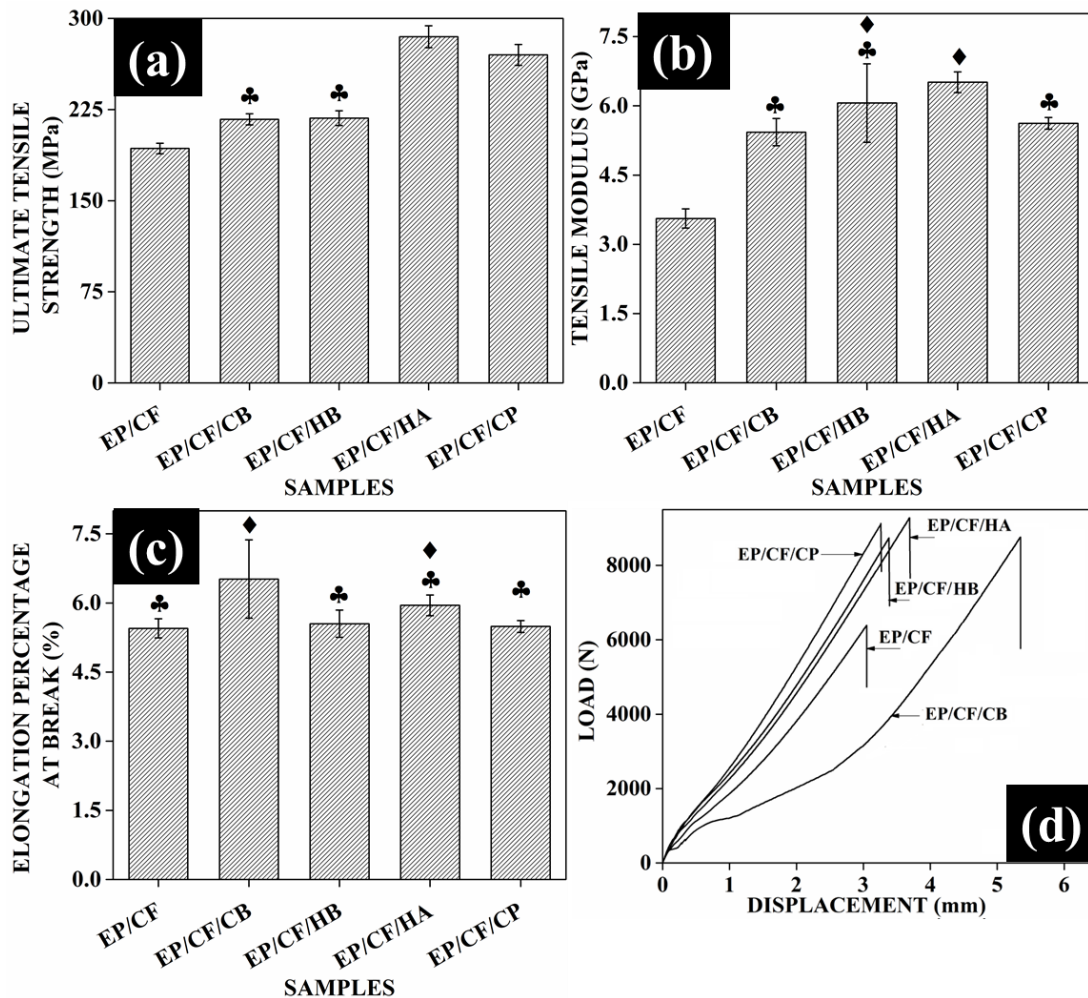


Figure 7.1. (a) Ultimate tensile strength, (b) Tensile modulus, (c) Elongation percentage at break and (d) Load Vs. displacement curve of EP/CF, EP/CF/CB, EP/CF/HB, EP/CF/HA and EP/CF/CP composites. Symbols, (inset in figure) indicate pairwise comparison, that they were not significantly different ($p \geq 0.05$).

Elongation percentage at break (EPB) for our hybrid composites along with unfilled carbon fiber/ epoxy composites are shown in Figure 7.1c. However, there was improvement in EPB value on all four hybrid composites, but it was not up to the substantial level. As compared to unfilled composites (EP/CF: 5.45%), there was no significant increment in EPB value found on EP/CF/HB (5.55%), EP/CF/HA (5.75%), and EP/CF/CP (5.49%) composites. Nevertheless, EP/CF/CB composites (6.52%) have significant improvement in EPB than unfilled composite and it shows the highest EPB

value among the hybrid composites. Addition of rigid filler particles in carbon fiber/epoxy composites tends the material become more brittle. From the results it denotes that micro size CB particles having better interaction with epoxy matrix rather than nano size HA and CP particles.

In figure 7.1c, insets indicates that EPB value of EP/CF/HB, EP/CF/HA and EP/CF/CP composites do not have significant difference with unfilled composite (EP/CF) ones. However, EPB value of EP/CF/CB composite is significantly higher than EP/CF, EP/CF/HB and EP/CF/CP composites. Moreover, there was no significant difference found between EP/CF/CB and EP/CF/HA composites.

Figure 7.1d, demonstrates the typical tensile load vs. deformation curve for unfilled carbon fiber/epoxy and four different hybrid composites. Apart from EP/CF/CB, remaining all four composites exhibit typical brittle behavior like large elastic deformation followed by sudden failure. These four composites deliver linear improvement without any yield point. Consequently, the improvement in strength and modulus was found in these composites. However, there was no significant improvement found in failure strain on EP/CF/HB, EP/CF/HA and EP/CF/CP composites than EP/CF. on the other hand, load Vs. deflection curve of EP/CF/CB composite shows linear behavior in elastic region. Further it starts yielding due to the presence of CB particles in epoxy matrix. Later on, it again shows linear improvement in curve which denotes failure in matrix and the load withstands by fiber ones. Moreover, there was significant improvement in EPB value found on EP/CF/CB composites than unfilled carbon fiber/epoxy composites.

The results concluded that nano size particle reinforced carbon fiber/epoxy composites have better tensile properties than micro size particle filled ones. Similar observation was made by several researchers for three phase hybrid composites (Hussain et al. 1996 & Su et al. 2006). In general, addition of high strength and modulus rigid particle in epoxy matrix may further enhance the properties of three phase hybrid composites. The improvement in tensile properties of EP/CF/HA and EP/CF/CP composites may due to the proper dispersion of nano size filler in epoxy matrix.

Furthermore, high surface energy of nano particle tends to enhance the bonding between carbon fiber and epoxy matrix. However, tensile modulus of EP/CF/CP composite was lesser than EP/CF/HB composites. The possible reason could be the uneven dispersion of CP particles in epoxy matrix leads to more agglomerated region which may reduce the interfacial adhesion between fiber and matrix. Consequently, the strength and modulus of composites was also reduced (Srikanth et al. 2012). The reduction in interfacial adhesion may also reduce the fracture strain of the composites. Less in EPB value of EP/CF/CP composite than other hybrid composites corroborates the reduction in interfacial bonding. The significant improvement in EPB value of EP/CF/CB composite denotes the better bonding of CB particle with epoxy matrix due to the presence of organic matters (Srikanth et al. 2012). Though the CB particles having better bonding with epoxy matrix, its tensile strength and modulus was lesser than EP/CF/HA composites. The possible reason could be the amount of mechanical interlocking between HA filler and epoxy matrix was higher due to its lesser particle size.

Figure 7.2 shows the flexural strength, flexural modulus and load vs. deformation curve of EP/CF and four different hybrid composites. The unfilled carbon fiber / epoxy composite have the flexural strength of 368MPa. As shown in Figure 7.2a, flexural strength of hybrid composites was comparatively higher than unfilled ones. The flexural strength of EP/CF/CB, EP/CF/HB, EP/CF/HA and EP/CF/CP composites was 435MPa, 417MPa, 647MPa and 598MPa, respectively. The EP/CF/HA and EP/CF/CP composites have higher flexural strength than EP/CF/CB and EP/CF/HB composites. The reason for enhancement of tensile strength at EP/CF/HA and EP/CF/CP composites could be the same for flexural strength viz. proper dispersion of nano size filler in epoxy matrix and good interfacial bonding between fiber and filler/matrix.

In figure 7.2a, insets indicate that filler reinforced hybrid composites has significant improvement in flexural strength than unfilled carbon fiber/epoxy composites. In that, EP/CF/CB and EP/CF/HB composites do not have significant difference between them. However, flexural strength of EP/CF/HA and EP/CF/CP composites has

significantly higher than EP/CF/CB and EP/CF/HB composites. Similarly, there was significant difference found between EP/CF/HA and EP/CF/CP composites.

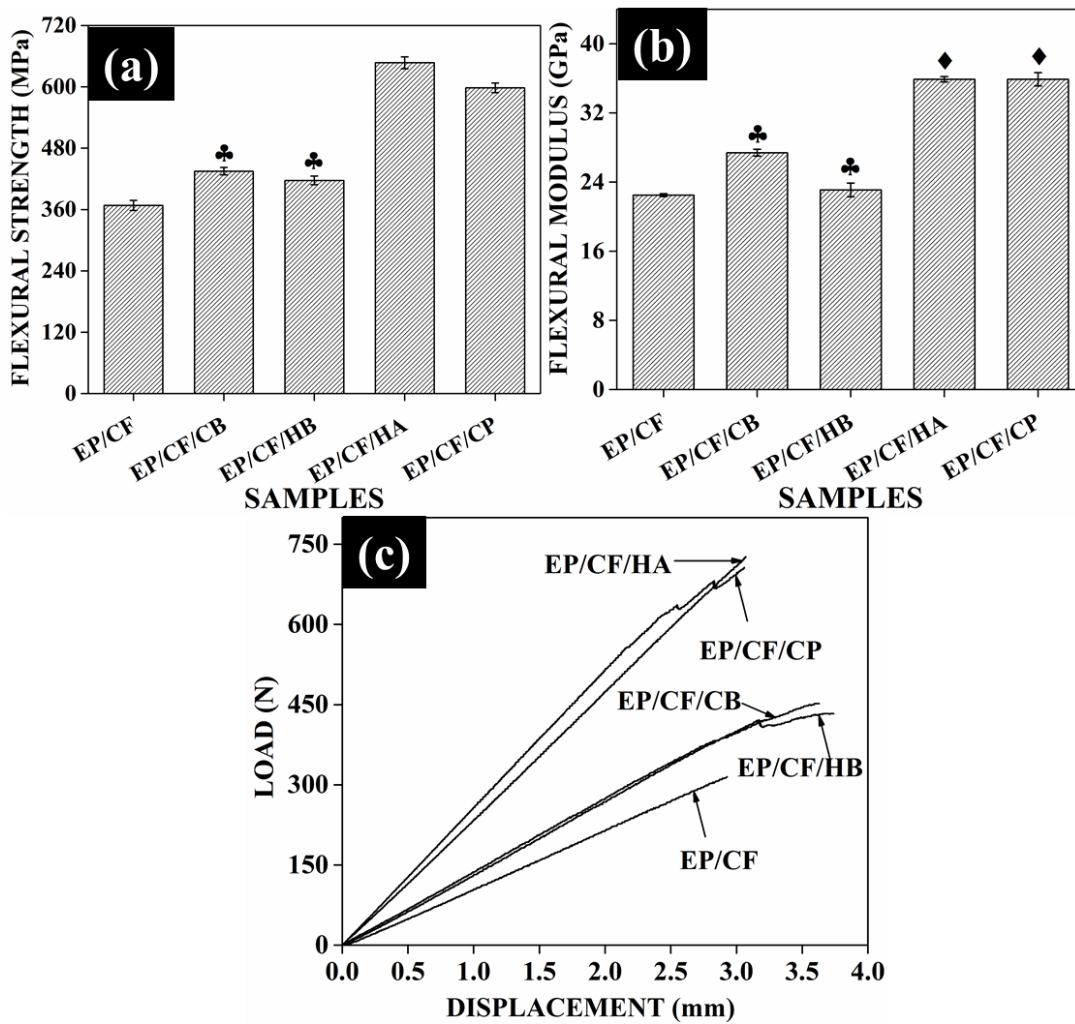


Figure 7.2. (a) Flexural strength, (b) Flexural modulus and (c) Load Vs. displacement curve of EP/CF, EP/CF/CB, EP/CF/HB, EP/CF/HA and EP/CF/CP composites. Symbols, (inset in figure) indicate pairwise comparison, that they were significantly not different ($p \geq 0.05$).

Flexural modulus of EP/CF and four different hybrid composites are shown in figure 7.2b. As like flexural strength, flexural modulus of all four hybrid composites was higher than unfilled carbon fiber/epoxy composites. The EP/CF has a flexural modulus value of 22.5GPa. The flexural modulus value of 27.4GPa, 23.1GPa, 35.9GPa and

35.9GPa was attained by EP/CF/CB, EP/CF/HB, EP/CF/HA and EP/CF/CP composites. This result shows that addition of nano size filler (HA and CP) in carbon fiber/epoxy matrix enhance the stiffness property of composites rather than micro size (CB and HB) filler particles.

Insets in figure 7.2b denote that four hybrid composites have significantly higher flexural modulus than unfilled carbon fiber/epoxy composites. The modulus values for EP/CF/HA and EP/CF/CP composites are significantly higher than EP/CF/CB and EP/CF/HB composites. However, there was no significant difference found between the combinations like EP/CF/HA & EP/CF/CP and EP/CF/CB and EP/CF/HB. Its states that EP/CF/HA and EP/CF/CP composite has better stiffness than EP/CF/CB and EP/CF/HB composites.

Figure 7.2c displays the flexural load vs. deflection curve of unfilled and four different hybrid composites. All five composites exhibit brittle kind of failure. The initial slope of hybrid composites was comparatively higher than unfilled composites ones. Simultaneously, failure strain of the hybrid composites was slightly increased compared to unfilled ones. Consequently, these behaviors enhance the stiffness and load taking capability of hybrid composites. However, failure at strain for EP/CF/CB and EP/CF/HB composites was substantially higher than EP/CF/HA and EP/CF/CP composites due to the presence of organic matters in cuttlebone derived bio fillers.

In general, fiber dominates the failure in bending test for fiber reinforced composites (Kornmann et al. 2005). For the two phase composite system (carbon fiber/epoxy composites), the type of failure is intra-laminar one. However, presences of rigid filler particle as third phase in hybrid composite system failed due to inter and intra laminar mechanism, while applying bending load. Moreover, addition of rigid filler particles (CB, HB, HA and CP) in epoxy matrix leads to the better bonding of matrix around the fiber surfaces. This phenomenon may effectively transfer the stress from filler-matrix phase to fiber phase which predominantly increase the flexural properties of hybrid composites (Ávila et al. 2012). Furthermore, higher flexural properties of EP/CF/HA and EP/CF/CP composites attributed by the high surface contact area of nano

fillers which improved the intermolecular interaction through hydrogen bonding between epoxy and nano fillers (Zulfli et al. 2013). Besides, HA and CP particles are having higher rigidity than CB and HB particles which contributes higher flexural properties for hybrid composites through the formation of tortuous crack path (He et al. 2011).

Figure 7.3 shows the impact strength and fracture toughness properties of unfilled carbon fiber/epoxy and four hybrid composites prepared using cuttlebone derived bio fillers and bio ceramics. As shown in Figure 7.3a the neat epoxy has impact strength of 197.28KJ/m^2 , and it has increased in all four hybrid composites. The impact strength of EP/CF/CB, EP/CF/HB, EP/CF/HA and EP/CF/CP composites was 223.66 KJ/m^2 and 209.64 KJ/m^2 , 280.99KJ/m^2 and 260.33 KJ/m^2 , respectively. Addition of rigid particles as third phase in hybrid composites tends to interlock the matrix and fiber phase which absorb more energy under impact loading. Based from the results, nano size bio ceramic filler (HA and CP) gave better interaction to fiber/matrix interface than micro filler (CB and HB) ones.

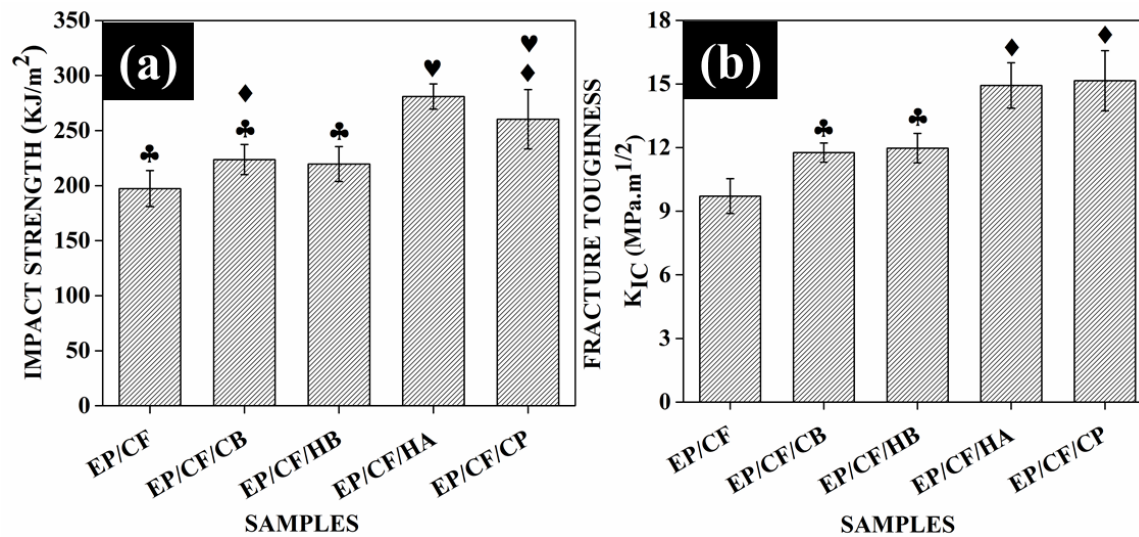


Figure 7.3. (a) Impact strength, and (b) Fracture toughness of EP, EP/CF/CB, EP/CF/HB, EP/CF/HA and EP/CF/CP composites. Symbols, (inset in figure) indicate pairwise comparison, that they were significantly not different ($p \geq 0.05$).

The inset in figure 7.3a indicates that addition of cuttlebone derived bio fillers (CB and HB) in carbon fiber/epoxy composites does not shown any significant with

unfilled carbon fiber/epoxy composites. However, cuttlebone derived bio ceramic (HA and CP) filled carbon fiber/epoxy composites shown significant improvement in impact strength than unfilled carbon fiber/epoxy composites. Besides, there was no significant difference found between the combinations like EP/CF/CB & EP/CF/HB, EP/CF/HA & EP/CF/CP and EP/CF/CB & EP/CF/CP composites.

Impact strength of four different hybrid composites is relatively higher than unfilled carbon fiber/epoxy composites. In general, carbon fiber/epoxy composites are brittle in nature and failed in fast manner under impact loading. This problem has been overcome by the addition of different toughening material like core-shell particles, liquid rubber and rigid particles in to the two phase composite systems (Sudheer et al. 2014). Improvement of fiber/matrix interfacial bonding through the inclusion of rigid filler tends to enhance the impact strength of the hybrid composites (Ahmed et al. 2011). Furthermore, these added fillers have the tendency to resist crack propagation in composite systems. In addition to that, nano fillers (HA and CP) have more interface region than micro filler (CB and HB) which give better adhesion of epoxy resin with carbon fiber and attributes the improvement in impact strength. Besides, the presence of OH group in HA and CP particles tends to interlinked with the COOH and OH group present in carbon fiber which makes better adhesion between them (Zulfli et al. 2013). This could be the possible reason for the higher impact strength in EP/CF/HA and EP/CF/CP composites.

Fracture toughness of EP/CF and four different hybrid composites is shown in figure 7.3b. The neat epoxy has the fracture toughness value of $9.71\text{MPa}\cdot\text{m}^{1/2}$. Addition of filler particles tends to improve the fracture toughness property in all four composites. The fracture toughness value of EP/CF/CB, EP/CF/HB EP/CF/HA and EP/CF/CP composites was $11.75\text{MPa}\cdot\text{m}^{1/2}$, $11.97\text{MPa}\cdot\text{m}^{1/2}$, $14.93\text{MPa}\cdot\text{m}^{1/2}$ and $15.15\text{MPa}\cdot\text{m}^{1/2}$, respectively. The results followed the similar trend of impact strength. Owing to proper interaction by nano filler particles (HA and CP) with epoxy resin than micro filled ones tends to enhance the interlocking mechanism between carbon fiber and epoxy. This will

restrict the crack propagation and absorbed more amount of energy followed by the improvement in fracture toughness (Zhu et al. 2012).

Insets in figure 7.3b denote that all four hybrid composites shown significant improvement in fracture toughness than unfilled carbon fiber/epoxy composite. In that, EP/CF/HA and EP/CF/CP composites have significantly higher fracture toughness value than EP/CF/CB and EP/CF/HB composites. Furthermore, combinations like EP/CF/CB & EP/CF/HB and EP/CF/HA & EP/CF/CP does not shown any significant difference. The results clearly indicate that addition of nano filler particles in carbon fiber/epoxy composites shown greater influence in the improvement of fracture toughness property.

In general, four major mechanisms contribute for the improvement in fracture toughness of hybrid composites. They are crack deflection, debonding between fiber and matrix, pull out and fiber bridging (Hussain et al. 1996). Few researchers found that the addition of rigid filler particles tends to increase the fracture toughness of hybrid composites (Gabr et al. 2010). The crack path might detour around the particles and/or blunting of crack tips by filler particles contributes the enhancement of fracture toughness (Srikanth et al. 2012). The deviation in crack path happened due to tilting and twisting mechanism. This mechanism leads the crack towards another particle and makes three dimensional pathways which contribute for fracture toughness enhancement (Srikanth et al. 2012). The higher fracture toughness of nano filler reinforced carbon fiber/epoxy composites could be contributed through the micro cracking mechanism and crazing process in the polymer matrix (Zulfli et al. 2013).

Shore D hardness and Interlaminar shear strength of unfilled carbon fiber/epoxy composites and four different hybrid composites are shown in figure 7.4. The neat carbon fiber/epoxy composite has a hardness value of 90.9 (shown in figure 7.4a). In all four hybrid composites, hardness value increased due to the addition of filler content. The hardness value of EP/CF, EP/CF/CB, EP/CF/HB, EP/CF/HA and EP/CF/CP composites were 91.6, 92.1, 92.3 and 93.3, respectively. In general, addition of rigid filler particles in carbon fiber/epoxy matrix enhanced the hardness of hybrid composites.

Inset in figure 7.4a indicates that there was no significant difference found between all five composites. However, addition of filler in carbon fiber/epoxy composites enhanced the hardness value, but it is not up to the significant level. It clearly indicates that cuttlebone derived bio fillers and bio ceramics does not influence much on the improvement of hybrid composite hardness value.

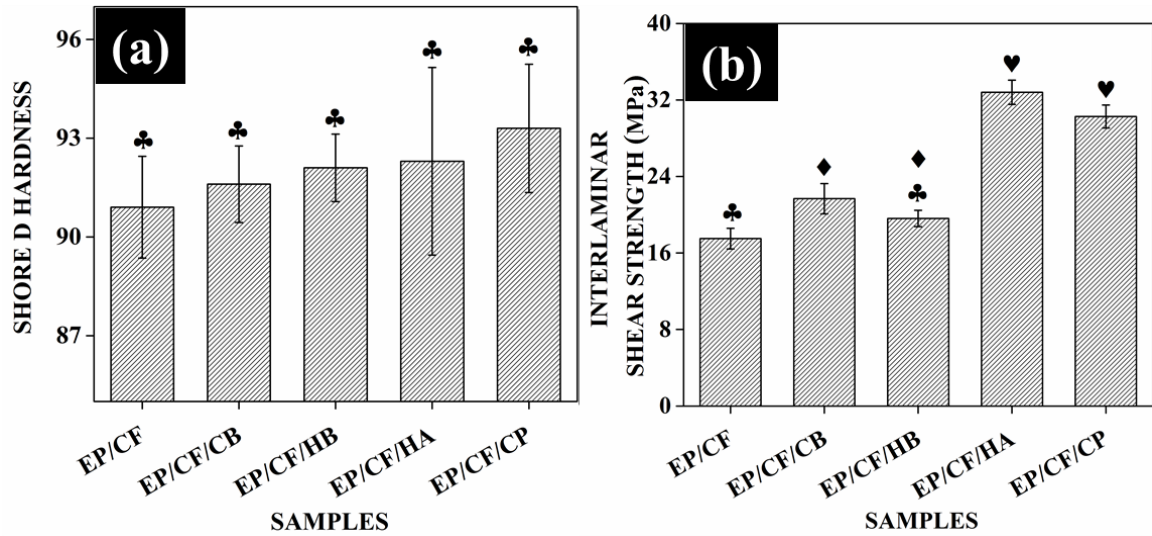


Figure 7.4. (a) Hardness and (b) Interlaminar shear strength of EP/CF, EP/CF/CB, EP/CF/HB, EP/CF/HA and EP/CF/CP composites. Symbols, (inset in figure) indicate pairwise comparison, that they were significantly not different ($p \geq 0.05$).

In general, addition of hard particles in epoxy matrix tends to the improvement in hardness of hybrid composites (Fombuena et al. 2014). The results clearly indicate that EP/CF/HA and EP/CF/CP composites have higher hardness value than other two hybrid composites. The cuttlebone derived hard bio ceramic particles (HA and CP) in nano size tends to absorb more energy due to better dispersion and does not allow to penetrate than micro size bio filler reinforced ones (CB and HB).

The Interlaminar shear strength (ILSS) of unfilled and four hybrid composites was presented in figure 7.4b. The unfilled carbon fiber/epoxy composite has ILSS of 17.5MPa. The results clearly indicates that addition of cuttlebone derived different filler particles (CB, HB, HA and CP) tends to improve the ILSS value of hybrid composites. The ILSS value of EP/CF, EP/CF/CB, EP/CF/HB, EP/CF/HA and EP/CF/CP composites

were 21.68MPa, 19.6MPa, 32.8MPa and 30.26MPa, respectively. As compared to EP/CF/CB and EP/CF/HB composites, EP/CF/HA and EP/CF/CP composites have higher ILSS value. The nano size HA and CP particles disperse evenly in epoxy matrix and makes better interaction between carbon fiber and matrix.

The inset in figure 7.4b denotes that EP/CF/CB, EP/CF/HA and EP/CF/CP composites are having significantly higher ILSS value than EP/CF composite. However, there was no significant difference found between EP/CF and EP/CF/HB composite. Simultaneously, EP/CF/HB composites do not have significant difference with EP/CF/CB composite. Similarly, there was no significant difference found between EP/CF/HA and EP/CF/CP composites. The results indicate that HA and CP particle reinforced carbon fiber/epoxy composites has greater influence on the improvement of ILSS value than other two hybrid composites. However, EP/CF/CB composite also having significant improvement than unfilled composites, but it is not up to level of EP/CF/HA and EP/CF/CP composites.

The major issue araised in fiber reinforced composite is delamination process. The durability and damage tolerance of this composite was evaluated through the delamination growth (He and Li 2012). This delamination failure occurred either in the matrix phase or at the interface region of fiber and matrix phase. The results indicate that addition of filler in carbon fiber/epoxy composites tends to improve the ILSS value than unfilled ones. The possible explanation for this enhancement is the modification of epoxy matrix by even dispersion of micro and nano size particles. This could lead the improvement of interface adhesion between modified matrix and carbon fiber (Hussain et al. 1996). As compared to EP/CF/CB and EP/CF/HB composites, EP/CF/HA and EP/CF/CP composite have better ILSS value. Addition of nano filler tends to increase the matrix strength substantially than micro filler ones. Hussian et al. 1996 identified that pressure was developed at the fiber surface due to the change in residual stress at epoxy matrix. Addition of rigid ceramic particles in epoxy matrix could increase the residual stress and attribute the improvement in adhesion strength between fiber and matrix (Aurrekoetxea et al. 2012). This may be the possible reason for the improvement in ILSS

value of EP/CF/HA and EP/CF/CP composites. Furthermore, EP/CF/CB composite have slightly higher ILSS value than EP/CF/HB composite due to the presence of organic matters in cuttlebone particles. Nonexistence of these organic matters in HB particles tends to reduce the ILSS value of hybrid composite, but it is not up to the significant level.

7.1.2 Fracture morphology studies of hybrid composites

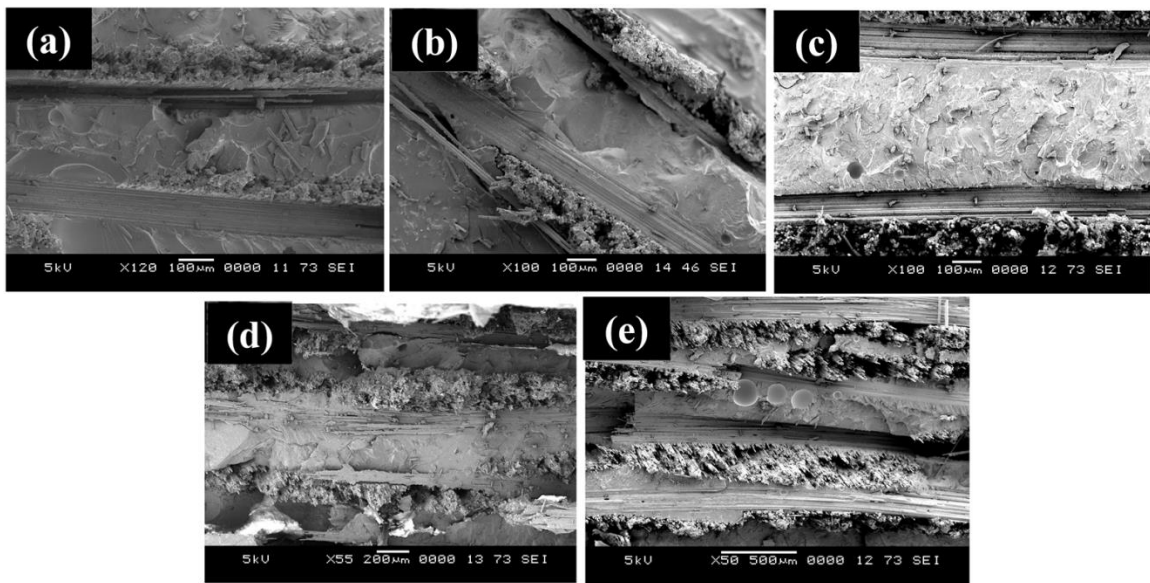


Figure 7.5. SEM micrograph of (a) EP/CF, (b) EP/CF/CB, (c) EP/CF/HB composites (d) EP/CF/HA composites and (e) EP/CF/CP composites.

SEM micrograph (Figure. 7.5) shows the fracture surface of the unfilled carbon fiber/epoxy and four hybrid composites. Fracture morphology of unfilled carbon fiber/epoxy composites (in Figure. 7.5a) did not show any noticeable gap and better interfacial bonding between fiber and matrix. While the fracture surface of EP/CF/HB and EP/CF/HA composites (in Figure. 7.5c & d) showed better adhesion between the fiber and matrix. Improvement in the interfacial adhesion of the hybrid composites can be attributed to the fibers being surrounded by the matrix material on the fracture surface. These improved interface toughness further resulted in obviously rough fracture surfaces. In case of EP/CF/CB and EP/CF/CP composites, poor interfacial region was identified by

the gap between matrix and fiber. Moreover, fiber extraction was identified on the fracture surface (in Figure. 7.5b & e). However, mild agglomerations identified at the fracture surface of the EP/CF/CP composite indicated the possible onset of crack propagation.

In unfilled carbon fiber/epoxy composites (shown in figure 7.5a) it is clearly evidenced that epoxy well adhered with carbon fiber. From figure 7.2b & d, the uniform dispersion of filler in epoxy matrix and the fiber surfaces was surrounded by filler-matrix adhesion was observed. The fiber pull out was reduced in these two hybrid composites and the carbon fiber was harmonized in epoxy matrix (Srikanth et al. 2012). This is attributed due to proper dispersion of filler material in epoxy matrix and good internal bonding between filler and epoxy matrix. This phenomenon could further explained that the presence of micro and nano filler at interface region act as anchor between carbon fiber and matrix. This may lead to strengthen the interface region and transfer the stress in uniform manner throughout the fiber surface (Kim et al. 2011). Figure 7.5b & e shows the delamination in fiber/matrix interface region and some amount of fiber pull out. This was happened due to the poor bonding between fiber and matrix which develops micro cracks at interfacial regions (He et al. 2011). Finally, these micro cracks propagate through interface regions and brings down the mechanical properties.

7.1.3 Density and voids percentage of hybrid composites

Table 7.1: Theoretical density, actual density and void percentage of unfilled carbon fiber/epoxy and four different hybrid composites

Composite	Theoretical Density (g/cm ³)	Actual Density (g/cm ³)	Void Content (%)
EP/CF	1.350	1.314	2.622
EP/CF/CB	1.397	1.351	3.248
EP/CF/HB	1.397	1.340	4.061
EP/CF/HA	1.382	1.320	4.482
EP/CF/CP	1.377	1.313	4.597

Theoretical and actual density along with voids percentage of unfilled carbon fiber/ epoxy composites and four different hybrid composites are presented in Table 7.1. The presence of voids has been confirmed from the reduction in actual density value of composite compared to theoretical density. The exact volume fraction of carbon fiber was identified through matrix digestion test according to ASTM 3171-09, in order to evaluate the theoretical density of hybrid composites. Theoretical and actual density of unfilled carbon fiber/epoxy composites was 1.35 and 1.314 g/cm³, respectively. Density of the hybrid composites was increased due to the addition of high density filler in epoxy matrix.

The hybrid composites were prepared through hand layup followed by hydraulic press method and the presence of voids are unavoidable. The voids percentage of unfilled carbon fiber/epoxy composite was 2.622% and it was increased in hybrid composites due to the addition of cuttlebone derived bio filler and bio ceramics. The existed voids percentage of EP/CF/CB, EP/CF/HB, EP/CF/HA and EP/CF/CP composites are 3.248%, 4.061%, 4.482% and 4.597%, respectively. Amongst the four hybrid composites, EP/CF/CB showed lesser voids percentage. The possible reason could be the presence of organic matters leads to improve the interfacial adhesion between matrix and fiber. However, it was comparatively higher than unfilled ones. Furthermore, there was no significant difference found on the voids percentage of remaining three composites. In general, addition of nano size filler in fiber reinforced composites tends to get agglomerated easily than micro filler ones. These agglomerated particles acts as flaws and initiate cracks in the interfacial region (Timmerman et al. 2002). This could be possible reason for the higher voids percentage in EP/CF/HA and EP/CF/CP composites. Though, the HB particles are in micron size range its corresponding composites shown merely same voids percentage of nano filled hybrid ones. The poor dispersion and weak adhesion of filler with epoxy matrix due to the absence of organic matters may leads to the increase in voids percentage. Besides, there might be some chance of misalignment of fibers mat and flash out of resin has taken place, while applying the compression load (Aurrekoetxea et al. 2012). This could enhance the voids percentage of composites.

7.1.4 Physical properties of hybrid composites

Figure 7.6 shows the water absorption behavior of unfilled carbon fiber/epoxy composites and four different hybrid composites. After 30 days, the maximum amount of water uptake for EP/CF, EP/CF/CB, EP/CF/HB, EP/CF/HA and EP/CF/CP composites was around 0.51%, 0.58%, 0.69%, 0.47% and 0.58%, respectively. However, the best fit curve equation for these five composites was in third order polynomial form with R^2 value of 0.98, 0.99, 0.99, 0.98 and 0.99, respectively.

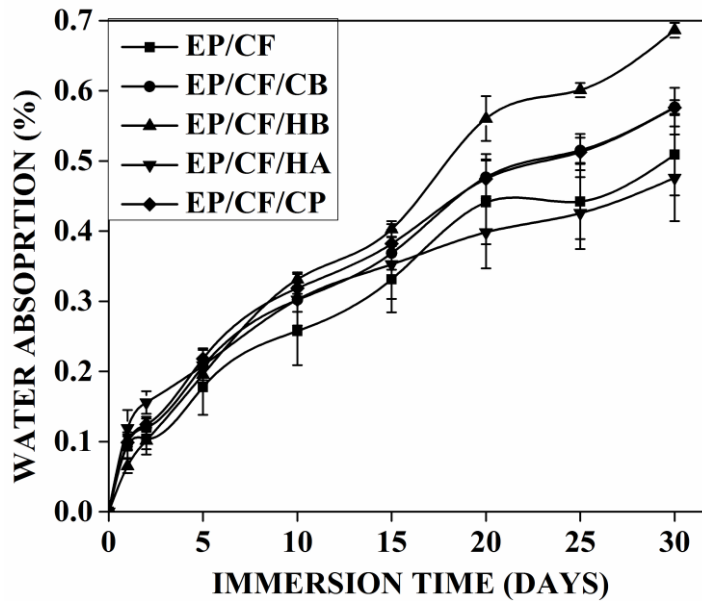


Figure 7.6: Water absorption percentage of EP/CF, EP/CF/CB, EP/CF/HB, EP/CF/HA and EP/CF/CP composites.

The corresponding best fit curve equation for EP/CF, EP/CF/CB, EP/CF/HB, EP/CF/HA and EP/CF/CP composites was mentioned in equation 7.1 to 7.5, respectively.

$$Y = 1 \times 10^{-3} X^3 - 0.0009 X^2 + 0.0312 X + 0.0343 \dots \dots \dots (7.1)$$

$$Y = 2 \times 10^{-5} X^3 - 0.0012 X^2 + 0.038 X + 0.0353 \dots \dots \dots (7.2)$$

$$Y = 1 \times 10^{-5} X^3 - 0.0009 X^2 + 0.0385 X + 0.0179 \dots \dots \dots (7.3)$$

$$Y = 3 \times 10^{-5} X^3 - 0.002 X^2 + 0.043 X + 0.0461 \dots \dots \dots (7.4)$$

$$Y = 3 \times 10^{-5} X^3 - 0.0016 X^2 + 0.0428 X + 0.0327 \dots \dots \dots (7.5)$$

The results indicate that addition of CB, HB, HA and CP particles in carbon fiber/epoxy composites tend to improve the water absorption properties of hybrid composites for a period of 30 days. It denotes that cuttlebone derived bio fillers and its derivative bio ceramics having the tendency of absorbing water. Consequently, the water uptake of these hybrid composites was increased. However, none of the composites reached the saturation level of water absorption even after 30 days. The impenetrable reinforcement particles in composites make the water molecules to diffuse in tortuous pathway which induce the unsaturation level of water absorption and also have the lower amount of water uptake ability at the end of experiment (Kornmann et al. 2005). Though the voids percentage is in considerable level, this could be the possible reason for the lower water uptake ability of EP/CF/HA composite. This result is further corroborated with the higher crosslink density of EP/CF/HA composite (which is discussed in upcoming topic). On the other hand, EP/CF/HB composite having the ability of higher water uptake percentage followed by EP/CF/CB and EP/CF/CP composites.

Moreover, these results are well agreed with contact angle studies. The water contact angle for E/CF, EP/CF/CB, EP/CF/HB, EP/CF/HA and EP/CF/CP composites was $73.01 \pm 1.07^\circ$, $76.76 \pm 1.13^\circ$, $63.64 \pm 1.15^\circ$, $72.16 \pm 1.91^\circ$ and $70.16 \pm 1.28^\circ$, respectively. All five composites showed a hydrophilic behavior because of its contact angle was less than 90° . Addition of reinforcement filler in epoxy matrix tends to increase the wettability of composites. In that, EP/CF/CB and EP/CF/HB composites have higher wettability/lower contact angle than EP/CF/HA and EP/CF/CP ones.

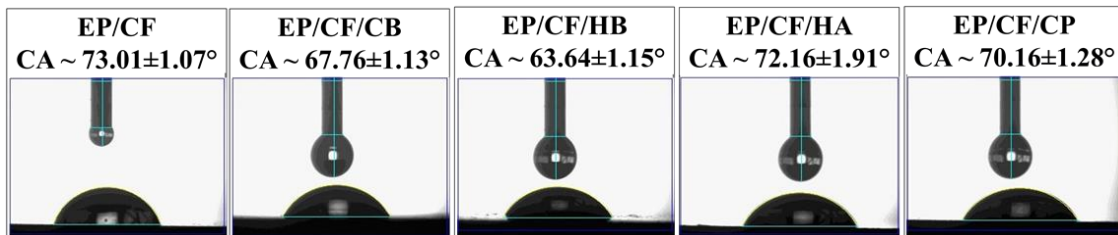


Figure 7.7: Wettability results of EP/CF, EP/CF/CB, EP/CF/HB, EP/CF/HA and EP/CF/CP composites.

7.1.5 Thermo-mechanical and thermal properties of hybrid composites

Figure 7.8a shows the thermal Stability of unfilled carbon fiber/epoxy (EP/CF) and four different hybrid composites (EP/CF/CB, EP/CF/HB, EP/CF/HA and EP/CF/CP). The hybrid composites exhibit two stage degradation. There was a minimal weight loss in all composites up to 250°C. Desorption of water molecules from composite is the reason behind the minimal degradation. The second degradation occurred with major weight loss in the temperature range of 300°C to 450°C, which was due to the thermal degradation of composites and epoxy network. Temperature at the maximum rate of degradation (T_{max}) was calculated from the DTG curve of composites (Figure 7.8b). Besides, thermal stability factors like activation energy (E_a), integral procedure decomposition temperature (IPDT) and char yield at 700°C (CY) were presented in table 7.2.

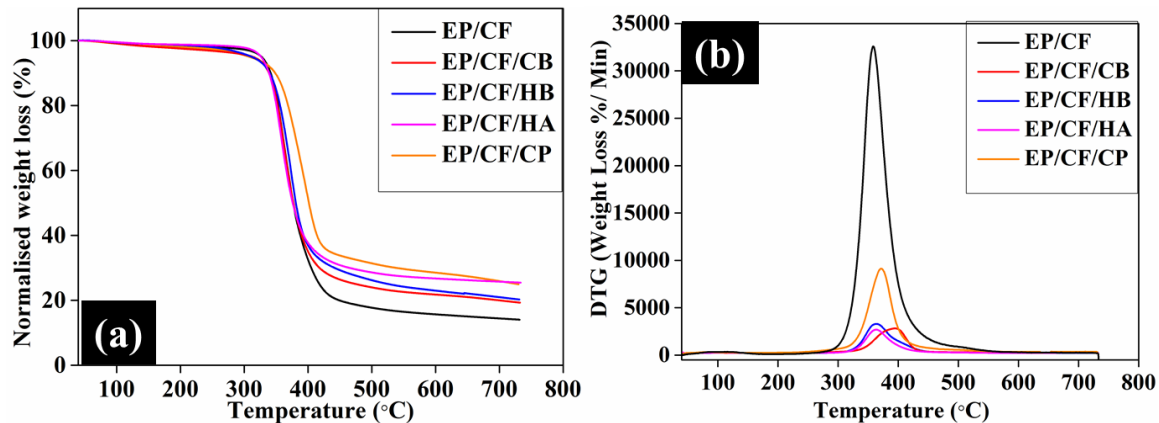


Figure 7.8 (a) TG and (b) DTG of curve EP, EP/CF/CB, EP/CF/HB, EP/CF/HA and EP/CF/CP composites

Figure 7.8b presents the DTG curve of unfilled carbon fiber/epoxy and four different hybrid composites which denote the rate of weight loss of material. As compared to unfilled ones, the DTG value of hybrid composites was smaller. The possible explanation could be the presence of filler components in composite can restrict the rate of thermal degradation (Chiang et al. 2007). Furthermore, the char yield percentage of hybrid composites was higher due to the filler content. Additionally, EP/CF/HA and EP/CF/CP composites have higher char yield than EP/CF/CB and EP/CF/HB composites. THE ceramic HA and CP particles won't degrade even after

700°C (which found from TGA curve of HA and CP particles) was the reason for the increment in char yield percentage. As like char yield, similar trend was followed in activation energy of composites. The higher activation energy required for EP/CF/HA and EP/CF/CP composites to thermal degradation was due to the more amount of interaction happened between fiber and matrix phase. In general, addition of thermal stable structures as third phase in fiber reinforced composites may improve the thermal stability of composites due to the increase in cross linking between polymer chains (Park et al. 2004). TGA results clearly indicate that the thermal stability of hybrid composites is higher than unfilled carbon fiber/epoxy composites due to the addition of inorganic components like cuttlebone derived bio fillers and bio ceramics. These filler can increase the van der Waals interaction between polymer chains which attributes the restriction in molecular mobility of polymer chains. Based on this phenomenon, the addition of filler may increase the cross linking between epoxy chains and tends to enhance the thermal stability of composites. The IPDT value of EP/CF/HA and EP/CF/CP composites which directly denotes the thermal stability of material was higher than EP/CF/CB and EP/CF/HB composites. The nano size HA and CP particles promotes more amount of successive crosslinking than micro size particle (CB and HB) added ones. Furthermore, these nano fillers gave better physical protective barrier against thermal degradation of composites (He et al. 2011).

Table 7.2: Thermal properties of EP/CF, EP/CF/CB, EP/CF/HB, EP/CF/HA and EP/CF/CP composites

Composite	T _{max} (°C)	IPDT (°C)	E _t (KJ/mol)	Char Yield (%)
EP/CF	358.55	538.81	123.98	14.06
EP/CF/CB	395.23	622.77	144.26	19.29
EP/CF/HB	364.59	644.94	152.41	20.27
EP/CF/HA	363.47	754.74	161.56	25.49
EP/CF/CP	371.69	745.21	169.40	24.97

Figure 7.9 shows the (a) storage modulus and (b) mechanical loss factor ($\tan\delta$) with respect to temperature for EP, EP/CF/CB, EP/CF/HB, EP/CF/HA and EP/CF/CP

composites. Furthermore, the storage modulus, gain in percentage of storage modulus and glass transition temperature of all four materials are summarized in table 7.3. The storage modulus for neat epoxy was 3.71GPa. By the addition of cuttlebone derived four different reinforcement particles (CB, HB, HA and CP) in epoxy matrix tends to increase the storage modulus of composites. The storage modulus of EP/CF/CB, EP/CF/HB, EP/CF/HA and EP/CF/CP composites was 4.10GPa, 4.60GPa, 5.63GPa and 5.31GPa, respectively. As presented in table 7.3, the increase in percentage of storage modulus for EP/CF/CB, EP/CF/HB, EP/CF/HA and EP/CF/CP composites with respect to neat epoxy was 10.51%, 23.99%, 51.75% and 43.13%, respectively. The increase in storage modulus of composites was probably due to the addition of rigid particles in epoxy matrix which restricts the molecular mobility (Ramdani et al. 2014).

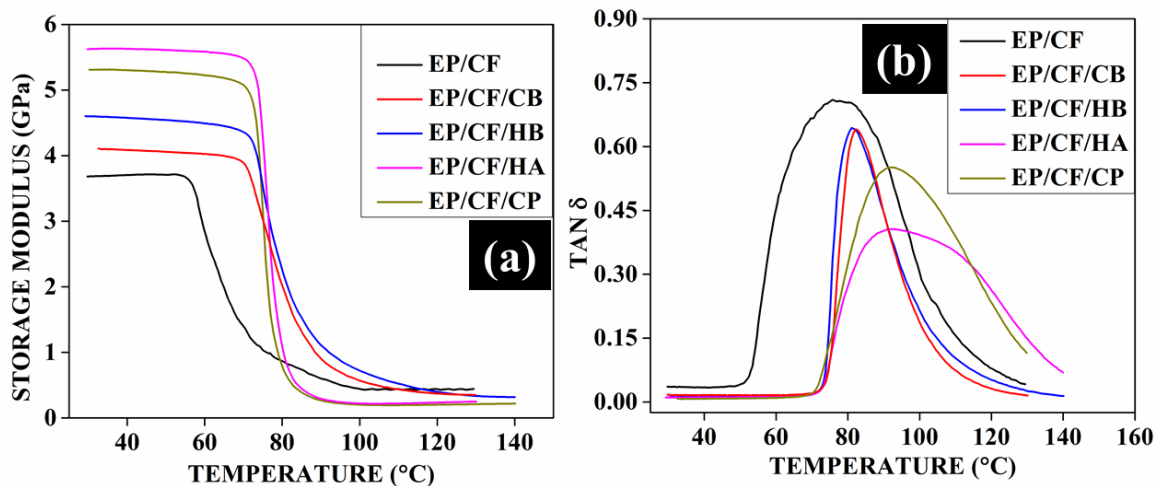


Figure 7.9 (a) Storage modulus and (b) $\tan\delta$ of EP/CF, EP/CF/CB, EP/CF/HB, EP/CF/HA and EP/CF/CP composites.

Consequently, the storage modulus of EP/CF/HA and EP/CF/CP composites was enhanced tremendously due to the increase in interfacial bonding between filler and matrix. Besides, the storage modulus of CB and HB particle reinforced hybrid composites was significantly lower than HA and CP particle reinforced hybrid composites. The possible reason could be the nano particles (HA and CP) have better dispersion and interaction than micro particle reinforced composites (Ramdani et al. 2014). As shown in

figure 7.9a, storage modulus of all five composites has a sudden drop at glass transition temperature and it denote that material has transferred from glassy to rubbery region.

The glass transition temperature (T_g) of composites was determined from the peak point of $\tan\delta$ curve (shown in figure 7.9b). As compared to unfilled carbon fiber/epoxy composites, hybrid composites filled with CB, HB, HA and CP particles as third phase has a relative improvement in T_g values. The T_g value of EP/CF, EP/CF/CB, EP/CF/HB, EP/CF/HA and EP/CF/CP composites was 75.76°C , 82.31°C , 81.05°C , 92.04°C and 92.01°C , respectively. The possible reason could be the presence of filler in epoxy matrix gave better fiber-matrix interaction in composites and also restricts the matrix mobility (Rahman et al. 2013). Apart from the T_g , damping factor of the prepared composites was extracted from the $\tan\delta$ curve (shown in figure 7.9b). Addition of rigid cuttlebone derived filler particles in epoxy matrix tends to decline in the damping factor through diminishes in peak intensity along with the peak broadening (Mohd Zulfli et al. 2013).

Table 7.3: Storage modulus and glass transition temperature of EP, EP/CF/CB, EP/CF/HB and EP/CF/HA and EP/CF/CP composites

Composites	Storage Modulus (GPa)	Gain in Storage Modulus (%)	Glass transition Temperature (T_g) ($^\circ\text{C}$)
EP/CF	3.71	-	75.76
EP/CF/CB	4.10	10.51	82.31
EP/CF/HB	4.60	23.99	81.05
EP/CF/HA	5.63	51.75	92.04
EP/CF/CP	5.31	43.13	92.01

The increase in storage modulus of EP/CF/HA and EP/CF/CP composites rather than EP/CF/CB and EP/CF/HB composites was due to the pseudo crosslink developed by fillers in epoxy matrix (Zulfli et al. 2013). Similarly, the enhancement in T_g value is mainly due to the increase in number of successive cross links and decrease in chain mobility of polymers. Furthermore, nano particles tend to occupy the voids area in epoxy matrix and reduce the free volume of polymers may help in the improvement of T_g value. (Yasmin and Daniel 2004). Additionally, inclusion of filler in fiber reinforced epoxy

composites tends to reduce the peak intensity of $\tan\delta$ due to the restriction of molecular mobility of matrix phase. Furthermore, addition of hard ceramic particles leads to the reduction in $\tan\delta$ peak intensity along with broadening of curve, due to the heterogeneity of polymer network (Núñez et al. 2002 and Timmerman et al. 2002).

The swelling ratio, crosslink density and molecular weight between crosslinks of EP, EP/CF/CB, EP/CF/HB and EP/CF/HA and EP/CF/CP composites were presented in table 7.4. The swelling ratio of EP/CF was 0.7038. Similarly, the swelling ratio of EP/CF/CB, EP/CF/HB and EP/CF/HA and EP/CF/CP composites was 0.4601, 0.5101, 0.1755 and 0.4488, respectively.

Table 7.4: Swelling ratio, crosslink density and molecular weight between crosslinks EP, EP/CF/CB, EP/CF/HB and EP/CF/HA and EP/CF/CP composites

Composites	Swelling ratio (S.R)	Crosslink density (ν) (mol/cm ³)	Molecular weight between crosslinks (M_c)
EP/CF	0.7038	0.0033	305.77
EP/CF/CB	0.4601	0.0046	213.82
EP/CF/HB	0.5101	0.0042	238.26
EP/CF/HA	0.1755	0.0117	85.61
EP/CF/CP	0.4488	0.0048	209.07

As compared to the unfilled carbon fiber/epoxy, the swelling ratio of all four hybrid composites was decreased. It showed that addition of hard bio fillers and ceramic particles in epoxy matrix tends to restrict the penetration of solvent in composites due to the better bonding between fiber and matrix material (Ku et al. 2013 and Ahmed 2015). Amongst the four composites, the swelling ratio was higher in EP/CF/HB followed by EP/CF/CB and EP/CF/CP. Addition of nano particles in polymer matrix tends to give better bonding than micro filled ones due to high surface contact area. Similarly, presence of hydroxyl group in HA samples have better interaction with epoxy matrix which tends to give lower swelling ratio in EP/CF/HA composite.

Addition of cuttlebone derived CB, HB, HA and CP particles in epoxy matrix tend to increase the cross link density of hybrid composites. As compared to unfilled

carbon fiber/epoxy composites (0.0033mol/cm^3), EP/CF/HA composites has higher cross link density (0.0117mol/cm^3) followed by EP/CF/CP (0.0048mol/cm^3), EP/CF/CB (0.0046mol/cm^3), and EP/CF/HB (0.0042mol/cm^3). This cross link density behavior of all four hybrid composites is well agreed with their corresponding glass transition temperature. The addition of thermally stable rigid filler in epoxy matrix attributes the interlocking formation between fiber and matrix which induces more cross link density (Ahmed et al. 2012 & Rahman et al. 2013). Furthermore, the average molecular weight between crosslinks was inversely proportional to cross link density. In that EP/CF/HB composite has lower value compare to other three hybrid composites.

7.1.6 Biocompatible properties of hybrid composites

In this topic four different groups of composites (EP/CF/CB, EP/CF/HB, EP/CF/HA and EP/CF/CP) were analyzed. Each test group consists of five different sets (cell control, 100%, 50%, 25% and 12.5% leach concentration). Results are expressed in the form of mean \pm Standard deviation of 6 experiments. Statistical analyses were performed by one-way ANOVA and Tukey's honestly significant difference method was used for all post hoc analysis to identify the significant difference between each set of individual test group. In all the tests, statistical significance was set at $p < 0.05$. Symbols (\clubsuit and \spadesuit), (\bullet , \blacklozenge and \heartsuit), (α , β , χ and δ) and (+) was used to denote the statistical results in EP/CF/CB, EP/CF/HB, EP/CF/HA and EP/CF/CP test group, respectively. Similarly, numbers (1), (2), (3) and (4 and 5) was used to denote the statistical results in leech concentration 100%, 50%, 25% and 12.5%, respectively.

Figure 7.10 shows the cell viability percentage of EP/CF/CB, EP/CF/HB, EP/CF/HA and EP//CF/CP composites at various leach concentration (LC). The cell viability percentage for EP/CF/CB composite at 100%, 50%, 25% and 12.5% leach concentrations were 83.82%, 87.17%, 92.11% and 112.87%, respectively. For EP/CF/HB composite, the cell viability percentage at 100%, 50%, 25% and 12.5% leach concentrations were 25.21%, 90.07%, 107.11% and 112.21%, respectively. Similarly for EP/CF/HA composite, the cell viability percentage at 100%, 50%, 25% and 12.5% leach

concentrations were 79.54%, 82.14%, 92.6% and 103.66%, respectively. Lastly for EP/CF/CP composites, the cell viability percentage at 100%, 50%, 25% and 12.5% LC were 33.36%, 61.61%, 87.78% and 96.49%, respectively. The results clearly indicate that out of four hybrid composites, EP/CF/CB do not show any toxic effect at all LC. While reducing the leach concentration from 100 to 12.5%, the percentage of metabolic activity (cell viability) was increased continuously and starts prolific the cell at 12.5% LC.

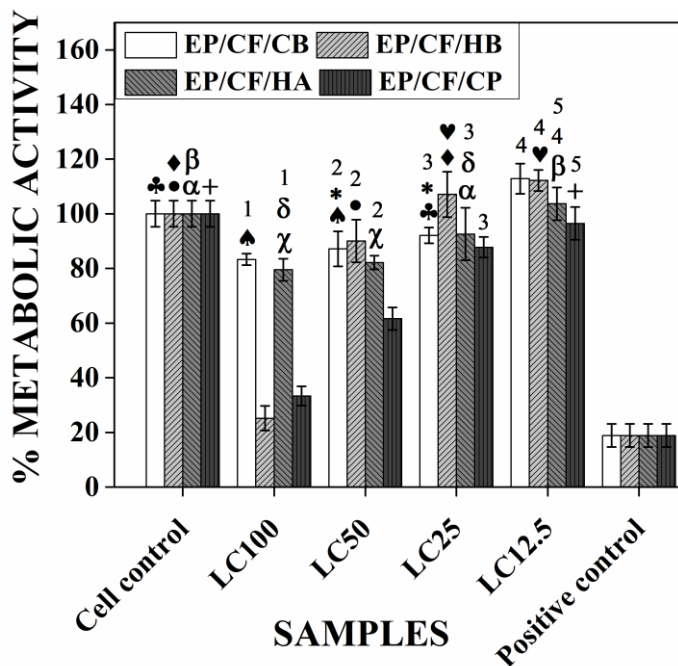


Figure 7.10 “*In vitro*” Cytotoxicity of EP/CF/CB, EP/CF/HB, EP/CF/HA and EP/CF/CP composites. Data are expressed as percentage of control mean± S.D. of six independent experiments. Symbols and numbers indicate pairwise comparison, that they were significantly not different ($p \geq 0.05$).

In EP/CF/CB composite, cell control and 25% LC does not shown any significant difference with cell control. However, reduction in cell viability at 100 & 50% LC has significantly different with cell control. Nevertheless, there was no significant difference found between 100 & 50% LC. Similarly, there no significant difference found between 50 & 25% LC. The 12.5%LC concentration sample showed cell proliferation and it’s significantly different with all other combinations.

EP/CF/HA composite showed slight toxic (negligible level) at 100% LC. Besides, the cell viability starts increasing by reducing the LC from 100 to 12.5%. Similarly as like EP/CF/CB, EP/CF/HA composite also starts proliferate the cell at 12.5% LC.

In EP/CF/HA composite, cell control sample does not have any significant difference with 50 & 12.5% LC samples. However, there was a significant difference found between 50 & 12.5% LC. Though the cell proliferation attained at 12.5% LC sample, but it was not significantly different with cell control. The reduction in cell viability at 100 (slight toxic sample) and 50% LC has significantly different with cell control. However, there was no significant difference found between the combinations like 100 & 50% and 100 & 25%.

In EP/CF/HB composite, severe toxic was identified in 100% LC sample. Nevertheless, it was non-toxic from 50 to 12.5% LC and it showed cell proliferation at 25 and 12.5% LC.

In EP/CF/HB composite, there was no significant difference found in the combinations like cell control & 50% LC and cell control & 25% LC. However, there was significant difference found between 50 & 25% LC samples. The reduction in cell viability at 100% LC sample significantly different with all other samples due to its severe toxicity. The 12.5% LC sample, starts proliferate the cell and it significantly different with cell control but not with 25% LC.

Finally, in EP/CF/CP composite toxicity was identified for 100 and 50% LC samples. However, in 25 and 12.5% LC sample does not show any toxic effect. In this cell control and 12.5% LC sample does not have any significant difference. However, all other combinations are significantly different. The toxic effect in 100 & 50% LC sample showed significant difference with cell control. Though 25 & 12.5% LC sample has nontoxic effect, only 12.5% LC and cell control sample are significant not different. It clearly indicates that in 25% LC sample the reduction in cell viability is significantly different with cell control.

Significant difference at particular LC for different composites also done through Tukey test. At 100% LC, EP/CF/CB and EP/CF/HA composite does not have any

significant difference. In 50% LC, except EP/CF/CP composite remaining three hybrid composites are significantly not different. It indicates that only EP/CF/CP composite shown toxicity at 50% LC. In 25% LC, except EP/CF/HB composite remaining three are significantly not different. The possible reason could be the cell proliferation at 25% LC in EP/CF/HB composite. In 12.5% LC, EP/CF/CB, EP/CF/HB and EP/CF/HA composite does not shown any significant difference due to the cell proliferation. Similarly in this same LC level, EP/CF/HA and EP/CF/CP composite does not shown any significant difference.

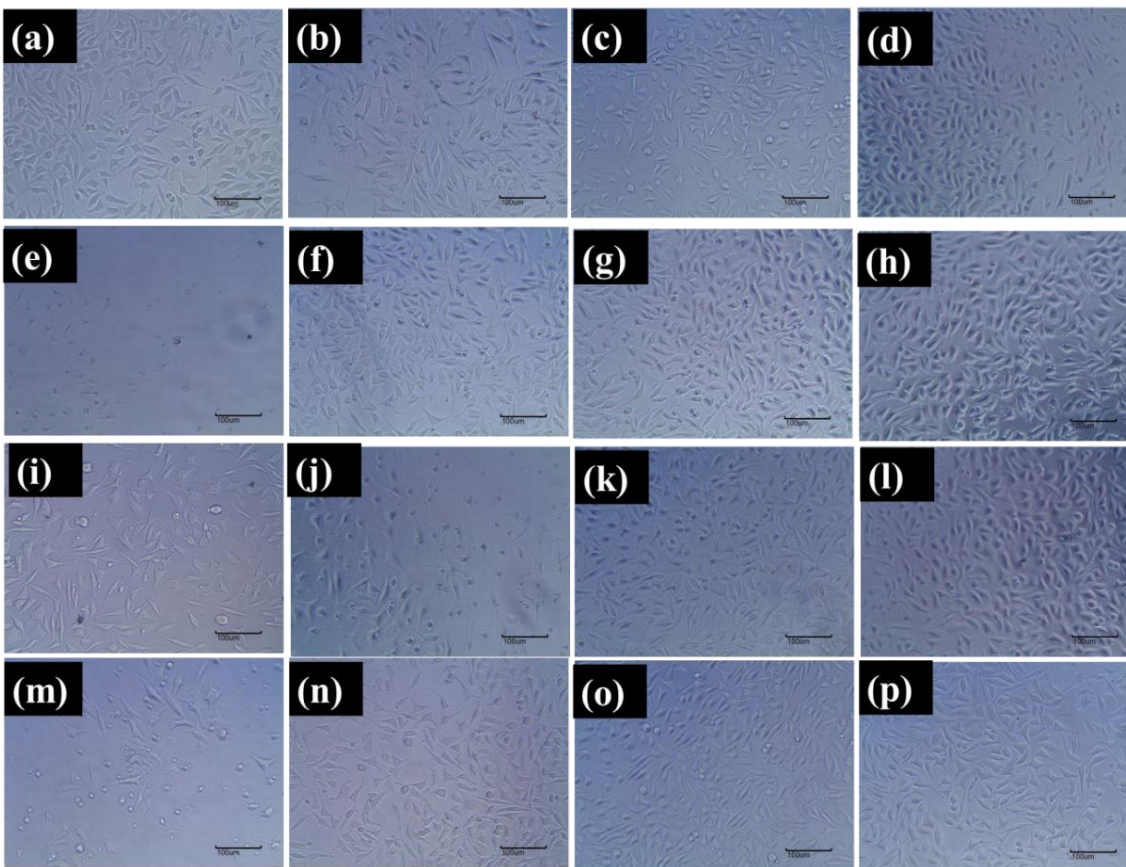


Figure 7.11 Microscopic images of viable cells for (a-d) EP/CF/CB composite prepared at 100, 50, 25 & 12.5% LC., (e-h) EP/CF/HB composite prepared at 100, 50, 25 & 12.5% LC., (i-l) EP/CF/HA composite prepared at 100, 50, 25 & 12.5% LC. and (m-p) EP/CF/CP composite prepared at 100, 50, 25 and 12.5% LC. (Scale bar: 100 μ m)

Figure 7.11 denotes the cell viability of four different hybrid composites at different leach concentration level. Based from the figure 7.11e & m, the images (EP/CF/HB & EP/CF/CP at 100% LC) clearly indicates the minimal amount of cell viability. Besides, EP/CF/CB & EP/CF/HA composite at 12.5% LC (figure 7.12d & i) and EP/CF/HB composite at 25 & 12.5% LC (figure 7.12g & h) has shown more amount of cell viability.

The cytotoxicity results concluded that addition of CB particles in carbon fiber/epoxy composite tends to improve the bioactivity property of material at all leach concentration level. Though there was a negligible amount of toxicity was identified at 100% LC in EP/CF/HA composite, it was diminished by reducing the leach concentration level. Besides, remaining two hybrid composites (EP/CF/HB and EP/CF/CP) showed severe toxicity at 100% LC. Therefore, EP/CF/CB composite was found as the only biocompatible hybrid composite.

Table 7.5: Hemolysis percentage of EP/CF/CB, EP/CF/HB, EP/CF/HA and EP/CF/CP composites.

Samples	% Hemolysis	Average Hemolysis %	Normal Hemolysis
EP/CF/CB	0.03	0.04	
EP/CF/HB	0.03	0.04	
EP/CF/HA	0.03	0.04	< 0.1%
EP/CF/CP	0.03	0.04	

Table 7.5 shows the hemolytic activity of the prepared composite samples. The average percentage of hemolysis was 0.04%. Hemolysis % of all four hybrid composites samples was found to be 0.03. From the above results it is concluded that all four hybrid composite samples are in non-hemolytic nature. There was no significant difference was found between these four composites. The observed results may confirm that addition of these fillers in carbon fiber/epoxy composites tend to improve the blood compatibility of composites.

7.1.7 Assessment on material properties for potential requirement of high load bearing implants application.

For few high load bearing clinical applications, the implants should be in the nature of non-degradable and bioactive. Some of the examples are femur bone fracture fixation devices like bone plate, screws, pins and rods (Saidpour 2006) and carnioplasty (Saringer et al. 2002). So far, titanium based bone plates, fiber reinforced non degradable polymer (like carbon fiber, PMMA and Epoxy) composites has been used for this application to attain its required mechanical properties (Mano et al. 2004). However, the nature of these implant materials are bio inert. These implant materials does not have better interaction with host tissue. Presence of bioactive material either on the implant surfaces or as a reinforcement in fiber reinforced polymer composites tends to make it as bioactive and it gets attached with host tissue in fast manner (Tanner 2010). For that, utilization of naturally derived bioactive material as third phase in fiber reinforced composite tends to change the nature of material from bio inert to bio active. However, care has to been taken for sustaining the mechanical and physical properties of composites.

In this present work, the prepared composites has comes under the category of fiber reinforced non-degradable (carbon fiber/epoxy composite) ones. However, utilization of cuttlebone derived bio fillers (CB, HB, HA and CP) at lower filler fraction (<9 wt%) as reinforcement in epoxy composites tends to improve the bioactive property of composites without sacrificing its mechanical properties. The tensile properties of these four hybrid composites has comes in the range of 220-290MPa (UTS), 5.25-6.25GPa (tensile modulus) and 5-6.5% (EPB). Similarly, attained flexural properties are in the range of 400-660MPa (flexural strength) and 24-36GPa (flexural modulus). Likewise impact strength Interlaminar shear strength and fracture toughness are comes in the range of 220-280KJ/m², 20-30MPa and 11-15MPa.m^{1/2}. The substantial improvement in mechanical properties tends to show the better interaction between filler and matrix. It indicates that obtained mechanical properties fulfill the required mechanical properties of implant material. Moreover, it's having similar modulus value of cortical bone and its

help to reduce the stress shielding effect during implant period (Bagheri et al. 2013). Besides, better thermal stability, crosslink density and moderate wettability also obtained in the prepared composites. It denotes that addition of bio fillers in epoxy matrix tends to make better bonding between fiber and matrix. Furthermore, the increase in cross link density reduced the uncured monomers presents in composite system which may help to improve the biocompatibility. Amongst the four hybrid composites, EP/CF/CB composite showed better biocompatibility (% of metabolic activity and % hemolysis) properties. It concludes that prepared EP/CF/CB composites has been found as alternate composite material for bio active high load bearing non degradable implants application. The major advantage of prepared composites is attained bioactivity properties without sacrificing its mechanical and physical properties. This may have better interaction with host tissue during “*in vivo*” condition for long term implant period.

7.1.8 Summary

To summarize the results from this chapter, material properties like mechanical, thermal, thermo-mechanical, physical and biocompatibility of carbon fiber/epoxy composites reinforced with four different cuttlebone derived bio filler (EP/CF/CB, EP/CF/HB, EP/CF/HA and EP/CF/CP) was compared.

Among the four different composites, EP/CF/HA and EP/CF/CP composites have better tensile, flexural, impact, hardness, fracture toughness and interlaminar shear strength properties. The results indicate that all four composites have good mechanical properties to satisfy the requirement for high load bearing implant applications. Besides, EP/CF/HA and EP/CF/CP composites has better thermal stability, storage modulus, glass transition temperature, cross link density and lower water uptake percentage rather than EP/CF/CB and EP/CF/HB composites. It denotes that addition of HA and CP particle as third phase in carbon fiber/epoxy composites makes the better interaction between fiber/matrix. Additionally, EP/CF/HA and EP/CF/CP composites have better wettability properties than EP/CF/CB and EP/CF/HB composites. In contrast, EP/CF/HA and EP/CF/CP composites has higher amount of voids percentage than other two hybrid composites. Though EP/CF/CB and EP/CF/HB composites have lesser thermal and

physical properties than EP/CF/HA and EP/CF/CP composites, but it fulfills the requirements for implants applications. Finally, EP/CF/CB composite has good biocompatibility property (% metabolic activity) than other three hybrid composites. Furthermore, blood compatibility was good in all four hybrid composites. It concludes that only EP/CF/CB composite has fulfilled the criteria (mechanical, physical and biocompatibility properties) for implant. These composite found suitable for the bioactive non degradable category implants destined for high load bearing applications.

CHAPTER 8

CHAPTER 8

CONCLUSIONS

The research conducted reveals that cuttlebone derived particles, cuttlebone derived bio ceramics as reinforcement in epoxy composites along with carbon fiber can be successfully implied as implants. Based on the results and discussion presented in the thesis, following conclusions were drawn.

- ❖ Cuttlebone particles consist of CaCO_3 in aragonite polymorph form with limited amount of organic matter; whereas, heat treated cuttlebone particles consists of CaCO_3 in calcite polymorph form. Heat treated cuttlebone reinforced composites have better tensile, hardness and fracture toughness properties; while raw cuttlebone reinforced composites have better flexural, compression and impact properties in conjunction with higher glass transition temperature and crosslink density. Though, both composites are hydrophilic in nature; they expressed low water absorption. These materialistic properties influences raw cuttlebone reinforced composite to express increased metabolic activity of L-929 fibroblast cells and its non-hemolytic nature.
- ❖ Cuttlebone derived hydroxyapatite particles are in biphasic crystalline form with the combination of hydroxyapatite and minimal amount of calcium oxide; whereas, tricalcium phosphate particles are in high purity level. Cuttlebone derived tricalcium phosphate reinforced composites has better tensile, compression, impact and hardness properties; while hydroxyapatite reinforced composite have better flexural and fracture toughness properties accompanied by higher glass transition temperature and crosslink density. Although, it is hydrophobic in nature; they possess favorable metabolic activity of L-929 fibroblast cells and expressed non-hemolytic nature. Finally, raw cuttlebone particles and cuttlebone derived hydroxyapatite particles reinforced epoxy composites have favorable materialistic properties for low load bearing implant applications.

- ❖ Among the four different hybrid composites, hydroxyapatite and tricalcium phosphate/carbon fiber reinforced epoxy composites have better mechanical, thermal, glass transition temperature, crosslink density and wettability properties than raw and heat treated cuttlebone reinforced carbon fiber epoxy composites. However, raw and heat treated cuttlebone / carbon fiber reinforced epoxy composites were found to attain the required materialistic properties for high load bearing implant applications. Finally, raw cuttlebone/carbon fiber reinforced epoxy composites have favorable biocompatibility property (metabolic activity and hemocompatibility) than the other three hybrid composites.
- ❖ Overall, a total of five cuttlebone derived bio-fillers were used as reinforcement in epoxy composites. Among the different composites, cuttlebone and hydroxyapatite reinforced epoxy composites showed better mechanical, physical, thermal and biocompatibility properties than other composites; even at a lower filler loading level ($\leq 9\text{wt}\%$). Material properties observed for these two composites showed them to be potential candidates for low load bearing implant applications. Cuttlebone derived particles and bio ceramics/carbon fiber reinforced hybrid composites showed better improvement in their mechanical, physical and thermal properties. Among the four different hybrid composites studied, raw cuttlebone/carbon fiber reinforced epoxy composite was found to become bioactive which was confirmed by its increased biocompatible properties. This materialistic property implies it as a potential candidate for high load bearing implant (bone plates) applications.

FUTURE WORK

Though the mechanical properties are adequate for implants application, biocompatible property of cuttlebone derived bioceramics particle reinforced composites is comparatively lower than raw cuttlebone particles reinforced composites. It has been improved by controlling the particle size, size distribution, crystallinity, stoichiometry and degree of agglomeration through different process parameters during synthesis. Moreover, different processing techniques to prepare the hybrid composites are required to achieve homogeneous dispersion of bioceramic fillers. The “*in-vitro*” bioactivity testing gave us information about the host tissue response to the biocomposite, the future studies could be more focused on “*in-vivo*” behavior.

REFERENCES

Abdul Khalil, H. P. S., Fizree, H. M., Bhat, A. H., Jawaid, M., and Abdullah, C. K. (2013). "Development and characterization of epoxy nanocomposites based on nano-structured oil palm ash." *Compos. Part B Eng.*, 53, 324–333.

Ahmed, K. (2015). "Hybrid composites prepared from Industrial waste: Mechanical and swelling behavior." *J. Adv. Res.*, 6(2), 225–232.

Ahmed, K. S., Mallinatha, V., and Amith, S. J. (2011). "Effect of ceramic fillers on mechanical properties of woven jute fabric reinforced epoxy composites." *J. Reinf. Plast. Compos.*, 30(15), 1315–1326.

Ahmed, K., Nizami, S., Raza, N., and Mahmood, K. (2012). "Mechanical, swelling, and thermal aging properties of marble sludge-natural rubber composites." *Int. J. Ind. Chem.*, 3(1), 21.

Ajikumar, P. K., Low, B. J. M., and Valiyaveetil, S. (2005). "Role of soluble polymers on the preparation of functional thin films of calcium carbonate." *Surf. Coatings Technol.*, 198(1-3), 227–230.

Ali, M. S., French, T. A., Hastings, G. W., Rae, T., Rushton, N., Ross, E. R., and Wynn-Jones, C. H. (1990). "Carbon fibre composite bone plates. Development, evaluation and early clinical experience." *J. Bone Jt. Surgery*, 72-B(4), 586–591.

Aminatun, Siswanto, Penga, Y. M., Istifarah, and Apsari, R. (2013). "The Effect of Sintering Process on the Characteristics of Hydroxyapatite from Cuttlefish Bone (*Sepia Sp.*)" *Res. J. Pharm. Biol. Chem. Sci.*, 4(4), 1431–1442.

Ang, K. C., Leong, K. F., Chua, C. K., and Chandrasekaran, M. (2015). "Compressive properties and degradability of poly(ϵ -caprolactone)/hydroxyapatite composites under accelerated hydrolytic degradation." *J. Biomed. Mater. Res.*, 80A(3), 654–660.

Aragón, J., González, R., Fuentes, G., Palin, L., Croce, G., and Viterbo, D. (2011). "Development and characterization of a novel bioresorbable and bioactive biomaterial

based on polyvinyl acetate, calcium carbonate and coralline hydroxyapatite.” *Mater. Res.*, 14(1), 25–30.

Aragón, J., González, R., Fuentes, G., Palin, L., Croce, G., and Viterbo, D. (2012). “In vitro release kinetics and physical, chemical and mechanical characterization of a POVIAC® /CaCO₃ /HAP-200 composite.” *J. Mater. Sci. Mater. Med.*, 23(2), 259–270.

Arnaud, E., Morieux, C., Wybier, M. and De-Vernejoul, M.C. (1994). “Potentiation of transforming growth factor (TGF- β 1) by natural coral and fibrin in a rabbit cranioplasty model. *Calcif. Tissue Int.*, 54(6), 493-498.

Auclair-Daigle, C., Bureau, M. N., Legoux, J. G., and Yahia, L. (2005). “Bioactive hydroxyapatite coatings on polymer composites for orthopedic implants.” *J. Biomed. Mater. Res. - Part A*, 73(4), 398–408.

Aurrekoetxea, J., Agirregomezkorta, A., Aretxaga, G., and Sarrionandia, M. (2012). “Impact behavior of carbon fiber/epoxy composite manufactured by vacuum-assisted compression resin transfer molding.” *J. Compos. Mater.*, 46(1), 43–49.

Ávila, A. F., Peixoto, L. G. Z. de O., Neto, A. S., Junior, J. de Á., and M. G. R. Carvalho. (2012). “Bending Investigation on Carbon Fiber / Epoxy Composites Nano- Modified by Graphene.” *J. Braz. Soc. Mech. Sci. Eng.*, XXXIV(3), 269–275.

Bader, R., Steinhäuser, E., Rechl, H., Siebels, W., Mittelmeier, W., and Gradinger, R. (2003). “Kohlenstofffaserverstärkte kunststoffe als implantatwerkstoff.” *Orthopade*, 32(1), 32–40.

Bagheri, Z. S., El Sawi, I., Bougherara, H., and Zdero, R. (2014). “Biomechanical fatigue analysis of an advanced new carbon fiber/flax/epoxy plate for bone fracture repair using conventional fatigue tests and thermography.” *J. Mech. Behav. Biomed. Mater.*, 35, 27–38.

Bagheri, Z. S., El Sawi, I., Schemitsch, E. H., Zdero, R., and Bougherara, H. (2013). “Biomechanical properties of an advanced new carbon/flax/epoxy composite material for bone plate applications.” *J. Mech. Behav. Biomed. Mater.*, 20, 398–406.

- Bagheri, Z. S., Giles, E., El Sawi, I., Amleh, A., Schemitsch, E. H., Zdero, R., and Bougherara, H. (2015). "Osteogenesis and cytotoxicity of a new Carbon Fiber/Flax/Epoxy composite material for bone fracture plate applications." *Mater. Sci. Eng. C. Mater. Biol. Appl.*, 46, 435–42.
- Bagheri, Z. S., Tavakkoli Avval, P., Bougherara, H., Aziz, M. S. R., Schemitsch, E. H., and Zdero, R. (2014). "Biomechanical analysis of a new carbon fiber/flax/epoxy bone fracture plate shows less stress shielding compared to a standard clinical metal plate." *J. Biomech. Eng.*, 136(9), 091002 1–10.
- Bai, W., Chen, D., Zhang, Z., Li, Q., Zhang, D., and Xiong, C. (2009). "Poly(paradioxanone)/inorganic particle composites as a novel biomaterial." *J. Biomed. Mater. Res. - Part B Appl. Biomater.*, 90 B(2), 945–951.
- Barakat, N. A. M., Khalil, K. A., Sheikh, F. A., Omran, A. M., Gaihre, B., Khil, S. M., and Kim, H. Y. (2008). "Physiochemical characterizations of hydroxyapatite extracted from bovine bones by three different methods: Extraction of biologically desirable HAp." *Mater. Sci. Eng. C*, 28(8), 1381–1387.
- Barakat, N. A. M., Khil, M. S., Omran, A. M., Sheikh, F. A., and Kim, H. Y. (2009). "Extraction of pure natural hydroxyapatite from the bovine bones bio waste by three different methods." *J. Mater. Process. Technol.*, 209(7), 3408–3415.
- Barinov, S. M. (2010). "Calcium phosphate-based ceramic and composite materials for medicine." *Russ. Chem. Rev.*, 79(1), 13–29.
- Ben-Nissan, B. (2003). "Natural bioceramics: From coral to bone and beyond." *Curr. Opin. Solid State Mater. Sci.*, 7(4-5), 283–288.
- Ben-Nissan, B., Milev, a, and Vago, R. (2004). "Morphology of sol-gel derived nano-coated coralline hydroxyapatite." *Biomaterials*, 25(20), 4971–5.
- Benoist, M. (1978). "Experience with 220 cases of mandibular reconstruction." *J. Maxillofac. Surg.*, 6(C), 40–49.

- Birchall, J. D. and Thomas, N.L. (1983). "On the architecture and function of cuttlefish bone." *J. Mater. Sci.*, 18(7), 2081–2086.
- Bonfield, W. (1988). "Hydroxyapatite-Reinforced Polyethylene as an Analogous Material for Bone Replacement." *Ann. N. Y. Acad. Sci.*, 523(1), 173–177.
- Bootklad, M., and Kaewtatip, K. (2014). "Biodegradability , Mechanical , and Thermal Properties of Thermoplastic Starch/Cuttlebone Composites." *Polym. Compos.*, 36(8), 1401–1406.
- Boutinguiza, M., Pou, J., Comesaña, R., Lusquiños, F., Carlos, A. D., and León, B. (2012b). "Biological hydroxyapatite obtained from fish bones." *Mater. Sci. Eng. C*, 32(3), 478–486.
- Bradley, J. S., Hastings, G. W., and Johnson-Nurse, C. (1980). "Carbon fibre reinforced epoxy as a high strength, low modulus material for internal fixation plates." *Biomaterials*, 1(1), 38–40.
- Brockett, C. L., John, G., Williams, S., Jin, Z., Isaac, G. H., and Fisher, J. (2012). "Wear of ceramic-on-carbon fiber-reinforced poly-ether ether ketone hip replacements." *J. Biomed. Mater. Res. - Part B Appl. Biomater.*, 100 B(6), 1459–1465.
- Cadman, J., Zhou, S., Chen, Y., Li, W., Appleyard, R., and Li, Q. (2010). "Characterization of cuttlebone for a biomimetic design of cellular structures." *Acta Mech. Sin.*, 26(1), 27–35.
- Canal, C., and Ginebra, M. P. (2011). "Fibre-reinforced calcium phosphate cements: A review." *J. Mech. Behav. Biomed. Mater.*, 4(8), 1658–1671.
- Cao, L., Jiang, J.-T., Wang, Z.-Q., Gong, Y.-X., Liu, C., and Zhen, L. (2014). "Electromagnetic properties of flake-shaped Fe–Si alloy particles prepared by ball milling." *J. Magn. Magn. Mater.*, 368, 295–299.
- Chen, F., Mao, T., Tao, K., Chen, S., Ding, G., and Gu, X. (2002). "Bone graft in the shape of human mandibular condyle reconstruction via seeding marrow-derived

osteoblasts into porous coral in a nude mice model.” *J. Oral Maxillofac. Surg.*, 60(10), 1155–1159.

Chen, J., Kinloch, A. J., Sprenger, S., and Taylor, A. C. (2013). “The mechanical properties and toughening mechanisms of an epoxy polymer modified with polysiloxane-based core-shell particles.” *Polym.*, 54(16), 4276–4289.

Chen, P. Y., Lin, A. Y. M., Lin, Y. S., Seki, Y., Stokes, A. G., Peyras, J., Olevsky, E. A., Meyers, M. A., and McKittrick, J. (2008). “Structure and mechanical properties of selected biological materials.” *J. Mech. Behav. Biomed. Mater.*, 1(3), 208–226.

Chiang, C. L., Chang, R. C., and Chiu, Y. C. (2007). “Thermal stability and degradation kinetics of novel organic/inorganic epoxy hybrid containing nitrogen/silicon/phosphorus by sol-gel method.” *Thermochim. Acta*, 453(2), 97–104.

Choi, S. H., Levy, M. L., and McComb, J. G. (1998). “A Method of Cranioplasty Using Coralline Hydroxyapatite.” *Pediatr Neurosurg*, 29(6), 324–327.

Chou, J., Ben-Nissan, B., Choi, A. H., Wuhner, R., and Green, D. (2007). “Conversion of coral sand to calcium phosphate for biomedical applications.” *J. Aust. Ceram. Soc.*, 43(1), 44–48.

Cieślik, M., Mertas, A., Morawska-Chochół, A., Sabat, D., Orlicki, R., Owczarek, A., Kró, W., and Cieślik, T. (2009). “The evaluation of the possibilities of using PLGA copolymer and its composites with carbon fibers or hydroxyapatite in the bone tissue regeneration process - In vitro and in vivo examinations.” *Int. J. Mol. Sci.*, 10(7), 3224–3234.

Coelho, T. M., Nogueira, E. S., Steimacher, A., Medina, A. N., Weinand, W. R., Lima, W. M., Baesso, M. L., and Bento, A. C. (2006). “Characterization of natural nanostructured hydroxyapatite obtained from the bones of Brazilian river fish.” *J. Appl. Phys.*, 100(9), 094312 1–6.

Coelho, T. M., Nogueira, E. S., Weinand, W. R., Lima, W. M., Steimacher, A., Medina, A. N., Baesso, M. L., and Bento, A. C. (2007). “Thermal properties of natural

nanostructured hydroxyapatite extracted from fish bone waste.” *J. Appl. Phys.*, 101(8), 084701 1–6.

Cusack, M., and Chung, P. (2014). “Crystallographic orientation of cuttlebone shield determined by electron backscatter diffraction.” *Jom*, 66(1), 139–142.

Demers, C. N., Tabrizian, M., Petit, A., Hamdy, R. C., and Yahia, L. (2002). “Effect of experimental parameters on the in vitro release kinetics of transforming growth factor β 1 from coral particles.” *J. Biomed. Mater. Res.*, 59(3), 403–410.

Denton, E. J., and Gilpin-Brown, J. B. (1961). “THE BUOYANCY OF THE CUTTLEFISH, SEPIA OFFICINAILS (L).” *J. Mar. biol. Ass.*, 41(02), 319–342.

Di Silvio, L., Dalby, M., and Bonfield, W. (1998). “In vitro response of osteoblasts to hydroxyapatite-reinforced polyethylene composites.” *J. Mater. Sci. Mater. Med.*, 9(12), 845–848.

Di Silvio, L., Dalby, M., and Bonfield, W. (1998). “In vitro response of osteoblasts to hydroxyapatite-reinforced polyethylene composites.” *J. Mater. Sci. Mater. Med.*, 9(12), 845–848.

Dimitrievska, S., Whitfield, J., Hacking, S. A., and Bureau, M. N. (2009). “Novel carbon fiber composite for hip replacement with improved in vitro and in vivo osseointegration.” *J. Biomed. Mater. Res. - Part A*, 91(1), 37–51.

Dorozhkin, S. V. (2012). “Biphasic, triphasic and multiphasic calcium orthophosphates.” *Acta Biomater.*, 8(3), 963–977.

Ferrari, M., Vichi, A., and García-Godoy, F. (2000). “Clinical evaluation of fiber-reinforced epoxy resin posts and cast post and cores.” *Am. J. Dent.*, 13, B15-B18.

Figueiredo, M., Henriques, J., Martins, G., Guerra, F., Judas, F., and Figueiredo, H. (2010). “Physicochemical characterization of biomaterials commonly used in dentistry as bone substitutes - Comparison with human bone.” *J. Biomed. Mater. Res. - Part B Appl. Biomater.*, 92(2), 409-419.

- Florek, M., Fornal, E., Gómez-romero, P., Zieba, E., Paszkowicz, W., Lekki, J., Nowak, J., and Kuczumow, A. (2009). "Complementary microstructural and chemical analyses of Sepia officinalis endoskeleton." *Mater. Sci. Eng. C*, 29(4), 1220–1226.
- Fombuena, V., Bernardi, L., Fenollar, O., Boronat, T., and Balart, R. (2014). "Characterization of green composites from biobased epoxy matrices and bio-fillers derived from seashell wastes." *Mater. Des.*, 57, 168–174.
- Fredriksson, M., Astbäck, J., Pamenius, M., and Arvidson, K. (1998). "A retrospective study of 236 patients with teeth restored by carbon fiber-reinforced epoxy resin posts." *J. Prosthet. Dent.*, 80(2), 151–157.
- Fu, T. A. O., and Zhao, J. (2004b). "Preparation of carbon fiber fabric reinforced hydroxyapatite / epoxy composite by RTM processing." *J. Mater. Sci.*, 39(4), 1411–1413.
- Fujihara, K., Huang, Z. M., Ramakrishna, S., Satknanantham, K., and Hamada, H. (2004). "Feasibility of knitted carbon/PEEK composites for orthopedic bone plates." *Biomaterials*, 25(17), 3877–3885.
- Fujihara, K., Kotaki, M., and Ramakrishna, S. (2005). "Guided bone regeneration membrane made of polycaprolactone/calcium carbonate composite nano-fibers." *Biomaterials*, 26(19), 4139–47.
- Gabr, M. H., Elrahman, M. A., Okubo, K., and Fujii, T. (2010). "A study on mechanical properties of bacterial cellulose/epoxy reinforced by plain woven carbon fiber modified with liquid rubber." *Compos. Part A Appl. Sci. Manuf.*, 41(9), 1263–1271.
- García-Enriquez, S., Guadarrama, H. E. R., Reyes-González, I., Mendizábal, E., Jasso-Gastinel, C. F., García-Enriquez, B., Rembao-Bojórquez, D., and Pane-Pianese, C. (2010). "Mechanical performance and in vivo tests of an acrylic bone cement filled with bioactive sepia officinalis cuttlebone." *J. Biomater. Sci. Polym. Ed.*, 21(1), 113–125.
- Ge, H., Zhao, B., Lai, Y., Hu, X., Zhang, D., and Hu, K. (2010). "From crabshell to chitosan-hydroxyapatite composite material via a biomorphic mineralization synthesis method." *J. Mater. Sci. Mater. Med.*, 21(6), 1781–7.

- Gergely, G., Wéber, F., Lukács, I., Tóth, A. L., Horváth, Z. E., Mihály, J., and Balázs, C. (2010). "Preparation and characterization of hydroxyapatite from eggshell." *Ceram. Int.*, 36(2), 803–806.
- Gopinath, C. S., Hegde, S. G., Ramaswamy, A. V, and Mahapatra, S. (2002). "Photoemission studies of polymorphic CaCO₃ materials." *Mater. Res. Bull.*, 37(7), 1323–1332.
- Gunduz, O., Sahin, Y. M., Agathopoulos, S., Ben-Nissan, B., and Oktar, F. N. (2014). "A new method for fabrication of nanohydroxyapatite and TCP from the sea snail *Cerithium vulgatum*." *J. Nanomater.*, 2014, 1–6.
- Ha, S. W., Giseop, A., Mayer, J., Wintermantel, E., Gruner, H., and Wieland, M. (1997). "Topographical characterization and microstructural interface analysis of vacuum-plasma-sprayed titanium and hydroxyapatite coatings on carbon fibre-reinforced poly(etheretherketone)." *J. Mater. Sci. Mater. Med.*, 8(12), 891–896.
- Hak, D. J., Mauffrey, C., Seligson, D., and Lindeque, B. (2014). "Use of carbon-fiber-reinforced composite implants in orthopedic surgery." *Orthopedics*, 37(12), 825–830.
- Hamester, M. R. R., Balzer, P. S., and Becker, D. (2012). "Characterization of calcium carbonate obtained from oyster and mussel shells and incorporation in polypropylene." *Mater. Res.*, 15(2), 204–208.
- He, H., and Gao, F. (2015). "Preparation and Characterization of Nano-Calcium Carbonate/Silane Coupling Agent Master Batch and Its Effect on Epoxy Resin." *J. Macromol. Sci. Part B*, 54(7), 879–885.
- He, H., and Li, K. (2012). "Silane Coupling Agent Modification on Interlaminar Shear Strength of Carbon Fiber/Epoxy/Nano-CaCO₃ Composites." *Polym. Compos.*, 33(10), 1755–1758.
- He, H., Li, K., Wang, J., Sun, G., Li, Y., and Wang, J. (2011). "Study on thermal and mechanical properties of nano-calcium carbonate/epoxy composites." *Mater. Des.*, 32(8-9), 4521–4527.

- He, H., Zhang, Z., Wang, J., and Li, K. (2013). "Compressive properties of nano-calcium carbonate/epoxy and its fibre composites." *Compos. Part B Eng.*, 45(1), 919–924.
- He, X., Zhang, D., Li, H., Fang, J., and Shi, L. (2011). "Shape and size effects of ceria nanoparticles on the impact strength of ceria/epoxy resin composites." *Particuology*, 9(1), 80–85.
- Hongmin, L., Wei, Z., Xingrong, Y., Jing, W., Wenxin, G., Jihong, C., Xin, X., and Fulin, C. (2015). "Osteoinductive nanohydroxyapatite bone substitute prepared via in situ hydrothermal transformation of cuttlefish bone." *J. Biomed. Mater. Res. Part B Appl. Biomater.*, 103(4), 1–9.
- Howard, C. B. (1985). "The Response of Human Tissues To Carbon Reinforced Epoxy Resin." *J. Bone Jt. Surgery.*, 67(4), 656–658.
- Hu, J., and Russell, J. J. (2001). "Production and analysis of hydroxyapatite from Australian corals via hydrothermal process." *J. Mater. Sci. Lett.*, 20, 85–87.
- Huang, J., Di Silvio, L., Wang, M., Tanner, K. E., and Bonfield, W. (1997). "In vitro mechanical and biological assessment of hydroxyapatite-reinforced polyethylene composite." *J. Mater. Sci. Mater. Med.*, 8(12), 775–779.
- Hui, P., Meena, S. L., Singh, G., Agarawal, R. D., and Prakash, S. (2010). "Synthesis of Hydroxyapatite Bio-Ceramic Powder by Hydrothermal Method." *J. Miner. Mater. Charact. Eng.*, 9(8), 683–692.
- Hussain, M., Nakahira, A., and Niihara, K. (1996). "Mechanical property improvement of carbon fiber reinforced epoxy composites by Al₂O₃ filler dispersion." *Mater. Lett.*, 26(3), 185–191.
- Ige, O. O., Umoru, L. E., and Aribo, S. (2012). "Natural Products: A Minefield of Biomaterials." *ISRN Mater. Sci.*, 2012, 1–20.
- Ignjatović, N., and Uskoković, D. (2008). "Biodegradable composites based on nanocrystalline calcium phosphate and bioresorbable polymers." *Adv. Appl. Ceram.*, 107(3), 142–147.

- Intharapat, P., Kongnoo, A., and Kateungngan, K. (2013). "The Potential of Chicken Eggshell Waste as a Bio-filler Filled Epoxidized Natural Rubber (ENR) Composite and its Properties." *J. Polym. Environ.*, 21(1), 245–258.
- Ivankovic, H., Gallego Ferrer, G., Tkalcec, E., Orlic, S., and Ivankovic, M. (2009). "Preparation of highly porous hydroxyapatite from cuttlefish bone." *J. Mater. Sci. Mater. Med.*, 20(5), 1039–1046.
- Ivankovic, H., Orlic, S., Kranzelic, D., and Tkalcec, E. (2010). "Highly Porous Hydroxyapatite Ceramics for Engineering Applications." *Adv. Sci. Technol.*, 63, 408–413.
- Ivankovic, H., Tkalcec, E., Orlic, S., Ferrer, G. G., and Schauperl, Z. (2010b). "Hydroxyapatite formation from cuttlefish bones: kinetics." *J. Mater. Sci. Mater. Med.*, 21(10), 2711–22.
- Jamali, A., Hilpert, A., Debes, J., Afshar, P., Rahban, S., and Holmes, R. (2002). "Hydroxyapatite/calcium carbonate (HA/CC) vs. plaster of Paris: A histomorphometric and radiographic study in a rabbit tibial defect model." *Calcif. Tissue Int.*, 71(2), 172–8.
- Janaki, K., Elamathi, S., and Sangeetha, D. (2008). "Development and Characterization of Polymer Ceramic Composites for Orthopedic Applications." *Trends Biomater. Artif. Organs*, 22(3), 169–178.
- Jasso-Gastinel, C. F., Enriquez, S. G., Flores, J., Reyes-González, I., and Mijares, E. M. (2009). "Acrylic Bone Cements Modified With Bioactive Filler." *Macromol. Symp.*, 283-284(1), 159–166.
- Jayabalan, M. (2009). "Studies on Poly(propylene fumarate-co-caprolactone diol) Thermoset Composites towards the Development of Biodegradable Bone Fixation Devices." *Int. J. Biomater.*, 2009, 486710.
- Jayabalan, M., Shalumon, K. T., Mitha, M. K., Ganesan, K., and Epple, M. (2010). "Effect of hydroxyapatite on the biodegradation and biomechanical stability of polyester nanocomposites for orthopaedic applications." *Acta Biomater.*, 6(3), 763–775.

- Jayasuriya, A. C., and Bhat, A. (2010). "Fabrication and characterization of novel hybrid organic/inorganic microparticles to apply in bone regeneration." *J. Biomed. Mater. Res. A*, 93A(4), 1280–8.
- Jianfeng, H., Juanying, L., Liyun, C., and Liping, Z. (2010). "Preparation and Properties of Carbon Fiber/ Hydroxyapatite-Poly(methyl methacrylate) Biocomposites." *J. of Applied Polymer Sci.*, 116(3), 1782–1787.
- Jin, F. L., and Park, S. J. (2009). "Thermal Stability of Trifunctional Epoxy Resins Modified with Nanosized Calcium Carbonate." *Bull. Korean Chem. Soc.*, 30(2), 334–338.
- Jin, F.-L., and Park, S.-J. (2008). "Interfacial toughness properties of trifunctional epoxy resins/calcium carbonate nanocomposites." *Mater. Sci. Eng. A*, 475(1-2), 190–193.
- Jin, F.-L., and Park, S.-J. (2012). "Thermal properties of epoxy resin/filler hybrid composites." *Polym. Degrad. Stab.*, 97(11), 2148–2153.
- Jinawath, S., Polchai, D., and Yoshimura, M. (2002). "Low-temperature , hydrothermal transformation of aragonite to hydroxyapatite." *Mater. Sci. Eng. C*, 22, 35–39.
- Jones, M. I., Barakat, H., and Patterson, D. A. (2011). "Production of hydroxyapatite from waste mussel shells." *ICC3 Symp. 13 Ceram. Med. Biotechnol. Biomimetics IOP Conf. Ser. Mater. Sci. Eng.* 18 192002, 192002 1–4.
- Jumahat, A., Soutis, C., Jones, F. R., and Hodzic, A. (2010). "Effect of silica nanoparticles on compressive properties of an epoxy polymer." *J. Mater. Sci.*, 45(21), 5973–5983.
- Kalaei, M., Akhlaghi, S., Nouri, A., Mazinani, S., Mortezaei, M., Afshari, M., Mostafanezhad, D., Allahbakhsh, A., Dehaghi, H. A., Amirsadri, A., and Gohari, D. P. (2011). "Effect of nano-sized calcium carbonate on cure kinetics and properties of polyester/epoxy blend powder coatings." *Prog. Org. Coatings*, 71(2), 173–180.

- Kamba, A. S., Ismail, M., Ibrahim, T. A. T., and Zakaria, Z. A. B. (2013). "Synthesis and Characterisation of Calcium Carbonate Aragonite Nanocrystals from Cockle Shell Powder (*Anadara granosa*)." *J. Nanomater.*, 2013, 1–9.
- Kango, S., Kalia, S., Celli, A., Njuguna, J., Habibi, Y., and Kumar, R. (2013). "Surface modification of inorganic nanoparticles for development of organic – inorganic nanocomposites - A review." *Prog. Polym. Sci.*, 38(8), 1232–1261.
- Kannan, S., Rocha, J. H. G., Agathopoulos, S., and Ferreira, J. M. F. (2007). "Fluorine-substituted hydroxyapatite scaffolds hydrothermally grown from aragonitic cuttlefish bones." *Acta Biomater.*, 3(2), 243–9.
- Kato, T., Nishimura, T. and Sakamoto, T. (2008). "Development of Inorganic/Organic Hybrid Thin-Films Inspired by Biomineralization." *J. Jpn. Assoc. Cryst. Growth*, 35, 145-148.
- Kauly, T., Siegmann, A., and Shacham, D. (2008). "Mechanical Behavior of Highly Filled Natural CaCO₃ Composites: Effect of Particle Size Distribution and Interface Interactions." *Polym. Compos.*, 29(4), 396–408.
- Kavitha, N., Balasubramanian, M., and Kennedy, A. X. (2012). "Investigation of impact behavior of epoxy reinforced with nanometer- and micrometer-sized silicon carbide particles." *J. Compos. Mater.*, 47(15), 1877–1884.
- Khalil, H. P. S. A., Fizree, H. M., Bhat, A. H., Jawaid, M., and Abdullah, C. K. (2013). "Composites : Part B Development and characterization of epoxy nanocomposites based on nano-structured oil palm ash." *Compos. Part B Eng.*, 53, 324–333.
- Khan, W., Muntimadugu, E., Jaffe, M. and Domb, A.J. (2014). "Implantable medical devices." Focal controlled drug delivery, A.J. Domb and W. Khan, eds., *Springer /controlled release Society*, 33-59.
- Khanal, S. P., Mahfuz, H., Rondinone, A. J., and Leventouri, T. (2016). "Improvement of the fracture toughness of hydroxyapatite (HAp) by incorporation of carboxyl

functionalized single walled carbon nanotubes (CfSWCNTs) and nylon.” *Mater. Sci. Eng. C*, 60, 204–210.

Kim, B. S., Kang, H. J., and Lee, J. (2013). “Improvement of the compressive strength of a cuttlefish bone-derived porous hydroxyapatite scaffold via polycaprolactone coating.” *J. Biomed. Mater. Res. - Part B Appl. Biomater.*, 101(7), 1302–1309.

Kim, B. S., Yang, S. S., and Lee, J. (2014). “A polycaprolactone/cuttlefish bone-derived hydroxyapatite composite porous scaffold for bone tissue engineering.” *J. Biomed. Mater. Res. - Part B Appl. Biomater.*, 102(5), 943–951.

Kim, G. M., and Michler, G. H. (1998). “Micromechanical deformation processes in toughened and particle filled semicrystalline polymers . Part 2 : Model representation for micromechanical deformation processes.” *Polymer*, 39(23), 5699–5703.

Kim, J. J., Kim, H. J., and Lee, K. S. (2008). “Evaluation of biocompatibility of pProus hydroxyapatite developed from edible cuttlefish bone.” *Key Eng. Mater.*, 361-363 I, 155–158.

Kim, M. T., Rhee, K. Y., Lee, J. H., Hui, D., and Lau, A. K. T. (2011). “Property enhancement of a carbon fiber / epoxy composite by using carbon nanotubes.” *Compos. Part B*, 42(5), 1257–1261.

Klungsuwan, P., and Poompradub, S. (2010). “Smart Green Composite: Effect of Cuttlebone Particle on the Mechanical Properties of NR Vulcanizates.” *Adv. Mater. Res.*, 150-151, 547–550.

Kobayashi, S., and Kawai, W. (2007). “Development of carbon nanofiber reinforced hydroxyapatite with enhanced mechanical properties.” *Compos. Part A Appl. Sci. Manuf.*, 38(1), 114–123.

Kornmann, X., Rees, M., Thomann, Y., Nocola, a., Barbezat, M., and Thomann, R. (2005). “Epoxy-layered silicate nanocomposites as matrix in glass fibre-reinforced composites.” *Compos. Sci. Technol.*, 65(14), 2259–2268.

- Kotela, I., Chlopek, J., Rosol, P., and Blazewicz, M. (2009). "Mechanical Assessment of Non-metallic Composite Clamps Designed for Orthopaedic Surgery." *J. Compos. Mater.*, 43(26), 3265–3274.
- Ku, H., Cardona, F., and Jamal Eddine, M. (2013). "Thermal properties of calcium carbonate powder reinforced vinyl ester composites: Pilot study." *J. Appl. Polym. Sci.*, 127(4), 2996–3001.
- Lee, H. S., Ha, T. H., Kim, H. M., and Kim, K. (2007). "Fabrication and Micropatterning of a Hybrid Composite of Amorphous Calcium Carbonate and Poly (ethylenimine)." *Bull. Korean Chem. Soc.*, 28(3), 457–462.
- Lee, S. J., and Oh, S. H. (2003). "Fabrication of calcium phosphate bioceramics by using eggshell and phosphoric acid." *Mater. Lett.*, 57(29), 4570–4574.
- Lee, S. J., Lee, Y. C., and Yoon, Y. S. (2007). "Characteristics of calcium phosphate powders synthesized from cuttlefish bone and phosphoric acid." *J. Ceram. Process. Res.*, 8(6), 427–430.
- Li, H.-Y., Chen, Y.-F., and Xie, Y.-S. (2004). "Nanocomposites of cross-linking polyanhydrides and hydroxyapatite needles: mechanical and degradable properties." *Mater. Lett.*, 58(22–23), 2819–2823.
- Li, H.-Y., Tan, Y.-Q., Zhang, L., Zhang, Y.-X., Song, Y.-H., Ye, Y., and Xia, M.-S. (2012). "Bio-filler from waste shellfish shell: preparation, characterization, and its effect on the mechanical properties on polypropylene composites." *J. Hazard. Mater.*, 217-218, 256–262.
- Li, L., Zou, H., Shao, L., Wang, G., and Chen, J. (2005). "Study on mechanical property of epoxy composite filled with nano-sized calcium carbonate particles." *J. Mater. Sci.*, 40(5), 1297–1299.
- Li, X., Zhao, Y., Bing, Y., Li, Y., Gan, N., Guo, Z., Peng, Z., and Zhu, Y. (2013). "Biotemplated Syntheses of Macroporous Materials for Bone Tissue Engineering Scaffolds and Experiments in Vitro and Vivo Biotemplated Syntheses of Macroporous

Materials for Bone Tissue Engineering Scaffolds and Experiments in Vitro and Vivo.” *ACS Appl. Mater. Interfaces*, 5(12), 5557–5562.

Li, X.-G., Lv, Y., Ma, B.-G., Wang, W.-Q., and Jian, S.-W. (2013). “Decomposition kinetic characteristics of calcium carbonate containing organic acids by TGA.” *Arab. J. Chem.*, 3, 1–4.

Lin, Z., Guan, Z., Chen, C., Cao, L., Wang, Y., Gao, S., Xu, B., and Li, W. (2013). “Preparation, structures and properties of shell/polypropylene biocomposites.” *Thermochim. Acta*, 551, 149–154.

Lucas-girot, A., Langlois, P., Sangleboeuf, J. C., Ouammou, A., Rouxel, T., and Gaude, J. (2002). “A synthetic aragonite-based bioceramic : influence of process parameters on porosity and compressive strength.” *Biomaterials*, 23(2), 503–510.

M.Selvakumar, Saravana Kumar Jaganathan, Golok B. Nando, S. C. (2014). “Synthesis and Characterization of Novel Polycarbonate Based Polyurethane / Polymer Wrapped Hydroxyapatite Nanocomposites: Mechanical Properties, Osteoconductivity and Biocompatibility.” *J. Biomedical Nanotechnol.*, 10, 1–15.

Macha, I. J., Ozyegin, L. S., Oktar, F. N., and Ben-Nissan, B. (2015). “Conversion of Ostrich Eggshells (*Struthio camelus*) to Calcium Phosphates.” *J. Aust. Ceram. Soc.*, 51(1), 125–133.

Mahshuri, Y., and Malina, M. A. (2014). “Hardness and compressive properties of calcium carbonate derived from clam shell filled unsaturated polyester composites.” *Mater. Res. Innov.*, 25(9), 1682–1690.

Mahyudin, F., Widhiyanto, L., and Hermawan, H. (2016). “Biomaterials in orthopaedics.” *Adv. Struct. Mater.*, 58, 161–181.

Manjubala, I., Sivakumar, M., Kumar, T. S. S., and Rao, K. P. (2000). “Synthesis and characterization of functional gradient materials using Indian corals.” *J. Mater. Sci. Mater. Med.*, 11(11), 705–709.

- Mano, J. F., Sousa, R. a, Boesel, L. F., Neves, N. M., and Reis, R. L. (2004). "Bioinert, biodegradable and injectable polymeric matrix composites for hard tissue replacement: state of the art and recent developments." *Compos. Sci. Technol.*, 64(6), 789–817.
- Medeiros, J.-R. J. I. K. (2007). "Effects of Calcium Carbonate Particulate Releasing Surgical Anchors on Bone and Tendon Healing." B. S. Thesis, Massachusetts Inst. Technol., Massachusetts, U.S.
- Mehta, M. S., and Singh, R. P. (2014). "Effect of Aging Time and Sintering Temperatures on Structural, Morphological and Thermal Properties of Coralline Hydroxyapatite." *Int. J. Res. Mech. Eng. Technol.*, 4(2), 62–67.
- Meyers, M. A., Chen, P.-Y., Lin, A. Y.-M., and Seki, Y. (2008). "Biological materials: Structure and mechanical properties." *Prog. Mater. Sci.*, 53(1), 1–206.
- Milovac, D., Ferrer, G. G., Ivankovic, M., and Ivankovic, H. (2014). "PCL-coated hydroxyapatite scaffold derived from cuttlefish bone: Morphology, mechanical properties and bioactivity." *Mater. Sci. Eng. C*, 34, 437-445.
- Milovac, D., Gamboa-Martínez, T. C., Ivankovic, M., Ferrer, G. G., and Ivankovic, H. (2014). "PCL-coated hydroxyapatite scaffold derived from cuttlefish bone: In vitro cell culture studies." *Mater. Sci. Eng. C*, 42, 264–272.
- Mirsalehi, S. A., Khavandi, A., Mirdamadi, S., Naimi-Jamal, M. R., and Kalantari, S. M. (2015). "Nanomechanical and tribological behavior of hydroxyapatite reinforced ultrahigh molecular weight polyethylene nanocomposites for biomedical applications." *J. Appl. Polym. Sci.*, 132(23), 1–11.
- Mishra, S., Sonawane, S., and Chitodkar, V. (2005). "Comparative Study on Improvement in Mechanical and Flame Retarding Properties." *Polym. Plast. Technol. Eng.*, 44(3), 37–41.
- Mohd Zulfli, N. H., Abu Bakar, A., and Chow, W. S. (2013). "Mechanical and thermal properties improvement of nano calcium carbonate-filled epoxy/glass fiber composite laminates." *High Perform. Polym.*, 26(2), 223–229.

- Mondal, S., Mondal, B., Dey, A., and Mukhopadhyay, S. S. (2012). "Studies on Processing and Characterization of Hydroxyapatite Biomaterials from Different Bio Wastes." *J. Miner. Mater. Charact. Eng.*, 11(1), 55–67.
- Murali, M., Finosh, G. T., and Jayabalan, M. (2013). "Studies on Biodegradable Polymeric Nanocomposites Based on Sheet Molding Compound for Orthopedic Applications." *Adv. Mater. Sci. Appl.*, 2(2), 73–87
- Mustata, F., Tudorachi, N., and Rosu, D. (2012). "Thermal behavior of some organic/inorganic composites based on epoxy resin and calcium carbonate obtained from conch shell of *Rapana thomasiana*." *Compos. Part B Eng.*, 43(2), 702–710.
- Nandi, S. K., Kundu, B., Mukherjee, J., Mahato, A., Datta, S., and Balla, V. K. (2015). "Converted marine coral hydroxyapatite implants with growth factors: In vivo bone regeneration." *Mater. Sci. Eng. C*, 49, 816–823.
- Navarro, M., Michiardi, A., Castaño, O. and Planell, J.A. (2008). "Biomaterials in orthopedics." *J. R. Soc. Interface*, 5(27), 1137-1158.
- Ngamcharussrivichai, C., Nunthasanti, P., Tanachai, S., and Bunyakiat, K. (2010). "Biodiesel production through transesterification over natural calciums." *Fuel Process. Technol.*, 91(11), 1409–1415.
- Njoku, R. E., Okon, A E., and Ikpaki, T. C. (2011). "Effects of Variation of Particle Size and Weight Fraction on the Tensile Strength and Modulus of Periwinkle Shell Reinforced Polyester Composite." *Niger. J. Technol.*, 30(2), 87–93.
- Núñez, L., Núñez, M. R., Villanueva, M., Castro, A., and Rial, B. (2002). "Study of the epoxy system BADGE (n = 0)/1,2-DCH/CaCO₃ filler by DMA and DSC." *J. Appl. Polym. Sci.*, 85(2), 366–370.
- Oktar, F. N., Agathopoulos, S., Ozyegin, L. S., Turner, I. G., Gunduz, O., Demirkol, N., Brück, S., Ben-Nissan, B., Samur, R., Kayali, E. S., and Aktas, C. (2012). "Nano-Bioceramic Production via Mechano-Chemical Conversion (Ultrasonication)." *Key Eng. Mater.*, 529-530, 609–614.

Oláh, L., and Tuba, F. (2010). "Investigation of Calcium Carbonates Enhanced Poly(ϵ -caprolactone) Materials for Biomedical Applications." *Macromol. Symp.*, 296(1), 371–377.

Olah, L., Filipczak, K., Jaegermann, Z., Czigany, T., Borbas, L., Sosnowski, S., Ulanski, P., and Rosiak, J. M. (2006). "Synthesis, structural and mechanical properties of porous polymeric scaffolds for bone tissue regeneration based on neat poly(ϵ -caprolactone) and its composites with calcium carbonate." *Polym. Adv. Technol.*, 17(11-12), 889–897.

Ooi, C. Y., Hamdi, M., and Ramesh, S. (2007). "Properties of hydroxyapatite produced by annealing of bovine bone." *Ceram. Int.*, 33, 1171–1177.

Öteyaka, M. Ö., Ünal, H. H., Nam, B. L. C., and Tafiçi, E. (2013). "Characterization of powdered fish heads for bone graft biomaterial applications." *Acta Orthop Traumatol Turc*, 47(5), 359–365.

Oudadesse, H., Derrien, A. C., Lucas-Girot, A., Martin, S., Cathelineau, G., Sauvage, T., and Blondiaux, G. (2004). "In vivo mineral composition evolution of a synthetic CaCO_3 aragonite used as biomaterial for osseous substitution." *Instrum. Sci. Technol.*, 32(5), 545–554.

Ozyegin, L. S., Sima, F., Ristoscu, C., Kiyici, I. A., Mihailescu, I. N., Meydanoglu, O., Agathopoulos, S., and Oktar, F. N. (2011). "Sea Snail: An Alternative Source for Nano-Bioceramic Production." *Key Eng. Mater.*, 493-494, 781–786.

Pai, R. K., Zhang, L., Nykpanchuk, D., Cotlet, M., and Korach, C. S. (2011). "Biomimetic Pathways for Nanostructured Poly(KAMPS)/aragonite Composites that Mimic Seashell Nacre." *Adv. Eng. Mater.*, 13(10), B415–B422.

Pallela, R., Venkatesan, J., and Kim, S. K. (2011). "Polymer assisted isolation of hydroxyapatite from *Thunnus obesus* bone." *Ceram. Int.*, 37(8), 3489–3497.

Park, K., and Vasilos, T. (1997). "Characteristics of carbon fibre-reinforced calcium phosphate composites fabricated by hot pressing." *J. Mater. Sci. Lett.*, 16(12), 985–987.

- Park, S. J., Lee, H. Y., Han, M., and Hong, S. K. (2004). "Thermal and mechanical interfacial properties of the DGEBA/PMR-15 blend system." *J. Colloid Interface Sci.*, 270(2), 288–294.
- Pattanayak, D., and Srivastava, D. (2005). "Evaluation of epoxy/sodium Bioglass ceramic composites in simulated body fluid." *Trends Biomater Artif.*, 18(2), 225–229.
- Patterson, A. L. (1939). "The scherrer formula for X-ray particle size determination." *Phys. Rev.*, 56(10), 978–982.
- Peter, S. J., Nolley, J. a, Widmer, M. S., Merwin, J. E., Yaszemski, M. J., Yasko, a W., Engel, P. S., and Mikos, a G. (1997). "In vitro degradation of a poly(propylene fumarate)/ β -tricalcium phosphate composite orthopaedic scaffold." *Tissue Eng.*, 3(2), 207–215.
- Petersen, R. C. (2011). "Bisphenyl-polymer/carbon-fiber-reinforced composite compared to titanium alloy bone implant." *Int. J. Polym. Sci.*, 2011, 1–11.
- Petersen, R. C. (2014). "Titanium Implant Osseointegration Problems with Alternate Solutions Using Epoxy/Carbon-Fiber-Reinforced Composite." *Metals*, 4(4), 549–569.
- Petite, H., Viateau, V., Bensaid, W., Meunier, A., Pollak, C.de., Bourguignon, M., Oudina, K., Sedel, L. and Guillemin, G. (2000). "Tissue Engineered Bone Regeneration." *Nat. Biotech.*, 18(9), 959-963.
- Poompradub, S., Ikeda, Y., Kokubo, Y., and Shiono, T. (2008). "Cuttlebone as reinforcing filler for natural rubber." *Eur. Polym. J.*, 44(12), 4157–4164.
- Prabakaran, K., and Rajeswari, S. (2006). "Development of hydroxyapatite from natural fish bone through heat treatment." *Trends Biomater. Artif. Organs*, 20(1), 20–23.
- Pramanik, S., Hanif, A. S. M., Pinguan-murphy, B., and Osman, N. A. A. (2013). "Morphological Change of Heat Treated Bovine Bone: A Comparative Study." *Materials*, 6, 65–75.

- Pramanik, S., Pinguan-Murphy, B., Cho, J., and Abu Osman, N. A. (2014). "Design and development of potential tissue engineering scaffolds from structurally different longitudinal parts of a bovine-femur." *Sci. Rep.*, 4, 5843.
- Rahman, M. M., Hosur, M., Zainuddin, S., Jajam, K. C., Tippur, H. V., and Jeelani, S. (2012). "Mechanical characterization of epoxy composites modified with reactive polyol diluent and randomly-oriented amino-functionalized MWCNTs." *Polym. Test.*, 31(8), 1083–1093.
- Rahman, M. M., Zainuddin, S., Hosur, M. V., Robertson, C. J., Kumar, A., Trovillion, J., and Jeelani, S. (2013). "Effect of NH₂-MWCNTs on crosslink density of epoxy matrix and ILSS properties of e-glass/epoxy composites." *Compos. Struct.*, 95, 213–221.
- Raju, G. U., and Kumarappa, S. (2011). "Experimental study on mechanical properties of groundnut shell particle-reinforced epoxy composites." *J. Reinf. Plast. Compos.*, 30(12), 1029–1037.
- Rakin, M., Sedmak, A. (2006). "Biomaterials – Joints and Problems of Contact Interfaces." *FME Trans.*, 34(2), 81–86.
- Ramdani, N., Wang, J., He, X., Feng, T., Xu, X., Liu, W., and Zheng, X. (2014). "Effect of crab shell particles on the thermomechanical and thermal properties of polybenzoxazine matrix." *Mater. Des.*, 61, 1–7.
- Rocha, J. H. G., Lemos, A. F., Agathopoulos, S., Valério, P., Kannan, S., Oktar, F. N., and Ferreira, J. M. F. (2005). "Scaffolds for bone restoration from cuttlefish." *Bone*, 37(6), 850–7.
- Rocha, J. H. G., Lemos, A. F., Kannan, S., Agathopoulos, S., and Ferreira, J. M. F. (2005). "Hydroxyapatite scaffolds hydrothermally grown from aragonitic cuttlefish bones." *J. Mater. Chem.*, 15, 5007–5011.
- Rodríguez-Lugo, V., Hernández, J. S., Arellano-Jimenez, M. J., Hernández-Tejeda, P. H., and Recillas-Gispert, S. (2005). "Characterization of Hydroxyapatite by Electron Microscopy." *Microscopy Microanal.*, 11, 516–523.

- Roeder, R. K., Converse, G. L., Kane, R. J., and Yue, W. (2008). "Hydroxyapatite-reinforced polymer biocomposites for synthetic bone substitutes." *Jom*, 60(3), 38–45.
- Roese, P. B., and Amico, S. C. (2009). "Thermal and Microstructural Characterization of Epoxy-Infiltrated Hydroxyapatite Composite." *Mater. Res.*, 12(1), 107–111.
- Rout, A. K., and Satapathy, A. (2012). "Study on mechanical and tribo-performance of rice-husk filled glass-epoxy hybrid composites." *Mater. Des.*, 41, 131–141.
- Roux, F.X., Brasnu, D., Loty, B., Georg,e B. and Guillemin, G. (1988). "Madreporic coral: A new bone graft substitute for cranial surgery." *J. Neurosurg.*, 69(4):510-513.
- Saidpour, S. H. (2006). "Assessment of carbon fibre composite fracture fixation plate using finite element analysis." *Ann. Biomed. Eng.*, 34(7), 1157–1163.
- Salernitano, E., and Migliaresi, C. (2003). "Composite materials for biomedical applications: a review." *J Appl Biomat Biomech*, 1, 3–18.
- Sanosh, K. P., Chu, M.-C., Balakrishnan, A., Kim, T. N., and Cho, S.-J. (2009). "Preparation and characterization of nano-hydroxyapatite powder using sol-gel technique." *Bull. Mater. Sci.*, 32(5), 465–470.
- Sarin, P., Lee, S.-J., Apostolov, Z. D., and Kriven, W. M. (2011). "Porous Biphasic Calcium Phosphate Scaffolds from Cuttlefish Bone." *J. Am. Ceram. Soc.*, 94(8), 2362–2370.
- Saringer, W., Nöbauer-Huhmann, I., and Knosp, E. (2002). "Cranioplasty with individual Carbon Fibre Reinforced Polymere (CFRP) medical grade implants based on CAD/CAM technique." *Acta Neurochir.*, 144(11), 1193–1203
- Scotchford, C. A., Garle, M. J., Batchelor, J., Bradley, J., and Grant, D. M. (2003). "Use of a novel carbon fibre composite material for the femoral stem component of a THR system: In vitro biological assessment." *Biomaterials*, 24(26), 4871–4879.
- Sezavar, A., Zebarjad, S., and Sajjadi, S. (2015). "A Study on the Effect of Nano Alumina Particles on Fracture Behavior of PMMA." *Technologies*, 3(2), 94–102.

Shang, S., Chiu, K.-L., Yuen, M. C. W., and Jiang, S. (2014). “The potential of cuttlebone as reinforced filler of polyurethane.” *Compos. Sci. Technol.*, 93, 17–22.

Shen, L., Yang, H., Ying, J., Qiao, F., and Peng, M. (2009). “Preparation and mechanical properties of carbon fiber reinforced hydroxyapatite/polylactide biocomposites.” *J. Mater. Sci. Mater. Med.*, 20(11), 2259–2265.

Shimpi, N. G., and Mishra, S. (2012). “Sonochemical Synthesis of Mineral Nanoparticles and Its Applications in Epoxy Nanocomposites.” *Polym. Plast. Technol. Eng.*, 51(2), 111–115.

Singh, A. (2012). “Hydroxyapatite, a biomaterial: Its chemical synthesis, characterization and study of biocompatibility prepared from shell of garden snail, *Helix aspersa*.” *Bull. Mater. Sci.*, 35(6), 1031–1038.

Sivakumar, M., and Rao, K. P. (2002). “Preparation, characterization and in vitro release of gentamicin from coralline hydroxyapatite – gelatin composite microspheres.” *Biomater.* 23, 23(15), 3175–3181

Sivakumar, M., Kumar, T. S. S., Shantha, K. L., and Rao, K. P. (1996). “Development of hydroxyapatite derived from Indian coral.” *Biomaterials*, 17(17), 1709–1714.

Ślósarczyk, A., Klisch, M., Blaziewicz, M., Piekarczyk, J., Stobierski, L. X., and Rapacz-Kmita, A. (2000). “Hot pressed hydroxyapatite-carbon fibre composites.” *J. Eur. Ceram. Soc.*, 20(9), 1397–1402.

Srikanth, I., Kumar, S., Kumar, A., Ghosal, P., and Subrahmanyam, C. (2012). “Effect of amino functionalized MWCNT on the crosslink density, fracture toughness of epoxy and mechanical properties of carbon–epoxy composites.” *Compos. Part A Appl. Sci. Manuf.*, 43(11), 2083–2086.

Su, F., Zhang, Z., and Liu, W. (2006). “Mechanical and tribological properties of carbon fabric composites filled with several nano-particulates.” *Wear*, 260(7–8), 861–868.

Sudheer, M., Prabhu, R., Raju, K., and Bhat, T. (2014). “Effect of Filler Content on the Performance of Epoxy / PTW Composites.” *Adv. Mater. Sci. Eng.*, 2014, 1-11.

- Sunny, A. T., Vijayan P., P., Adhikari, R., Mathew, S., and Thomas, S. (2016). "Copper oxide nanoparticles in an epoxy network: microstructure, chain confinement and mechanical behaviour." *Phys. Chem. Chem. Phys.*, 18(29), 19655–19667.
- Suping, H., Baiyun, H., Kechao, Z., and Zhiyou, L. (2004). "Effects of coatings on the mechanical properties of carbon fiber reinforced HAP composites." *Mater. Lett.*, 58(27-28), 3582–3585.
- Su-ping, H., Ke-chao, Z., and Zhi -you, L. (2008). "Preparation and mechanism of calcium phosphate coatings on chemical modified carbon fibers by biomineralization." *Trans. Nonferrous Met. Soc. China*, 18(1), 162–166.
- Suter, A. J., Molteno, A. C. B., Bevin, T. H., Fulton, J. D., and Herbison, P. (2002). "Long term follow up of bone derived hydroxyapatite orbital implants." *Clin. Sci.*, 86(11), 1287–1292.
- Tanner, K. E. (2010). "Bioactive Composite Materials for Bone Augmentation." *J. R. Soc. Interface*, 7, S541–S557.
- Tas, A. C. (2007). "Porous , Biphasic CaCO₃ -Calcium Phosphate Biomedical Cement Scaffolds from Calcite (CaCO₃) Powder." *Int. J. Appl. Ceram. Technol.*, 4(2), 152–163.
- Tayton, K., Phillips, G., and Ráliš, Z. (1982). "Long-term effects of carbon fibre on soft tissues." *J. Bone Jt. Surgery.*, 64(1), 112–114.
- Teh, P. L., Jaafar, M., Akil, H. M., Wagiman, A. N. R., and Beh, K. S. (2008). "Thermal and mechanical properties of particulate fillers filled epoxy composites for electronic packaging application." *Polym. Adv. Technol.*, 19, 308–315.
- Timmerman, J. F., Hayes, B. S., and Seferis, J. C. (2002). "Nanoclay reinforcement effects on the cryogenic microcracking of carbon fiber / epoxy composites." *Compos. Sci. Technol.*, 62, 1249–1258.
- Tkalčec, E., Popović, J., Orlić, S., Milardović, S., and Ivanković, H. (2014). "Hydrothermal synthesis and thermal evolution of carbonate-fluorhydroxyapatite scaffold from cuttlefish bones." *Mater. Sci. Eng. C*, 42(1), 578–86.

Tsafnat, N., Fitz Gerald, J. D., Le, H. N., and Stachurski, Z. H. (2012). “Micromechanics of Sea Urchin Spines.” *PLoS ONE*, 7(9), 1–10

Tuba, F., Oláh, L., and Nagy, P. (2010). “Characterization of the Fracture Properties of Aragonite- and Calcite-Filled Poly (ϵ -Caprolactone) by the Essential Work of Fracture Method.” *J. Appl. Polym. Sci.*, 120(5), 2587–2595.

Vacanti, C.A., Bonassar, L.J., Vacanti, M.P. and Shufflebarger J. (2001). “Replacement of an avulsed phalanx with tissue-engineered bone.” *N. Engl. J. Med.*, 344, 1511–1514.

Vecchio, K. S., Zhang, X., Massie, J. B., Wang, M., and Kim, C. W. (2007). “Conversion of sea urchin spines to Mg-substituted tricalcium phosphate for bone implants.” *Acta Biomater.*, 3(5), 785–793.

Venkatesan, J., Qian, Z. J., Ryu, B., Thomas, N. V., and Kim, S. K. (2011). “A comparative study of thermal calcination and an alkaline hydrolysis method in the isolation of hydroxyapatite from *Thunnus obesus* bone.” *Biomed. Mater.*, 6(3), 035003 1-12.

Verma, D., Gope, P. C., and Shandilya, A. (2014). “Evaluation of Mechanical Properties and Morphological Studies of Bagasse Fibre (Chemically Treated/Untreated)-CaCO₃ Epoxy Hybrid Composites.” *J. Inst. Eng. Ser. D*, 95(1), 27–34.

Wang, C., He, C., Tong, Z., Liu, X., Ren, B., and Zeng, F. (2006). “Combination of adsorption by porous CaCO₃ micro particles and encapsulation by polyelectrolyte multilayer films for sustained drug delivery.” *Int. J. Pharm.*, 308(1-2), 160–7.

Wang, J., and Qin, S. (2007). “Study on the thermal and mechanical properties of epoxy – nanoclay composites: The effect of ultrasonic stirring time.” *Mater. Lett.*, 61, 4222–4224.

Wang, J., and Shaw, L. L. (2009). “Synthesis of high purity hydroxyapatite nanopowder via sol-gel combustion process.” *J. Mater. Sci. Mater. Med.*, 20(6), 1223–1227.

- Wang, M., Joseph, R., and Bonfield, W. (1998). "Hydroxyapatite-polyethylene composites for bone substitution: effects of ceramic particle size and morphology." *Biomaterials*, 19(24), 2357–2366.
- Williams, D.F. and Cunningham, J. (1979). *Materials in clinical dentistry*, Oxford University Press, UK.
- Xu, S., Girouard, N., Schueneman, G., Shofner, M. L., and Meredith, J. C. (2013). "Mechanical and thermal properties of waterborne epoxy composites containing cellulose nanocrystals." *Polymer*, 54(24), 6589–6598.
- Yao, Z. T., Chen, T., Li, H. Y., Xia, M. S., Ye, Y., and Zheng, H. (2013). "Mechanical and thermal properties of polypropylene (PP) composites filled with modified shell waste." *J. Hazard. Mater.*, 262, 212–7.
- Yao, Z., Xia, M., Ge, L., Chen, T., Li, H., Ye, Y., and Zheng, H. (2014). "Mechanical and thermal properties of polypropylene (PP) composites filled with CaCO₃ and shell waste derived bio-fillers." *Fibers Polym.*, 15(6), 1278–1287.
- Yasmin, A., and Daniel, I. M. (2004). "Mechanical and thermal properties of graphite platelet/epoxy composites." *Polymer*, 45(24), 8211–8219.
- Younesi, M., Javadpour, S., and Bahrololoom, M. E. (2010). "Effect of Heat Treatment Temperature on Chemical Compositions of Extracted Hydroxyapatite from Bovine Bone Ash." *J. Mater. Eng. Perform.*, 20(8), 1484–1490.
- Yukna, R. (1994). "Clinical evaluation of coralline calcium carbonate as a bone replacement graft material in human periodontal osseous defect." *J. Periodontol.*, 65(2), 177-185.
- Zabihi, O., Mostafavi, S. M., Ravari, F., Khodabandeh, A., Hooshafza, A., Zare, K., and Shahizadeh, M. (2011). "The effect of zinc oxide nanoparticles on thermo-physical properties of diglycidyl ether of bisphenol A/2,2'-Diamino-1,1'-binaphthalene nanocomposites." *Thermochim. Acta*, 521(1–2), 49–58.

- Zhang, X., and Vecchio, K. S. (2007). "Hydrothermal synthesis of hydroxyapatite rods." *J. Cryst. Growth*, 308(1), 133–140.
- Zhang, X., and Vecchio, K. S. (2013). "Conversion of natural marine skeletons as scaffolds for bone tissue engineering." *Front. Mater. Sci.*, 7(2), 103–117.
- Zhang, Y., and Tanner, K. E. (2008). "Effect of filler surface morphology on the impact behaviour of hydroxyapatite reinforced high density polyethylene composites." *J. Mater. Sci. Mater. Med.*, 19(2), 761–766.
- Zhang, Y., Yin, Q. S., Xia, H., Ai, F. Z., Jiao, Y. P., and Chen, X. Q. (2010). "Determination of antibacterial properties and cytocompatibility of silver-loaded coral hydroxyapatite." *J. Mater. Sci. Mater. Med.*, 21(8), 2453–2462.
- Zhao, C.-X., and Zhang, W.-D. (2008). "Preparation of waterborne polyurethane nanocomposites: Polymerization from functionalized hydroxyapatite." *Eur. Polym. J.*, 44(7), 1988–1995.
- Zhao, J-L., Fu, T., Han, Y., and Xu, K-W. (2004). "Reinforcing hydroxyapatite /thermosetting epoxy composite with 3-D carbon fiber fabric through RTM processing." *Mater. Lett.*, 58(1-2), 163–168.
- Zhaolin, L., Wen, L., Zunzhao, B., Qingshui, Y., and Yu, Z. (2009). "Study on the physical properties and chemical compositions of artificially synthesized coral hydroxyl apatite (CHA) bone." *Chinese J. Geochemistry*, 28(4), 421–426.
- Zhu, L., Jin, F., and Park, S. (2012). "Thermal Stability and Fracture Toughness of Epoxy Resins Modified with Epoxidized Castor Oil and Al₂O₃ Nanoparticles." *Bull. Korean Chem. Soc.*, 33(8), 2513–2516.
- Zhu, Y., Wu, S., and Wang, X. (2011). "Nano CaO grain characteristics and growth model under calcination." *Chem. Eng. J.*, 175, 512–518.
- Zuiderduin, W. C. J., Westzaan, C., Huétink, J., and Gaymans, R. J. (2003). "Toughening of polypropylene with calcium carbonate particles." *Polymer*, 44(1), 261–275.

Zulfli, N. H. M., Bakar, A. A., and Chow, W. S. (2013). "Mechanical and thermal properties improvement of nano calcium carbonate-filled epoxy/glass fiber composite laminates." *High Perform. Polym.*, 26(2), 223–229.

LIST OF PUBLICATIONS

In Refereed International Journals

1. **Kamalbabu, P.**, and Mohan Kumar, G. C. (2016). "Sea-coral derived cuttlebone reinforced epoxy composites: characterization and tensile properties evaluation with mathematical models", *Journal of Composite Materials*, 50(6), 807-823.
2. **Kamalbabu, P.**, and Mohan Kumar, G. C., (2014). "Effects of particle size on tensile properties of marine coral reinforced polymer composites". *Procedia Materials Science*, 5, 802-808.

International Conference Proceedings

1. Mohan Kumar G. C. and **Kamalbabu P.** (February 2017). "Bio-ceramics reinforced polymer composites for biomedical applications". *Proceedings of the 8th International conference on advancements in polymeric materials- APM 2017*, Centre for Scientific and Industrial Consultancy, IISc, Bengaluru, pp:83.
2. G. C. Mohan Kumar and **Kamalbabu P.** (December 2016). "Mechanical Properties of Treated cuttlebone TCP Reinforced Composites for biomedical Applications". *Proceedings of the 3rd International conference on Mechanical Properties of Materials -ICMPM 2016*, Centro culturale Don Orione Artigianelli, Venice, Italy, pp:PM-208.
3. G. C. Mohan Kumar and **Kamalbabu P.** (May 2016). "Processed Marine Corals Reinforced Polymer Bio-Composites". *Proceedings of the International conference on Advanced Materials & Technology -ICMAT 2015*, Sri Jayachamarajendra College of Engineering, Mysuru, Karnataka, India, pp:73-74.

4. Mohan Kumar, G. C., and **Kamalbabu, P.** (October-2015). “Experimental Studies of Marine Coral (Cuttlebone) Reinforced Polymer Composites”. *23rd Annual meeting of the Bio-Environmental Polymer Society -BEPS 2015*, Laboratory of Applied Chemistry, Institute of Organic Chemistry, Karlsruhe Institute of Technology, Karlsruhe, Germany, pp:28.
5. **Kamalbabu, P.**, and Mohan Kumar. G. C. (December-2014). “Thermal studies of Marine coral/Epoxy composites”. *International conference on polymer composites-ICPC 2014*, Department of Mechanical Engineering, National Institute of Technology Karnataka, Surathkal, India. pp:82.
6. **Kamalbabu, P.**, and Mohan Kumar. G. C. (December- 2013). “Effects of coralline CaCO₃ reinforced epoxy composites for biomedical applications”. *6th International conference on Bangalore India Nano -2013*, Department of IT, BT and science and technology, Govt. of Karnataka, Bangalore, India, pp:35.
7. **Kamalbabu, P.**, and Mohan Kumar. G. C., (October- 2012). “Cuttlebone filled polymer composites for biomedical applications”. *3rd International conference on Natural Polymer (ICNP)-2012*, M. G. University, Kottayam, Kerala India, pp: 94-95.

BIO-DATA

Name : KAMALBABU P.
Date of Birth : 07-07-1983
Permanent address : 80-2, NEW QUARTERS, KONGU NAGAR,
DEVASTHANAM PUDUR,
NAMAGIRIPET POST, RASIPURAM (T.K.),
NAMAKKAL (D.T). -637406
TAMILNADU STATE, INDIA.
E-mail : kamalbabu83@gmail.com
Contact number : +91-9945038652

Academic Qualification

- ◆ **Bachelor of Engineering (B.E.):** Mechanical Engineering, K. S. Rangasamy college of technology, Tiruchengode, Tamilnadu.
- ◆ **Master of Engineering (M.E.):** Engineering Design, Kongu engineering college, Perundurai, Tamilnadu.